ABSTRACT

Title of Dissertation: FUNCTIONAL CONNECTIVITY PATTERNS ASSOCIATED WITH AGING, PHYSICAL ACTIVITY, AND GENETIC RISK FOR ALZHEIMER'S DISEASE IN HEALTHY HUMAN BRAIN NETWORKS.

Theresa Jeanne Chirles
Doctor of Philosophy, 2017

Dissertation directed by: Dr. J. Carson Smith, Associate Professor, Department of Kinesiology

Leisure time physical activity (PA) and exercise training help to improve and maintain cognitive function in healthy older adults and in adults with the APOE-ε4 allele, a genetic risk for Alzheimer's Disease (AD). Earlier work finding increased functional connectivity in the Default Mode Network (DMN) after a 12-week walking intervention in 16 older adults with mild cognitive impairment is presented in Chapter 3. The primary dissertation study investigating differences in brain function depending on PA level and genetic risk for AD prior to changes in cognition is presented in Chapters 4-6.

Useable resting state and anatomical MRI scans were collected from 69 healthy adults (22-51 years) as well as saliva for APOE genotyping (carriers defined as homozygotes or heterozygotes of the ε4 allele) and responses to the Paffenbarger

Physical Activity Questionnaire (High PA >1500 kcal, Low PA <1500 kcal per week). The following network measures of functional connectivity were calculated: global efficiency; node strength of Default Mode Network (DMN) and Fronto-Parietal Network (FPN) hubs and hippocampal subsections; and long-range connectivity of the medial prefrontal cortex (mPFC) and posterior cingulate cortex (PCC) in the DMN.

Multiple linear regression analysis revealed statistically significant results for the long-range connectivity of the left PCC, a prominent hub of the DMN, and left mPFC. The differences in projected trajectories of the connectivity are potentially reflective of the compensatory time-course in our participants based on interactions of PA level and APOE status. The Low PA non-carriers had a positive slope indicating increased connectivity with age while carriers and non-carriers in the High PA category had horizontal aging trajectories. PA is associated with cognitive reserve (CR), a term describing the protection and adaptation of cognitive processes through neural efficiency and compensation mechanisms, and it is possible the Low PA non-carriers exhibited compensatory increases in connectivity of the left mPFC-PCC earlier than High PA study participants due to lower levels of CR. The promising findings that rs-fMRI can be used as an early detection of brain changes sensitive to PA levels and APOE-ε4 status are critical to the research and treatment of AD.

FUNCTIONAL CONNECTIVITY PATTERNS ASSOCIATED WITH AGING, PHYSICAL ACTIVITY, AND GENETIC RISK FOR ALZHEIMER'S DISEASE IN HEALTHY HUMAN BRAIN NETWORKS.

by

Theresa Jeanne Chirles

Dissertation submitted to the Faculty of the Graduate School of the
University of Maryland, College Park, in partial fulfillment
of the requirements for the degree of
Doctor of Philosophy
2017

Advisory Committee:
Associate Professor J. Carson Smith, Chair
Associate Professor Donald J. Bolger
Assistant Professor Shuo Chen
Professor James M. Hagberg
Associate Professor Tracy Riggins, Dean's Representative
Professor Stephen Roth

Acknowledgements

There are many individuals to thank and acknowledge for assistance and guidance in completing this dissertation. To begin, the support and reassurance I received from the members of my dissertation committee enabled me to complete my degree. This adventure would not have been possible without my advisor, Dr. J. Carson Smith. His willingness to accept a 'non-traditional' student into his lab was the reason this process could begin, and I have learned much from him over the course of the past five years. I have benefitted from his genuine kindness, and I value the opportunities he has provided to me and the friendship that has developed.

Five other professors joined my dissertation committee, and they were all vital to my progress and development. I did not meet Dr. Donald Bolger until my fourth year, but his assistance in my understanding of research, his encouraging teaching style, and his willingness to provide me access to invaluable data for my project propelled me to the completion of my dissertation. I look forward to continued collaboration with his lab. I approached Dr. Shuo Chen to assist me in understanding the mathematics of resting state fMRI analyses, and he enthusiastically came on board. His reassuring guidance helped me understand the strengths and weaknesses of this approach, and this knowledge is integral to my continuation in this field. I began this graduate program without knowing any brain anatomy, yet almost from the first day I heard references to "the hippocampus." I knew I needed to understand this memory system player, and Dr. Tracy Riggins joined my committee to help me in this quest. I cannot thank her enough for her guidance and willingness to share information, methods, and resources. She has become a valuable mentor to me, and I

am immensely grateful. Dr. James Hagberg is the professor from whom I have taken the most courses during my time at the University of Maryland, and I was privileged to be his teaching assistant. He has been a father figure to me, and words cannot express how grateful I am to him. Dr. Stephen Roth is another person to whom I owe a great deal of thanks that cannot be accurately reflected in the written word. We first met in his office when I was beginning the application process to graduate school, and I have benefited from his wisdom throughout my time as a graduate student. I will continue to follow his example as I move forward in life and career.

This project was very enjoyable because of the collaboration needed to gather and analyze the data. I am in great debt to Dustin Moraczewski for his assistance with the resting state fMRI data processing. I do hope the project was the beginning of our collaborative relationship. This dissertation would not be possible without the data collection efforts by the students in the Bolger and Dougherty laboratories and the genotyping done by Dr. Maureen Kellogg Kayes and Dr. Andrew Venezia. Dr. Lesley Sand aided in starting the FreeSurfer process, and Sarah Dean, an undergraduate in Dr. Riggin's lab, took the time to train me in identifying anatomical markers of the hippocampus for segmentation. Dr. Hyuk Oh, Farzad Ehtemam, and Sarah Blankenship kindly shared what they knew when I either literally or figuratively caught them in the hallway to ask a question. I am thankful for the scientific friendship of Dr. Rian Landers-Ramos, Dr. Kristen Hamilton, and Dr. Ana Valencia who took time out of their schedules to listen and discuss my ideas about the data results. Shelley Diaz and Sylvie Carson made efforts to read and review sections of this document, and I am most grateful.

Appreciation must be extended to the individuals who helped me with my teaching duties during the time I was analyzing the dissertation data and writing the results and discussion. Isabelle Shuggi, Theresa Hauge, Farzad Ehtemam, and Dr. Rudolphe Gentili made KNES385 such an enjoyable team effort. Jo Zimmerman, Dr. Ana Palla-Kane, and Andrew Ginsberg made accommodations to allow me to be a teaching assistant for an online course, enabling me to stay home with my newborn son. I could not have completed this dissertation without the assistance of fantastic babysitters: Fernanda Byars, Nafisha Low, Ashley Moore, David and Cara Versace, my sister, Dr. Eleanor Smith, and my mother, Jeanne Smith. I was so fortunate to have a wonderful and supportive roommate for four years of my graduate school career, Dr. Eleanor Donaghue.

Finally, I extend sincere and heartfelt thanks to the two men who have been with me through the ups and downs of this doctoral program adventure: my son, Dominic, and my husband, Kevin. Dominic began his life as I began my dissertation proposal, and he was with me for almost every moment of the data analysis and writing of the dissertation. He was always a source of joy and comfort. Only Kevin knows how much I depended on his love and support to get me to the finish line. Thank you.

Table of Contents

List of Tables

List of Figures

List of Abbreviations

AD	Alzheimer's Disease
DMN	Default Mode Network
ADHD	Attention-deficit/hyperactivity disorder
AFNI	Analysis of Functional NeuroImages
APOE	Apolipoprotein E
BA	Brodmann area
BMI	Body mass index
BOLD	Blood oxygen level dependent
CA1	Cornus ammonis (Latin), region I of hippocampus proper
CA3	Cornus ammonis (Latin), region III of hippocampus proper
CDR	Clinical dementia rating
CI	Confidence interval
CR	Concept to describe the disjunction between degree of brain damage and clinical outcome.
CSF	Cerebral spinal fluid
DA	Axial diffusivity
DG	Dentate gyrus, sub-region of hippocampus
DLPFC	Dorso lateral prefrontal cortex
DNA	Deoxyribonucleic acid
DTI	Diffusion tensor imaging
EC	Entorhinal cortex, subregion of hippocampus
EEG	Electroencephalogram
FA	Fractional anisotropy
FDR	False discovery rate
fMRI	Functional magnetic resonance imaging
FOV	Field of view
HM	Famous research subject with hippocampal damage
HR	Heart rate
ICA	Independent component analysis

INVADE	Intervention project on cerebrovascular disease and dementia in the community of Ebersberg, Bavaria
IR	Inversion recovery
MCI	Mild Cognitive Impairment
MD	Mean diffusivity
MET	Metabolic equivalent
mPFC	Medial prefrontal cortex
MTL	Medial temporal lobe
OR	Odds ratio
PA	Physical activity
PAR-Q	Physical Activity Readiness Questionnaire
PC/p	Posterior cingulate/precuneus
PCA	Principle component analysis
PCC	Posterior cingulate cortex
PET	Positron emission tomography
PiB	Pittsburgh compound B
PLV	Phase locked synchrony
RAVLT	Rey Auditory Verbal Learning Test
RD	Radial diffusivity
ROI	Regions of interest
SD	Standard deviation
TA	Acquisition time
TE	Echo time
TR	Repetition time
VO_2	Volume of oxygen
WM	Cerebral white matter

Chapter 1: Introduction

As increasing numbers of people are living longer (World Population Ageing Report, United Nations, 2015), memory decline due to physiological aging and pathophysiological changes is growing as a public health issue (World Health Organization). Alzheimer's disease (AD) will be growing in prevalence because of the swelling proportion of elderly in the global population, and this will come with great social and financial cost. AD is the most expensive disease in the United States, and there is no current cure (Alzheimer's Association, 2016). If the onset of AD could be delayed by a few years, costs would vastly decrease and a greater number of older adults would complete their lives with memories and personalities intact. One of the difficulties in treating AD is that we do not fully understand how the healthy brain functions and adapts.

The fronto-parietal network, responsible for executive control, and the default mode network, important for episodic memory, are disrupted during the aging process. Additionally, the hippocampus, also important for episodic memory, decreases in volume with aging. Volume decreases in anterior white matter (part of the fronto-parietal network) do not appear to be accelerated in early AD, indicating that these are age related disruptions (Head et al., 2004), but the DMN has a greater loss of communication in AD patients compared to age matched healthy controls (Damoiseaux, Prater, Miller, & Greicius, 2012). The combination of age related fronto-parietal disruptions and AD pathology beginning in the medial temporal lobe (MTL) is devastating to cognition (Buckner, 2004).

It is well established that PA protects cognition in healthy aging and reduces the likelihood of experiencing cognitive decline (Cotman & Berchtold, 2002; Etgen et al., 2010;

Laurin, Verreault, Lindsay, MacPherson, & Rockwood, 2001; Middleton, Barnes, Lui, & Yaffe, 2010; Middleton et al., 2011; Scarmeas et al., 2009). The mechanisms by which PA protects and preserves cognition in older adults are still being explored, but suggestions include exercise induced neurogenesis in the hippocampus (Erickson et al., 2011; Pereira et al., 2007) and protection of the white matter tracts (Oberlin et al., 2016; J. C. Smith et al., 2016) vulnerable to aging (Buckner, 2004). Thus, PA has been implicated as an ideal intervention to preserve memories and delay cognitive decline, thus reducing both financial and societal costs of AD. Continued investigation of the mechanisms by which PA protects cognition will assist in our understanding of how the brain functions and adapts, and perhaps give us insights into the pathophysiology of AD.

While PA is a protector against cognitive decline, carriers of the ε4 allele of the APOE gene are at increased risk for cognitive decline and AD (Farrer et al., 1997). APOE is involved in lipid transport (Bu, 2009; Holtzman, Herz, & Bu, 2012), and while the mechanisms that increase the risk are still not determined, some potential neural explanations include increased amyloid burden (Chételat & Fouquet, 2013; Reiman et al., 2009), smaller grey matter volumes (K. Chen et al., 2007; Honea, Vidoni, Harsha, & Burns, 2009; O'Dwyer et al., 2012; Plassman et al., 1997; Shaw et al., 2007; Wishart et al., 2006), altered metabolism (Jagust, Landau, & Initiative, 2012; Knopman et al., 2014; Perkins et al., 2016) and connectivity changes of the posterior cingulate cortex and precuneus that mirror AD (Fleisher et al., 2009; McKenna, Koo, Killiany, & Initiative, 2015; Sheline et al., 2010). However, not all ε4 carriers will be diagnosed with AD (Saunders et al., 1993), and perhaps there are some lifestyle behaviors, such as PA, that can moderate this genetic risk. A possible explanation of this apparent moderation of genetic risk is that PA may augment a person's ability to withstand brain disruption or damage.

Investigating the effects of PA in vulnerable networks of healthy carriers of genetic risk is important in the effort to understand these moderating mechanisms.

PA may increase the brain's ability to tolerate damage and recruit alternate networks by increasing levels of cognitive reserve. Cognitive reserve (CR) is a concept to explain why individuals with identical observed evidence of brain disruption will have different clinical diagnoses based on cognitive performance (Buckner, 2004; Stern, 2009). An individual with higher CR would be able to withstand greater amounts of brain damage than an individual with less CR before a critical threshold is reached and cognitive processes decline (Barulli & Stern, 2013). One neural implementation of CR that enables this greater capacity to withstand damages is the ability to recruit alternate brain network (Stern, 2009). PA has been implicated as one of the factors that increases cognitive reserve (Fratiglioni, Paillard-Borg, & Winblad, 2004), and it is possible that PA protects against cognitive decline by aiding the ability of the brain to recruit existing and alternate networks. Our laboratory has shown that 12 weeks of walking in older adults already experiencing cognitive decline due to AD, with a diagnosis of mild cognitive impairment, enabled the recruitment of frontal and parietal regions implicating enhanced ability to compensate (Chirles et al., 2017). This enhanced compensation would increase cognitive reserve and thus possibly delay cognitive decline.

Despite the evidence that PA protects cognition, few studies have investigated the effects of PA on brain networks throughout the lifespan. The effects of PA on the networks disrupted by the aging process need to be studied at all stages in order to more fully understand the influence of PA on brain plasticity. Additionally, despite the evidence that carriers of the APOE-ε4 allele have disrupted networks similar to the changes observed in aging and AD before non-

carriers (Sheline et al., 2010), there has not been research to illuminate the interactive effects of PA and APOE-ε4 allele on these networks.

Specific Aim 1: To investigate the association of self-reported leisure-time PA on the fronto-parietal network, DMN, and hippocampal connectivity in young adulthood to middle adulthood.

Specific Aim 2: To investigate the association of the interaction of PA and APOE-ε4 status on the fronto-parietal network, DMN, and hippocampal connectivity from young adulthood to middle adulthood.

The following chapter reviews the literature necessary to address these specific aims and lay the theoretical foundation for the study described in Chapters 4-6. First, a review is presented on the effects of aging and AD on the fronto-parietal network, the DMN, and hippocampus. Secondly, resting state functional connectivity and the benefits of using a network approach to understand the brain are explored. This section includes subsections covering changes in the networks due to aging and AD, as well as the effect of APOE-*ε4* status on connectivity. Finally, the protective effects of PA on cognition in healthy adults and in those at risk for AD are described, and the literature describing the current understanding of PA's effect on resting state network functional connectivity are presented.

Chapter 2: Literature Review

Section 2.1: Brain, Age and Alzheimer's Disease

Subsection 2.1.1: Effect of Aging and AD on Frontal-Striatal Circuits

Evidence suggests that frontal white matter is particularly vulnerable to aging, and while there is age related loss throughout all brain regions, it is greatest in the frontal cortex than compared to other cortical and subcortical regions (Buckner, 2004). These age related changes to volume and structure of cerebral white matter (WM) (Bartzokis et al., 2004; Paus, Pesaresi, & French, 2014; Peters, 2002) have been identified as a possible neuroanatomical substrate of the cognitive differences and decline that are exhibited with increasing age (Bartzokis et al., 2004; Bender, Prindle, Brandmaier, & Raz, 2016; Bennett & Madden, 2014; Walhovd, Johansen-Berg, & Káradóttir, 2014). The regions included in this network are the anterior prefrontal cortex, insular and frontal operculum cortices, the temporo-parietal junction, and the dorsal posterior and anterior cingulate gyri (Dosenbach et al., 2006; Rushworth, Walton, Kennerley, & Bannerman, 2004). These areas are involved in executive function, a network responsible for task switching and controlling attention. In this system, 65% of older adults over the age of 75 years show white matter abnormalities (Ylikoski et al., 1995).

Older adults without dementia do experience difficulty on cognitive tasks that require attention and executive function (Craik, Morris, Morris, & Loewen, 1990; West, 1996), and consistently research has shown that these attention and executive function difficulties are distinct from memory loss due to Alzheimer's disease(Buckner, 2004). Some memory functions, such as word retrieval and vocabulary, that are disrupted in AD remain relatively constant throughout the healthy aging process (Nyberg, Bäckman, Erngrund, Olofsson, & Nilsson, 1996;

Park et al., 1996; Schaie & Willis, 2010), and difficulties in However, what is so devastating in AD is that predicted memory impairment from AD pathology is synergistically worse with frontal-striatal circuit disruptions (Buckner, 2004). If these frontal-striatal circuits can be protected, then AD symptomology will be mitigated.

Subsection 2.1.2: Distinct Effects of Aging and AD on the Hippocampus

The famous study participant, HM, instigated the intense research and study of the role of the hippocampus in memory (Squire, 2004). This subject's unique damage to the hippocampus and resultant memory symptoms implicated the hippocampus as having an integral role in declarative memory (Eichenbaum, 2004), and as subsequent lesion studies have demonstrated, the hippocampus is vital in the encoding and retrieval of specific personal experiences, otherwise known as episodic memory (Schacter, 1997, 2000) . The encoding and retrieval of episodic memories that include spatial, temporal, and sensory integration utilize the circuit properties of the hippocampus subfields (Eichenbaum, 2004).

Higher resolution fMRI research techniques have made it possible to investigate the subfields of the hippocampus (Yassa & Stark, 2011), and this has led to the amassing of evidence suggesting region specific effects of healthy aging and AD on the hippocampus (S. A. Small, Schobel, Buxton, Witter, & Barnes, 2011). The entorhinal cortex (EC), dentate gyrus (DG), CA1, and CA3, all subregions of the hippocampus, appear to be preferentially vulnerable to either aging or AD pathology. The EC is the first region to exhibit AD pathology (Gómez-Isla et al., 1996; S. A. Small et al., 2011) yet is preserved in aging as evidenced by older adults in their 9th decade showing little change in the EC (Hedden & Gabrieli, 2004). Effects of aging are predominately in the DG (Yassa & Stark, 2011) CA3 and CA1. The DG has a primary role in discriminating between two similar objects or events (S. A. Small et al., 2011; Yassa & Stark,

2011), and this ability is altered in aging (Yassa & Stark, 2011). Due to the difficulty of separating it anatomically from the DG, the CA3 is often lumped together with DG as the same region of interest (ROI) and has also had the role of object discrimination attributed to it (S. A. Small et al., 2011; Yassa & Stark, 2011). The CA3 is particularly sensitive to increases in cortisol, and as cortisol most often increases with age, this may explain the deterioration of the CA3 over the course of aging (S. A. Small et al., 2011). The CA1, responsible for re-coding the incoming information into bundles, otherwise called chunking (Kesner, Lee, & Gilbert, 2004), and appears to be highly sensitive to vascular disease and high glucose levels (S. A. Small et al., 2011). Again, this area is vulnerable to the aging process as age is a risk factor for vascular disease and disrupted glucose clearance (Basu et al., 2003).

While the total hippocampal volume decreases in both aging and AD, the hippocampus in AD patients is consistently smaller (Jack et al., 1997). In a meta-analysis of 28 studies (n = 3422, age range = 24.5-84) Fraser et al. (2015) determined that the average rate of hippocampal atrophy is 0.85% per year. This rate does change over the lifespan, however, and was calculated to be 0.38% per year when age is less than 55, 0.98% per year during ages 55 to less than 70, and at 1.12% per year in studies when the subjects were 70 years or older. Other research studies have determined atrophy of the hippocampus to about 2-3% decrease per decade through the aging process and observed increases to about 1% per annum after age 70 (Hedden & Gabrieli, 2004). An interesting caveat to aging and AD research is that there is often the "contamination" of healthy elder subjects with elders who are in the preclinical stages of AD (Buckner, 2004). This may explain the predominance of medial temporal lobe (MTL) dysfunction in aging studies when this may be the antecedent of AD. In fact, 30-60% of neuron loss previously associated with aging is absent in older adults in their 9th decade who do not show any AD pathology, and

the meta-analysis by Frasser et al. (2015) did not distinguish between healthy aging and elders in the preclinical stages of AD.

Subsection 2.1.3: Effects of Age and AD on Default Mode Network

The default mode network (DMN) spans the frontal, temporal, and parietal regions of the brain. These areas the posterior cingulate, ventral and superior frontal medial cortices, and bilateral occipital cortices, middle frontal cortices, and middle temporal cortices including the hippocampus and parahippocampus (Buckner, Andrews-Hanna, & Schacter, 2008; Fox et al., 2005; M. D. Greicius, Srivastava, Reiss, & Menon, 2004). This network was first identified as a "task negative" network by Fox et al. (2005) as these regions consistently had BOLD fMRI activity during the absence of a task compared to task conditions. While at first this "task negative" status induced a confusion and uncertainty about purpose of this network, it is now believed to be involved in flexible self-relevant mental reflections and explorations that anticipate and evaluate possible future events (Buckner et al., 2008). Additionally, this network overlaps and is strongly integrated in episodic memory (Buckner et al., 2008; Vincent et al., 2006).

The DMN has attracted much attention in neuroscience research because of its relevance to aging and disease (Buckner, 2013; Buckner et al., 2008; Buckner et al., 2009; Buckner, Snyder, Sanders, Raichle, & Morris, 2000). The purpose of this section is to give a general presentation of the changes that occur in the DMN over the course of aging and throughout the AD progression. In order to do so, many of these studies include the term "functional connectivity". While this term and studies are more fully developed and explored in a later section, for the present we will consider this term to mean communication between spatially separate brain regions.

Damoiseaux et al. (2012) measured the modularity of the DMN in AD patients over the course of 2 to 4 years. The posterior default mode network at baseline had reduced connectivity, but the anterior and ventral default mode networks had increased connectivity compared to controls. At follow up, however, the entire DMN had reduced connectivity compared to controls. Hillary et al. (2015) effectively summarized the connectivity changes that are expected due to the neuronal disruption in AD. First, there is compensatory hyperconnectivity in the frontal/parietal regions, and then overall loss of connectivity as AD progresses. In aging, these connections are not lost, but anterior to posterior connections are weakened (Andrews-Hanna et al., 2007).

A hypothesized underlying neural substrate for functional connectivity is the white matter structural architecture (Honey, Kötter, Breakspear, & Sporns, 2007), and white matter integrity is also a subject of aging studies relating to the DMN. In one of the few longitudinal studies investigation the relationship between white matter changes and cognitive performance, Bender et al. (2016) conducted a two year longitudinal study in 96 healthy adults (baseline age range = 18-79). Diffusion tensor imaging (DTI) was used to measure fractional anisotropy (FA), mean diffusivity (MD), axial diffusivity (DA) and radial diffusivity (RD), and changes in white matter structure were found in the episodic memory network that highly overlaps with the DMN. These changes were coupled with improved cognitive scores on associative memory tasks. Interestingly, while increased FA and lower RD was associated with better performance at baseline, a reversal of these indices in the two-year time-period was connected to positive changes in cognition. While the longitudinal design gives a unique insight into the WM changes over time that concur with cognitive improvements, individual genetic and environmental influences in network structure (e.g. APOE status and PA status) were not considered in the analyses.

Section 2.2: Resting State Functional Connectivity

Subsection 2.2.1: General Description

Functional connectivity is a method to study spatial and temporal properties of brain regions using the spontaneous BOLD activity that stems from the brain's energy metabolism (Fox & Raichle, 2007). While much of the original fMRI research focused on task based activations, there is less than a 5% change in signal induced by tasks (Raichle & Mintun, 2006). This change in signal is independent and additive to the underlying spontaneous activity. Most of the signal, with accounts for 20% of the total body energy metabolism, is accounted for by the 'resting' brain (Fox & Raichle, 2007; Raichle, 2011). This signal of the resting brain can be distinguished from cardiac and respiratory noise factors because of its 1/frequency distribution: there is greater power to detect this signal at lower frequencies (Zarahn, Aguirre, & D'Esposito, 1997). Noise has a flat power density function: there is an equal distribution across frequencies. During the beginning of fMRI usage, the signal during this resting state was considered to be noise, yet consistent findings in the functional connectivity research find that brain regions known to be functionally related tend to have correlated spontaneous BOLD activity (Fox & Raichle, 2007). Repeatedly, complex systems that have been identifies using various task paradigms also demonstrate this correlated spontaneous BOLD activity, and this connectivity survives different states of task, sleep, and anesthesia. Differences in functional connectivity have been associated with variability in human behavior (Fox & Raichle, 2007).

Functional connectivity has been described as an interesting window on the underlying synchrony of neuronal process (Varoquaux & Craddock, 2013). While these signals are meaningful, the underlying physiology explaining these signals is still unknown. It is believed to

have a different underlying physiology than task based induced BOLD. Nitric oxide synthesis blocker successfully blocked stimulus-related increases in blood flow, but the spontaneous BOLD was unchanged (Golanov, Yamamoto, & Reis, 1994).

One must be careful about how functional connectivity is interpreted. While correlations of spontaneous activity do exist in neuro-anatomical systems, this analysis technique is unable to distinguish direct anatomical pathways and polysynaptic pathways (Fox & Raichle, 2007). The particular parcellation for the connectivity analysis also will determine the conclusions that may be made from the results, and current parcellations are on the macroscopic, not neuronal, scale. (de Reus & van den Heuvel, 2013).

Currently, there are three predominate theories to explain the role of spontaneous BOLD. First, it is a record or memory of previous use (D. J. Foster & Wilson, 2006; Kenet, Bibitchkov, Tsodyks, Grinvald, & Arieli, 2003) . Thus, regions that are activated for the same task will have spontaneous correlations during no task. Secondly, the organization and coordination of neuronal activity will be greater in areas that are routinely enrolled in similar tasks, and this is reflected in the spontaneous signal (Salinas & Sejnowski, 2001; Shatz, 1996). Finally, a theory that is gaining more experimental support is that the coordinated spontaneous activity is a prediction of expected use and not a record of past use (Körding & Wolpert, 2006; Pouget, Dayan, & Zemel, 2003).

Despite the uncertainly on the function of spontaneous BOLD, resting state connectivity is quickly becoming a marker for diagnostic and prognostic information (Fox & Raichle, 2007). Differences in the intrinsic activity structure have been found in Alzheimer's disease, multiple sclerosis, depression, schizophrenia, ADHD, autism, epilepsy, blindness, and spatial neglect following stroke (Fox & Raichle, 2007).

In this dissertation, the subject area is aging and Alzheimer's disease. A vast amount of research is being done studying the functional connectivity changes that are due to physiological and pathological reasons. In fact, resting state functional connectivity is emerging as a new biomarker that may potentially be more sensitive to neuronal network integration and function that is necessary for higher level cognition and so horribly attacked in AD. This method has been used to identify network differences before the presentation of any cognitive difficulties in individuals at risk for AD in older adults (Sperling et al., 2011), and is emerging as a viable method to detect the efficacy of treatments in patients with AD (Goveas et al., 2011; Li et al., 2012).

Resting state functional connectivity has been used to test the efficacy of drug interventions in mild AD. Basal forebrain medial cholinergic pathways are altered in aging and AD, and acetylcholinesterase inhibitors, such as donepezil, are administered to reinstate the cholinergic innervation. Areas of increased blood flow in the medial cholinergic pathway after 12 weeks of donepezil treatment have also been found to have increased functional connectivity (Li et al., 2012). The hippocampal network is an area of high cholinergic innervation, and 12 weeks of donepezil have increased the connectivity between the hippocampus, insula, and thalamus (Goveas et al., 2011). In these drug treatment interventions, increases in connectivity were associated with increases in the AD rating scale – cognitive subset.

Subsection 2.2.2: Methods to Measure Functional Connectivity

In the seed based approach to functional connectivity, the time course from one region of interest, the seed, is extracted. This time course is then correlated with the rest of the brain, and the assumption is that a correlation in the time series indicates that the spatially separate brain regions are functionally connected. It is important to remember that the correlations are

truncated, thus not normally distributed, and typically a Fisher to z transformation is performed before the statistical analysis steps. In one sense, this method is very simple and yet has a very straightforward interpretation (Fox & Raichle, 2007). In resting state research, the seed based approach is the most common method employed, and comparisons between studies are possible. As a result of the simplicity, there are weaknesses to this method. The results do depend on the choice of seed, and it is possible that the seedtime course is not statistically independent from the remaining time courses in the brain. Importantly, multiple brain systems cannot be simultaneously studied (Fox & Raichle, 2007), and it is impossible to make conclusions about networks (Habeck & Moeller, 2011). Despite the weaknesses, when the research question concerns the connectivity of one region of interest, this is an appropriate approach.

In fMRI research, methods exist to account for the mass univariate testing in the statistical analysis steps. Multiple comparisons are an issue as the data most often includes more than 80,000 voxels. The most typical method in the seed based approach to account for this issue is by using cluster extent thresholding (Woo, Krishnan, & Wager, 2014). From an arbitrary primary threshold, clusters of contiguous voxels with a voxel-wise statistic value above this threshold are detected. The false positive probability of this region as a whole is controlled and not for each voxel. This limits how many comparisons are done. The family-wise error rate is obtained from a sampling distribution of the largest null hypothesis cluster size among the suprathreshold voxels within the brain. This method had relatively high sensitivity and dramatically decreases the type II errors likely with Bonferroni corrections. Unfortunately, many researchers then make conclusions that are not supported by this statistical correction (Woo et al., 2014). The null-hypothesis for this test is that there is no significant correlation with any voxel in that cluster. Thus, the rejection of the null hypothesis is that there is a correlation with at

least one voxel in that cluster, and the cluster-level p value is the probability that there is a correlation somewhere in the cluster. Yet, many papers exist claiming correlations with an entire cluster that covers several anatomical regions (Woo et al., 2014).

Independent component analysis (ICA) or principal component analysis (PCA) is a data driven approach to analyze resting state networks with functional connectivity (Fox & Raichle, 2007). In this method, linear combinations of multiple effects are unmixed and spatial maps are created that capture functional networks or noise. This method assumes that brain networks are mutually orthogonal, and it is a very useful method for isolating sources of noise and for data reduction (Habeck & Moeller, 2011). Statistically, the signals is decomposed so that the components are maximally independent (Fox & Raichle, 2007). Despite these strengths, there are some difficulties in the interpretation of this method, and due to these issues, the resulting components may not be intrinsically meaningful. Additional evidence needs to be provided for these analysis (Habeck & Moeller, 2011). One of the major issues stems from the dependence of the results on the number of components the algorithms is requested to find, and the determination of which components reflect neuro-anatomical systems or noise depends entirely upon the user (Fox & Raichle, 2007). This method assumes orthogonal or independent networks, but that in fact may not be the case.

Brain networks are complex systems, and many complex systems are represented mathematically as a network defined by a collection of nodes (vertices) and links (edges) between pairs of nodes (Rubinov & Sporns, 2010). These networks can be quantified into single metrics that limit multiple comparison issues. The first step is to define these nodes that can be determined in using several methods (Bullmore & Sporns, 2009), and the result of the subsequent metrics depends greatly on the node selection(N : number of nodes). The

assumption is that these nodes are spatially separate and cover the entire cortex (Rubinov & Sporns, 2010) and match functional units (Varoquaux & Craddock, 2013). Once nodes are determined, the second step is to define the association between these nodes (Bullmore & Sporns, 2009). The most common method for determining an association between nodes is correlation measures, but time series are dynamic and time sliding windows are also used to capture the dynamism of the signal. Whether a link exists between two nodes is determined by thresholding (Rubinov & Sporns, 2010), and this is part of step three. An association matrix is generated from all the pairwise associations, and each element has an arbitrary threshold applied to produce a binary or undirected adjacency matrix (NxN) (Bullmore & Sporns, 2009). The final step is to calculate the network parameter that is of interest to the research question and compare this parameter to a population of random networks with equivalent network characteristics such as number of nodes, links, and the degree distribution (Rubinov & Sporns, 2010). Rubinov and Sporns (2010) provide mathematical definitions of several network metrics, and Table 1 defines terms used in this paper.

Table 1: Definition of Network Terms

Centrality	A measure of how central or influential a node is relative to the rest of the network.
Clusters	Densely interconnected groups of brain regions.
Degree distribution	The summarization of all the node degrees across a whole network.
Edge	Pairs of nodes are linked by edges, also called links or connections.
Global efficiency	A measure of functional integration that is the average inverse shortest path length.
Hubs	Hubs may be identified on the basis of several network measures, including high degree, short average path length, or high betweenness centrality.
Local efficiency	A measure of functional segregation: efficiency within a module.
Modularity	Degree to which a given network can be decomposed into a set of non-overlapping, overlapping, or hierarchically arranged modules.
Motif	A small subset of network nodes and edges, forming a subgraph.
Network	Set of nodes (elements) and edges (relations).
Node	A network element which may represent a neuron, a neuronal population, a brain region, a brain voxel, or a recording electrode. Nodes are also referred to as vertices.
Node degree	The number of connections (incoming and outgoing) that are attached to a given node.
Path length	In weighted graphs, the length of the path is the sum of the edge lengths, which can be derived by transforming the edge weights.
Small worldness	A property of networks that combines high clustering with a short characteristic path length compared to a population of random networks composed of the same number of nodes and connections.

Definitions from "Networks of the Brain" by Olaf Sporns (2011).

The assumption in graph network studies is that all networks found in natural and technological systems have non-random features that deviate from randomness. These deviation

reflects the specific characteristics and functionality of that network (Bullmore & Sporns, 2009). Thus, the final step in complex network measures is to generate statistics calculated on null-hypothesis random networks that share the basic network characteristics. There are many strengths to this method, and it is quickly becoming the method of choice for research studies investigation functional connectivity and networks (Rubinov & Sporns, 2010). Network measures have shown consistent overlap of anatomical and functional modules in the macaque cortex, and complex brain networks can be reliably quantified with easily computable measures that are neurobiologically meaningful (Rubinov & Sporns, 2010). Small-worldness, and other large-scale organizational aspects of network are consistent across different anatomical parcellation templates.

In fact, differences between individual subjects network characteristics were preserved across several parcellation templates when there were more than 200 nodes (de Reus & van den Heuvel, 2013). In a study using computational modeling of a macaque monkey cortex using the structural anatomy as a substrate for spontaneous activity, structural-functional connections were consistent at multiple time scales (Honey et al., 2007). The computationally induced episodes of synchronization were consistent with experimental observations, and the models suggest that the cortical resting state consists of multiple time scale oscillations that are shaped by the anatomical structure. While the BOLD signal reflects spontaneous fluctuations at a slow time scale (~0.10Hz), these observations may be an aggregate of many couplings and decouplings that occur at a far more rapid pace (~10Hz).

Despite the strengths of this method, there are weaknesses that must be acknowledged and addressed in research studies employing network measures. Networks using different parcellation schemes or network order (N) will not result in identical numerical values of

network measures and cannot be quantitatively compared (de Reus & van den Heuvel, 2013; Rubinov & Sporns, 2010). Additionally, links are the result of arbitrary thresholding and results are most informative is shown across a range of thresholds (Rubinov & Sporns, 2010). Currently, in the mathematical definitions of network measures, negative weights (as a result of negative correlations) are not able to be quantified and thus are currently discarded (Rubinov & Sporns, 2010). Anatomically, nodes that are in structurally confined areas will have a lower degree distribution, and thus a lower probability of high degree nodes, due to their limited capacity of making connections (Bullmore & Sporns, 2009; de Reus & van den Heuvel, 2013).

The weaknesses of graph theory do not discredit the method, but rather are important to understand to develop appropriate methods for particular research questions and inform the researcher on the conclusions that can be made from the results. For instance, while a greater number of nodes allow for greater special resolution, the researcher must be aware that this increases the probability of measuring intrinsic smoothness inducing spurious connections (de Reus & van den Heuvel, 2013). While the practice of comparing structural and functional connectivity networks is quickly gaining group, there are innate differences in network density (functional networks will have greater density) that makes direct comparisons difficult.

The differences in sparsity must be addressed when comparing systematic differences between groups. One method to address such sparsity differences is to apply different link thresholds for each matrix (de Reus & van den Heuvel, 2013). Neurobiological interpretation of network topology depends on the parcellation scheme (either anatomical, randomly generated, voxel based) and the determination of links (de Reus & van den Heuvel, 2013; Rubinov & Sporns, 2010), and the choice of parcellation should be related to the research questions.

Normalization is a key step in graph theory analysis. This is due to the fact that there are both intrinsic and transient structures in a network, and it is the intrinsic structures that are of interest to the researcher (Zalesky, Fornito, & Bullmore, 2012). Using correlation as a connectivity measures inherently gives rise to more clusters than random networks due to the transitive property (Zalesky et al., 2012). This is due to indirect paths and their corresponding direct connections are more likely to both be present in the link measure, while in a randomly generated network these would not be both present. Measures of small-worldness, such as modularity, efficiency, and centrality, will all be influenced by the transitive nature of correlation measures (Zalesky et al., 2012). One must be aware that small-world networks can be overestimated. Ensuring that the random networks generated also have the transitive nature will give credence to the network measures generated from the data (Zalesky et al., 2012).

The calculation of the network measure of interest, F, in the observed network, captures the networks intrinsic and transient structure. Fnull is the same network measure calculated for the null hypothesis. This is generated from the repeated calculations of the F measure averaged over a collection of generated random networks, and Fnull should capture only the transient structure. Thus, when normalization is performed, F/Fnull will result in a network measure that only reflects the intrinsic structure of the network.

One of the major benefits of using network measures in research is that it limits mass-univariate testing. The number of tests performed "scales" as the number of regions used, and thus correcting for these multiple comparisons will greatly reduce the statistical power of finding real differences (Varoquaux & Craddock, 2013). A less stringent method is to control for the false discover rate (FDR), but often the assumptions needed to apply FDR are not met (Varoquaux & Craddock, 2013).

By using a network approach with resting-state fMRI, a unified approach to the neural substrates of cognition may be investigated (Voytek & Knight, 2015) across aging and disease states that is not possible with basic task activation studies. There is difficulty in studying the changes of structural connections across the lifespan because of the changes in myelination that occur adds difficulty to diffusion tensor imaging interpretations, but observational captures of the spontaneous neuronal activity is important in understanding the development of the brain (Sporns, 2011) and how it naturally compensates to neurological disruption (Hillary et al., 2014; Hillary et al., 2015). The brain has been called the most complex organism in the universe, and it is only logical to use complex network analysis when trying to comprehend the amazing dimensions of the organ that sits in our own heads.

As with any approach, strengths and limitations must be understood and used properly in interpretation of results. Models should be chosen to match the question being asked in the situation at hand (Varoquaux & Craddock, 2013). As George Box has said, "All models are wrong; some models are useful."

Subsection 2.2.3: Using resting state functional connectivity to understand the role of the hippocampus, fronto-parietal network, DMN, and changes due to aging and AD.

Resting state functional connectivity and the many models using this concept have provided researchers with important insights into how the brain develops, operates, and changes due to aging and pathologies. Simple correlation measurements between ROI's have revealed the importance of the connectivity of the PCC and hippocampus in episodic memory. Wang et al. (2010) found that greater connectivity between the PCC and hippocampus was associated with better performance on a face/name recall task involving episodic memory. Wang et al. (2010) also investigated the importance of inter-hemisphere connectivity and memory performance.

Greater bilateral hippocampus connectivity was associated with better performance on a word recall task. This was not a global connectivity effect as the hippocampus connectivity correlation was much more significant than the inter-hemisphere connectivity of the motor cortex.

Aging and development also alters the fronto-parietal network as shown through resting state functional connectivity studies. Fair et al. (2009) was able to demonstrate that fronto-parietal network brain regions that are closely segregated in childhood become more diverse as a young adult. In this sample, the connectivity strength decreased in local regions and becomes stronger with regions further away anatomically in young adults and this appeared to be true across several networks. Archard and Bullmore (2007) found decreases in global efficiency (thus an increase in path length) in adults over the age of 60. While small-worldness is maintained across the lifespan, a rebalancing of functional segregation and integration occurs through childhood development, and young, middle, and late adulthood, and this rebalancing is a possible neural substrate for cognitive changes (Sporns, 2011).

In the DMN, young children have very sparse anterior-posterior connections that are highly connected in young adults (ages 21-31) (Fair et al., 2008). These are the same connections that are disrupted with aging (Andrews-Hanna et al., 2007), and as mentioned previously, these aging effects are synergistically devastating when coupled with AD pathology (Buckner, 2004). An intervention, such as physical activity, that protects these connections will have vast benefits to the growing aging population.

In the AD literature, resting state functional connectivity is emerging as a viable biomarker to detect changes before clinical symptoms emerge (Sperling et al., 2011). Hedden (2009) investigated the activations in the DMN and hippocampal network in PiB+ (amyloid

deposition at levels of those with AD) and PiB- healthy older adults. PiB+ older adults had similar hypo activity as found in MCI patients - that included a decreased deactivation of the DMN areas during the task. This decreased activation correlated to a decreased connectivity of the hippocampus with the PCC. These results could not be explained by atrophy or age, and it was network unique – similar differences in connectivity were not found in the visual cortex. Drzezga (2011) investigated cluster loss (as measured by voxel wise whole brain connectivity) in healthy elders PiB-, healthy elders PiB+, and MCI with PiB+ results The healthy PiB- adults showed similar cluster (also called hub) distribution as young adults in a study performed by Buckner et al. (2009), but the PiB+ group had significant loss of clusters in the PCC and angular gyrus regions. The MCI group had an absence of clusters in the PCC, angular gyrus, and disrupted cluster distribution in the temporal memory related regions. These results could not be explained due to atrophy. These disruptions are similar to what is found in patients already diagnosed with AD. Sans-Agrita (2010) measured functional connectivity using clustering from graph theory to compare cognitively healthy older adults and AD patients. There was a significant loss of global integration, and the AD presented clustering closer to a random network. These pre-clinical studies illustrate that communications between brain areas are disrupted and network alterations occur before clinical symptoms appear. This network approach allows for such preemptive detections and perhaps more effective treatments.

[More information on network disruptions on the AD continuum are included in Chapter 3].

Subsection 2.2.4: Effects of APOE-ε4 on Network Connectivity

Healthy adults with the APOE-ε4 allele have consistently been shown to have deficiencies in episodic memory (Wisdom, Callahan, & Hawkins, 2011), and this coincides with

disruptions in the connectivity of the hippocampus, disruptions in the DMN, and disruptions in the fronto-parietal network – all of which are involved in episodic memory. Harrison et al. (2016) measured the connectivity differences of the subregions of the hippocampus in APOE-ε4 carriers (n = 34) and non-carriers (n = 46) during an associative memory task. Carriers were found to have lower function connectivity of the anterior hippocampus with several regions of the DMN during encoding and retrieval. This is consistent with the theory that the AD progression begins in the anterior regions, the EC, of the hippocampus. Heise et al. (2014) found an overall reduction of the functional connectivity between the hippocampus and PCC in female APOE-ε4 carriers. This was found in a sample of 86 cognitively healthy adults (age range = 30 – 78). This reduction in functional connectivity was accompanied with increased MD, DA, and DR in the white matter of left and right cingulum tracts. No measures of PA were included in this study.

Goveas et al. (2013) conducted a seed based analysis in middle age adults (age range 45 – 60) in APOE-ε4 carriers (n = 20) and non-carriers (n = 26) to investigate the communication of the hubs of the fronto-parietal network and the DMN. The PCC was used as the seed for the DMN, and the dorsolateral prefrontal cortex was used as a seed for the fronto-parietal network. In both networks, carriers had diminished functional connectivity, and this was in subjects without cognitive decline or gray-matter atrophy. In another study investigating internetwork communication, Chen et al. (2015) found significant loss of small worldness (as measured by pathlength) in the functional connectivity networks in APOE-ε4 allele carries as compared to non-carriers in cognitively healthy older adults. This was due primarily to the loss of connectivity in the PCC.

Healthy adults with the APOE-ε4 allele have similar disrupted functional connectivity of the precuneus, as those on the AD progression (Sheline et al., 2010). In 100 cognitively intact older adults (CDR=0) without amyloid plaque buildup or decreased CSF A_{42}, APOE-ε4 carriers had greater connectivity of the precuneus than APOE-ε4 negative adults with the medial prefrontal cortex and BA10 (Sheline et al., 2010). The APOE-ε4 carriers also had negative correlations with the caudal oribital cortex and dorsal occipital cortex (BA19), while the non-carriers had positive correlations. The non-carriers had negative correlations and the APOE-ε4 carries had positive correlations with the following areas: right gyrus rectus, right hippocampus, and left superior temporal gyrus/frontoparietal operculum (BA22). Thus, with a few exceptions, the APOE-ε4 positive, cognitively intact adults, show increased connectivity of the precuneus with brain regions in the DMN compared to low risk groups (Fleisher et al., 2009; McKenna et al., 2015; Sheline et al., 2010). While tempting to infer that increased connectivity is a negative outcome and an indicator of decline because of the association with at risk populations, this increased connectivity in the DMN has been shown to correlate with improved episodic memory performance in ε4 carriers (Matura et al., 2014). In fact, increased connectivity appears to be a compensatory response to neuronal disruption (Hillary et al., 2015). Interventions that increase the connectivity of the precuneus with the DMN may in fact be increasing the brains ability to compensate to neuronal disruption. Consequently, however, when age increases and AD pathology develops, these carriers may not be able to further compensate and this may explain the increased incidence of AD in APOE-ε4 carriers.

Resting state functional connectivity is a viable method for detecting the neuronal substrates of changes in cognitive abilities across the lifespan and in APOE-ε4 carriers. Simple correlations between hub regions, network level metrics, and node degree have all provided

insights into the brain connections that enhance cognition. Factors that protect or augment these connective properties will aid in preserving the cognitive abilities of our growing older population. In the following sections, evidence that physical activity is a candidate protective factor against detrimental aging effects and alterations in the connectivity patterns of APOE-ε4 carriers is presented.

Section 2.3: Protective Effects of Exercise

Subsection 2.3.1: Evidence for Protection in Healthy Aging

There is accumulating evidence that higher levels of physical activity offer protection against cognitive decline in older adults. Etgen et al. (2010), as part of the prospective cohort INVADE study, published results from 3,903 cognitively intact adults over the age of 55 years. These participants took the 6-Item Cognitive Test cognitive test, similar to the Mini Mental State Exam, at baseline and again two years later. Physical activity (PA) was assessed by simply asking the participants the number of days they participated in strenuous physical activity. The subjects were divided into three PA groups: no PA (no regular PA), moderate PA (less than 3 times per week) and high PA (3 or more times per week). At baseline, 418 participants were classified with cognitive impairment. Across the entire cohort, the risk of developing cognitive impairment was significantly reduced in the high and moderate PA groups as compared to the no PA group (odds ratio[OR] 0.57, 0.37-0.87 95% confidence interval [CI], p = 0.01, and OR, 0.54, 95% CI, 0.35-0.83, p = 0.005, respectively). When further analysis was done on the participants without prodromal phase dementia or cognitive impairment, the reduction was even greater for the high PA and moderate PA groups (OR, 0.44, 95% CI, 0.24-0.83, p = 0.01, and OR, 0.46, 95% CI, 0.25-0.85, p = 0.01, respectively). While the large sample size and measurement of

many cardiovascular health measures added to the strength of this study, conclusions about the mechanisms of this protective effect cannot be addressed. Additionally, while the 6-Item Cognitive Test has been indicated to be sensitive to mild cognitive impairment and correlates well to the Mini Mental State Exam, it is not a comprehensive neuropsychological exam, and specific memory domains and cognitive functions are not measured.

Middleton et al. (2010) found in 9,344 women over the age of 65 who self-reported activity during teenage years had a reduced incidence of cognitive impairment, as defined by 1.5 standard deviations below the age group mean. Additionally, women who reported becoming active later in life also had a lower incidence of cognitive decline than those who remained inactive throughout their life. Thus, the findings indicated that physical activity at any point during the life span reduced the risk of cognitive impairment. Middleton et al. (2011) also used more objective measures of total physical activity to correlate with reduced incidence of cognitive decline. Activity energy expenditure was calculated using doubly labeled water to measure total energy expenditure and indirect calorimetry to measure resting metabolic rate. In the 197 men and women in the study, there was a significantly reduced incidence of cognitive decline in those in the highest tertile of activity expenditure compared to the lowest tertile. Cognitive decline was defined as a reduction of 1 standard deviation on the Mini Mental State Exam at the 2-year or 5-year follow up.

As part of the Canadian Study of Health and Aging, Laurin et al. (2001) found that participants in the 4,615 person sample with a self-report of high or moderate sessions of leisure time activity at least 3 times per week had a reduced risk of Alzheimer's disease compared to those that reported no activity. Scarmeas et al. (2009) found that in a prospective cohort study comprising of 1,880 older adults that were initially cognitively healthy, 282 incidents of

Alzheimer's disease were documented in an average follow up of 5.4(3.3) years. Adherence to a Mediterranean diet and physical activity were independently had a reduced hazard ratio compared to not adhering to the diet or no physical activity. The combination of diet adherence and physical activity also resulted in a lower hazard ratio compared to no diet adherence and no physical activity. Buchman et al. (2012) found total daily physical activity was associated with a reduced incident of Alzheimer's disease in 716 older adults who wore wrist activity monitors and followed for 4 years.

In a review of physical activity studies in cognitively healthy older adults, increases in physical fitness have corresponded to improvements in executive control and cognitive inhibition, but the results were varied in the exact cognitive functions that were improved, and several studies had no significant result (Angevaren, Aufdemkampe, Verhaar, Aleman, & Vanhees, 2008). Despite the fact that consistent cognitive improvements were not observed, the benefit of physical activity extends into the realm of cognitive reserve. The functional definition of cognitive reserve is the ability to effectively recruit brain networks (Habeck et al., 2003; Scarmeas et al., 2003; Stern, 2003; Stern et al., 2005), which suggests PA may be changing the organization of the networks in a protective manner, independent of any behavioral effects on cognition.

The hippocampus is a focus of many research studies attempting to explain the protective effects of PA. Erickson et al. (2011) measured changes in hippocampal volume in a randomized controlled study in 120 older adults. Subjects in the moderate exercise group demonstrated a 2% volume increase in the anterior hippocampus after 12 months of aerobic exercise compared to subjects in the stretching control group. This effectively delayed age-related decline in the hippocampus volume by 1 to 2 years, and the hippocampal volume increase in the exercise group

was correlated with improvement on spatial learning tasks [left hippocampus; $r = 0.23$, $p < 0.05$; right hippocampus: $r = 0.29$, $p < 0.02$]. The spatial learning task consisted of a computerized program requiring the participants to remember the location of one, two, or three black dots on the screen. Subjects with higher initial fitness in the controlled group had an attenuated decline in hippocampal volume compared to the low fitness controlled group members. Pereira et al. (2007) provided a proxy in vivo measurement in rats of exercise induced neurogenesis in the hippocampus by correlating BrdU labeling of neurogenesis with increased cerebral blood volume MRI measurements in the hippocampus. Eleven healthy human subjects, 21 – 44 years old, participated in a 12-week running program and demonstrated similar increases in hippocampal cerebral blood volume. More recently, Kleemeyer et al. (2016) found increased fitness was associated with increased hippocampal volume in older adults. These effects have also been found in middle adulthood (Thomas et al., 2016), and yet six weeks of no aerobic activity was enough time for the hippocampus to return to baseline volumes.

While increased hippocampal volume does induce great excitement as a mechanism for the protection against cognitive decline and AD, few tests have been done to assess the functionality of new neurons in the hippocampus after PA interventions. Additionally, memory engrams are not contained solely in the hippocampus but is spread throughout the cortex and require healthy connections to cortical regions.

As a response to the requirement of healthy connections to serve brain function and higher-level cognition, several recent studies have investigated the connection between WM structure and PA or physical fitness. The fact that evidence suggest WM changes can occur quickly and are accompanied with cognitive improvements (Engvig et al., 2012; Hofstetter, Tavor, Tzur Moryosef, & Assaf, 2013; X. Wang, Casadio, Weber, Mussa-Ivaldi, & Parrish,

2014) is a strong indicator that this may be the mechanism by which physical activity protects against age related cognitive decline and alters resting state brain networks. Oberlin et al. (2016) found VO_{2max}, a measure of cardiorespiratory fitness, was associated with WM microstructure corona radiate, anterior internal capsule, fornix, cingulum, and corpus callosum in two experiments (N = 113, mean age = 66.61, and N = 154, mean age = 65.66). They found higher VO_{2max} correlated with greater FA values in these tracts, and a mediation analyses revealed these tracts established an indirect path between VO_{2max} and spatial working memory performance. While the samples were from randomized controlled exercise intervention trials, only baseline measurements were included in this paper. Additionally, while this study had consistent results across samples, they did not measure APOE-ε4 status. Smith et al. (2016) did investigate the interaction of APOE-ε4 status and physical activity on white matter microstructure in healthy older adults (N = 88, age range = 65 – 89). Interaction of APOE-ε4 status and PA levels (measured using self-report questionnaire) were found in many white matter tracts. In tracts related memory, higher FA and lower RD were associated with greater levels of PA in older adults without the APOE-ε4 allele, but sedentary ε4 positive older adults had higher FA values and lower RD values than the active ε4 positive older adults. The sedentary ε4 positive group had shown decline in episodic memory during a previous 18-month period, yet they had similar directional FA and RD values as the APOE-ε4 negative group that did not show decline.

In a review of fMRI studies investigating PA, WM, and age, Sexton et al. (2016) found that these studies emphasize the between subject variability in WM measures. Reviews on PA's effect on grey matter in the brain consistently show increased volumes in the hippocampal and prefrontal regions (Erickson, Weinstein, & Lopez, 2012), yet the directionality of WM microstructure and locations of these changes are inconsistent (Sexton et al., 2016). A common

interpretation of these inconsistencies in the literature is that DTI measures of WM do not only measure the integrity of the white matter but are also influenced by the directionality of the fibers in each voxel, and that these changes are indicative of unique reorganization of these tracts (Bender et al., 2016; Johansen-Berg, 2012; Sexton et al., 2016; J. C. Smith et al., 2016). The directionality of the white matter fibers and the instance of crossing fibers influence the eigenvectors in each voxel that are used to calculate RD and DA (Wheeler-Kingshott & Cercignani, 2009), and FA is inversely related to RD and DA. The individualistic development of networks influenced by intrinsic and extrinsic factors (example genetics and PA) (Sporns, 2011) make white matter fibers a heterogeneous arrangement. Thus, WM tracts vary across people in their interconnections and crossing fibers, despite having a common primary architecture. In fact, crossing fibers construct 60-90% of voxels in WM (Jeurissen, Leemans, Tournier, Jones, & Sijbers, 2013; Vos, Jones, Jeurissen, Viergever, & Leemans, 2012). The inconsistent findings of PA on DTI measurements of WM do match the network approach to the brain and would be explained by re-organization of the white matter fibers rather than solely due to changes of the myelination. An area that still needs to be addressed is that the development of the networks, and the genetic and environmental influences, PA being the primary environmental variable of interest, on these networks, needs to be studied over the entire lifespan.

Subsection 2.3.2: Protection in Older Adults at Risk for Alzheimer's Disease

Two of the risk factors for AD are a diagnosis of mild cognitive impairment and the APOE-ε4 allele, and several studies have shown PA or exercise training has a protective effect in subjects with these risk factors. MCI is a classification for older adults with memory decline that do not yet meet the criteria for AD (Petersen, 2004; Petersen et al., 1999). Within 5 years 50% of these individuals progress to AD (Gauthier et al., 2006). In 179 subjects meeting the criteria for

MCI, higher physical activity scores reduced the risk of conversion to dementia over an average 2.59 year follow up (Grande et al., 2014). Individuals diagnosed with MCI were also investigated by Smith et al. (2013). Healthy elders and those with MCI (total of 33 subjects) underwent a 12-week walking intervention that improved VO_{2peak} by about 10%. A semantic memory task was performed in the MRI before and after the exercise intervention. Both the healthy elders and the MCI seemed to improve neural efficiency as demonstrated by decreased activation when comparing familiar vs. unfamiliar activations during correct responses. Both groups also improved in trial 1 learning of the RAVLT. In this same sample, increased fitness scores were correlated with increases in cortical thickness (Reiter et al., 2015). In two other intervention studies with similar sample sizes, one study found cognitive improvement only in the women (Baker, Frank, Foster-Schubert, Green, Wilkinson, McTiernan, Plymate, et al., 2010), and the other found no cognitive improvement at all (Miller et al., 2011). These results exemplify what a meta-analysis of random controlled exercise training studies in MCI found – inconsistency in cognitive improvements (Gates, Fiatarone Singh, Sachdev, & Valenzuela, 2013). This does not indicate that the interventions with no cognitive improvements were ineffective, however. It is plausible that unmeasured alterations to networks occurred, despite small or no behavioral changes. The need for functional connectivity studies to be done in MCI with exercise interventions would address this possibility.

The APOE-ε4 allele is a genetic risk factor for sporadic AD (Corder et al., 1993), and evidence is starting to amass that indicate PA has a strong protective effect in individuals with this particular allele (J. C. Smith, K. A. Nielson, J. L. Woodard, et al., 2013). Woodard et al. (2012) conducted a longitudinal study investigating the interactive effects of cognitive activity, hippocampal volume, APOE status, and physical activity levels on cognitive decline. Cognitive

decline was defined as one standard deviation below a baseline measurement on the Dementia Rating Scale (a measure of global cognitive functioning), or the Rey Auditory Learning Test Immediate Recall or Delayed Recall (a measure of learning capacity and episodic memory). Hippocampal volume, APOE status, self-reported cognitive activity (such as creative writing or reading), and self-reported physical activity were collected at baseline, and after 18 months, neuropsychological testing was repeated. The researchers found a significant interaction effect of APOE-ε4 status and physical activity levels in predicting cognitive decline. Subjects with the APOE-ε4 allele and low physical activity had a higher likelihood of cognitive decline than subjects with the APOE-ε4 allele and high physical activity. Interestingly, reported cognitive activities did not predict decline nor interact with PA or APOE genotype. Schuit et al. (Schuit, Feskens, Launer, & Kromhout, 2001) followed 560 Dutch men over 3 years, and the odds ratio for cognitive decline was greater for APOE-ε4 carriers compared to non-carriers [OR: 3.7, 95% CI: 1.1–12.6]. However, in the APOE-ε4 group, higher self-reported levels of PA greatly decreased the odds ratio compared to carriers with lower levels of self-reported PA [active carriers as reference group, OR:3.9, 95% CI: 1.2–12.9].

In unique studies investigating the interaction of self-reported PA and the APOE on fMRI semantic memory activation(J. C. Smith et al., 2011) and hippocampal volume changes in cognitively healthy older adults (J. C. Smith et al., 2014), subjects were classified by their genotype (High Risk – having at least one ε4 allele) and by their PA (High PA, leisure time physical activities 3 or more times per week). The High Risk/High PA group had the greatest activation during the semantic name task, and these activations appear to be protective. After 18 months, the Low Risk (both high and low PA) maintained hippocampal volume, as well as the High Risk/High PA subjects. However, the High Risk/Low PA group decreased hippocampal

volume by 3%. Head et al. (2012) also investigated the interaction between PA and APOE status in cognitively healthy older adults. Subjects with the APOE-ε4 allele positive or negative were classified as high or low PA using self-report. While overall the ε4 positive subjects had higher amyloid burden (part of the AD pathology) as measured by PiB-PET than the ε4 negative subjects, it was the low PA ε4 positive subjects that had the highest burden. There was no effect of PA on amyloid burden in the ε4 allele negative group. Again, while low PA did not have an adverse effect on subjects without the APOE-ε4 allele, high PA did have a positive protective effect on the APOE-ε4 allele carriers. Both studies provide evidence that PA may be most beneficial for those who are at genetic risk for AD.

Section 2.4: Evidence for Physical Activity Protecting Resting State Networks

Subsection 2.4.1: Young Adults

Young adults are often used as a control for older adults in functional connectivity studies, but very few have inspected the relationship between PA and network connectivity in young adults. Kamijo et al. (2010) looked at the connectivity within the executive function network in 20 sedentary and 20 active young adults (mean age =21.2) during an executive control task. Phase locked synchrony (PLV) between 19 electrodes was calculated to determine strength of connectivity, and the strength of the PLV was stronger in the active group at the 300-400ms time epoch. In a study comparing seed based connectivity in the FPN and DMN of collegiate male runners and healthy non-athlete controls, several connections in the FPN were stronger in the athlete group (Raichlen et al., 2016). These results were due to positive correlations in the athlete group between the right parietal region FPN seed and the middle/superior frontal regions and correlations not different from zero in the non-athlete

controls, as well as strong positive correlations in the athlete group between the left anterior region FPN seed and the superior/mid frontal regions and anticorrelations in the control group. In the DMN, there were anti-correlations of DMN seeds with clusters in motor control, somatosensory, and visual networks in the athlete group that were not present in the control group. The anti-correlation of the DMN with task-positive regions has been associated with improved cognitive performance (Guerra-Carrillo, Mackey, & Bunge, 2014). The conclusion of the authors of the male collegiate athlete /non-athlete connectivity study is that the co-activation of brain regions during endurance running enhances the connectivity of resting state networks that may explain the protection of physical activity against cognitive decline in older adults.

Subsection 2.4.2: Middle Aged Adults

A database search did not result in any findings investigating the effects of PA on resting state networks in middle-aged adults. Yet, the development of networks is throughout the entire lifespan, and plasticity during middle age will affect the plasticity of the older brain. Research investigating how PA influences resting state networks in this period before the onset of age related cognitive decline is of utmost importance in understanding how the healthy brain functions.

Subsection 2.4.3: Healthy Elders

The literature on the effects of PA on resting state networks in healthy older adults is more expansive and yields promising results. Burdette et al. (2010) conducted a four month exercise intervention in older adults with a control group learning about healthy aging (age 70-85 years, total n =11). Resting state connectivity was measured using node degree and modularity calculated from a voxel level binary connectivity matrix. Hubs were defined as being in the top

15% of node degree, and hubs were found in the hippocampus of the exercise group while this was not the case in the control group. When whole brain metrics were used, no differences were found between groups (Burdette et al., 2010). The small sample size may be the reason differences were not detected at the whole brain network measurements level.

Voss et al. (2010) conducted a randomized one-year exercise intervention in older adults (walking group: mean age = 67.3, n = 30; control group: mean age = 65.4, n = 35), with a young adult control group (mean age = 23.9 , n=32). Functional connectivity was measured as the strengths of the z-transformed correlation of time-series between ROI's in networks shown to be disrupted in aging. Several regions in the DMN and fronto-executive network were stronger in the walking group compared to older adult controls. Network metrics were not measured in this study.

Boraxbekk et al. (2016) analyzed functional connectivity changes over the course of 10 years as part of the Betula prospective cohort study. Subjects used in this study had current and accumulated physical activity (as indexed from BMI, waist circumference, pulse, blood pressure,and maximum grip strength) and resting state scans (n = 196, age range = 25 – 80). The results showed PA was associated with increased functional voxel wise connectivity of the PCC, a hub of the DMN that is disrupted with age and connected with age related cognitive decline. While the variables for the PA index score have been associated with PA, the levels of PA for the individuals in this study were not directly measured.

A review of PA studies and brain networks consistently found increased connectivity in fronto-executive networks and the DMN in older adults (P. Huang, Fang, Li, & Chen, 2016), but there were few additional studies included other than those mentioned above.

Subsection 2.4.4: Adults with MCI

While studies have indicated that PA delays the conversion of MCI to AD, there is very limited research investigating changes in functional connectivity due to PA in adults with MCI. Klados et al. (2016) used resting state electroencephalogram (EEG) to measure of strength of node connectivity before and after a randomized combined cognitive and physical training in older adults (n = 25 in each group, mean age = 68.8) meeting MCI criteria. Connectivity was measured using the square of the magnitude of coherence between the node signals, and node strength was calculated as the sum of the edges weights. After the intervention, more bilateral connections were found in the combined group compared to the controls in parietal, prefrontal, occipital, and temporal regions.

Seed based results that were obtained from data collected in our laboratory have indicated increased connectivity of the PCC, a hub of the DMN, with frontal and parietal regions after a 12-week walking intervention in healthy older adults and in those with MCI (Smith et al., in review). The paper is included in Appendix A of this proposal. The conclusion of this paper was that the walking intervention increased the ability of the PCC to recruit frontal and parietal brain regions, which may reflect enhanced compensation. This increased recruitment may indicate more cognitive reserve, and thus may explain PA's role in reducing the incidence of cognitive decline.

Section 2.5: What is missing in the literature?

There is an utmost need to understand how the healthy brain functions and adapts to the aging process. This will aid in the effort to preserve cognitive function in the increasing proportion of elderly persons in our global population and inform treatment research for neurological diseases, such as AD. Despite the evidence that PA protects cognition, very few

studies have been done investigating the effects of PA on brain networks in older adults and minimal studies in young adults. Middle adulthood, as the preceding stage of older adulthood, will continue to lay the formation of networks in the brain and will influence the plasticity of these networks as older adults. The effects of PA on the networks disrupted by the aging process need to be studied at all stages. Additionally, despite the literature demonstration that carriers of the APOE-ε4 allele have disrupted networks similar to the changes observed in aging and AD before non-carriers, there has not been research to illuminate the interactive effects of PA and APOE-ε4 allele on these networks. The overarching goal of the dissertation research was to begin the research to fill in these gaps. We expected in to find that PA increased the integration of networks and the node strength of the hubs of these networks, and the strongest effects would be found in APOE-ε4 carriers. While not testable with methods and data available, it is plausible that the underlying cause of these effects of PA are the protection of the white matter tracts in the fronto-striatal circuit that are so disrupted in aging. It is through the preservation and enhancement of these white matter connections that counteract the age-related decline in cognition and increase the cognitive reserve that delays symptomology when AD pathologies have begun.

Chapter 3: Published Study: Exercise Training and Functional Connectivity Changes in MCI and Healthy Elders

Exercise Training and Functional Connectivity Changes in MCI and Healthy Elders

Published in Journal of Alzheimer's Disease, Vol 57 (2017)

Theresa J. Chirles[a], Katherine Reiter[b], Lauren R. Weiss[a], Alfonso J. Alfini[a], Kristy A. Nielson[b, c], & J. Carson Smith*[a]

[a] University of Maryland, College Park, Maryland

[b] Marquette University, Milwaukee, Wisconsin

[c] Medical College of Wisconsin, Milwaukee, Wisconsin

*Corresponding Author: J. Carson Smith, PhD

Address: Department of Kinesiology, 2351 SPH Bldg #255, College Park, MD, 20742

Telephone: 301-405-0344

Fax: 301-405-5578

Email: carson@umd.edu

Keywords: Alzheimer's disease, connectivity, cognitive disorders, aging, default mode network, posterior cingulate, precuneus, exercise interventions, resting state fMRI.

Section 3.1: Abstract

Background: Effective interventions are needed to improve brain function in Mild Cognitive Impairment (MCI), an early stage of Alzheimer's disease (AD). The posterior cingulate cortex (PCC)/precuneus is a hub of the Default Mode Network (DMN) and is preferentially vulnerable to disruption of functional connectivity in MCI and AD.

Objective: We investigated whether 12 weeks of aerobic exercise could enhance functional connectivity of the PCC/precuneus in MCI and healthy elders.

Methods: Sixteen MCI and 16 healthy elders (age range = 60-88) engaged in a supervised 12-week walking exercise intervention. Functional MRI (fMRI) was acquired at rest; the PCC/precuneus was used as a seed for correlated brain activity maps.

Results: A linear mixed effects model revealed a significant interaction in the right parietal lobe: the MCI group showed increased connectivity while the healthy elders showed decreased connectivity. In addition, both groups showed increased connectivity with the left postcentral gyrus. Comparing pre to post intervention changes within each group, the MCI group showed increased connectivity in 10 regions spanning frontal, parietal, temporal and insular lobes and the cerebellum. Healthy elders did not demonstrate any significant connectivity changes.

Conclusion: The observed results show increased functional connectivity of the PCC/precuneus in individuals with MCI after 12 weeks of moderate intensity walking exercise training. The protective effects of exercise training on cognition may be realized through the enhancement of neural recruitment mechanisms, which may possibly increase cognitive reserve. Whether these effects of exercise training may delay further cognitive decline in patients diagnosed with MCI remains to be demonstrated.

Section 3.2: Introduction

Neuropathological changes associated with Alzheimer's disease (AD) occur many years before the onset of clinical symptoms (Jack et al., 2010). Older adults who have declined cognitively but who do not meet criteria for a diagnosis of AD are often classified as having Mild Cognitive Impairment (MCI) (Petersen, 2004; Petersen et al., 1999), and more than half of these individuals progress to an AD diagnosis within five years (Gauthier et al., 2006). There is an urgency to identify biomarkers for preclinical detection of neuropathology prior to the onset of symptoms in order to inform treatment strategies and to aid in the understanding of AD progression (Pievani, de Haan, Wu, Seeley, & Frisoni, 2011). Resting state functional connectivity is emerging as a viable biomarker and predictor of future conversion to AD (Albert et al., 2011; M. Greicius, 2008; Pievani, Filippini, van den Heuvel, Cappa, & Frisoni, 2014; Yamasaki, Muranaka, Kaseda, Mimori, & Tobimatsu, 2012) and as an indicator of treatment efficacy (Goveas et al., 2011; Li et al., 2012).

Resting state functional connectivity in this paper is based on the correlations of spontaneous blood oxygenation level-dependent (BOLD) functional magnetic resonance imaging (fMRI) signals during the absence of an external task. It is assumed to reflect the underlying anatomy of the neuronal architecture (Buckner et al., 2009) through direct and indirect neural networks consisting of monosynaptic and polysynaptic connections (Allen et al., 2005; Vincent, Kahn, Snyder, Raichle, & Buckner, 2008; Vincent et al., 2007). Temporal correlations of spatially distinct brain regions indicate either direct or indirect neuronal connections, and resting state functional connectivity has been found to predict performance on higher order cognitive tests (Andrews-Hanna et al., 2007; L. Wang, Laviolette, et al., 2010; L. Wang, Negreira, et al., 2010). Higher order cognitive processes require the integration of several segregated, domain-specific neural processing pathways (Buckner et al., 2009), and these diverse pathways intersect

in regions of the brain called ‘hubs’, characterized by a disproportionately high number of functional, and often concurrently anatomical, connections (O. Sporns, Honey, & Kötter, 2007). These hubs, while few in number, may limit the large metabolic cost of neural communication by integrating otherwise disparate networks (Bassett & Bullmore, 2006) and play an important role in information flow (Power, Fair, Schlaggar, & Petersen, 2010). The posterior cingulate (PCC) and precuneus regions together constitute a key hub of the default mode network (DMN). This hub fosters efficient communication between the DMN and the medial temporal lobe (MTL) network, a network with an important role in memory processes (Alvarez & Squire, 1994) that is highly vulnerable to AD pathology (Albert, 2011). The PCC/precuneus is also an area associated with the accumulation of amyloid-β (Aβ) plaque, a hallmark of AD pathology (Buckner et al., 2009). The PCC/precuneus exhibits reduced functional connectivity in MCI, early AD (M. D. Greicius & Menon, 2004; Zhou et al., 2008), and in clinically normal older adults that test positive for brain amyloid burden (Drzezga et al., 2011; Hedden et al., 2009). Changes in the functional connectivity of the PCC/precuneus have also been associated with accelerated atrophy and other preclinical pathological changes associated with AD (Buckner et al., 2005; C. Huang, Wahlund, Svensson, Winblad, & Julin, 2002; Zhou et al., 2008), underscoring its potential role as a predictive biomarker. Thus, alterations in resting state functional connectivity, while concurrently associated with cognitive decline, may also precede measureable cognitive changes.

Prior to evidence of cognitive decline in AD, the PCC/precuneus exhibits increased connectivity with frontal and parietal brain regions that do not show AD pathology until very late disease stages (Zhang et al., 2009), and there is growing evidence that increased recruitment of these frontal regions in older adults is a compensatory response to aging (Buckner, 2004).

Although this compensatory response is associated with neuronal damage (Hillary et al., 2015), it is also thought to be indicative of maintaining cognitive function (Reuter-Lorenz & Park, 2010, 2014). In individuals diagnosed with MCI and AD, declines in connectivity have been noted in brain areas affected early in the progression of AD, such as the MTL (Albert, 2011). Interventions or treatments that preserve and/or increase the connectivity of the PCC/precuneus with available frontal and parietal resources in older adults may help promote cognitive stability.

It is well established that both leisure time physical activity and exercise training help to improve and maintain cognitive function in healthy older adults (Cotman & Berchtold, 2002; Kramer, Erickson, & Colcombe, 2006), even in those at increased risk for AD (Gates et al., 2013; Heyn, Abreu, & Ottenbacher, 2004; J. C. Smith, K. A. Nielson, J. L. Woodard, et al., 2013; Woodard et al., 2012). Aerobic training in healthy elders appears to increase the functional connectivity within the DMN (Voss et al., 2010) and hippocampal networks (Burdette et al., 2010). Furthermore, although local neuronal networks exhibit deterioration in healthy elders, high levels of physical activity have been shown to protect these networks (Heisz, Gould, & McIntosh, 2015). Exercise training in individuals diagnosed with MCI has been shown to improve cognition (Baker, Frank, Foster-Schubert, Green, Wilkinson, McTiernan, Plymate, et al., 2010; Gauthier et al., 2006; Lautenschlager et al., 2008; J. C. Smith, K. A. Nielson, P. Antuono, et al., 2013) and increase neuronal efficiency during a semantic memory retrieval task (J. C. Smith, K. A. Nielson, P. Antuono, et al., 2013), but it is not known if exercise training results in changes to neural network functional connectivity in older adults diagnosed with MCI. If exercise training does increase the connectivity of hubs enhancing network recruitment in this population, it may indicate a gain of cognitive reserve that would help to preserve cognitive abilities and possibly delay cognitive decline. Cognitive reserve is a concept that explains the

typically nonlinear relationship between cognitive performance and neuronal damage or brain disruption (Buckner, 2004), and is associated with the ability to recruit additional brain networks when the primary networks are disrupted (Stern, 2009) as in MCI. Greater levels of cognitive reserve proxies, such as education, have been associated with increased functional connectivity (Arenaza-Urquijo et al., 2013), and physical activity (PA) also has been implicated as one of the factors that increases cognitive reserve (Fratiglioni et al., 2004).

The current study extends this literature with evidence that aerobic exercise training may stimulate functional connectivity of the PCC/precuneus in individuals diagnosed with MCI. This is a continuation of our previously published paper that reported a 12-week walking intervention resulted in decreased fMRI activation in several cortical regions during a semantic memory-related task (J. C. Smith, K. A. Nielson, P. Antuono, et al., 2013). We hypothesized that healthy elders and individuals diagnosed with MCI would demonstrate *increased* connectivity between the PCC/precuneus and frontal-parietal cortices from before to after the intervention, indicating enhanced network recruitment capabilities. We expected increased connectivity to the MTL in the MCI group, as the MTL is particularly vulnerable to AD progression (Albert, 2011).

Section 3.3: Material and Methods

Participants and pre-screening

This study used resting state fMRI data from participants (17 MCI and 18 healthy elders) described in previous work (J. C. Smith, K. A. Nielson, P. Antuono, et al., 2013), except that resting state fMRI data were missing for one MCI and two healthy elder participants. Community dwelling older adults, ages 60 to 88, were recruited through physician referrals, local newspaper advertisements, and in-person informational sessions at retirement communities and recreational centers. Interested volunteers who were still eligible after a phone interview met

face-to-face with a study team member to review all procedures, expectations, possible risks, and a physician approval form for moderate intensity exercise was obtained. A neurological evaluation completed the eligibility evaluation. Informed consent was obtained from all individual participants included in the study. All procedures were in accordance with the ethical standards of the institutional and/or national research committee and with the 1964 Helsinki declaration and its later amendments or comparable ethical standards.

Inclusion and exclusion criteria

In order to maximize the effect of exercise training, all study participants indicated they engaged in only light physical activity two or fewer days/week for the past six months. Participants were excluded if they reported a history or evidence of: 1) medical illnesses or conditions that may affect brain function (including glaucoma, chronic obstructive pulmonary disease, and untreated hypertension); 2) neurological illnesses or conditions (including cerebral ischemia, vascular headache, head trauma with loss of consciousness (>30 min), epilepsy, carotid artery disease, cerebral palsy, brain tumor, normal-pressure hydrocephalus, chronic meningitis, pernicious anemia, multiple sclerosis, Huntington's disease, Parkinson's disease or HIV infection); 3) current untreated Axis I psychiatric disturbance meeting DSM-IV Axis I criteria (including substance abuse or dependence and severe depressive symptoms); 4) exclusion criteria specific to MR scanning (such as pregnancy, history of claustrophobia, weight inappropriate for height, and ferrous objects within the body); 5) any unstable or severe cardiovascular disease or asthmatic condition; 6) left-handedness (laterality quotient [LQ] <50) (Oldfield, 1971); 6) current use of psychoactive medications, except stable doses of antidepressants; and 7) history of transient ischemic attack or >4 on the modified Hachinski ischemic scale. Participants were also excluded if they scored >15 on the Geriatric Depression

Scale (GDS) (Yesavage, 1988) or showed relatively impaired activities of daily living (ADL) using the Lawton and Brody Self-Maintaining and Instrumental Activities of Daily Living Scale.

Neuropsychological test battery and clinical criteria for MCI

The Neuropsychological test battery included the Mini-Mental State Exam (Folstein, Folstein, & McHugh, 1975), Mattis Dementia Rating Scale-2 (DRS) (Jurica, Leitten, & Mattis, 2001), Rey Auditory Verbal Learning Test (AVLT) (Rey, 1964), Logical Memory and Letter-Number Sequencing subtests of the Wechsler memory Scale-III (Wechsler, 1997), Symbol-Digit Modalities Test (A. Smith, 1991), Controlled Oral Word Association Test (Benton & Hamsher, 1978), animal fluency, and the Clock Drawing Test (Cosentino, Jefferson, Chute, Kaplan, & Libon, 2004). This comprehensive battery was administered before and after the exercise intervention, and alternate forms of the AVLT and DRS were used at each testing session.

Cognitive status of the participants was determined using the core clinical criteria set by the NIH-Alzheimer's association workgroup on MCI due to AD (Albert et al., 2011). MCI was defined as a subjective concern regarding a change in cognition supported by an informant, impairment in one or more cognitive domains (defined as 1.5 standard deviations below age and education matched means on delayed recall on the AVLT), and intact activities of daily living. Three neuropsychologists (including K.A.N.) reached a consensus on impairment. A neurologist ruled out all other possible etiologies. Healthy elders had no specific cognitive complaint, intact cognitive performance in all domains, and intact activities of daily living.

Exercise test

Participants completed a submaximal exercise test on a motorized treadmill (General Electric, Milwaukee, WI) to estimate peak aerobic capacity ($\dot{V}O_{2peak}$) before and after the exercise intervention. The exercise test used a modified Balke-Ware protocol of 2.0 miles/hr

beginning with a 0^0 grade and increasing 1^0 per minute (American College of Sports Medicine, 2010). Concentrations of oxygen and carbon dioxide in expired air were collected every 15 seconds by a metabolic measurement system (ParvoMedics, Sandy, UT). Each test included measurements of heart rate, blood pressure (every 2 minutes), and ratings of perceived exertion (RPE; each minute). Test termination criteria included reaching 85% of age-predicted heart rate max, a diastolic blood pressure greater than 110 mmHg, or the participant's desire to stop. The peak rate of oxygen uptake ($\dot{V}O_{2peak}$) was estimated from the highest $\dot{V}O_2$ value achieved during the test (expressed as ml/kg/min at STPD) (American College of Sports Medicine, 2010). Additional details have been described by Smith et al. (2013).

Exercise intervention

A qualified personal fitness trainer or an exercise physiologist supervised the participants in the 12-week intervention at fitness centers located near the participants' homes or within their communities. The exercise intensity, session duration, and weekly frequency were increased during the first four weeks until the participants were walking for 30 minutes, four times a week, at approximately 50-60% of HRR (heart rate reserve). Each session began and ended with 10 minutes of light walking and flexibility exercises. Participants wore a Polar® heart rate monitor and provided subjective RPE's using the Borg 6-20 RPE scale throughout each exercise session at minutes 5, 15, and 30 (Borg, 1998; Cook, O'Connor, Eubanks, Smith, & Lee, 1997). The treadmill grade and/or speed were modified to moderately challenge the participant based on the heart rate and perception of effort (not more than 15 on the Borg scale). This is considered a moderate intensity exercise for older adults (Mazzeo & Tanaka, 2001).

MRI acquisition procedures

Prior to the first MRI acquisition using a General Electric (Waukesha, WI) 3.0 Tesla scanner, participants were familiarized with the MRI environment by lying in a mock scanner. During MRI acquisition, participants were instructed to lie as still as possible and foam padding was used to limit movement and improve comfort. Anatomical and resting state sequences were run during the scanning session. High-resolution, three-dimensional spoiled gradient-recalled at steady-state (SPGR) anatomic images were acquired (TE = 3.9ms; TR = 9.6ms; inversion recovery (IR) preparation time = 450ms; flip angle = 12°; number of excitations (NEX) = 1; slice thickness = 1.0mm; FOV = 240mm; resolution = 256 x 224). During the resting state scan, participants were instructed to keep their eyes open and to look at a fixation cross. A gradient-echo, echo-planar pulse sequence sensitive to blood oxygenation level-dependent (BOLD) contrast were acquired (TE = 25ms; TR = 2000ms; flip angle = 77°; NEX = 1; 36 axial slices; 4.0 mm isotropic voxels; FOV = 240mm; resolution = 64 x 64; duration 6 minutes).

MRI preprocessing

Preprocessing steps were done using tools from the Analysis of Functional NeuroImages (AFNI) software package (Cox, 1996). During the initial preprocessing and analysis, the researcher (TC) was blind to each participant's group classification. Time series and anatomical images were aligned and skull-stripping, slice time correction, and motion correction procedures were performed. The first 3 TRs were removed, a 0.005 to 0.10 Hz bandpass filter was applied, and the following sources of noise were regressed out: six-parameter rigid body head motion, ventricle signal, white matter signal, mean global signal, and the derivatives of the motion parameters, white matter signal, and ventricle signal. The time series data were smoothed using

a 4mm full-width at half-maximum Gaussian blur and normalized to Montreal Neurological Institute (MNI) space.

Seed based analysis

The seed based analysis was also conducted using AFNI. The seed region of interest (ROI) was defined using a 5mm spherical mask surrounding the MNI coordinates -2, -50, 36, the peak voxel coordinates of the PCC/precuneus reported by Buckner and colleagues (Buckner et al., 2009). The time course in the ROI was extracted, and seed correlation maps for all participants at each testing session were formed by correlating the seed ROI with all other voxels in the brain. A Fisher's r to z transformation was implemented to normalize the correlation coefficients. Group and Time differences were analyzed using linear mixed effects (G. Chen, Saad, Britton, Pine, & Cox, 2013) and cluster-based analysis (after interpolation to 2 mm^3 voxels, 105 voxels or more with primary threshold = 0.01; cluster-based statistic $p < 0.05$, FWER controlled). This allows for sensitivity (minimizing Type II errors), while maintaining some spatial specificity. The AFNI 3dLME command was used to run the linear mixed effects model using age as a covariate. This is an ideal analysis for repeated measures analyses because it allows for random intercepts; thus initial variability in the correlations are taken into account. F-statistics indicate main effects and interactions, and we also conducted post hoc paired sample t-tests within each group to assess changes from baseline to post-intervention.

Section 3.4: Results

Participant and baseline characteristics

Usable resting state fMRI data were available for 16 healthy elders and 16 participants diagnosed with MCI. As shown in Table 1, the healthy elders and individuals diagnosed with MCI did not significantly differ in sex, age, education, depression or activities of daily living.

As expected, the MCI group exhibited poorer baseline performance than the healthy group on all but two neuropsychological subtests (DRS Attention and DRS Construction). Participants' baseline characteristics are presented in *Table 1*.

Table 1. Demographic data and baseline characteristics of the participants diagnosed with mild cognitive impairment (MCI) and the healthy elders (HE).

Table 2: Demographic Data and Baseline Characteristics of Published Study.

Variables	**MCI (n=16) Mean (SD)**	**HE (n=16) Mean (SD)**	**Group Difference p-value**
Demographics			
Age (y)	79.6 (6.8)	76.1 (7.2)	0.167
Education (y)	15.6 (3.1)	16.6 (2.1)	0.322
Sex*	6M, 10F	3M, 13F	0.238
Depression Symptoms and Activities of Daily Living			
GDS	4.9 (4.1)	3.8 (2.8)	0.386
Lawton ADL	4.7 (0.5)	4.8 (0.5)	0.705
Neuropsychological Testing			
Logical Memory IR	27.1 (12.7)	43.1 (6.6)	<0.001
Logical Memory DR	15.9 (10.4)	25.9 (5.8)	0.002
Logical Memory Recognition	22.9 (3.7)	26.0 (1.8)	0.005
DRS Total	128.1 (13.3)	140.3 (2.5)	0.001
LNS Total	6.9 (2.7)	9.4 (1.9)	0.005
BDS	17.1 (2.1)	18.8 (0.5)	0.004
COWS FAS	29.8 (12.1)	41.9 (9.4)	0.003
Category Fluency - Animals	12.4 (6.5)	20.4 (4.2)	<0.001
Clock Drawing Test	2.6 (1.2)	1.4 (0.9)	0.003

Logical Memory, Wechsler Memory Scale-III subtest: IR, immediate recall; DR, delayed recall; DRS, Mattis Dementia Rating Scale-2; LNS, Wechsler Adult Intelligence Scale-III Letter Number Sequencing; BDS, Behavioral Dyscontrol Scale; COWA, Controlled Oral Word Association Test; GDS, Geriatric Depression Scale (scores were available for 14 MCI, 15 HE); ADL, activities of daily living. *p-value based on chi-sq.

Exercise intervention fidelity

The mean (SD) number of exercise sessions attended, adherence rate, exercise intensity and perceived exertion over the first 4 weeks and during weeks 5-12 of the intervention did not differ between groups. Out of a total of 44 sessions, 42.3 (2.2) were completed resulting in a 96.1 (5.0) % adherence rate. During weeks 1-4 and weeks 5-12, the mean intensity was 46.9 (7.1) %HRR and 54.7 (11.0) %HRR, respectively. RPEs were most closely associated with the verbal descriptor "light" at 10.6 (1.8) and 10.8 (2.0) during the first 4 weeks and last 8 weeks, respectively. There was also a mean increase over the 12-week intervention in $\dot{V}O_{2peak}$ by 2.0ml/kg/min – an approximate 10.6% increase in cardiorespiratory fitness. More details regarding the change in cardiorespiratory fitness can be found in Smith et al. (2013).

Neuropsychological test performance

Neuropsychological test results for the entire sample (35 participants) have been previously reported (J. C. Smith, K. A. Nielson, P. Antuono, et al., 2013). The results reported here are consistent with those reported by Smith et al. (2013), and reflect the slightly smaller sample size (32 participants) in the current study. A repeated measures ANOVA revealed a significant effect of Time in Trial 1 of AVLT ($p = .013$), where both groups demonstrated improvement from baseline to post-intervention (mean (SD): MCI pre: 3.75 (2.02), MCI post: 4.81 (1.97)); healthy elders pre: 5.50 (2.00) healthy elders post: 6.38 (1.57)). The Group by Time interaction for Trial 1 was not significant ($p = 0.800$), and there were no significant changes in the other Rey AVLT indices.

Seed based functional connectivity: Group by Time interaction

Connectivity results are based on the correlation maps of the mean BOLD time course from the PCC/precuneus seed ROI and the remaining voxels in the brain. One significant Group

by Time interaction was observed and is presented in *Figure 1A* and *Table 2*. The MCI group showed an increased correlation between the PCC/precuneus and right inferior parietal lobe (IPL). The healthy elders showed a decreased correlation with the cluster in the right IPL.

Seed based functional connectivity: Time main effects

A Time main effect, reflecting significant changes from before to after the intervention on average collapsed across both groups, was found in the left postcentral gyrus. There was an increased correlation of the PCC/precuneus with this cluster, and the region is presented in *Figure 1B* and *Table 2.*

Table 2. Regions that showed a significant Group by Time interaction and Time main effect for functional connectivity changes with the PCC/Precuneus from before to after a 12-week exercise training intervention in older adults diagnosed with mild cognitive impairment (MCI; n = 16) and healthy elders (HE; n = 16).

Table 3: Regions that Showed a Significant Group by Time Interaction and Time Main Effect in Published Study.

Region	**BA**	**k**	**Peak Voxel**			**F**	**MCI**		**HE**	
			x	**y**	**z**		**Pre (r)**	**Post (r)**	**Pre (r)**	**Post (r)**
Group by Time interactions										
Parietal Lobe										
R IPL	39	110	48	-70	38	36.66	0.31[a]	0.46[a]	0.49[b]	0.28[b]
Time main effects										
Parietal Lobe										
L Postcentral Gyrus	40	213	-44	-34	50	24.77	0.01	0.12	-0.14	0.01

Common superscript within region indicates significant difference, $p<0.01$. BA: Brodmann Area; k: cluster size; r and F: correlation and statistic of the peak, respectively; MCI: mild cognitive impairment; HE: healthy elders; L: left hemisphere; R: right hemisphere; IPL: inferior parietal lobule. xyz: MNI coordinates. Pre indicates baseline; Post indicates after exercise intervention. Shown in *Figure 1.*

Figure 1: Group by time interactions and main effects of time for functional connectivity of the PCC/precuneus in response to a 12-week walking exercise intervention in older adults diagnosed with mild cognitive impairment and healthy elders.

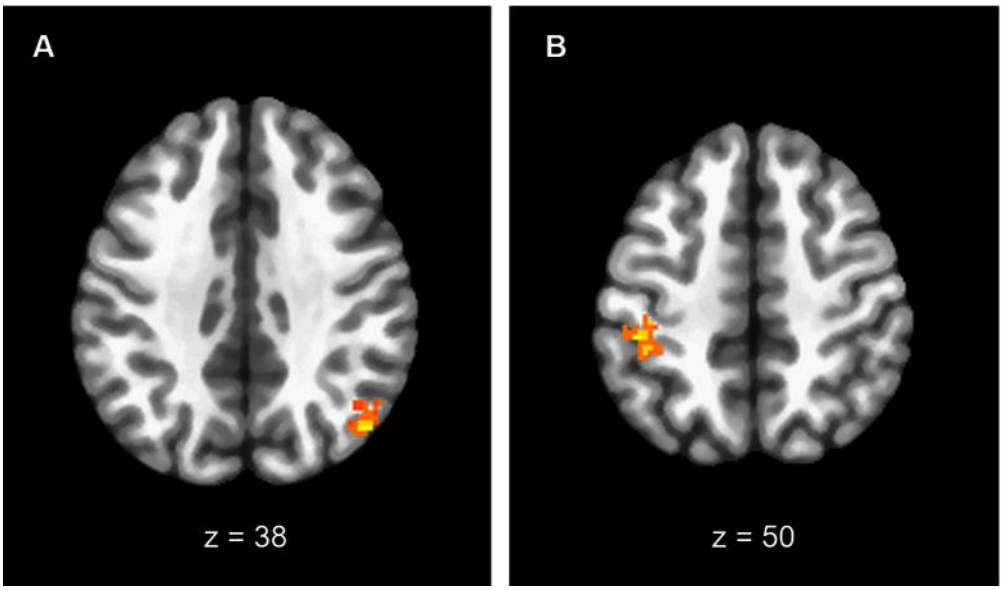

Statistically significant (family-wise error corrected, $p < .05$) Group by Time interactions and main effects of Time for functional connectivity of the PCC/precuneus in response to a 12-week walking exercise intervention in older adults diagnosed with mild cognitive impairment (MCI; n = 16) and healthy elders (HE; n = 16). The mean correlation coefficients, MNI coordinates, and cluster size for each region are shown in Table 2. Panel A: A significant Group by Time interaction was found in the right inferior parietal lobule (IPL), where functional connectivity with the PCC/precuneus increased after exercise training in the MCI group and decreased in the HE group. Panel B: Functional connectivity significantly increased between the PCC/precuneus and the postcentral gyrus after exercise training in both the MCI and HE groups.

Seed based functional connectivity: Post-hoc t-tests: Changes within each group

Significant changes in the MCI group are identified in *Table 3* and *Figure 2A.* The MCI group exhibited increased correlations after the exercise intervention in ten regions. Clusters had

peak voxels in the right MFG, superior frontal gyrus, postcentral gyrus, PHG, and claustrum. Clusters were also found in the left IPL and bilateral precentral gyrus (two clusters in the left precentral gryrus) and culmen. No significant clusters demonstrating changes in connectivity across time were found in the healthy elders group.

Table 3. Regions that showed a significant change in functional connectivity with the PCC/precuneus from before to after a 12-week exercise training intervention in older adults diagnosed with mild cognitive impairment (MCI; n = 16).

Table 4: Regions that Showed a Significant Change in Functional Connectivity with the PCC/precuneus in Published Study.

Region	BA	k	x	y	z	t-statistic
MCIpost>MCIpre						
Frontal Lobe						
R Middle Frontal Gyrus	6	187	30	-4	64	4.41
R Precentral Gyrus	6	193	48	-4	38	5.00
R Superior Frontal Gyrus	10	170	32	56	2	4.87
L Precentral Gyrus	6	177	-24	-16	74	4.59
	6	147	-44	-12	32	4.43
Parietal Lobe						
R Postcentral Gyrus	3	215	48	-22	44	4.74
L IPL	40	167	-50	-34	46	3.93
Temporal Lobe						
R PHG	30	139	12	-48	2	3.94
Insular Lobe						
R Claustrum	13	128	36	-2	4	4.33
Cerebellum						
L Culmen		173	-32	-48	-36	4.83

BA: Brodmann Area including the peak voxel; k: cluster size; xyz: peak voxel MNI coordinates; MCI: mild cognitive impairment. L: left hemisphere; R: right hemisphere; IPL: inferior parietal lobule; HP: hippocampus; PHG: parahippocampal gyrus. Pre indicates baseline; Post indicates after exercise intervention. Shown in *Figure 2.*

Figure 2: Resting state functional connectivity changes with the PCC/precuneus seed region in response to a 12-week walking exercise intervention in older adults diagnosed with MCI and healthy elders.

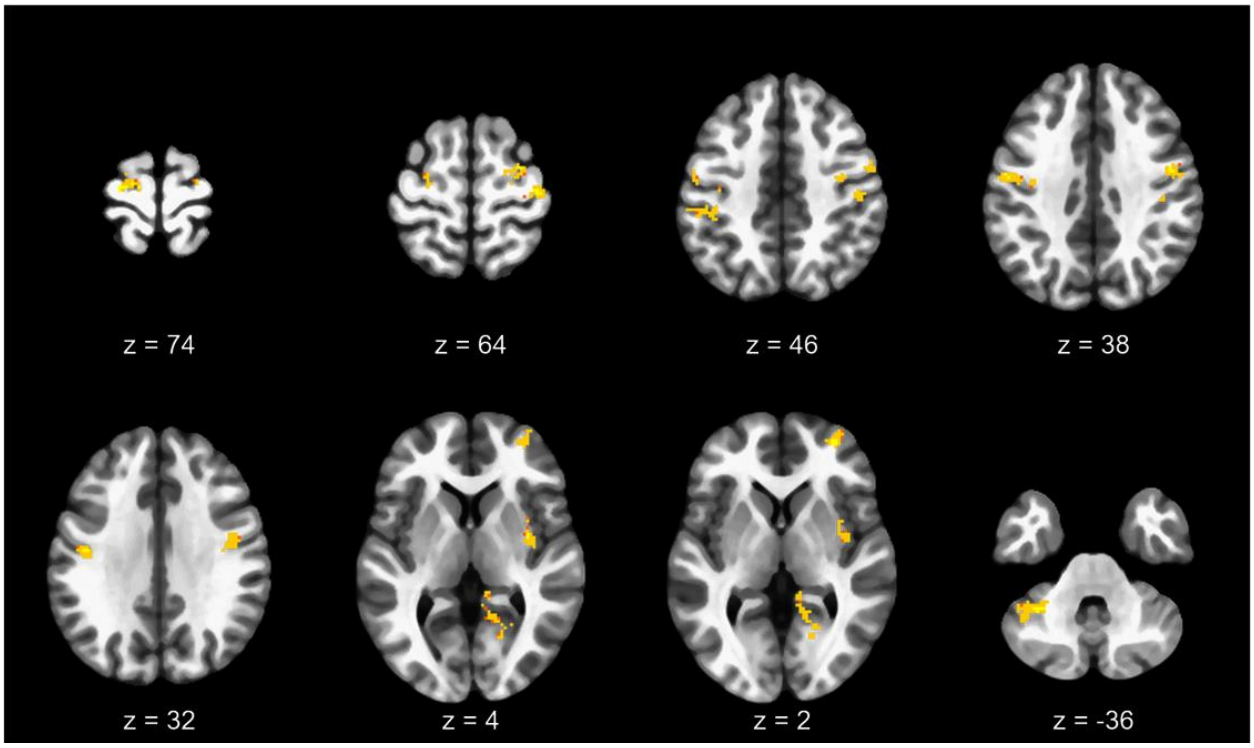

Figure 2. Resting state functional connectivity changes with the PCC/precuneus seed region in response to a 12-week walking exercise intervention in older adults diagnosed with mild cognitive impairment (MCI; n = 16). All 10 highlighted brain regions indicate increased functional connectivity with the PCC/precuneus from before to after exercise training (family-wise error corrected, $p < .05$). The MNI coordinates and cluster sizes for each region are shown in Table 3.

Section 3.5: Discussion

We investigated the effects of a 12-week walking intervention on the functional connectivity of the PCC/precuneus in individuals diagnosed with MCI and healthy elders. We hypothesized that both the MCI group and healthy elders would show increased connectivity with frontal and parietal regions, suggestive of enhanced recruitment of preserved brain regions.

We also hypothesized that the intervention would increase PCC/precuneus connectivity with MTL regions in the MCI group. We did find the hypothesized changes in functional connectivity of the PCC/precuneus with frontal, temporal, and parietal brain regions in the MCI group, but only one region, the left postcentral gyrus, showed increased connectivity in both groups. Additionally, a group by time interaction in the right IPL revealed that the MCI group showed the expected increased connectivity while the healthy elders demonstrated decreased connectivity in this region. These results, in conjunction with the findings from our previously published paper on the same subjects (J. C. Smith, K. A. Nielson, P. Antuono, et al., 2013), may indicate that exercise training has divergent effects on neural compensation and neural efficiency in the MCI group compared to healthy elders.

In developing our hypotheses for this study, we focused primarily on neural compensation as demonstrated by increased connectivity of the PCC/precuneus with preserved brain regions as a mechanism to increase cognitive reserve. After exercise training, the MCI group, presumed to be on the AD continuum, did demonstrate increased synchrony between compensatory networks and the PCC/precuneus, a region preferentially targeted in AD pathology. We expected, but did not observe, a similar increase in connectivity after exercise training in the healthy elders. This prediction was based on a previous report by Voss and colleagues (Voss et al., 2010), which found trends of connectivity changes in the DMN after 6 months of exercise training. However, these effects did not reach statistical significance in their study until after the 12-month intervention. As our intervention lasted only 3 months, it is possible that a longer exercise intervention is needed to observe connectivity changes in cognitively healthy older adults.

Another hypothesized mechanism to increase cognitive reserve is augmenting neural reserve – an indicator of neural efficiency (Barulli & Stern, 2013). In our previous paper utilizing the same subjects (J. C. Smith, K. A. Nielson, P. Antuono, et al., 2013) , we found group differences in activation changes in the precuneus and PCC during a famous name discrimination task. While both groups maintained equal task performance, the activation intensity decreased in the healthy elders after the exercise intervention, while there were no changes in the MCI group. This suggests increased neural efficiency in the healthy elders (as found in several other regions of the semantic memory network), and a need to maintain a compensatory response in the MCI group, as this region is targeted by AD pathology. Unfortunately, we were not able to measure levels of amyloid deposition or neurological damage in either group, so this possibility needs to be further explored. However, our current results are consistent with this interpretation and suggest that the MCI group demonstrated neural compensation through increased connectivity of the PCC/precuneus, while the healthy elders, who appear to not have reached a critical threshold for age related changes, did not require neural compensation (Barulli & Stern, 2013). Rather, exercise training may have resulted in increased neural reserve (or efficiency) of the PCC/precuneus, as indicated by our previously published findings of reduced activation during memory retrieval (J. C. Smith, K. A. Nielson, P. Antuono, et al., 2013). While the participants diagnosed with MCI did not differ in education from the healthy elders group (both were highly educated), the presence of cognitive impairment indicates a critical threshold was reached through combined age-related and AD processes. Thus, in those diagnosed with MCI, our findings support the idea that exercise training may stimulate increased cognitive reserve through enhanced recruitment of compensatory networks, such as increased function connectivity with a key neural hub in the PCC/precuneus.

As a first attempt to examine changes in resting state functional connectivity in MCI after an exercise intervention, we conducted *a priori* post hoc analyses to further explore the functional connectivity changes within this group. Results showed that the MCI group demonstrated increased connectivity of the PCC/precuneus with frontal and parietal regions from pre to post intervention. These effects suggest improved coordination of intrinsic activity of PCC/precuneus and several network regions including the fronto-parietal network (bilateral precentral gyrus and right middle frontal gyrus), the somatosensory network (right postcentral gyrus), and DMN regions (right superior frontal gyrus and left IPL). There was also increased connectivity between the PCC and the right parahippocampal gyrus, a region that links the DMN to the medial temporal lobe system (Ward et al., 2014). The increased connectivity suggests possible enhancement of posterior-anterior connections vulnerable to aging (Andrews-Hanna et al., 2007; Buckner, 2004). Our findings raise the possibility that these increased compensatory connections across networks connected to the PCC/precuneus may in part explain the neural protective effects of physical activity in MCI. This pattern of stronger connectivity with the PCC/precuneus after exercise training is a stark contrast to the typical progression of connectivity disruptions with the emergence of clinical symptoms. As AD progresses there has been shown to be an initial decrease in functional connectivity within the DMN, followed by compensatory hyperconnectivity in the frontal/parietal network regions, and ultimately, with severe dementia, an overall loss of connectivity (Hillary et al., 2015). The increased functional connectivity after exercise training observed in the MCI group between the PCC/precuneus and the other 10 regions suggests a possible reversal of the expected progression of connectivity decrements in MCI and, furthermore, enhancement of recruitment mechanisms that would

increase cognitive reserve and possibly delay cognitive decline. Future randomized controlled trials should test this hypothesis.

Interestingly, the MCI group showed increased connectivity with regions in the insular lobe and cerebellum after the walking intervention. Connectivity in insular networks are reported to correspond to cognitive performance in individuals with amnesic MCI and cognitively healthy older adults (Xie et al., 2012). Additionally, while we focused on the recruitment of frontal and parietal regions by the PCC/precuneus as an example of increased compensation to protect the DMN, the cerebellar region identified in our study corresponds to regions identified to be functionally related to the DMN (2011). Our results may indicate that the insular lobe and cerebellum are additional resources of reserve for the DMN. These results should be interpreted with some caution due to lower signal to noise ratio in these regions and particularly in the cerebellum.

Future research on the effects of an exercise intervention on functional connectivity in MCI and healthy elders should address potential mechanisms for these effects. Candidate measures that have been linked to exercise training would be BDNF, which has been found to modify functional connectivity (P. P. Foster, 2015), cerebral blood flow (Burdette et al., 2010), hippocampal brain volume (Erickson et al., 2011; J. C. Smith et al., 2014) white matter integrity (J. C. Smith et al., 2016), and Aβ plaque burden (Head et al., 2012). Given the evidence that exercise may oppose the actions of acetylcholinesterase in the hippocampus and cerebral cortex of rats (Pihlajamaki & Sperling, 2009), the effects of exercise training on the cholinergic system should also be considered. We have also recently reported, in this same cohort, that increased cardiorespiratory fitness after the exercise intervention was positively correlated in both groups with increased cortical thickness in regions including the precuneus, posterior cingulate cortex,

pre-central and post-central gyri, and the medial and middle frontal gyri (Reiter et al., 2015); regions that partly overlap with the areas that showed changes in resting state connectivity in the current analysis. Future studies should focus on multimodal imaging techniques to understand the mechanisms of exercise on neural plasticity in older adults and if this changes by disease state.

The lack of a non-exercise control group is a limitation of this study, and some caution is warranted in the interpretation of these effects. We cannot rule out the possibility that the walking intervention and its social context (most participants exercised alone under the supervision of a certified personal trainer) combined to produce changes in connectivity. However, the passage of time does not seem to be a plausible explanation for the changes we observed, as a longitudinal study in healthy older adults (ages 49 to 79) found functional connectivity within the DMN to be stable over a period of six years (Persson, Pudas, Nilsson, & Nyberg, 2014). We observed that several regions showed bilateral increases in functional connectivity, and the fact that the effects were more pronounced in those diagnosed with MCI argues against a generalizable influence of the experimental context.

Many longitudinal studies have shown that the risk of cognitive decline is reduced in older adults who are physically active (Etgen et al., 2010; Middleton et al., 2011) and cognition is protected in individuals with MCI who have greater physical activity (Baker, Frank, Foster-Schubert, Green, Wilkinson, McTiernan, Plymate, et al., 2010; Lautenschlager et al., 2008). Our results indicate that these protective effects may manifest in individuals with MCI through the enhanced recruitment of the PCC/precuneus, an important hub for higher order cognitive processes, and the preservation of posterior-anterior resting state functional connections. These connections are vulnerable in normal aging, and when these aging effects are combined with AD,

the results are even more devastating to cognition (Buckner, 2004). The pathological processes of AD and normal aging have divergent effects on brain networks (Hedden & Gabrieli, 2004; S. A. Small et al., 2011), and the differential effects of exercise training on functional connectivity in our study suggest that exercise-induced neural plasticity may vary based on AD progression and available cognitive reserve. While it remains to be conclusively demonstrated that exercise training may delay the conversion of individuals diagnosed with MCI to AD, or delay the onset of MCI among the cognitively intact, these results further underscore the complexity and pleiotropic nature of exercise as a potential intervention to modify neural network connectivity along the AD continuum.

Acknowledgements

We thank the participants for their time and dedication to this project. The authors also thank Piero Antuono, Alissa Butts, Ryan Hanson, Nathan Hantke, Mahshid Najafi, Karen Outzen, Hyuk Oh, Mihai Sirbu, and Matthew Verber for assistance with various phases of this study.

This study was supported by the University of Wisconsin-Milwaukee Graduate School Research Growth Initiative; and the National Center for Advancing Translational Sciences, National Institutes of Health grant numbers 8UL1TR000055 and 8KL2TR000056. Its contents are solely the responsibility of the authors and do not necessarily represent the official views of the NIH.

Chapter 4: Dissertation Study Introduction and Methods

Section 4.1: Introduction

As increasing numbers of people are living longer (World Population Ageing Report, United Nations, 2015), memory decline due to physiological aging and pathophysiological changes is growing as a public health issue (World Health Organization). Alzheimer's disease (AD) will be growing in prevalence because of the swelling proportion of elderly in the global population, and this will come with great social and financial cost. AD is the most expensive disease in the United States, and there is no current cure (Alzheimer's Association, 2016). If the onset of AD could be delayed by a few years, costs would vastly decrease and a greater number of older adults would complete their lives with memories and personalities intact. One of the difficulties in treating AD is that we do not fully understand how the healthy brain functions and adapts.

To address these research needs, we propose using resting state function connectivity and complex network graph theory. Resting state functional connectivity is a measure of coherent spontaneous blood oxygenation level-dependent (BOLD) functional magnetic resonance imaging (fMRI) signals during the absence of an external task. It is assumed to reflect the underlying white matter structural connectivity (M. D. Greicius, Supekar, Menon, & Dougherty, 2009) (Buckner et al., 2009) and synchronous neural activity (Fox & Raichle, 2007). Observational captures of the spontaneous neuronal activity are important in understanding the development of the brain (Sporns, 2011) and how it naturally compensates to neurological disruption (Hillary et al., 2014; Hillary et al., 2015). By using a network approach, a unified approach to the neural substrates of cognition may be investigated (Voytek & Knight, 2015) across aging and disease states that is not possible with basic task activation studies. The brain has been called the most

complex organism in the universe, and the use of complex network theory allows for single metrics that quantify the topologies of the networks of interest.

The networks of interest in this study are the fronto-parietal network and the default mode network (DMN). The fronto-parietal network, responsible for executive control, and the DMN, important for episodic memory (Buckner et al., 2008; Vincent et al., 2006) and overlapping with semantic memory systems (Binder, Desai, Graves, & Conant, 2009), are disrupted during the aging process. Anterior-posterior connections also diminish with age, and the medial prefrontal cortex (mPFC) and posterior cingulate cortex (PCC) have been shown to have a reduction in connectivity with age that correlated with poorer cognitive performance (Andrews-Hanna et al., 2007). Communication between brain regions is accomplished via white matter tracts, and age related changes to the volume and structure of white matter (WM) (Bartzokis et al., 2004; Paus et al., 2014; Peters, 2002) have been identified as a possible neuroanatomical substrate of the cognitive differences and decline that are exhibited with increasing age (Bartzokis et al., 2004; Bender et al., 2016; Bennett & Madden, 2014; Walhovd et al., 2014).

Although there are apparently no additional effects on anterior white matter tracts involved in the fronto-parietal network due to early AD (Head et al., 2004; Head, Snyder, Girton, Morris, & Buckner, 2005), the DMN has a greater loss of communication in AD patients compared to age matched healthy controls (Damoiseaux et al., 2012; Hillary et al., 2015; Sanz-Arigita et al., 2010). The combination of age-related disruptions to fronto-parietal circuits and AD pathology beginning in the MTL is devastating to cognition (Buckner, 2004).

Observed evidence that factors indicating brain disruption do not completely predict individual cognitive performance is referred to as cognitive reserve (Buckner, 2004). Cognitive

reserve is also referred to as the ability to recruit brain networks (Stern, 2009). Physical activity (PA) has been implicated as one of the factors that increases cognitive reserve (Fratiglioni et al., 2004), and it is well recognized that both leisure time PA and exercise training help to improve and maintain cognitive function in healthy older adults (Cotman & Berchtold, 2002; Kramer et al., 2006), and in those at increased risk for AD (Gates et al., 2013; Heyn et al., 2004; J. C. Smith, K. A. Nielson, J. L. Woodard, et al., 2013; Woodard et al., 2012). Evidence also exists that PA influences the integrity and organization of the white matter tracts (Bender et al., 2016; Oberlin et al., 2016; Sexton et al., 2016; J. C. Smith et al., 2016) so disrupted in the aging process.

Resting state functional connectivity is an apt method for investigating the interactive effects of PA and age on the brain networks as the underlying anatomical neural substrate for intrinsic functional connectivity appears to be the structural white matter connections (Honey et al., 2007; van den Heuvel & Sporns, 2013) vulnerable to aging. Thus PA has been shown to increase connectivity in the brain networks disconnected during the aging process (P. Huang et al., 2016). Four months of an exercise intervention in older adults found the hippocampus had greater overall connectivity as measured by the number of connections to other brain regions (Burdette et al., 2010), and twelve months of an exercise intervention increased the connections between brain regions in the DMN and fronto-executive network in older adults compared to controls (Voss et al., 2010). In a cohort study covering 10 years (subjects' age ranged from 25-80 years) higher levels of PA was associated with increased functional voxel wise connectivity of the PCC, a hub of the DMN. We have shown with data from our lab that 12 weeks of walking in healthy older adults and in older adults diagnosed with mild cognitive impairment (MCI), a risk factor of AD, increased the connectivity of the posterior cingulate/precuneus (PC/p) with

frontal and parietal regions (Chirles et al., 2017). These increases in connectivity are apparent compensatory mechanisms protecting connections disrupted with age, perhaps through the protection and reorganization of white matter tracts, which would increase cognitive reserve and thus delay cognitive decline.

Despite the evidence that PA protects cognition, few studies have investigated the effects of PA on brain networks throughout the lifespan and middle adulthood has not been included at all. Yet, as Sporns (2011) asserts in the book, Networks of the Brain, the influences of the middle adulthood stage lay the foundation for network plasticity in late adulthood While small-worldness (a measure of non-randomness in complex graph theory) is maintained across the lifespan, a rebalancing of functional segregation and integration occurs through childhood development, and young, middle, and late adulthood, and this rebalancing is a possible neural substrate for cognitive changes (Sporns, 2011).. The effects of PA on the networks disrupted by the aging process need to be studied at all stages.

In the literature investigating the effects of PA on functional connectivity across the lifespan, one important variable is missing. Despite the findings that among carriers of the APOE-ε4 allele (a genetic risk factor for AD) (Corder et al., 1993; Okuizumi et al., 1994) PA appears to provide greater protection of cognition and hippocampal volume compared to APOE-ε4 non-carriers (Head et al., 2012; J. C. Smith et al., 2014; J.C. Smith, K.A. Nielson, J.L. Woodard, M. Seidenberg, & S.M. Rao, 2013; Woodard et al., 2012), there has not been research to illuminate the interactive effects of PA and APOE-ε4 allele on the functional connectivity of these networks.

Connectivity studies in cognitively healthy APOE-ε4 carriers have shown disrupted functional connectivity similar to changes observed in aging and AD (Sheline et al., 2010).

Older APOE-ε4 carriers have shown lower functional connectivity between the anterior hippocampus, important for episodic memory (Squire, 2004), and several regions of the DMN during encoding and retrieval (Harrison et al., 2016). Additionally, an overall reduction of the functional connectivity between the hippocampus and the PCC was found in female APOE-ε4 carriers ages 30-78 (Heise et al., 2014). In middle aged adults, the PCC and dorsolateral prefrontal cortex (DLPFC), hubs of the DMN and fronto-parietal network respectively, showed diminished functional connectivity (Goveas et al., 2013). A different effect is found with the precuneus, and with a few exceptions, studies have found cognitively intact adults with the APOE-ε4 allele demonstrate increased connectivity of the precuneus with brain regions in the DMN compared to low risk groups (Fleisher et al., 2009; McKenna et al., 2015; Sheline et al., 2010). This increased connectivity in the DMN has been shown to correlate with improved episodic memory performance in ε4 carriers (Matura et al., 2014). In fact, increased connectivity appears to be a compensatory response to neuronal disruption (Hillary et al., 2015). Consequently, however, when age increases and AD pathology develops, these carriers may not be able to further compensate and this may explain the increased incidence of AD in APOE-ε4 carriers.

Aging is a lifetime process, and how networks develop and establish connections over this lifetime will affect the response to any treatment or stimulus. The interaction of PA, APOE-ε4 status, and age on network connectivity measures in healthy adults is needed to appreciate the natural adaptations of the brain to overcome neurological disruption. This knowledge will help to preserve and protect the memories of our elders by informing AD treatment research.

Section 4.2: Specific Aims

Subsection 4.2.1: PA and Age Interactions on Network Connectivity Measures

Specific Aim 1: To investigate the association of self-reported leisure-time PA on the fronto-parietal network, DMN, and hippocampal connectivity in young adulthood to middle adulthood.

Hypotheses:

1) Global efficiency in the DMN and fronto-parietal network, node degree, and long-range connectivity between the PCC and mPFC will decrease with increased age.
2) Subjects who meet the weekly recommendations for moderate to vigorous intensity PA will have greater measures of network integration (global efficiency) in the DMN and fronto-parietal network than the low PA group across the entire age range.
3) Subjects who meet the weekly recommendations for moderate to vigorous intensity PA will have greater node strength of the hippocampal subregions, precuneus, PCC, and DLPFC than the low PA group across the entire age range.
4) Subjects who meet the weekly recommendations for moderate to vigorous intensity PA will show greater connectivity between the mPFC and PCC than the low PA group across the entire age range.

Subsection 4.2.2: PA, APOE-ε4 Status, and Age Interactions

Specific Aim 2: To investigate the association of the interaction of PA and APOE-ε4 status on the fronto-parietal network, DMN, and hippocampal connectivity from young adulthood to middle adulthood.

Hypotheses:

1) APOE-ε4 carriers will have smaller measures of network integration (global efficiency) in the DMN than the non-carrier group across the age range.

2) APOE-ε4 carriers will have smaller measures of node strength of the anterior hippocampus and PCC compared to the non-carrier group across the age range.
3) The APOE-ε4 carriers will have larger measures of node strength of the precuneus compared to the non-carrier group across the age range.
4) APOE-ε4 carriers with levels of PA that meet the weekly recommendations for moderate to vigorous intensity PA will have connectivity measures that are not different from the non-carriers who meet the recommendations for moderate to vigorous intensity PA.

Section 4.3: Description of Study

Subsection 4.3.1: Summary of Overall Study

The current study is a secondary analysis from a primary study aimed at the cognitive benefits of cognitive training via computer games. The study was approved by the University of Maryland, College Park Institutional Review Board (IRB) and conducted in accordance with the Federal Policy for the Protection of Human Subjects. A total of 264 participants were recruited through University of Maryland electronic list serves, local community online newsletters, craigslist.org, and flyers. The recruitment literature described the study as looking for participants interested in improving memory by using "brain games." The desired age range was 20-50 years old. Volunteers who had 1) neurological illnesses or conditions; 2) medical illnesses or conditions that may affect brain function; 3) current untreated Axis I psychiatric disturbance meeting DSM-IV Axis I criteria; or 4) contraindications for MRI scanning (ex. ferrous objects in body, pregnancy, claustrophobia, left-handedness (laterality quotient [LQ] <50 (Oldfield, 1971) were not included in the study.

After screening performed by research team members in the Psychology department, participants were provided with information about the study and signed an informed consent form. Participants were also informed of a $100 stipend. Day one of the study included the collection of physical activity and estimated cardiovascular fitness measures. Physical activity was assessed using the Paffenbarger Physical Activity Questionnaire (Paffenbarger, Blair, Lee, & Hyde, 1993; Paffenbarger, Wing, & Hyde, 1978), readiness to perform exercise was assessed using the Physical Activity Readiness Questionnaire (PAR-Q), and VO_{2max} was estimated using the YMCA cycle protocol (W. R. Thompson, Gordon, & Pescatello, 2010). Saliva was collected to determine APOE genotype.

Subjects Used in this Study:

Of the 264 subjects collected in the parent study, 77 of these subjects had baseline fMRI scans and self-reported physical activity collected. Subjects self-reported education levels (1 = less than high school degree; 2 = high school degree; 3 = some college; 4 = bachelor's degree; 5 = some graduate school; 6 = master's degree; 7 = PhD, MD, JD).

Physical Activity Readiness Questionnaire (PAR-Q):

The physical activity readiness questionnaire from the Public Health Agency of Canada, the PAR-Q, was administered to assess the participants' ability to perform the sub maximal test to estimate cardiovascular fitness. The seven questions in this questionnaire determine if the individual should obtain a physician's approval before activity. All subjects were found to be ready to perform the YMCA cycle protocol.

Paffenbarger Physical Activity Questionnaire:

This questionnaire was employed to assess weekly caloric expenditure due to physical activity. Also known as the College Alumnus Activity Survey (Paffenbarger, Blair, Lee, &

Hyde, 1993), these eight questions assess the average weekly time spent performing sport and recreational activities over the past year. Estimated intensity of these activities is used to calculate the metabolic equivalent units of task (MET), and total expenditure also includes an estimation of blocks walked and stairs climbed.

YMCA cycle protocol:

This protocol measures a subject's heart rate at a series of submaximal work rates (W. R. Thompson et al., 2010). The age predicted heart rate max is also used to extrapolate the individual's VO_2max. In this test, the two to four 3-minute stages of continuous pedaling on a cycle ergometer are performed with heart rate measured during the last 15 to 20 seconds of minute 2 and minute 3. If the subject's heart rate varies more than five beats per minute, then this state should continue for an additional minute. The first stage is set at a work rate of 0.5kg at 50 rpms (or 150 kg/min), but subsequent stage work rates depend on the subject's heart rate. Once the test is completed (with at least 2 stages of steady state continuous cycling), HR during the last minute of each steady-state stage is plotted against work rate. The line defined by these points is then extended to the age predicted HR max (220-age). A vertical line is then dropped to the x-axis to estimate the maximal effort work rate. This is then used in the following equation to predict the individual's VO_2max.

$$\textit{Eq 1)}\ VO_2\text{max} = SM_2 + [b \times (HR_{max} - HR_2)];$$

where SM_2 is the sub-maximal VO_2 at the last workload, HR_2 is the individual's HR at the last workload, and b is the multi-stage slope prediction.

Other calculations needed are:

$$\textit{Eq a)}\ SM_2 = (\text{Last Workload(W)}/\text{Body mass (kg)}) * 10.8 + 7$$

$$\textit{Eq b)}\ SM_1 = (\text{Previous Workload(W)}/\text{Body mass (kg)}) * 10.8 + 7$$

$$\textit{Eq c)}\ b = (SM_2 - SM_1)/(HR_2 - HR_1)$$

APOE genotyping:

DNA samples were obtained using a mouthwash procedure (Lum & Marchand, 1998). Participants abstained from food or drink for one hour before the collection and rinsed with 10ml of mouthwash for 45 seconds before spitting into a 30-ml test tube. Research assistants labeled and stored the samples at -20^{o} C. The unprocessed samples were stored for one to five months before DNA isolation and genotyping. Participants were classified as ε4 carriers if their genotype was either heterozygous (ε3/ε4 or ε2/ε4) or homozygous (ε4/ε4).

DNA Isolation Procedures

Isolation of the DNA followed methods prescribed by Puregene EP DNA Purification Kit (Gentra). DNA samples were centrifuged for 10 minutes, and the supernatant was poured off before 1 ml of cell lysis solution was added. The samples were vortexed for 20 seconds and then incubated for 15 minutes at room temperature. Before the samples for vortexed for 20 seconds again, 10μL of proteinase K solution (20mg/mL) were added to cells. Samples were incubated a second time for 10 minutes at room temperature. The samples were then vortexed for 20 seconds after adding 340 μL of protein precipitation solution and then incubated at 4^{o} C for 10 minutes.

Following incubation, supernatant was poured into 15-mL tubes containing 1 mL of 100% isoproponal. Samples were inverted 50 times and then centrifuged for 10 minutes, and the supernatant poured off. Next, 1 mL of 70% ethanol was added to the sample and tubes were inverted 5 times, followed by a 1 minute centrifuge. The samples were centrifuged for 1 minute after the ethanol was poured off. Before placing the samples in an incubator at 37^{o} C for 10 minutes to dry, residual ethanol was removed using a pipette. Incubation at the same temperature continued for 48 hours after adding 400μL of DNA hydration solution to the samples.

After the 48-hour incubation period, the supernatant was poured off and 2 mL of cell lysis solution added to the samples to begin a second isolation procedure. Samples were vortexed for 20 seconds and then incubated in a 65º C water bath for one hour. Samples were vortexed again for 20 seconds and centrifuged for 15 minutes after adding 800 µL of protein precipitation solution.

The supernatant was poured into 2.4 mL of 100% isopropanol in 15-ml tubes. Tubes were gently inverted 50 times and centrifuged for five minutes. Next, 2.4 mL of 70% ethanol were added to samples after the supernatant was poured off, and tubes were inverted five times. Samples were centrifuged for three minutes and ethanol was poured off. After samples were centrifuged again for three minutes, a pipette was used to remove residual ethanol from tube. Samples were incubated at 37º C for 10 minutes to dry. Samples were incubated for 48 hours at 37º C after adding 400 µL of DNA hydration solution to tube. Upon completion of incubation, samples were centrifuged for one minute and stored at 4º C in 1.5 mL Eppendorf tubes.

DNA Genotyping

The following primers were used to genotype APOE ε2, ε3, and ε4 alleles: F-5' ACT GAC CCC GGT GGC GGA GGA GAC- 3'; R-5' TGT TCC ACC AGG GGC CCC AGG CGC TC- 3'. The following steps constituted the thermal profiling cycle profile: 1) incubation at 95º C for 5 minutes; 2) 45 cycles of 95º C for 30 seconds, 63º C for 30 seconds, and 72º C for 30 seconds; and 3) incubation at 72º C for 5 minutes. Two restriction digests were used (15 µL of PCR product and either 0.2 µl of HaeII OR 0.75 µl of AflIII) and were incubated at 37º C overnight. Digests were analyzed separately on a 3% agarose gel for two hours, and genotypes were determined according to observed fragment sizes. DNA sequence-verified controls with each genotyping reaction determined genotype accuracy.

MRI acquisition procedures:

Participants were scanned on the second day of coming to the lab, and an additional scan was performed after the 5-week cognitive training. A 3.0 Tesla Siemens TRIO scanner (Siemens Medical Systems, Erlangen, Germany) with a 32-channel head coil at the Maryland Neuroimaging Center was used. During MRI acquisition, participants were instructed to lie as still as possible and foam padding was used to limit movement and improve comfort. Anatomical and resting state sequences were run during the scanning session. High-resolution, three-dimensional multi planar reconstructed (mpr) anatomic images were acquired (TE = 2.32ms; TR = 1900ms; inversion recovery (IR) preparation time = 900ms; flip angle = 9°; slice thickness = 0.9 mm; voxel size = 0.9x0.9x0.9mm; FOV = 230mm; resolution = 256 x 192, acquisition time (TA) = 4:26 minutes). During the resting state scan, participants were instructed to keep their eyes open and to look at a fixation cross. A gradient-echo, echo-planar pulse sequence sensitive to blood oxygenation level-dependent (BOLD) contrast were acquired (TE = 24ms; TR = 2000ms; TR delay = 10ms; flip angle = 70°; 36 axial slices, interleaved; 3x3x3.2mm voxels; FOV = 192mm; resolution = 64 x 64; 160 volumes; duration 5:26 minutes).

Preprocessing steps:

Preprocessing steps were performed using tools from the Analysis of Functional NeuroImages (AFNI) software package (Cox, 1996) and FreeSurfer image analysis suite, version 5.3.0 (http://surfer.nmr.mgh.harvard.edu) In FreeSurfer, high-resolution structural data were used to create individual parcellations. The first step included reconstruction of the brain using motion correction and conformation, non-uniform intensity normalization, and talairach transform computation. The second reconstruction step drew the pial and white matter surfaces. Each subject was viewed and edited for surface smoothness and minor pial edits were necessary

for 18 subjects. Each subject's cortical areas were transferred to a default mesh (fsaverage) and converted to the 17 sub-network parcellation from the Yeo et al. (2011) paper (http://www.freesurfer.net/fswiki/CorticalParcellation_Yeo2011).

In AFNI, the functional time series were aligned to the anatomical images, and slice time correction, motion correction procedures, and intensity normalization to percent signal change were performed. The first 3 TRs were removed, a 0.005 to 0.10 bandpass filter applied, and the following sources of noise were regressed out: six-parameter rigid body head motion, the derivatives of the motion parameters, ventricle signal, and white matter signal. The time series data were smoothed using a 6mm full-width at half-maximum Gaussian blur. Due to the importance of accounting for motion in functional connectivity analyses (Power, Barnes, Snyder, Schlaggar, & Petersen, 2012), any subject with a maximum head movement greater than 6mm (2 voxels) was completely eliminated from the analysis as well as scrubbing individual time points with movement greater than 0.5mm from the analyses. Subjects were also eliminated from the analysis if more than 10% of the TRs were censored. Two subjects were removed due to more than 10% of TRs being censored. Group difference in motion was checked using t-tests on the mean frame displacement in each group (APOE-ε4 status and PA status).

Functional Connectivity Measurements:

The time courses of all the voxels in each ROI defined by the parcellations from the Yeo atlas were averaged. Using the Matlab toolbox for complex network measures (http://www.brain-connectivity-toolbox.net), weighted, undirected complex network measures were calculated from the *n*x*n* adjacency matrix for each participant. Each element *ij* in the matrix was the z-transformed Pearson correlation between nodes *i* and *j*. Negative correlations

were replaced with a zero and not used in these calculations for network-based measures. (Rubinov & Sporns, 2010)

Global efficiency and local efficiency in the DMN and fronto-parietal network, as measures of integration and segregation, respectively, were calculated. The mathematical equations used were:

Weighted Global Efficiency

$$E^w = \frac{1}{n}\Sigma_{i\in N}\frac{\Sigma_{j\in N, j\neq i}\left(d_{ij}^w\right)^{-1}}{n-1}$$

Weighted Local Efficiency

$$E_{loc}^w = \frac{1}{2}\Sigma_{i\in N}\frac{\Sigma_{j,h\in N, j\neq i}\left(w_{ij}w_{ih}\left[d_{jh}^w(N_i)\right]^{-1}\right)^{\frac{1}{3}}}{k_i(k_i-1)}$$

(Rubinov & Sporns, 2010)

mPFC and PCC Connectivity:

The element in each subject's adjacency matrix corresponding to mPFC-PCC connection in each hemisphere was used as a dependent variable measuring long-range connectivity.

Node Degree of the hippocampus subregions, Precuneus, PCC, and DLPFC,:

The precuneus, PCC, dorsal PFC, and lateral PFC were identified from the 17-subnetwork FreeSurfer derived cortical parcellation. However, the hippocampus is a subcortical region, and the following sections described how the hippocampal subregions were identified.

Hippocampal Subregions

The methods used to identify the hippocampus and segmenting the hippocampus into three subregions (head, body, and tail) followed the methods described in the Weiss et al. (2005) paper. FreeSurfer volumes were aligned into anterior commissure-posterior commissure space, thus dispensing with distortions due to reorientation and allowing for assessment of hippocampal volumes. The uncal apex was used for the segmentation as an easily recognizable landmark. The anterior slice of the hippocampus is identifiable by FreeSurfer and identified the anterior end of the hippocampal head. The posterior hippocampal head was identified moving caudally through

the images to the last slice in which the uncal apex was still visible. The landmark for the most anterior slice of the hippocampal tail was identified as when the fornix separates from the hippocampus and is clearly visible (Watson et al, 1992). Parcellation algorithms for the whole hippocampus in FreeSurfer identified the posterior slice of the tail.

Masks were created from these identified subregions in each subject and used to create hippocampal head, body, and tail ROIs in the functional resting state data. The time-series in these ROIs were averaged.

Calculating Node Strength

Using the Matlab (The Mathworks, Inc., Natick, MA, USA) toolbox, the weighted degree of each node (hippocampal subregions, precuneus, PCC, dorsal and lateral PFC) were calculated.

$$\text{Weighted degree (or node strength) of i: } k_i^w = \sum_{j \in N} w_{ij}$$

Subsection 4.3.2: Data Analysis

Multiple linear regression models were used for each of the dependent variables (global efficiency, local efficiency, node strength, and PCC-mPFC connectivity). All dependent variables were continuous. The independent variables were defined as the following: APOE status (ε4 positive (value 1), ε4 negative (value 2)), PA status (PA>1500 kcal/week (value 2), PA<1500 kcal/week (value 1)); Age (continuous); and the interaction predictors: APOExAge, PAxAge, APOExPA, APOExPAxAge. The data were checked for the following model assumptions: homogeneity (via scatterplot of studentized residuals vs. predicted values and vs. values of independent variables), normality (via S-W test for normality, skewness, and kurtosis), linearity (via review of independent vs. dependent variable scatterplots), and noncollinearity (via tolerance tests). Multiple comparison corrections were performed using Bonferonni corrections.

Chapter 5: Results

Two subjects of the original 77 were excluded from the analyses because of movement during the resting state scan, one was not included due to a diagnosis of anxiety, and 5 had missing anatomical or resting data. Thus, 69 participants were included in the final analyses.

Section 5.1: Demographics

The demographics of the overall sample as well as the demographics of groups by APOE-ε4 status and PA level are presented in Table 5. Demographics of the sample split into 4 groups (Low PA carriers and non-carriers, High PA carriers and non-carriers) are presented in Table 6.

Table 5: Subject Demographics

	Entire Sample N = 69		**APOE-ε4 Non-carriers N = 50**	**APOE-ε4 Carriers N = 19**	**APOE Group Differences**	**Low PA Group N = 27**	**High PA Group N = 42**	**PA Group Differences**
	Range	**Mean (SD)**	**Mean(SD)**	**Mean(SD)**	**t-statistic (p value)**	**Mean(SD)**	**Mean(SD)**	**t -statistic (p value)**
Sex (M/F)		28/41	21/29	7/12	0.152(0.457)*	9/18	19/23	0.966(0.452)*
Age(years)	22 - 51	31.69(8.4)	31.5(8.8)	32.3(7.4)	0.351(0.727)	32.0(8.0)	31.5(8.7)	0.214(0.831)
Weekly kcal	56 - 8878	2353.4(1834.7)	2430.6(1916.1)	2150.4(1631.5)	0.564(0.575)	875.1(374.6)	3303.8(1768.9)	7.016(<0.001)
Kcal > 6 METS	0 - 6923	824.9(1117.2)	904.5(1224.8)	619.5(764.2)	0.943(0.349)	262.3(346.6)	1195.4(1287.7)	3.670(<0.001)
Time per week (min)	0 - 1153	227.6(241.2)	239.0(260.8)	198.2(184.1)	0.623(0.535)	75.7(79.8)	327.5(259.8)	4.876(<0.001)
Time sitting (hours)	2 - 16	6.9(3.5)	6.7(3.5)	7.6(3.5)	1.017(0.313)	7.1(3.3)	6.8(3.7)	0.270(0.788)
Bouts of Vigorous Exercise per week	0 - 7	2.9(2.2)	2.8(2.1)	3.0(2.4)	0.225(0.833)	1.4(1.7)	3.9(1.9)	5.487(<0.001)
Estimated VO_{2max} (mlO_2/min/kg)	18 - 49	31.7(8.4)	33.0(8.6)	30.1(5.6)	1.052(0.297)	31.2(6.7)	33.1(8.7)	0.879(0.383)

*Chi squared used. Estimated VO_{2max} scores available for 59 subjects (16 ε4 positive and 43 ε4 negative). One e4 negative subject is missing 6 MET information, time per week, sitting hours per day.

No significant differences were found in sex distribution, age, weekly kcal, kcal > 6 METS, time per week, time sitting, bouts of vigorous exercise per week, or estimated VO_{2max} when comparing groups by APOE-ε4 status. When comparing the groups by PA status (meeting 1500 kcal per week or not), predictably there were significant differences between groups on Kcal > 6 Mets, time per week, and bouts of vigorous exercise per week. There were no significant differences in time sitting, age, sex distribution, or APOE-ε4 status. No differences were found in estimated VO_{2max}.

Table 6: Subject Demographics by PA and APOE-ε4 Group.

	Low PA Carriers Group N = 8	Low PA Non-carriers Group N = 19	High PA Carriers Group N = 11	High PA Non-carriers Group N = 31	Group Differences	
	Mean (SD)	Mean (SD)	Mean (SD)	Mean (SD)	F -statistic	p value
Sex (M/F)	2/6	7/12	5/6	14/17	1.294*	0.731
Age(years)	29.34(2.86)	33.07(9.22)	34.40(9.04)	30.50(8.55)	0.969	0.413
Weekly kcal	961.75(321.38)	838.58(397.28)	3014.82(1663.30)	3406.32(1820.11)	16.302	<0.001
Education	4.71 (1.50)	3.88 (1.46)	5.00 (1.00)	4.11 (1.40)	1.421	0.247

*Chi squared used. The Low PA groups are significantly lower in weekly kcal than the High PA groups. Education Level was collected for 7 Low PA carriers, 16 Low PA non-carriers, 7 High PA carriers, and 27 High PA non-carriers.

Section 5.2: Motion Displacement

A one-way ANOVA was conducted on the mean frame displacement (FD) due to motion for each group during the resting state fMRI scan, and there were no statistical differences [$F(3,65) = 0.481$, $p = 0.696$]. A one-way ANOVA was also conducted on the maximum FD due to motion, and again no differences were found between the four groups [$F(3,65) = 0.698$, $p = 0.557$].

Section 5.3: Hippocampal Volumes

All hippocampal volumes were corrected for intracranial volume using previously established methods (Raz et al., 2005). A one-way ANOVA was conducted on the volumes of the right hippocampal head [$F(3,65) = 0.0.374$, $p = 0.772$], body [$F(3,65) = 0.997$, $p = 0.400$], tail [$F(3,65) = 0.419$, $p = 0.740$], total hippocampus [$F(3,65) = 0.568$, $p = 0.638$], and left hippocampal head [$F(3,65) = 0.640$, $p = 0.592$], body [$F(3,65) = 0.578$, $p = 0.632$], tail [$F(3,65) = 0.294$, $p = 0.829$], and total hippocampus [$F(3.65) = 0.376$, $p = 0.770$]. No statistical differences were found between the four groups.

Section 5.4: Model Description

Several multiple linear regression models were conducted to determine if the dependent variables in this study could be predicted by the following models of independent predictors: 1) Age; 2) Age, PA level, PA levelxAge; 3) Age, APOE level, APOExAge; and 4) Age, APOE level, PAxAPOE, and PAxAPOExAge. The null hypotheses tested were that the adjusted R^2 was equal to 0 and that the regression coefficients (i.e., the slopes) were equal to zero. The data were screened for missing values and violation of assumptions. There were no missing data.

Tests of Assumptions

In the previously mentioned models, there are three variables that are not interactions: Age, PA level ((PA>1500 kcal/week, PA<1500 kcal/week), and APOE level (ε4 carriers or non-carriers). Of the three, only age is continuous, and thus tests of linearity only included age as an independent variable.

Section 5.5: Global Efficiency

The four multiple linear regression models were run with global efficiency as the dependent variable. The results are presented in Table 9, but no models reached significance.

Linearity: Reviews of the partial scatterplots of the independent variable (age) and the dependent variable (Global Efficiency) indicated linearity was not violated. Additionally, a residual plot vs age demonstrated a random horizontal band within an absolute value of 2 or 3, also indicating linearity, with one data point as an exception.

Normality: Review of the S-W test for normality ($SW = 0.823$, $df = 69$, $p < 0.001$) and the skewness (2.110) and kurtosis (6.571) statistics suggested that normality was an issue. The Box-Cox power transformation was performed due to the S-W test result, but when the regression model was run again, there were no significance differences in the outcome model.

Homogeneity of variance: A relatively random display of points, where the spread of residuals appears fairly constant over the range of values of the independent variables (in the scatterplots of studentized residuals versus predicted values and studentized residuals against values of the independent variables) would provide evidence of homogeneity of variance. In models 1 and 2, this evidence was clear. However, in model 3, the studentized residuals vs. APOExAge displayed a possible negative trend as the right side of the graph had a much smaller spread of residuals. Again, in model 4, a smaller spread of residuals on the right side was exhibited in the studentized residuals vs. APOExPAxAge. In this model, the residuals vs. predicted values appeared to have a smaller spread on the left side of the graph. While the graphs did not indicate major violations of the homogeneity of variance, there may be an increased likelihood of type II error.

Multicollinearity: Due to the inclusion of interaction variables in the models, multicollinearity did exist (view Table 8). Table 7 illustrates the tolerance, and values less than 0.10 suggest that multicollinearity is an issue. This table is the same for all models of dependent variables in the result section.

Table 7: Tolerance for Models

Independent Variable	Tolerance
Model 1	
Age	1.00
Model 2	
Age	0.077*
PA Level	0.061*
PA x age	0.036*
Model 3	
Age	0.101
APOE Level	0.053*
APOE x age	0.034*
Model 4	
Age	0.195
APOE Level	0.482
APOE x PA	0.059*
APOE x PA x age	0.047*

*Multicollinearity is an issue. Analyses were redone with centering corrections to reduce multicollinearity, and significance findings of the models did not change.

Table 8: Correlations of all Independent Variables

Correlations

	Age	PA Level	APOE Level	PAxAge	APOE xAge	PAxAPOE	PAx APOExAge
Age	1.000	-0.026	0.043	.641**	.587**	0.061	.493**
PA Level	-0.026	1.000	-0.038	.726**	-0.003	.628**	.513**
APOE Level	0.043	-0.038	1.000	0.039	.812**	.720**	.628**
PAxAge	.641**	.726**	0.039	1.000	.425**	.533**	.758**
APOExAge	.587**	-0.003	.812**	.425**	1.000	.637**	.832**
PAxAPOE	0.061	.628**	.720**	.533**	.637**	1.000	.871**
PAxAPOExAge	.493**	.513**	.628**	.758**	.832**	.871**	1.000

**Correlation is significant at the 0.01 level (2-tailed).

Screening for Influential Points: Model 1: In model one, the maximum value for Cook's distance is 0.265, and the maximum centered leverage value is 0.078, both under points of concern (value of 1 for Cook's distance and 0.5 for maximum centered leverage)(Lomax & Hahs-Vaughn, 2012). The maximum Mahal's distance is 5.30, less than the chi-squared critical value of 5.99. These values all indicated there are no data points exerting undue influence on the model.

Model 2: In model two, the maximum value for Cook's distance was 0.219, under the point of concern. The maximum centered leverage value was 0.173, again under the point of concern. However, the maximum Mahal's distance was 11.75, greater than the chi-squared critical value of 9.49. While two of the three values indicated there are no data points exerting undue influence on the model, the identified possible outlier was removed from the data and the model was run again. The model did not change in significance.

Model 3: In model three, the maximum value for Cook's distance was 0.556, under the point of concern. The maximum centered leverage value was 0.393, greater than ideal (0.2) but below the value of concern. The maximum Mahal's distance was 26.725, greater than the chi-squared critical value of 9.49. While two of the three values indicated there are no data points exerting undue influence on the model, the identified possible outlier was removed from the data and the model was run again. The model did not change in significance.

Model 4: In model four, the maximum value for Cook's distance was 0.781, under the point of concern. The maximum centered leverage value was 0.360, again not indicating any points with undue influence. The maximum Mahal's distance was 24.484, greater than the chi-squared critical value of 11.07. While two of the three values indicated there were no data points exerting undue influence on the model, the identified possible outlier was removed from the data and the model was run again, but the model did not change in significance. As there were no reasons to believe the outlier was due to error or incorrectly measured data, and the outlier did not create nor negate a significate association, the possible outlier was included in the reported results.

Table 9: Model Summary and Coefficients for Models of Global Efficiency

	Global Efficiency				
Model Summary	F	Adj R^2	p-value	Std β	p-value
Model 1	0.335	-0.100	0.565		
Age				-0.710	0.565
Intercept				0.511	<0.001
Model 2	0.404	-0.270	0.751		
Age				-0.089	0.843
PA Level				-0.132	0.791
PAxAge				0.023	0.972
Intercept				0.574	0.024
Model 3	1.682	0.029	0.180		
Age				0.598	0.116
APOE Level				1.086	0.041
APOExAge				-1.218	0.063
Intercept				0.096	0.650
Model 4	0.961	-0.002	0.435		
Age				0.252	0.363
APOE Level				0.235	0.185
PAxAPOE				0.469	0.353
PAxAPOExAge				-0.733	0.194
Intercept				0.276	0.097

None of the models for Global Efficiency reached significance levels.

Section 5.6: Long Range Connectivity of the mPFC-PCC

Subsection 5.6.1: Right Hemisphere

The same four multiple linear regression models were run with the right mPFC-PCC correlation as the dependent variable. The results are presented in Table 10, but no models reached significance.

Linearity: Reviews of the partial scatterplots of the independent variable (age) and the dependent variable (the correlation between the PCC and mPFC in the right hemisphere) indicated linearity was not violated. Additionally, a residual plot vs. age demonstrated a random horizontal band within an absolute value of 3, also indicating linearity, with two data points as an exception.

Normality: Review of the S-W test for normality (SW = 0.960, df = 69, p = 0.026) and the skewness (-.505) and kurtosis (2.083) statistics suggested in aggregate that normality was an issue (skewness statistic is in acceptable range). The Box-Cox power transformation was performed due to the S-W test result, but when the regression models were run again, there were no significance differences in the outcome model.

Homogeneity of variance: In models 1, 3 and 4, this evidence to support the assumption of homogeneity of variance was clear. However, in model 2, the studentized residuals vs. predicted values displayed a possible negative trend as the right side of the graph had a much smaller spread of residuals, but not enough to warrant concern.

Screening for Influential Points: Model 1: In model one, the maximum value for Cook's distance was 0.344, under the point of concern. The maximum centered leverage value was 0.078, again under the point of concern. The maximum Mahal's distance was 5.30, less than the chi-squared critical value of 5.99. These values all indicated there were no data points exerting undue influence on the model.

Model 2: In model two, the maximum value for Cook's distance was 0.254, under the point of concern. The maximum centered leverage value was 0.173, again under the point of concern. However, the maximum Mahal's distance was 11.75, greater than the chi-squared critical value of 9.49. While two of the three values indicated there were no data points exerting

undue influence on the model, the identified possible outlier was removed from the data and the model was run again. The model did not change in significance. As there were no reasons to believe the outlier was due to error or incorrectly measured data, and the outlier did not create nor negate a significate association, the possible outlier was included in the reported results.

Model 3: In model three, the maximum value for Cook's distance was 0.750, under the point of concern. The maximum centered leverage value was 0.393, not indicating any undue influence. The maximum Mahal's distance was 26.725, greater than the chi-squared critical value of 9.49. While two of the three values indicated there were no data points exerting undue influence on the model, the identified possible outlier was removed from the data and the model was run again. The model did not change in significance. As there were no reasons to believe the outlier was due to error or incorrectly measured data, and the outlier did not create nor negate a significate association, the possible outlier was included in the reported results.

Model 4: In model four, the maximum value for Cook's distance was 0.498and the maximum centered leverage value of 0.360, both under the points of concern. The maximum Mahal's distance was 24.484, greater than the chi-squared critical value of 11.07. While Cook's distance and the centered leverage value indicated that there were no data points exerting undue influence on the model, the identified possible outlier was removed from the data and the model was run again. The model did not change in significance. As there were no reasons to believe the outlier was due to error or incorrectly measured data, and the outlier did not create nor negate a significate association, the possible outlier was included in the reported results.

Subsection 5.6.2: Left Hemisphere

The same four multiple linear regression models were run with the left mPFC-PCC correlation as the dependent variable. The results are presented in Table 10, and models 3 and 4 were significant.

Linearity: Reviews of the partial scatterplots of the independent variable (age) and the dependent variable (the correlation between the PCC and mPFC in the left hemisphere) indicated linearity was not violated. Additionally, a residual plot vs age demonstrated a random horizontal band within an absolute value of 3, also indicating linearity.

Normality: Review of the S-W test for normality (SW = 0.963, df = 69, p = 0.039) and the skewness (0.289) and kurtosis (1.677) statistics suggested in aggregate that normality was not an issue. The Box-Cox power transformation was performed due to the S-W test result, and when the regression model was run again, there were no significance differences in the outcome model.

Homogeneity of variance: In models 1, 3 and 4, there was a constant spread of residuals over the range of values of the independent variables and the predicted values indicating homogeneity.

Screening for Influential Points: Model 1: In model one, the maximum value for Cook's distance was 0.400, under the point of concern. The maximum centered leverage value was 0.078, again under the point of concern. The maximum Mahal's distance was 5.30, less than the chi-squared critical value of 5.99. These values all indicated there were no data points exerting undue influence on the model.

Model 2: In model two, the maximum value for Cook's distance (0.277) and the maximum centered leverage value (0.173), did not raise any concerns. However, the maximum Mahal's distance was 11.75, greater than the chi-squared critical value of 9.49. While two of the

three values indicated there were no data points exerting undue influence on the model, the identified possible outlier was removed from the data and the model was run again. The model did not change in significance. As there were no reasons to believe the outlier was due to error or incorrectly measured data, and the outlier did not create nor negate a significate association, the possible outlier was included in the reported results.

Model 3: In model three, the maximum value for Cook's distance was 1.268, and the maximum centered leverage value was 0.393, both indicating at least one influential point. The maximum Mahal's distance was 26.725, greater than the chi-squared critical value of 9.49. The identified possible outlier was removed from the data and the model was run again. The model did not change in significance.

Model 4: In model four, the maximum value for Cook's distance was 0.960, and the maximum centered leverage value was 0.360, both under the point of concern. The maximum Mahal's distance was 24.484, greater than the chi-squared critical value of 11.07. The identified possible outlier was removed from the data and the model was run again. The model did not change in significance. As models 3 and 4 had significant outcomes, the models without the outliers and with normality corrections are also presented in Table 11.

Table 10: Models for Connectivity between mPFC and PCC

	Right mPFC-PCC					Left mPFC-PCC				
Model Summary	F	Adj R^2	p-value	Std β	p-value	F	Adj R^2	p-value	Std β	p-value
Model 1	0.891	-0.002	0.349			0.051	-0.014	0.822		
Age				0.004	0.349				0.028	0.822
Intercept				1.114	<0.001				0.998	<0.001
Model 2	1.211	0.009	0.313			2.451	0.060	0.071		
Age				0.558	0.205				1.129	**0.010**
PA Level				0.805	0.103				1.260	**0.010**
PAxAge				-1.016	0.114				-1.666	**0.009**
Intercept				0.303	0.555				-0.229	0.632
Model 3	1.695	0.300	0.177			3.510	0.100	**0.020**		
Age				0.579	0.128				1.133	**0.003**
APOE Level				1.062	0.460				1.604	**0.002**
APOExAge				-1.258	0.055				-1.999	**0.002**
Intercept				0.265	0.548				-0.242	0.553
Model 4	1.941	0.052	0.114			3.743	0.139	**0.008**		
Age				0.486	0.074				0.907	**0.001**
APOE Level				0.034	0.841				0.043	0.791
PAxAPOE				1.210	**0.016**				1.668	**0.001**
PAxAPOExAge				-1.371	**0.014**				-1.995	**0.00027**
Intercept				0.330	0.325				-0.050	0.871

Table 11: Significant Models for Connectivity of mPFC-PCC without Outliers and with Normality Corrections

	Left mPFC-PCC*					Left mPFC-PCC*				
Model Summary	F	Adj R2	p-value	Std β	p-value	F	Adj R2	p-value	Std β	p-value
Model 3	4.595	0.139	**0.006**			2.884	0.078	**0.043**		
Age				**1.287**	**0.001**				1.071	**0.005**
APOE Level				1.807	**0.001**				1.445	**0.006**
APOExAge				-2.213	**0.001**				-1.773	**0.006**
Intercept				-0.359	0.343				0.399	0.106
Model 4	4.498	0.173	**0.003**			3.160	0.114	**0.020**		
Age				0.996	**0.000**				0.889	**0.001**
APOE Level				0.103	0.525				0.033	0.842
PAxAPOE				1.738	**0.000**				1.558	**0.002**
PAxAPOExAge				-2.126	**0.0001**				-1.822	**0.001**
Intercept				-0.113	0.690				-0.510	0.094

*Without outliers.**With Box-Cox Transformation.

The results of the multiple linear regression models 3 and 4 suggest that a portion of the total variation in the long-range connectivity of the mPFC and PCC in the left hemisphere was predicted by Age, APOE level, and APOExAge in model 3, and Age, PAxAPOE, and PAxAPOExAge in model 4.

Model 3: The equation for this model was mPFC-PCC = 0.039*Age + 1.022*APOE Level – 0.031* APOExAge. For age, the unstandardized partial slope (0.039) and standardized partial slope (1.133) are statistically different from 0 (t = 3.132, df = 65, p = 0.003). For APOE Level, the unstandardized partial slope (1.022) and standardized partial slope (1.604) are significantly different from 0 (t = 3.197, df = 65, p = 0.002). For the interaction effect, the unstandardized partial slope (-0.031) and standardized partial slope (-1.999) are statistically different from 0 (t = -3.227, df = 65, p = 0.002). The model suggests there are changes in connectivity with every year increase in age, and that connectivity controlling for age would depend on APOE level, but due to multicollinearity issues with the interaction terms, it is very difficult to describe main effects. The interaction indicates that the changes in connectivity due to age are different between the APOE Levels. Further investigation of the directionality of these changes was conducted using GraphPad Prism 7.0 (results presented in Figures 4 and 5). Simple linear regression analysis revealed the carriers of the APOE-ε4 allele showed decreased connectivity by 0.016 each year while the non-carrier group did not change with age. The intercept in model 3 (which does not hold a significant meaning as it would not make sense for all the independent variables to be 0) was not statistically significantly different from 0 (t = -0.596, df = 65, p = 0.553). The R^2 value indicates that 10% of the variation in connectivity of the mPFC and PCC was predicted by age and APOE status (or level). Interpreted according to Cohen (1988), this suggests a small effect.

Model 4: The equation for this model was mPFC-PCC = 0.031*Age + 0.028*APOE Level + 0.497*PAxAPOE – 0.015* PAxAPOExAge. For age, the unstandardized partial slope (0.031) and standardized partial slope (0.907) were statistically different from 0 (t = 3.561, df = 64, p = 0.001). For APOE Level, the unstandardized partial slope (0.028) and standardized partial slope (0.043) were not significantly different from 0 (t = 0.266, df = 64, p = 0.791). For PAxAPOE, the unstandardized partial slope (0.497) and standardized partial slope (1.668) were statistically different from 0 (t = 3.586, df = 64, p = 0.001). For PAxAPOExAge, the unstandardized partial slope (-0.15) and standardized partial slope (-1.995) were significantly different from 0 (t = -3.853, df = 64, p = 0.00027). The model suggested there were changes in connectivity with every year increase in age, but that APOE level did not predict connectivity when controlling for age and PA level. The PAxAPOE interaction indicated that when controlling for age, connectivity was predicted not by APOE status alone but was predicted by the PA level in the APOE category. The PAxAPOExAge interaction indicated that the changes in connectivity due to age were different based on PA level, but depended on APOE status (or PA level). Further investigation of the directionality of these differences was conducted using GraphPad Prism 7.0 (results presented in Figures 4 and 5). Simple linear regression analysis revealed the non-carriers in the Low PA group increased connectivity by 0.0198 per year, while carriers and non-carriers in the High PA group did not have slopes different from 0 (thus showing no change in connectivity with increased age). In the High PA group, the slopes of the carriers and non-carriers did differ, but again, neither slope was different from 0. The Low PA carriers did not have a slope different from 0, and did not show differences with any other group across age. The intercept in model 4 (which does not hold a significant meaning as it would not make sense for all the independent variables to be 0) was not statistically significantly different

from 0 (t = -0.163, df = 64, p = 0.871). The R^2 value indicates that about 14% of the variation in connectivity of the mPFC and PCC was predicted by age, APOE status (or level), and PA level. Interpreted according to Cohen (1988), this suggests a small effect.

Additional Analyses: The low PA ε4 positive group only has 9 subjects all under the age of 35 years. The above analysis was redone including only subjects under the age of 35. There were no significant findings in this analysis. Additionally, a 2(APOE level) x 2(PA level) ANOVA did not reveal any significant findings when performed on all subjects or when restricted to only subjects under the age of 35.

To visually inspect the differing effects based on group, the graphs in Figure 3 and 4 and equations were generated using GraphPad Prism 7.0.

Figure 3: Correlation of left hemisphere mPFC and PCC by PA or APOE- ε4 group.

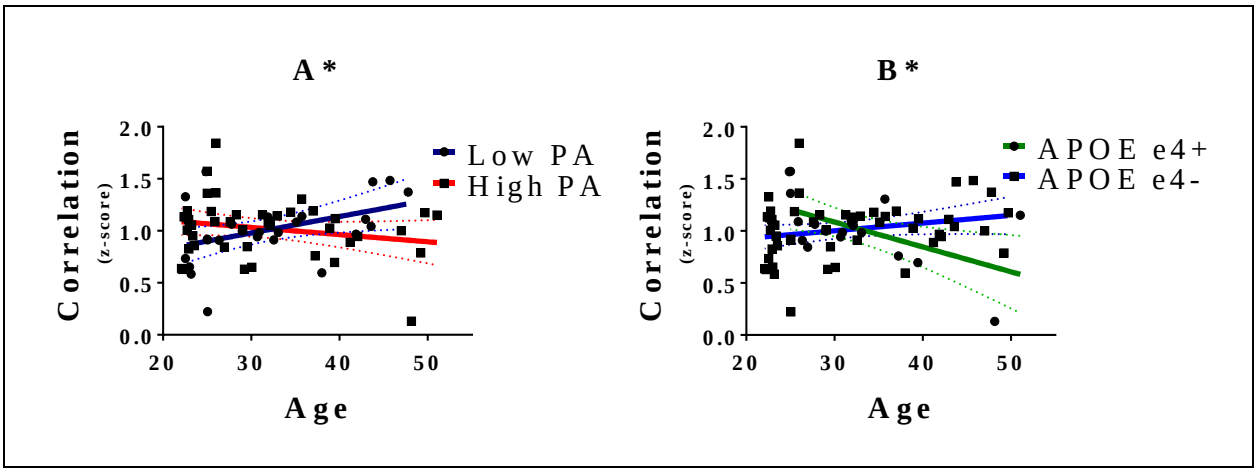

Legend: Panel A: Graphs show the linear regression line when plotting the correlation of the rs-fMRI timeseries of the mPFC and PCC in the left hemisphere versus age. Panel A: Comparing the regression lines of High and Low PA. Low PA: dark blue line and circle data points. High PA: red line and square data points. *The slopes of the two equations were significantly different (F(1,65) = 7.263, p = 0.0090) indicating the Low PA group was increasing while the High PA group was not changing. Panel B: Comparison of the regression lines of APOE-ε4 carriers and non-carriers. APOE-ε4 carriers: green line and circle data points. APOE-ε4 non-carriers: blue line and square

data points. *The slopes of the two equations were significantly different ($F(1,65) = 10.39$, $p = 0.0020$), indicating the carriers were decreasing in connectivity while the non-carriers were not changing. Both slope comparisons survived the Bonferroni correction for two comparisons ($q = 0.025$).

Equations for each group in Figure 3:

1) Low PA: $y = 0.01579x + 0.5056$

The slope was significantly different from 0 ($F(1,25) = 5.6$, $p = 0.0260$), but did not survive the correction for multiple comparisons (Bonferroni correction for 4 comparisons to 0, $q = 0.0125$)

2) High PA: $y = -0.006923x + 1.24$

   The slope was not significantly different from 0 ($F(1,40) = 1.897$, $p = 0.1761$).

3) APOE ε4 positive: $y = -0.0239x + 1.802$

   The slope was significantly different from 0 ($F(1,17) = 7.501$, $p = 0.0140$), but just missed surviving the multiple comparison correction threshold.

4) APOE ε4 negative: $y = 0.085x + 0.7295$

   The slope was not quite significantly different from 0 ($F(1,50) = 3.455$, $p = 0.0690$).

Figure 4: Effects of PA and APOE-ε4 groups on correlation of left hemisphere mPFC-PCC.

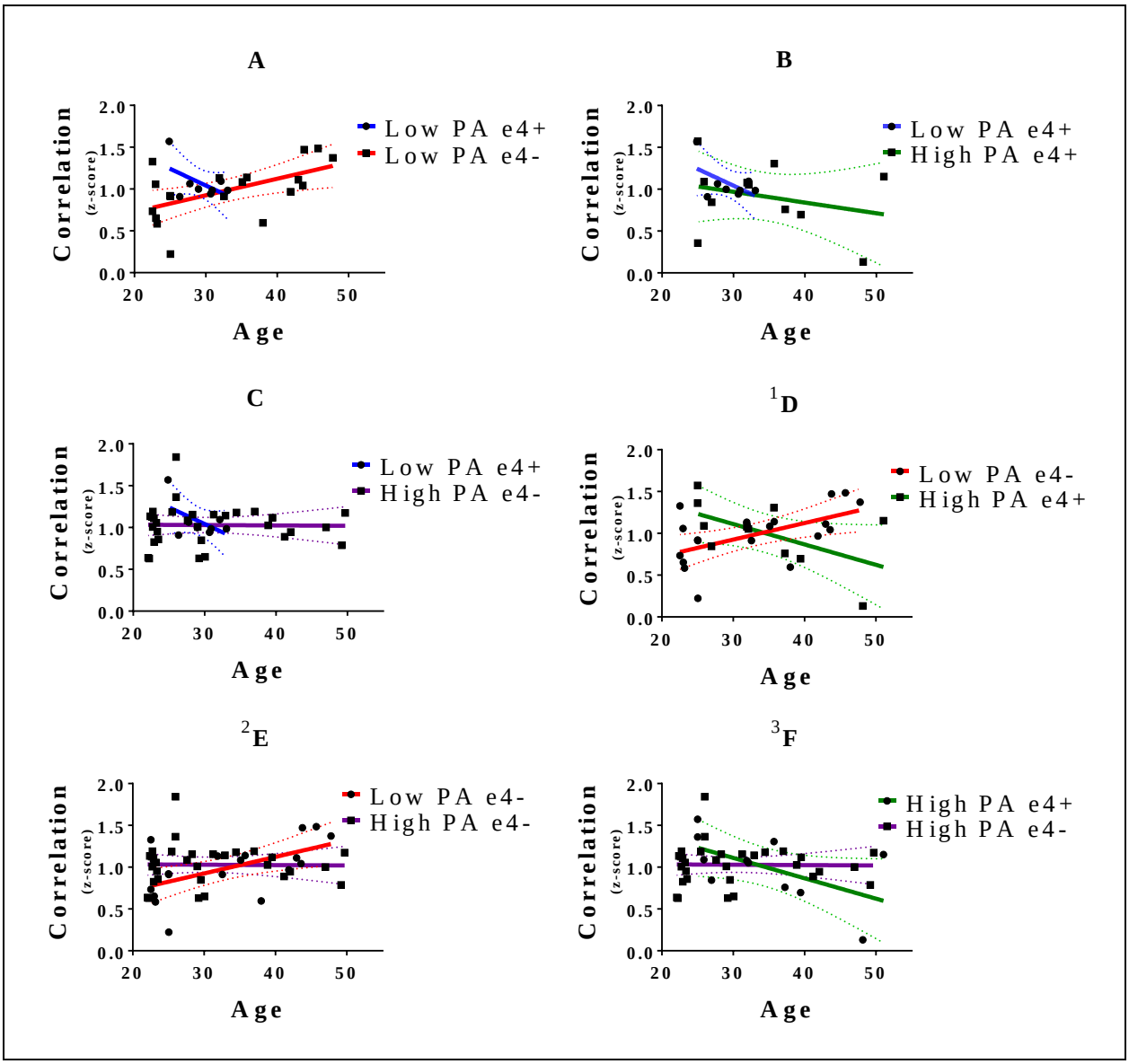

Legend: Graphs show the linear regression line when plotting the Fisher's z-transformed correlation of the rs-fMRI timeseries of the mPFC and PCC in the left hemisphere versus age. Blue line and circle data points: Low PA APOE-ε4 carriers; Red line and square data points: Low PA APOE-ε4 non-carriers; Green line square data points: High PA APOE-ε4 carriers; Purple line square data points: High PA APOE-ε4 non-carriers. Panel A: Comparing the regression lines of APOE-ε4 carriers and non-carriers in the Low PA category. The slopes of the

regression lines were not significantly different from each other ($F(1,23) = 2.929$, $p = 0.1005$); Panel B: Comparing the regression lines of APOE-ε4 carriers in the High and Low PA categories. The slopes were not significantly different from each other ($F(1,15) = 0.1768$, $p = 0.6805$); Panel C: Comparing the regression lines of Low PA APOE-ε4 carriers and High PA APOE-ε4 non-carriers. The slopes were not significantly different from each other ($F(1,35) = 1.501$, $p = 0.2287$); Panel D: Comparing the regression lines of Low PA APOE-ε4 non-carriers and High PA APOE-ε4 carriers. [1]The slopes were significantly different from each other ($F(1,26) = 11.51$, $p = 0.0022$); Panel E: Comparing the regression lines of APOE-ε4 non-carriers with High and Low PA levels. [2]The slopes were significantly different from each other ($F(1,46) = 5.472$, $p = 0.0237$); Panel F: Comparing the regression lines of APOE-ε4 carriers and non-carriers in the High PA category. [3]The slopes were significantly different from each other ($F(1,38) = 4.597$, $p = 0.0385$). The Bonferroni corrected significance level for 6 comparisons was $p = 0.008$.

The following equations were generated for each line in Figure 4:

1) Low PA ε4 positive: $y = -0.03971x + 2.234$

The slope was not significantly different from 0 ($F(1,6) = 2.449$, $p = 0.1686$).

2) Low PA ε4 negative: $y = 0.01981x + 0.3304$

The slope was significantly different from 0 ($F(1,17) = 7.755$, $p = 0.0127$) and just missed surviving the multiple comparison correction threshold ($p = 0.0125$).

3) High PA ε4 positive: $y = -0.0244x + 1.843$

The slope was not significantly different from 0 ($F(1,9) = 4.229$, $p = 0.0669$).

4) High PA ε4 negative: $y = -0.0004362x + 1.042$

The slope was not significantly different from 0 ($F(1,29) = 0.006761$, $p = 0.9350$).

Section 5.7: DMN Hubs

Four models were used to explain the node strength of four identified hubs of the DMN: bilateral precuneus and bilateral PCC. The assumptions of linearity, normality, homogeneity of variance, and screening for influential points were examined. None of the models reached significance (results presented in Table 13). There were no changes in significance of the models when an assumption appeared to be violated and then appropriately accounted for in the model.

Linearity: Reviews of the partial scatterplots of the independent variable (age) and the dependent variables (node strength of the left and right precuneus, left and right PCC) indicated linearity was not violated. Additionally, a residual plot vs age demonstrated a random horizontal band within an absolute value of 3, also indicating linearity, with one data point consistently as an exception.

Normality: Review of the S-W test for normality and the skewness and kurtosis statistics [right hemisphere: precuneus (SW = 0.834, df = 69, $p < 0.001$; skewness (1.774); kurtosis (3.669)); PCC (SW = 0.833, df = 69, $p < 0.001$; skewness (1.742); kurtosis (3.429)); left hemisphere: precuneus (SW = 0.810 df = 69, $p < 0.001$; skewness (2.026); kurtosis (5.243)); PCC (SW = 0.817, df = 69, $p < 0.001$; skewness (2.137); kurtosis (6.494))] statistics suggested in aggregate that normality was an issue (skewness statistic was in acceptable range for the right hemisphere precuneus and PCC). The Box-Cox power transformation was performed to normalize the data, but when the regression models were run again, there were no significance differences in the outcome models.

Homogeneity of variance: When examining the models explaining the node strength of the 4 identified hubs of the DMN, there was a constant spread of residuals over the range of values

of the independent variables and the predicted values indicating homogeneity. However, there were some minor deviations in some graphs. In the left precuneus and right PCC models, model 3 had a larger spread at smaller independent variable values when graphing APOExAge vs. residuals, and the same was true in model 4 when graphing APOExPAxAge vs. residuals. In the left PCC, model 2 had a larger spread of residuals at lower independent variable values when graphing vs. age and PAxAge. This was also true in model 4 when graphing residuals vs. APOExPAxAge. While the graphs did not indicate major violations of the homogeneity of variance, there may be an increased likelihood of type II error.

Screening for Influential Points: Table 12 presents Cook's distance, centered leverage values, and Mahal's distance (and the chi-squared critical values to compare to the Mahal's distance). In model one, all values indicated that there were no data points exerting undue influence. However, in models 2, 3, and 4, Mahal's distance was greater than the critical value. The models were re-run with the identified outlier removed, but all the models remained non-significant. As there were no reasons to believe the outlier was due to error or incorrectly measured data, and the outlier did not create nor negate a significate association, the possible outlier was included in the reported results.

Table 12: Influential Points Statistics for DMN

	Cook's Distance	Centered Leverage	Mahal's Distance	Chi^2 Critical Value
Model 1		0.078	5.302	5.990
R Precuneus	0.194			
R PCC	0.186			
L Precuneus	0.226			
L PCC	0.251			
Model 2		0.173	11.749	9.490
R Precuneus	0.169			
R PCC	0.169			
L Precuneus	0.195			
L PCC	0.251			
Model 3		0.393	26.725	9.490
R Precuneus	0.376			
R PCC	0.386			
L Precuneus	0.478			
L PCC	0.511			
Model 4		0.360	24.484	11.070
R Precuneus	0.563			
R PCC	0.536			
L Precuneus	0.697			
L PCC	0.770			

Table 13: Node Strength in the DMN.

	Right Precuneus					Left Precuneus				
Model Summary	F	Adj R^2	p-value	Std β	p-value	F	Adj R^2	p-value	Std β	p-value
Model 1	0.398	-0.009	0.530			0.604	-0.006	0.440		
Age				-0.077	0.530				-0.095	0.440
Intercept				51.645	<0.001				52.525	<0.001
Model 2	0.940	0.042	0.426			0.866	0.038	0.463		
Age				-0.096	0.828				-0.170	0.701
PA Level				-0.205	0.678				-0.250	0.612
PAxAge				0.021	0.974				0.107	0.867
Intercept				67.165	0.087				71.554	0.070
Model 3	2.255	0.052	0.900			1.581	0.025	0.202		
Age				0.702	0.063				0.588	0.123
APOE Level				1.256	0.017				1.055	0.047
APOExAge				-1.417	0.029				-1.239	0.059
Intercept				-23.884	0.467				-11.128	0.739
Model 4	1.348	0.020	0.262			0.866	-0.008	0.490		
Age				0.283	0.302				0.202	0.467
APOE Level				0.293	0.095				0.209	0.239
PAxAPOE				0.474	0.343				0.382	0.450
PAxAPOExAge				-0.814	0.146				-0.666	0.239
Intercept				10.691	0.677				21.018	0.421
	Right Posterior Cingulate Cortex					Left Posterior Cingulate Cortex				
	F	Adj R^2	p-value	Std β	p-value	F	Adj R^2	p-value	Std β	p-value
Model 1	0.495	-0.007	0.484			0.499	-0.007	0.482		
Age				-0.086	0.484				-0.086	0.482
Intercept				47.305	<0.001				44.834	<0.001
Model 2	0.350	0.016	0.789			1.162	0.007	0.331		
Age				-0.147	0.742				0.202	0.646
PA Level				-0.158	0.752				0.139	0.777
PAxAge				0.090	0.890				-0.443	0.488
Intercept				58.717	0.121				34.965	0.337
Model 3	1.545	0.023	0.211			2.011	0.043	0.121		
Age				0.614	0.108				0.592	0.117
APOE Level				1.061	0.046				1.133	0.032
APOExAge				-1.268	0.054				-1.237	0.057
Intercept				-13.697	0.667				-19.168	0.536
Model 4	0.645	0.039	0.633			1.807	0.045	0.138		
Age				0.227	0.417				0.290	0.283
APOE Level				0.129	0.468				0.355	0.042
PAxAPOE				0.505	0.323				0.445	0.367
PAxAPOExAge				-0.708	0.214				-0.850	0.124
Intercept				16.701	0.505				3.890	0.870

Section 5.8: FPN Hubs

Four models were used to explain the node strength of four identified hubs of the FPN: bilateral dorsal and lateral PFC. The assumptions of linearity, normality, homogeneity of variance, and screening for influential points were examined. None of the models reached significance (results presented in Table 15). There were no changes in significance of the models when an assumption appeared to be violated and then appropriately accounted for in the model.

Linearity: Reviews of the partial scatterplots of the independent variable (age) and the dependent variables (node strength of the left and right d-PFC and l-PFC) indicated linearity was not violated. Additionally, a residual plot vs age demonstrated a random horizontal band within an absolute value of 3, also indicating linearity, with one data point as an exception in all but the right dorsal PFC.

Normality: Review of the S-W test for normality and the skewness and kurtosis statistics [right hemisphere: dorsal PFC (SW = 0.864, df = 69, $p < 0.001$; skewness (1.460); kurtosis (2.040)); lateral PFC (SW = 0.904, df = 69, $p < 0.001$; skewness (1.498); kurtosis (4.350)); left hemisphere: dorsal PFC (SW = 0.877 df = 69, $p < 0.001$; skewness (1.609); kurtosis (3.833)); lateral PFC (SW = 0.845, df = 69, $p < 0.001$; skewness (1.922); kurtosis (5.654))] statistics suggested in aggregate that normality was an issue (only skewness statistic remains in acceptable range). The Box-Cox power transformation was performed to normalize the data, but when the regression models were run again, there were no significance differences in the outcome models.

Homogeneity of variance: When examining the models explaining the node strength of the 4 identified hubs of the FPN, there was a constant spread of residuals over the range of values of the independent variables and the predicted values indicating homogeneity. However, there were

some minor deviations in some graphs. In the bilateral dorsal PFC models, model 2 had a larger spread at smaller independent variable values when graphing age and PAxAge vs. residuals, and the same was true in model 3 when graphing APOExAge vs. residuals. The right dorsal PFC model 4 also had the same larger spread at smaller independent variable values when graphing residuals vs. APOExPAxAge. While the graphs did not indicate major violations of the homogeneity of variance, there may be an increased likelihood of type II error.

Screening for Influential Points: Table 14 presents Cook's distance, centered leverage values, and Mahal's distance (and the chi-squared critical values to compare to the Mahal's distance). In model one, all values indicated that there were no data points exerting undue influence. However, in models 2, 3, and 4, Mahal's distance was greater than the critical value. The models were re-run with the identified outlier removed, but no model changed in significance findings. The results remained nonsignificant, and the possible outlier was included in the results.

Table 14: Influential Points Statistics for FPN.

	Cook's Distance	Centered Leverage	Mahal's Distance	Chi^2 Critical Value
Model 1		0.078	5.302	5.990
R d-PFC	0.130			
R l-PFC	0.229			
L d-PFC	0.211			
L l-PFC	0.257			
Model 2		0.173	11.749	9.490
R d-PFC	0.170			
R l-PFC	0.205			
L d-PFC	0.178			
L l-PFC	0.213			
Model 3		0.393	26.725	9.490
R d-PFC	0.171			
R l-PFC	0.467			
L d-PFC	0.409			
L l-PFC	0.540			
Model 4		0.360	24.484	11.070
R d-PFC	0.295			
R l-PFC	0.680			
L d-PFC	0.587			
L l-PFC	0.775			

Table 15: Node Strength in the FPN.

	Right Dorsal PFC					Left Dorsal PFC				
Model Summary	F	Adj R^2	p-value	Std β	p-value	F	Adj R^2	p-value	Std β	p-value
Model 1	1.204	0.003	0.276			1.289	0.004	0.260		
Age				-0.133	0.276				-0.137	0.260
Intercept				50.131	<0.001				47.037	<0.001
Model 2	1.194	0.052	0.319			0.994	0.000	0.401		
Age				-0.217	0.621				-0.051	0.907
PA Level				-0.274	0.576				-0.055	0.912
PAxAge				0.120	0.851				-0.136	0.831
Intercept				68.987	0.053				50.997	0.172
Model 3	2.055	0.044	0.115			2.575	0.065	0.061		
Age				0.452	0.230				0.472	0.205
APOE Level				1.015	0.054				1.091	0.037
APOExAge				-1.070	0.099				-1.116	0.082
Intercept				-5.394	0.857				-15.730	0.614
Model 4	1.599	0.091	0.185			1.884	0.049	0.124		
Age				0.097	0.720				0.194	0.471
APOE Level				0.356	0.042				0.340	0.050
PAxAPOE				0.185	0.709				0.463	0.347
PAxAPOExAge				-0.521	0.346				-0.759	0.168
Intercept				21.691	0.350				5.786	0.810
	Right Lateral PFC					Left Lateral PFC				
	F	Adj R^2	p-value	Std β	p-value	F	Adj R^2	p-value	Std β	p-value
Model 1	0.062	-0.014	0.804			0.016	-0.015	0.901		
Age				0.030	0.249				0.015	0.901
Intercept				43.975	<0.001				43.611	<0.001
Model 2	0.521	-0.022	0.669			0.612	-0.017	0.610		
Age				0.215	0.629				0.294	0.509
PA Level				0.072	0.885				0.174	0.725
PAxAge				-0.285	0.659				-0.427	0.509
Intercept				39.080	0.269				31.174	0.399
Model 3	1.467	0.020	0.232			1.487	0.021	0.226		
Age				0.569	0.137				0.673	0.079
APOE Level				0.947	0.075				1.064	0.046
APOExAge				-0.985	0.132				-1.197	0.069
Intercept				-7.188	0.810				-16.767	0.594
Model 4	1.273	0.016	0.290			1.132	0.008	0.349		
Age				0.334	0.225				0.376	0.175
APOE Level				0.324	0.066				0.270	0.126
PAxAPOE				0.369	0.460				0.481	0.339
PAxAPOExAge				-0.689	0.218				-0.814	0.148
Intercept				9.934	0.667				5.968	0.806

Section 5.9: Hippocampus Subsections

Four models were used to explain the node strength of the three subsections of the hippocampus in both hemispheres: head, body, and tail. The assumptions of linearity, normality, homogeneity of variance, and screening for influential points were examined. None of the models reached significance (results presented in Table 17). There were no changes in significance of the models when an assumption appeared to be violated and then appropriately accounted for in the model.

Linearity: Reviews of the partial scatterplots of the independent variable (age) and the dependent variables (node strength of the head, body, and tail of the hippocampus in both hemispheres) indicate linearity was not violated. Additionally, a residual plot vs age demonstrated a random horizontal band within an absolute value of 3, also indicating linearity, with one data point as an exception in in the left body and tail and right tail.

Normality: Review of the S-W test for normality and the skewness and kurtosis statistics [right hemisphere: head (SW = 0.956, df = 69, p = 0.016; skewness (0.724); kurtosis (0.208)); body (SW = 0.897, df = 69, p < 0.001; skewness (1.428); kurtosis (3.284)); tail (SW = 0.924, df = 69, p < 0.001; skewness (1.126); kurtosis (1.681)); left hemisphere: head (SW = 0.945 df = 69, p = 0.004; skewness (0.880); kurtosis (0.680)); body (SW = 0.897, df = 69, p < 0.001; skewness (1.428); kurtosis (3.284)); tail (SW = 0.910, df = 69, p < 0.001; skewness (1.247); kurtosis (2.718))] statistics suggested in aggregate that normality was an issue (only skewness statistic remains in acceptable range, and kurtosis is in range for the right head, tail, and left head). The Box-Cox power transformation was performed to normalize the data, but when the regression models were run again, there were no significance differences in the outcome models.

Homogeneity of variance: When examining the models explaining the node strength of the 4 identified hubs of the FPN, there was a constant spread of residuals over the range of values of the independent variables and the predicted values indicating homogeneity. However, in the left tail there was a wider spread of residuals when graphing vs. APOExAge at smaller independent variable values. While the graph did not indicate a major violation of the homogeneity of variance, there may be an increased likelihood of type II error.

Screening for Influential Points: Table 16 presents Cook's distance, centered leverage values, and Mahal's distance (and the chi-squared critical values to compare to the Mahal's distance). In model one, all values indicated that there were no data points exerting undue influence. However, in models 2, 3, and 4, Mahal's distance was greater than the critical value. The models were re-run with the identified outlier removed, but no model changed in significance findings. The results remained nonsignificant, and the possible outlier was included in the results.

Table 16: Influential Points Statistics for Hippocampal Subsections.

	Cook's Distance	Centered Leverage	Mahal's Distance	Chi^2 Critical Value
Model 1		0.078	5.302	5.990
R Head	0.138			
R Body	0.128			
R Tail	0.120			
L Head	0.143			
L Body	0.206			
L Tail	0.184			
Model 2		0.173	11.749	9.490
R Head	0.160			
R Body	0.142			
R Tail	0.148			
L Head	0.166			
L Body	0.156			
L Tail	0.137			
Model 3		0.393	26.725	9.490
R Head	0.213			
R Body	0.233			
R Tail	0.156			
L Head	0.235			
L Body	0.446			
L Tail	0.402			
Model 4		0.360	24.484	11.070
R Head	0.284			
R Body	0.352			
R Tail	0.105			
L Head	0.269			
L Body	0.537			
L Tail	0.427			

Table 17: Node Strength of Hippocampal Subsections

	Right Head					Right Body					Right Tail				
Model Summary	F	Adj R2	p-value	Std β	p-value	F	Adj R2	p-value	Std β	p-value	F	Adj R2	p-value	Std β	p-value
Model 1	0.052	-0.014	0.819			0.002	-0.015	0.962			1.825	0.012	0.181		
Age				-0.028	0.819				-0.006	0.962				-0.163	0.181
Intercept				23.713	<0.001				24.796	<0.001				26.629	<0.001
Model 2	0.599	-0.018	0.618			0.359	-0.029	0.783			1.585	0.025	0.202		
Age				0.523	0.241				0.151	0.735				-0.501	0.251
PA Level				0.592	0.235				0.061	0.902				-0.556	0.254
PAxAge				-0.835	0.199				-0.243	0.709				0.505	0.425
Intercept				-1.579	0.943				22.315	0.290				51.442	0.025
Model 3	0.765	-0.010	0.518			2.419	0.059	0.074			1.073	0.003	0.367		
Age				0.487	0.208				0.907	0.017				-0.053	0.889
APOE Level				0.668	0.213				1.382	0.009				0.303	0.568
APOExAge				-0.926	0.163				-1.655	0.011				-0.209	0.750
Intercept				1.040	0.957				-19.588	0.264				15.897	0.423
Model 4	0.716	-0.017	0.584			1.346	0.020	0.263			1.972	0.054	0.109		
Age				0.341	0.222				0.455	0.099				-0.300	0.265
APOE Level				0.023	0.896				0.230	0.188				0.389	0.025
PAxAPOE				0.579	0.256				0.667	0.184				-0.621	0.207
PAxAPOExAge				-0.823	0.148				-1.039	0.065				0.322	0.556
Intercept				7.208	0.624				0.085	0.995				29.174	0.052
	Left Head					Left Body					Left Tail				
	F	Adj R2	p-value	Std β	p-value	F	Adj R2	p-value	Std β	p-value	F	Adj R2	p-value	Std β	p-value
Model 1	2.373	0.020	0.128			2.552	0.022	0.115			0.157	-0.013	0.693		
Age				-0.185	0.128				-0.192	0.115				-0.048	0.693
Intercept				31.620	<0.001				32.565	<0.001				21.658	0.003
Model 2	2.136	0.048	0.104			1.941	0.040	0.132			1.771	0.033	0.161		
Age				0.633	0.144				0.528	0.224				0.747	0.088
PA Level				0.931	0.056				0.861	0.077				1.037	0.035
PAxAge				-1.238	0.051				-1.086	0.087				-1.199	0.060
Intercept				-4.514	0.816				-5.998	0.789				-29.988	0.233
Model 3	1.442	0.019	0.239			2.238	0.052	0.092			1.144	0.006	0.338		
Age				0.279	0.462				0.514	0.171				0.602	0.118
APOE Level				0.726	0.171				1.033	0.049				0.938	0.080
APOExAge				-0.843	0.197				-1.277	0.049				-1.176	0.075
Intercept				9.258	0.588				-4.173	0.830				-15.399	0.486
Model 4	1.614	0.035	0.182			2.029	0.057	0.101			2.010	0.056	0.104		
Age				0.283	0.298				0.364	0.177				0.566	0.038
APOE Level				0.079	0.647				0.035	0.837				-0.116	0.498
PAxAPOE				0.876	0.080				1.056	0.034				1.364	0.007
PAxAPOExAge				-1.065	0.057				-1.261	0.023				-1.404	0.012
Intercept				7.944	0.542				1.817	0.903				-15.563	0.348

Chapter 6: Discussion

In this study, we used rs-fMRI (resting state fMRI) and graph theory to investigate whether age, PA, APOE-ε4, and the interactions of these variables predict global efficiency, long-range connectivity in the DMN, node strength of hubs in the DMN, FPN, and the subsections of the hippocampus in young adulthood to middle adulthood. We aimed to determine if the selected metrics could capture differences in brain function depending on PA level and genetic risk for AD. We hoped to add to the literature of how PA protects cognition by describing the natural adaptations to resting state networks, even in those with genetic risk for AD, prior to declines in cognitive abilities. By understanding the connectivity patterns, we may better predict future cognitive changes, but the current study only begins to address this question.

While our results do not comprehensively describe and capture brain alterations prior to cognitive decline, we did gain insights into how changes in the functional connectivity of the mPFC-PCC relate to meeting health requirements of PA and genetic risk. Our findings raise awareness that PA and APOE genotype may alter the time-course of compensatory increased functional connectivity of this connection, and effective protective interventions in individuals will either increase or decrease connectivity depending on the relationship between the time of treatment implementation and the point of compensatory increased functional connectivity. Due to the dependency of expected outcomes on this time-course, PA and APOE genotype must be included when using rs-fMRI as an outcome measurement of intervention or clinical trials in AD research. Precision medicine is a medical model utilizing environment, lifestyle, and biology to design specific prevention and treatment strategies to treat an individual, and our findings will assist in identifying target populations and expected outcomes on connectivity by informing

expectations of functional connectivity patterns of the mPFC-PCC and how they relate to PA and APOE genotype.

We began the study with the following specific aims:

Specific Aim 1: To investigate the association of self-reported leisure-time PA on the fronto-parietal network, DMN, and hippocampal connectivity in young adulthood to middle adulthood.

Specific Aim 2: To investigate the association of the interaction of PA and APOE-ε4 status on the fronto-parietal network, DMN, and hippocampal connectivity from young adulthood to middle adulthood.

We had several hypotheses related to each aim, but we will begin this discussion with the significant findings and address possible reasons for the non-findings in the following sections.

Section 6.1: Findings on Connectivity of the mPFC-PCC in the Left Hemisphere

Specific Aim 1: Hypothesis 4: Subjects who meet the weekly recommendations for moderate to vigorous intensity PA will show greater connectivity between the mPFC and PCC than the low PA group across the entire age range.

In our analysis, Model 2 with the mPFC-PCC as the dependent variable was designed to test Specific Aim 1, hypothesis 4. While this model did not quite reach significance, a subsequent analysis using PAxAge as the sole predictor found in the Low PA group, each year increase in age corresponded with a 0.016 increase in connectivity. The High PA group was found to have a slope not different from zero indicating there were not changes in connectivity due to age in this sample. However, as the slopes did significantly differ from each other, we could not test the elevations of the lines and a *post hoc ANOVA* did not reveal any difference between the means of the High and Low PA groups. Thus, our results indicated that the High PA group did not have a

greater correlation of the mPFC-PCC in the left hemisphere as we had expected. This finding caused us to review our earlier expectations, and while in advanced aging the correlation of these brain regions was positively correlated with episodic memory performance (Andrews-Hanna et al., 2007; Zhao et al., 2012), this may not be the case in young adults. We further discuss the renewed look at our results in terms of CR and underlying biological mechanisms in future sections.

> ***Specific Aim 2: Hypothesis 4:*** APOE-ε4 carriers with levels of PA that meet the weekly recommendations for moderate to vigorous intensity PA will have connectivity measures that are not different from the non-carriers who meet the recommendations for moderate to vigorous intensity PA.

When we ran Model 3 with the mPFC-PCC as the dependent variable, there were main effects of age and APOE level, but the interaction revealed that carriers decreased in connectivity while the non-carriers did not have a regression slope different from zero (we focus on the interaction predictors because of the multicollinearity issue). This indicated an apparent downward trajectory for the carriers and a horizontal trajectory for the non-carriers. Model 4 investigated the interactive effects of PA and APOE, directly testing Specific Aim 2, Hypothesis 4. We found the carriers and non-carriers in the High PA category did have different slopes of the regression lines. However, neither the slope for the carriers nor the slope for the non-carriers was different from zero, indicating horizontal trajectories for those with High PA regardless of APOE status. The Low PA non-carriers had positive slope indicating increased connectivity with age, and this trajectory was significantly different from both the carriers and non-carriers in the High PA category. The Low PA carriers did not have a slope different from zero, nor did the slope differ from any other group. However, we believe this is due to limitations in our data

(discussed in later sections) and not a representation of the trajectory of this group across our age range. Thus, we did find that carriers and non-carriers had horizontal trajectories in our age range while the Low PA non-carriers increased. It is harder to determine if there is a difference between carriers based on PA levels, but we have explanations of our data in relation to other studies in the following section.

Section 6.2: Findings and Relationship to Cognitive Reserve Theory

In the cognitive reserve (CR) theory, neural compensation is the recruitment of alternate neural networks to perform the same cognitive processes that were disrupted due to pathology or age related changes, but this may occur in conjunction with improved or unchanged cognitive performance – an indication of maintenance (Barulli & Stern, 2013). Rs-fMRI functional connectivity has the potential to be a unique tool to measure these compensatory recruitments. Currently, using rs-fMRI in relation to CR is not a customary practice, despite the apparent advantages to interpretation. The compensation neural mechanism underlying CR is frequently studied using brain activation during a cognitive task, yet brain changes and aging both increase subjective difficulty (Barulli & Stern, 2013), and thus it is difficult to find the appropriate task and level of difficulty that would be comparable across a wide range of individuals. The paradigms chosen are often very simple cognitive tasks that do not reflect experiences outside the scanner. Functional connectivity analysis using rs-fMRI data is advantageous because it does not rely on task or performance, but is rather an observational capture of spontaneous neuronal activity reflecting brain communication regardless of the undertaken task. Another benefit to using rs-fMRI is the promise of being an early biomarker of brain changes, and this early detection before the onset of cognitive decline is critical to the development of treatments to prevent AD (Albert et al., 2011).

The left PCC is a prominent hub of the DMN (Buckner et al., 2009), and it is possible the differences in the projected trajectories of the connectivity of this hub with the mPFC is reflective of the compensatory time-course in our participants based on the interactions of PA level and APOE status. Unfortunately, the current study is cross-sectional in design, and there are no longitudinal measurements of changes in cognitive performance. We cannot with certainty claim increased connectivity of the mPFC-PCC was correlated with improved or maintained cognition and thus meeting the criteria for a compensatory response. Interestingly, these regions do overlap with the significant areas of the PA main effect and PAxAPOE-ε4 status interactions on semantic memory in the Smith et al. (2011) fMRI study. Additionally, a recently published study (Weng et al., 2017) endeavored to uncover the neural mechanisms underlying PA protective effects on cognition using core networks as seeds in a rs-fMRI analysis, and the PCC was included in the core network for the DMN. After an acute bout of moderate intensity exercise, these researchers found there were transient increases in correlation of the spontaneous BOLD signal of the core DMN with several regions including the mPFC, thus again overlapping with the connection we found to have significance in the current study. It may be that these transient increases of connectivity lay the groundwork for future compensatory recruitment as concurrent activation induces white matter connections between brain regions (Sporns, 2011).

Figure 5 is an illustration expanding upon the CR construct provided by Barulli and Stern (2013) to elucidate the timing of different events preceding cognitive decline and the relationship between levels of cognitive reserve, cognition status, and functional connectivity of the mPFC-PCC. The CR model published by Barulli and Stern (2013) is one of several models attempting to describe the adaptations and workings of the brain, but one of the other prominent theories is the STAC model by Reuter-Lorenz and Park (2014). This theory proposes the recruitment of

alternate networks and the reorganization of functional connections to maximize performance (such as in learning) or to minimize impact on cognition due to brain changes is a property of the brain at all stages of life. While some proponents of this model claim it differs from CR theory, we view the STAC model as a detailed description of how life-long exposures build up CR to better adapt to normal aging or pathology as well as conceivably reducing the rate of these alterations (Barulli & Stern, 2013). PA is one of the life experiences that has been shown to increase CR (Stern, 2006), and our measurement of the mPFC-PCC connectivity in the left hemisphere appeared to be the most sensitive to the timing of neural compensation processes in our sample. Future studies will need to investigate other resting state connections and graph metrics to determine the dynamic patterns preceding cognitive changes and dementia in individuals with differing levels of CR as well as confirm the validity of the proposed model in Figure 5.

Figure 5: Adaptation of the CR mediation role with AD pathology and clinical diagnosis.

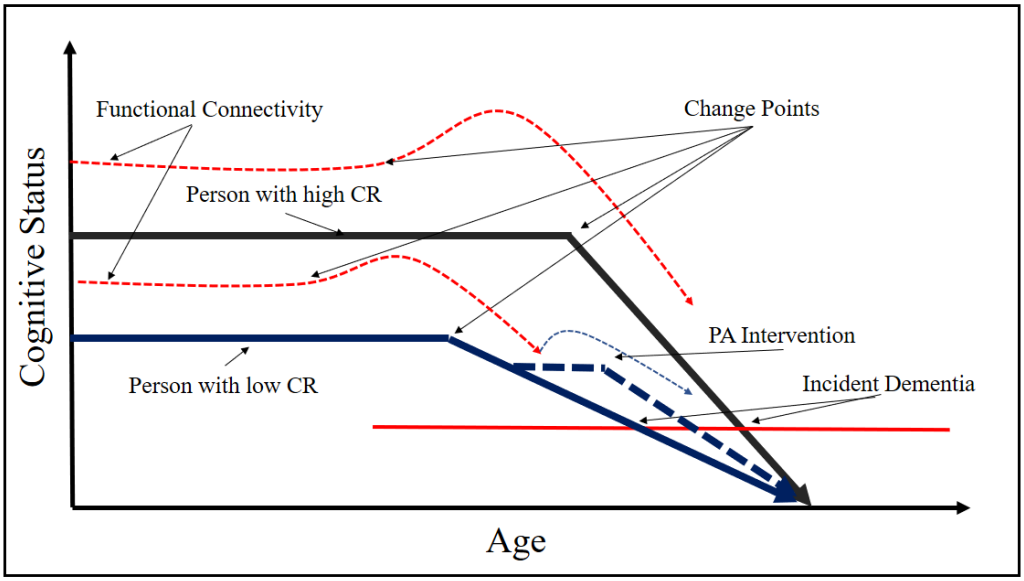

Adaptation of the CR mediation role with AD pathology and clinical expression presented by model presented by Barulli and Stern (2013). The x-axis in this model indicates time progression, and age-related changes as well as increases of AD neuropathology occur along this continuum. Cognitive function is reflected along the y-axis, and the higher the CR, the more AD pathology and age-related changes are needed before the change points (Amieva et al., 2005; Hall et al., 2007) and clinical diagnostic criteria are met for AD. While it is likely that these concurrent brain changes progress at different rates, once the change point is reached, the decline of cognition is more rapid in the person with higher CR (Hall et al., 2007; Stern, 2006) due to the evidence that AD pathology will be more severe (Ewers, Insel, Stern, Weiner, & (ADNI), 2013; Stern, Alexander, Prohovnik, & Mayeux, 1992). The new additions to this model are the superimposed red dotted lines indicating the proposed connectivity of the mPFC-PCC in relation to cognitive changes. The connectivity pattern is placed on the graph in relation to the solid line indicating cognitive status and is not related to the y axis. Increases in connectivity occur prior to changes in cognition, and the pattern would explain the direction of the regression lines in the current study. The blue dotted line illustrates what we hypothesize would occur (based on our Chirles et al. 2017 study) as a result of a PA intervention in an individual already experiencing cognitive decline.

In a prior study, we demonstrated evidence that PA interventions in older adults with MCI aid in the recruitment of alternate brain networks to protect against cognitive decline (Chirles et al., 2017). After 12 weeks of walking, a seed region including part of the PCC

increased connectivity with frontal regions in the participants diagnosed with MCI while there were no effects in the healthy elders. Interpreting these results as they relate to CR, the participants in the MCI group had already experienced enough brain changes to exhaust the compensatory increased connectivity of the PCC region with frontal areas (evidenced by the declines in cognitive abilities). The PA intervention enabled compensatory responses of the PCC to function again and protect cognition by delaying the downward connectivity trajectory. While also speculative, we interpreted the non-findings in our healthy elders to be consistent with our assertion that higher levels of CR (assumed to be true as the healthy elders were of the same age as the MCI group yet were not exhibiting cognitive decline) would prolong the period of effective compensation. While the PA intervention did not increase the connectivity of the PCC in our healthy elders, it may have additionally prolonged the effective compensatory period. Future intervention studies need to confirm these theoretical explanations by measuring rates of cognitive decline and incidence of dementia over the course of several years.

The current study's findings also fit into the model explained in Figure 5, and proposed connectivity trajectories captured in the current study are presented in Figure 6. The fact that our High PA subjects did not show any connectivity changes in the left hemisphere corresponds with the horizontal line segment of functional connectivity preceding the change point indicated with arrows. PA increases CR (we describe potential mechanisms in the Biological Plausibility section), and we hypothesize the amount of brain changes due to age (as they are younger than 50 years) and any existing pathology in these subjects does not yet require adaptation (proposed connectivity pattern Fig.6, Panel B). We assume our Low PA group has lower levels of CR, and thus would have a change point in connectivity preceding a change in cognition earlier than the High PA group. Our results support this as the Low PA non-carriers do show greater

connectivity as a function of age (proposed connectivity pattern Fig. 6, Panel C). APOE-ε4 carriers have been shown to have greater amounts of amyloid burden than age-matched non-carriers (Morris et al., 2010), and brain regions first exhibiting these deposits are associated with earlier compensatory mechanisms evidenced by increased connectivity and subsequent loss of connectivity (Buckner et al., 2009; Hillary et al., 2015). The current study results indicated the APOE-ε4 carriers decreased connectivity with age, and it is possible that our older carriers were indicating the loss of connectivity preceding cognitive decline. However, the linear regression models employed in this study would not detect non-linear relationships and would miss if there were an increase in connectivity prior to the decrease in connectivity (proposed connectivity pattern Fig. 6, Panel D). Regardless, we do not feel a loss of connectivity adequately explains our results as we did find the High PA carriers did not have slopes, as a function of age, that were significantly different from zero. Our Low PA carriers were all younger than 32 years, and thus only carriers with High PA made up the data points at the older end of our age range. It is possible that our Low PA carriers were exhibiting increased connectivity due to compensatory mechanisms, even at this early age, while the High PA carriers had a horizontal trajectory, indicating functional connections that did not yet require compensation (compensatory activations have been previously reported in young APOE-ε4 carriers (Matura et al., 2014)). The two trajectories superimposed upon each other would indicate a negative slope across our study's age range in APOE-ε4 carriers (proposed connectivity pattern, Fig. 6, Panel E). This interpretation of our results would suggest functional connectivity evidence that PA can mitigate the increased risk of decreased connectivity in APOE-ε4 carriers. However, this is an interpretation that will need to be confirmed with future studies.

Figure 6: Proposed progression along the general functional connectivity pattern of the left mPFC-PCC related to levels of CR that would explain the results of the multiple linear regression analysis.

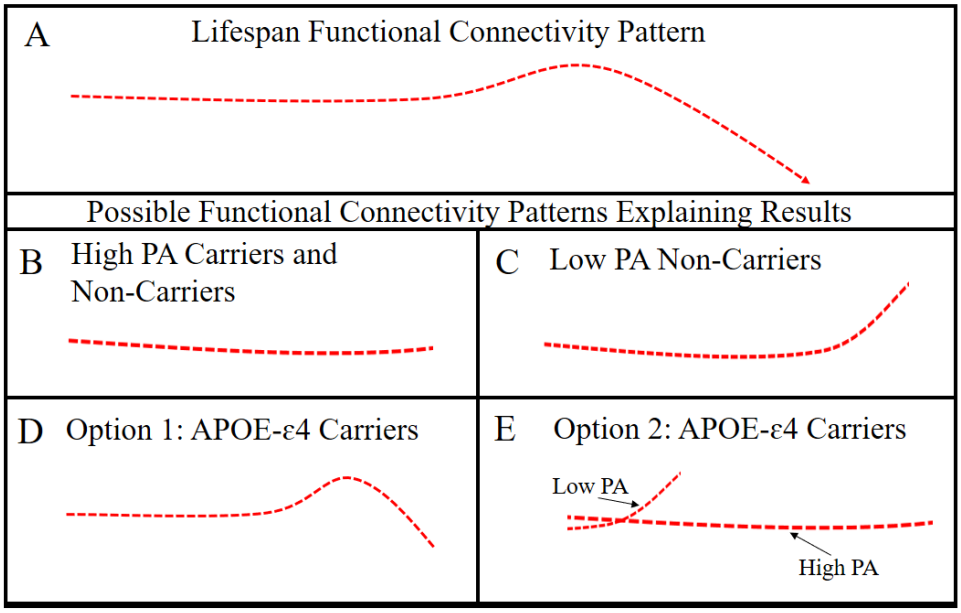

A) Lifespan functional connectivity pattern: changes in cognition are preceded by changes in connectivity. B) The High PA carriers and non-carriers have enough neural reserve to not yet require compensatory recruitment. C) The Low PA Non-carriers have less CR and need to begin compensation demonstrated by increased connectivity. D) The increased rate of amyloid deposition in carriers of the APOE-ε4 allele along with age related changes initiate compensatory increased connectivity at an earlier age, and the compensation period is limited. E) Low PA carriers have begun compensatory increases in connectivity, but the High PA carriers have not yet reached a critical threshold of brain changes to initiate the compensatory mechanisms.

We are not the first study to examine trajectories of function in relation to the APOE-ε4 allele, and our interpretation of our results do coincide with another cross-sectional study investigating the effects of age and APOE genotype on rs-fMRI functional connectivity (Shu et

al., 2016). Despite opposite susceptibilities to AD, cognitively normal carriers of the ε2 and ε4 allele were found to have similar fMRI activations during memory tasks (Trachtenberg, Filippini, Cheeseman, et al., 2012) and intrinsic connectivity (Trachtenberg, Filippini, Ebmeier, et al., 2012), and this apparently confusing finding is perhaps explained by the single time point comparisons rather than understanding the trajectory of the connectivity pattern. Shu et al. (2016) modeled the connectivity of the PCC in a rs-fMRI seed based analysis in cognitively healthy ε2 and ε4 carriers. In this cross-sectional study, significant effects of the different alleles were found in the connectivity of the PCC with the precuneus and ACC. The ε4 carrier model demonstrated a decrease in functional connectivity in the DMN in the age range studied (54 to 80 years), and the ε2 carriers demonstrated a positive aging trajectory – thus indicating an increase in connectivity with age. If we view these results in conjunction with the CR model, the protective effect of ε2 carriers against the development of AD is demonstrated by increasing compensatory recruitment by the PCC during this age range while the ε4 carriers are already exhibiting the downward trajectory after peak compensatory connectivity in this age range leading towards cognitive decline. It is this trajectory that explains the different risk ratios better than any single timepoint comparison.

Higher levels of CR may set the groundwork for future adaptations and minimize the effect of brain changes on cognition by delaying pathology and increasing the recruitment of alternate brain networks (Barulli & Stern, 2013). Our study is unique in using rs-fMRI to detect differences in connectivity prior to changes in cognition in subjects with different PA levels and APOE-ε4 status. Our limited age range does challenge our ability to interpret our results as different points of alteration of the connectivity pattern across the lifespan, but the model does explain the results of connectivity studies in AD and healthy at-risk adults. If the pattern of this

early detection of brain changes can be established, then we will better understand how the brain naturally adapts and this will inform AD treatment strategies. However, there is danger of confusing inter-subject variability with intra-subject variability in this cross-sectional approach (W. K. Thompson, Hallmayer, O'Hara, & Initiative, 2011) to modeling connectivity patterns prior to cognitive decline. We may not be presenting a genuine effect of age but rather individual or generational differences, and future longitudinal studies need to confirm that PA can protect against harmful brain changes to cognition and improve the ability to recruit alternate brain networks regardless of APOE-ε4 status, thus increasing CR and delaying cognitive decline and incidence of dementia.

Section 6.3: Biological Plausibility

It is established that higher levels of PA reduce the incidence of cognitive decline (Etgen et al., 2010; Laurin et al., 2001; Middleton et al., 2010; Middleton et al., 2011), and we now present biological plausibility that PA can change the connectivity trajectory of the mPFC-PCC that would explain this protection in both carriers and non-carriers of the APOE-ε4 allele. There are many hypothesized neurophysiological mechanisms that may explain the protection of brain structure and function in human aging due to PA, but few have been confirmed in human brains and depend upon animal studies. Cholinergic function in the hippocampus and cerebral cortex of rats has been shown to be improved by exercise (Ben et al., 2009), and rodent studies have demonstrated improved brain lipid metabolism and reduced neuroinflammation after PA interventions, thus counteracting the physiologic impact of the APOE-ε4 allele in the hippocampus (Intlekofer & Cotman, 2013). Neurotrophic effects supporting neurogenesis in the dentate gyrus of rodents due to PA has been well supported (Trejo, Carro, & Torres-Aleman, 2001; van Praag, Shubert, Zhao, & Gage, 2005), and this is an effect also seen in humans

(Erickson et al., 2011; Pereira et al., 2007). While the hippocampus is a brain region inherently involved in cognitive processes involving memory, it is not where we found significant results in the current study. Due to this discrepancy, we focus our explanations of biological plausibility on amyloid beta deposition and altered glucose metabolism that do occur in the PCC of humans and have links to changes in functional connectivity.

While findings are still inconsistent, most studies have found APOE-ε4 carriers to have a higher cortical Aß load compared to non-carriers (Fouquet, Besson, Gonneaud, La Joie, & Chételat, 2014). However, given that PA levels have been implicated in reducing Aß load in carriers comparable to non-carriers (Head et al., 2012), the inconsistency may be due to measurements of PA not being included in data collection and thus subsequent analyses. Amyloid plaque is a common subject of AD studies and has been linked to altered connectivity of cortical hubs in asymptomatic human subjects (Drzezga et al., 2011). However, it is unlikely in the current study that we are seeing changes in the connectivity of the mPFC-PCC due primarily to amyloid deposition as most studies have found amyloid pathology to begin after our age range (Jack et al., 2010), differences between carriers and non-carriers in amyloid burden manifest in adults older than 50 years (Fouquet et al., 2014), and rs-fMRI differences between carriers and non-carriers of the ε4 allele have been found in the absence of amyloid pathology in older adults (Sheline et al., 2010). Moreover, functional activation differences between carriers and non-carriers in young adults (20-38 years) during episodic memory tasks (Matura et al., 2014) also indicates differences in brain function occur long before the presence of AD pathology. Despite the fact it is unlikely that connectivity alterations in the age range of the current study are due to amyloid plaque buildup, there is evidence that the accumulation of amyloid beta is not the cause of AD but rather a downstream effect of differences in neural

metabolic function (Stranahan & Mattson, 2012). Thus, our findings of differences in connectivity of the PCC, a target brain region of later amyloid plaque deposition reaching clinical levels in the AD continuum, supports the theory that this biomarker is a result of earlier pathologies increasing the risk of an AD diagnosis.

The more likely candidate to explain our connectivity findings is differences in glucose metabolism that could reduce the ability to form resilient white matter architecture. Type II diabetes and insulin resistance increase the risk of cognitive decline (Ott et al., 1996; Velayudhan et al., 2010; Yen et al., 2010), and improved glycemic control has been associated with improved cognitive abilities in non-diabetic individuals (Rolandsson, Backeström, Eriksson, Hallmans, & Nilsson, 2008), indicating a metabolic continuum that effects the ability of the brain to be protected against changes (Stranahan & Mattson, 2012). While age is a risk factor for insulin resistance and developing type 2 diabetes (DeFronzo, 1981), findings of altered metabolism in young APOE-ε4 carriers (20-39 years old) have been demonstrated in the PCC and prefrontal cortex (Reiman et al., 2004). These areas have been shown to exhibit hypometabolism in older cognitively intact adults at genetic risk for AD (Reiman et al., 1996; G. W. Small et al., 1995). The PCC, as a hub of the DMN, utilizes glycolysis (Vaishnavi et al., 2010) to meet the high energy demand (Buckner et al., 2005), and Perkins et al. (2016) found upregulated GLUT1 and GLUT3 transporters in postmortem PCC brain tissue of these young adult APOE-ε4 carriers compared to non-carriers. GLUT1 is involved in the transportation of glucose across the blood brain barrier, and as this increase in protein levels of GLUT1 were not accompanied by increases in the mRNA levels, it is indicative of increased regulation of translational activity shifts (Perkins et al., 2016). Additionally, APOE binds to rab11, a protein involved in GLUT3 trafficking to the neuron membrane surface, and this may explain the

apparent contradictory findings that protein levels were upregulated in areas associated with hypometabolism. Hexokinase-1 sequesters imported glucose via phosphorylation, and Perkins et al. (2016) also found increased protein levels as another possible compensatory response to impaired glucose transport functionality in the young carriers. Another apparent compensatory response in these young carriers were the increased protein levels of complexes I, II, and IV of the electron transport chain(ETC), necessary to mitochondrial function. These same carriers have also been shown to have lower levels of mitochondrial cytochrome oxidase activity than noncarriers in the PCC indicative of declining mitochondrial function (Valla et al., 2010). This in conjunction with findings of altered synaptic structure in infants (Dean et al., 2014; Dumanis et al., 2009; Knickmeyer et al., 2014) provide more evidence that this upregulation of proteins may be indicative of early compensatory responses to altered energy metabolism pathways in the PCC of young adult APOE-ε4 carriers (Perkins et al., 2016). The increased risk of cognitive decline in APOE-ε4 carriers and individuals on the more critical end of the metabolism continuum might result from the same metabolic inefficiency effects.

Efficient metabolism in older adults is indicative of a reserve to function despite AD related changes (Cohen et al., 2009; Stranahan & Mattson, 2011, 2012), and it is possible this efficient metabolism is necessary in young and middle adulthood to lay the groundwork of white matter connections necessary for the recruitment of alternate brain networks when brain changes have hindered the function of the typical network paths. Interestingly, Middleton et al. (2010) found higher levels of PA reported during teenage years of women over the age of 65 were associated with a reduced incidence of cognitive impairment, which would fit with the hypothesis of earlier foundations of connections necessary for protected cognition. White matter tracts require a high metabolic cost (Tomasi, Wang, & Volkow, 2013), and inefficient

metabolism will not allow for easy formation of white matter tracts beyond what is necessary for brain function. Thus, when the recruitment of alternate pathways is needed to maintain function due to brain alterations, carriers and adults with reduced metabolic efficiency are limited in alternate connections and thus must require increased communication along these relatively sparse existing pathways earlier in life than adults with a varied and strong white matter network. This may be what we are measuring in our current study.

There is much evidence that PA improves glucose tolerance and insulin sensitivity (Heath et al., 1983; Rogers et al., 1988; Seals, Hagberg, Allen, et al., 1984; Seals, Hagberg, Hurley, Ehsani, & Holloszy, 1984) and that these improvements are associated with increased performance on executive function tasks (Baker, Frank, Foster-Schubert, Green, Wilkinson, McTiernan, Cholerton, et al., 2010). The mechanisms through which PA improves glycemic control and increases insulin sensitivity may be the reason PA reduces the risk of cognitive decline in the general population, and this reduced risk supports the conceptual understanding that metabolic reserve protects against cognitive decline, including AD. However, while PA potentially has a plethora of effects at various stages of glycolysis, we propose a few mechanisms by which PA would result in improved glucose transport resulting in more efficient metabolism necessary for neural protection and plasticity (Stranahan & Mattson, 2011).

First, GLUT3 trafficking to the neuron surface membrane is regulated by synaptic activity (Ferreira, Burnett, & Rameau, 2011), and it may be through the transitional activity induced by afferent projections from the motor cortex during acute bouts of PA that aid in the transport of GLUT3, thus reducing the dysregulatory effect of APOE-ε4 allele on protein functionality and improving glucose transport into the neuron. Secondly, PA also increases levels of BDNF (Cotman & Berchtold, 2002), a neurotrophic factor implicated in improved glucose

transport in cerebral cortical neurons (Burkhalter, Fiumelli, Allaman, Chatton, & Martin, 2003), again negating adverse effects of impaired glucose delivery into the neuron. This dual effect on increased metabolic efficiency via PA may allow for enough energy to 'wire' together the neurons that "fire" together (paraphrase of Hebb's Law: "Neurons that fire together wire together") and enhance CR by enabling the establishment of a durable white matter network.

While peripheral levels of insulin are decreased with PA (Heath et al., 1983) and associated with cognitive improvements (Tarumi et al., 2013), it still remains to be established that PA increases insulin sensitivity in the central nervous system, perhaps through the mechanisms mentioned previously. IDE (insulin-degrading enzyme) clears amyloid beta as well as insulin, and hyperinsulinemia, due to impaired glucose transport, would divert enzymatic resources from clearing the amyloid beta. PA increases insulin sensitivity, thus reducing the amount of diverted IDE and increasing the clearance of amyloid beta as evidenced in PA studies in APOE-ε4 carriers (Head et al., 2012). Sequentially, improved glucose transport leads to increased clearance of amyloid, and implicitly is one of the more compelling arguments that the accumulation of amyloid beta is a downstream effect of inefficient glucose metabolism and not the instigator of AD pathology. While the amyloid plaques do additionally damage neurons and interneuronal communication, they may not be the initial cause of the dysfunction. Thus, PA protects cognition not only by increasing CR through improving metabolic efficiency, but through the prevention of additional secondary pathology that disrupts brain function.

In summary, there is evidence of dysregulated metabolism in young APOE-ε4 carriers decades before the accumulation of amyloid plaque buildup indicating early compensatory measures due to reduced functional glucose transport across the blood brain barrier and into the neuron. Accumulated evidence that PA influences the efficiency of glucose metabolism would

explain why PA reduces the risk of developing AD in the general population as well as in those with genetic risk for AD. The results from the current study could indicate that PA levels do alter the time course of compensatory connectivity increases of the PCC, which are related to metabolic processes. However, it is necessary to confirm this speculation with empirical data.

Section 6.4: Methodological Differences from Previous Literature

Our first specific aim of the current study was to investigate the association of self-reported leisure-time PA on the fronto-parietal network, DMN, and hippocampal connectivity in young adulthood to middle adulthood. Other than interactions of PA with age and APOE on the long-range connectivity in the left hemisphere, we failed to reject the null hypothesis with all other dependent variables. We believe our non-findings may be explained due to methodological differences with the studies cited in our rationale. Primarily, the differences in the age of our participants, the network measures used, and the subjective measure of PA may explain why we did not obtain significant results when testing the following hypotheses of **Specific Aim 1:**

> ***Hypothesis 1:*** Global efficiency in the DMN and fronto-parietal network, node degree, and long range connectivity between the PCC and mPFC will decrease with increased age.
>
> ***Hypothesis 2:*** Subjects who meet the weekly recommendations for moderate to vigorous intensity PA will have greater measures of network integration (global efficiency) in the DMN and fronto-parietal network than the low PA group across the entire age range.
>
> ***Hypothesis 3:*** Subjects who meet the weekly recommendations for moderate to vigorous intensity PA will have greater node strength of the hippocampal subregions, precuneus, PCC, and DLPFC than the low PA group across the entire age range.

Age is a factor that might account for the limited findings in this study. Our oldest participant was 50, yet previous PA and connectivity studies demonstrating increased connectivity in the DMN defined the lower limit of their older participants to be 55 (Voss et al., 2010) or 60 (Chirles et al., 2017). Another exercise intervention study found greater node degree of the hippocampus in the exercisers, but again this study included cognitively healthy adults over the age of 70 years (Burdette et al., 2010). Including participants older than 60 years would have extended our regression lines and perhaps allowed us to detect differences in middle age. Another possibility is that our sample is too young to have age related brain changes requiring compensatory recruitment to such an extent that differences in network measures (global efficiency, node degree) would be measurable. The two PA intervention studies finding increased recruitment in the DMN measured connectivity as the correlation between two brain regions (Chirles et al., 2017; Voss et al., 2010) and did not use network measures. Our significant result in the current study was a measure of the correlation between two brain regions, and it is possible in these cognitively healthy adults that there were not enough single connection differences to be detected by the network measures.

The sums of the link strengths were calculated in the equations we used for global efficiency and node strength (defined below).

Global efficiency: $E^w = \frac{1}{n} \Sigma_{i \in N} \frac{\Sigma_{j \in N, j \neq i} \left(d_{ij}^w\right)^{-1}}{n-1}$

Weighted degree (or node strength) of i: $k_i^w = \sum_{j \in N} w_{ij}$

If some connections have compensatory increases in connectivity due to decreases in other connections, these changes are negated by the summation. It is possible that our non-findings using global efficiency and node strength as dependent variables are indicative of successful

adaptations in these young and middle-aged adults. The benefit of the network measures is that they encapsulate the organization and function of the brain in a holistic approach, but the downfall is that meaningful single connections indicative of brain changes may be missed.

The choice of node size and number for the network influences the outcome measurements, and this may also explain our non-findings in this study. Burdette et al (2010) used 15,000 network nodes and found the node degree of the hippocampus in older adults after a 4-month exercise intervention increased due to connections with the anterior cingulate cortex (ACC). The ACC was comprised of numerous network nodes, while in our study this region comprised 4 of 234 nodes. The combination of variance and not enough connections to the ACC would mask any differences in the node strength of the subsections of the hippocampus if effects of PA on connections to the hippocampus were limited to this region. While not strictly using network analysis, Boraxbekk et al. (2016) found voxel-wise connectivity of the PCC was positively correlated with current and accumulated PA over the course of 10 years. Again, this study utilized a greater number of connections to determine an index of connectivity compared to the current study.

The Paffenbarger Physical Activity Questionnaire was used to determine the physical activity status in this study as PA questionnaires are commonly employed by researchers investigating PA and the brain. For example, white matter is evidenced to be the underlying neural substrate supporting functional connectivity, and Smith et al. (2016) found self-reported PA did have interactive effects with APOE-ε4 status on white matter integrity as measured using DTI. The Paffenbarger Questionnaire of total Index of weekly kilocalories correlates moderately strongly with VO_{2max} (correlation coefficient 0.60) (Ainsworth, Leon, Richardson, Jacobs, & Paffenbarger, 1993), and physical fitness (as measured by VO_{2max}) has been shown to have

associations with functional connectivity in networks affected by aging (Voss et al., 2016). When the analyses for the current study were redone with an estimated VO_{2max} continuous measure, we did not uncover any additional significant findings. While there is evidence to support using self-reported PA, a weakness in the current study is that while the reliability of the Paffenbarger Questionnaire is high for retest after one month interval (0.72) it decreases to 0.34 after an interval of eight months (Ainsworth et al., 1993). Thus, we cannot assume that the questionnaire results collected for this study accurately reflect PA habits for past year nor do we have a measure of life-long PA habits.

Our second specific aim of the current study was to investigate the association of the interaction of PA and APOE-ε4 status on the fronto-parietal network, DMN, and hippocampal connectivity from young adulthood to middle adulthood. Again, other than our findings related to the long-range connectivity of the mPFC-PCC in the left hemisphere, we failed to reject the null hypothesis with all other dependent variables. We believe these non-findings when testing the following hypotheses of **Specific Aim 2** are due primarily to the choice of metrics for our network analysis as well as the limited age range of the Low PA carrier group.

Hypothesis 1: APOE-ε4 carriers will have smaller measures of network integration (global efficiency) in the DMN than the non-carrier group across the age range.

Hypothesis 2: APOE-ε4 carriers will have smaller measures of node strength of the anterior hippocampus and PCC compared to the non-carrier group across the age range.

Hypothesis 3: The APOE-ε4 carriers will have larger measures of node strength of the precuneus compared to the non-carrier group across the age range.

In our younger sample, the non-findings concerning global efficiency and node strength may indicate compensatory mechanisms in the APOE-ε4 carrier group are successful and

network brain function has been maintained. While differences have been found when comparing patient groups (Zhao et al., 2012), it is likely, as explained in an earlier section, that there are not enough single connection differences to be detected after summation. Given our non-result when testing global measures, future investigations should investigate single connection differences between carriers and non-carriers.

In the APOE-ε4 studies previously cited, hippocampal connectivity differences between carriers and non-carriers were limited to single connections or seed-based analyses during task-based connectivity (Harrison et al., 2016; Heise et al., 2014). In 95 cognitively healthy individuals, age range 50-80, APOE-ε4 carriers had greater correlations of rs-fMRI time series between the hippocampus and posterior regions of the DMN that extended into the PCC (Westlye, Lundervold, Rootwelt, Lundervold, & Westlye, 2011). The Heise et al. (2014) study found the reduced connectivity of the hippocampus with the PCC in female carriers, and Goveas et al. (2013) found carriers had greater functional connectivity of the PCC and precuneus in a seed based analysis. Koch et al. (2012) was not able to use connectivity of the PCC in the DMN to distinguish between cognitively healthy older adult carriers and non-carriers of the APOE-ε4 allele nor between adults diagnosed with MCI or AD and concluded that single connections were of little diagnostic value. PA levels were not included in this analysis, which may explain why differences were not found based on APOE status, and while single connections may be of predictive value of future cognitive decline they are not a distinguishable attribute when compensatory processes are no longer protecting cognition. In cognitively intact individuals, single connection compensatory responses are successful and clinical criteria are not met, but in patient groups, the increased connectivity of single connections have not successfully inhibited cognitive changes, and thus cognitive difficulties manifest.

Hypothesis 4: APOE-ε4 carriers with levels of PA that meet the weekly recommendations for moderate to vigorous intensity PA will have connectivity measures that are not different from the non-carriers who meet the recommendations for moderate to vigorous intensity PA.

It was not possible to determine APOE-ε4 status prior to recruitment and enrollment in our current study. Subsequently, our Low PA APOE-ε4 carrier group was very small and not adequately represented across the age span. Results for this group could not be extrapolated beyond the age of 30 years. This limited any statistical ability to determine differences in the regression models, and it may explain why we did not find the Low PA APOE-ε4 carrier group to differ from the non-carriers and the High PA groups. This severely limited our ability to determine if higher levels of PA attenuated early compensation in carriers.

Section 6.5: Future Directions

Our current study implicates PA as another factor to consider in understanding the connectivity pattern trajectory in individuals with genetic risk for AD, but a limitation is that we did not separate the different genotypes. We based our analysis solely on having or not having the ε4 allele, yet the estimated risks for AD of the isoforms vary greatly [0.6 for APOE 2/2 or 2/3; 2.6 for APOE 2/4; 3.2 for APOE3/4; and 14.9 for APOE 4/4 (Farrer et al., 1997)]. We included and APOE 2/4 participant in the carrier group, yet and carriers of the ε4 and ε2 allele have been shown to have different aging trajectories (Shu et al., 2016). Increasing our sample size would allow us to investigate the aging trajectory of each isoform.

The limited age range of the Low PA APOE-ε4 carriers as well as the entire sample is a limitation, but the recruitment of older subjects or the inclusion of publicly available data is a solution to this issue. Future studies should also include a network node structure with smaller

nodes and higher spatial resolution, particularly in the ACC, to increase sensitivity to differences in brain function. We would also need to expand data collection to include life-time exposures that have been reported to increase cognitive reserve and affect brain network connectivity for future longitudinal studies. Such exposures would be enriching experiences such as the intellectual stimulation associated with higher education (Coffey, Saxton, Ratcliff, Bryan, & Lucke, 1999), specialized occupation (Gaser & Schlaug, 2003), and literacy (Carreiras et al., 2009). Moreover, PA levels need to be through questionnaire and VO_{2max} tests repeatedly across the age span and not just for the current year. While socioeconomic status, IQ, education, and occupation have opportunistic or financial limitations, PA is lifetime exposure that can be altered at any time regardless of previous behavior, and it is a prime method to use in intervention studies (Stern, 2006). It is encouraging that in the current study leisure activities meeting the recommended amounts for general health appeared to indicate a delay in the need for compensation. However, future longitudinal studies need to confirm this, and endpoints in this study need to include rates of slowed dementia and incidence of dementia that would require sensitive neuropsychological testing. Table 18 describes some of the research questions that should be addressed in these future longitudinal studies.

Table 18: Additional Questions for Future Research.

1. Does lifetime PA increase the length of the compensation period (as measured using functional connectivity) and further delay cognitive decline in APOE-ε4 carriers and non-carriers to the same extent? If so, is this augmented ability to compensate regulated to specific brain networks or hubs, or is it a global effect?
2. Are there graph metrics sensitive to brain changes prior to change in cognitive status, or are single connections the best indicators? Are there directionality differences depending on the metric used due to the dynamic and integrated nature of the brain?
3. Does delayed change in connectivity delay change in cognitive status?

Section 6.6: Conclusion

This novel study used rs-fMRI connectivity and graph metrics to investigate the interactive effects of age, APOE-ε4, and PA on brain networks altered by AD and age and related these findings to levels of cognitive reserve. We found the long-range connectivity of the mPFC-PCC in the left hemisphere had a positive age trajectory in our Low PA non-carriers, but a horizontal age trajectory in the High PA carriers and non-carriers of the APOE-ε4 allele. This may indicate the Low PA non-carriers, due to lower levels of CR, were demonstrating compensatory increases in connectivity while High PA carriers and non-carriers in our age range did not yet require protective compensatory mechanisms. We suggest that perhaps due to more efficient glucose metabolism, higher levels of PA allow the development of a more robust network architecture, thus increasing CR and reducing the risk of cognitive decline regardless of

APOE-ε4 status. The validity of using rs-fMRI to detect differences in the time-course connectivity patterns sensitive to levels of CR still needs to be established, but the proposed future directions will aid this effort and are critical to the research and treatment of AD. These future directions will also determine if delayed compensatory increases in functional connectivity of the mPFC-PCC in the DMN is indicative of delayed declines in episodic memory, the memory system supported by the DMN. Early detection may be the key to identifying appropriate target populations for specific treatment studies allowing precision medicine to delay cognitive decline and preserve memories. Our study adds to the literature describing adaptations of the brain networks prior to clinical diagnoses, and uniquely relates these adaptations to PA level and genetic risk for AD.

Appendix

Additional Graphs for Data

Figure A1: Global Efficiency by PA or APOE-ε4 Group.

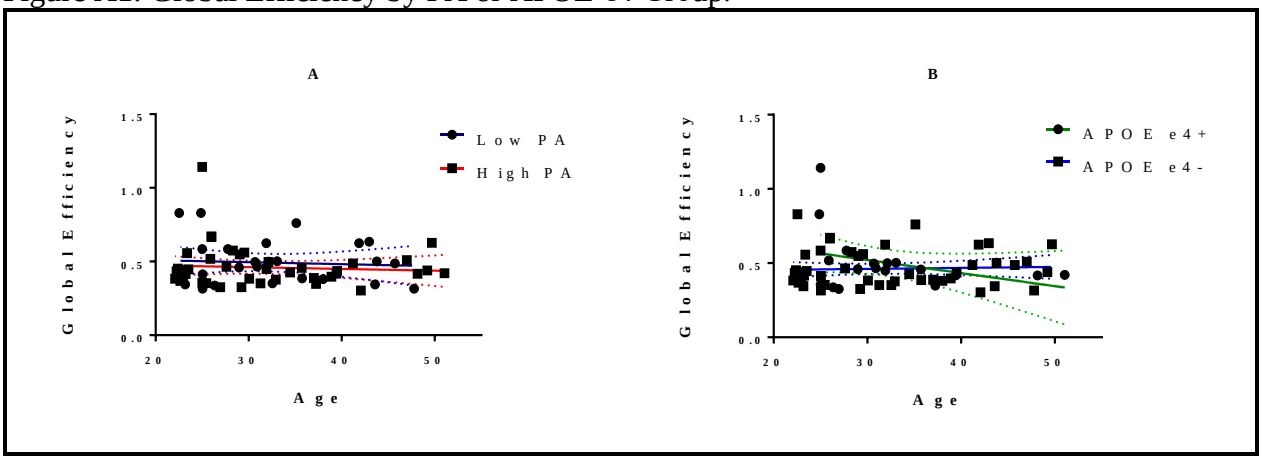

Legend: Panel A: Graphs show the linear regression line when plotting the global efficiency versus age. Panel A: Comparing the regression lines of High and Low PA. Low PA: dark blue line and circle data points. High PA: red line and square data points. The slopes of the two equations are not significantly different ($F(1,65) = 0.001234$, $p = 0.9721$). Panel B: Comparing the regression lines of APOE-ε4 carriers and non-carriers. APOE-ε4 carriers: green line and circle data points. APOE-ε4 non-carriers: blue line and square data points. The slopes of the two equations are not quite significantly different ($F(1,65) = 3.583$, $p = 0.0628$).

Equations of regression lines in Figure A1 generated by GraphPad Prism 7.0 software.

1) Low PA: $y = -0.001351x + 0.536$

The slope is not significantly different from 0 ($F(1,25) = 0.133$, $p = 0.7184$).

2) High PA: $y = -0.001196x + 0.4976$

The slope is not significantly different from 0 ($F(1,40) = 0.2269$, $p = 0.6364$).

3) APOE-ε4 positive: $y = -0.008819x + 0.7856$

The slope is not significantly different from 0 ($F(1,17) = 2.267$, $p = 0.1505$).

4) APOE-ε4 negative: $y = 0.0006761x + 0.4407$

The slope is not significantly different from 0 ($F(1,48) = 0.1177$, $p = 0.7331$).

Equations of regression lines in Figure A2 generated by GraphPad Prism 7.0 software.

5) Low PA APOE-ε4 positive: $y = -0.0201x + 1.111$

The slope is not significantly different from 0 ($F(1,6) = 1.18$, $p = 0.3190$).

6) Low PA APOE-ε4 negative: $y = -0.0001572x + 0.4859$

The slope is not significantly different from 0 ($F(1,17) = 0.001516$, $p = 0.9694$).

7) High PA APOE-ε4 positive: $y = -0.008292x + 0.7714$

The slope is not significantly different from 0 ($F(1,9) = 1.115$, $p = 0.3185$).

8) High PA APOE-ε4 negative: $y = 0.0008641x + 0.4242$

The slope is not significantly different from 0 ($F(1,29) = 0.1734$, $p = 0.6802$).

Figure A2: Global Efficiency versus Age by PA and APOE-ε4 Groups.

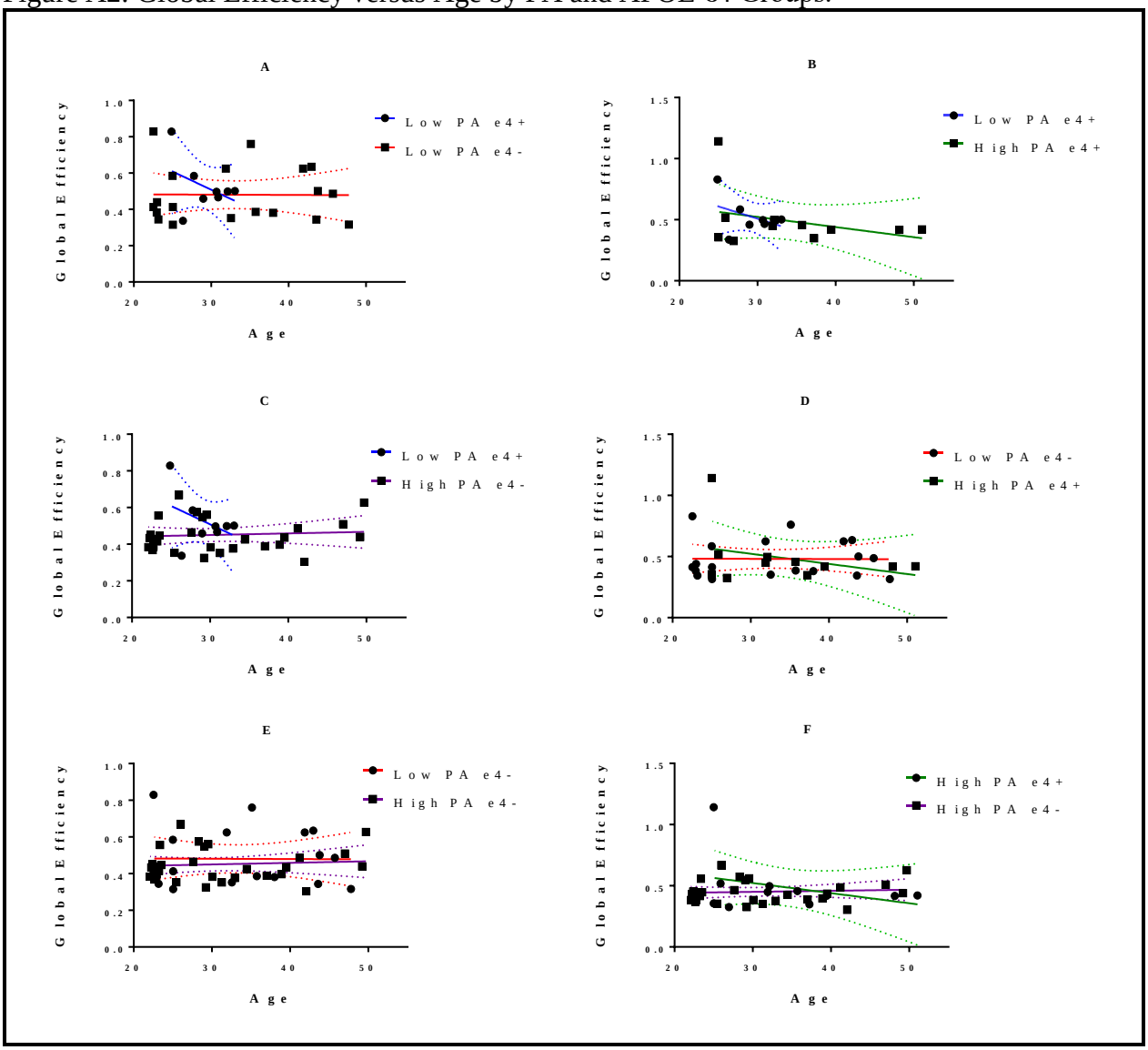

Legend: Graphs show the linear regression line when plotting global efficiency versus age. Blue line and circle data points: Low PA APOE-ε4 carriers; Red line and square data points: Low PA APOE-ε4 non-carriers; Green line square data points: High PA APOE-ε4 carriers; Purple line square data points: High PA APOE-ε4 non-carriers. Panel A: Comparing the regression lines of APOE-ε4 carriers and non-carriers in the Low PA category. The slopes of the regression lines are not significantly different from each other ($F(1,23) = 0.9338$, $p = 0.3439$); Panel B: Comparing the regression lines of APOE-ε4 carriers in the High and Low PA categories. The slopes are not significantly different from each other ($F(1,15) = 0.1964$, $p = 0.6640$); Panel C: Comparing the regression lines of Low PA APOE-ε4 carriers and High PA APOE-ε4 non-carriers. The slopes are not significantly different from each other ($F(1,35) = 2.197$, $p = 0.1472$); Panel D: Comparing the regression lines of Low PA APOE-ε4 non-carriers and High PA APOE-ε4 carriers. The slopes are not significantly different from each other ($F(1,26) = 1.044$, $p = 0.3162$); Panel E: Comparing the regression lines of APOE-ε4 non-carriers with High and Low PA levels. The slopes are not significantly different from each other ($F(1,46) = 0.06196$, $p = 0.8045$); Panel F: Comparing the regression lines of APOE-ε4 carriers and non-carriers in the High PA category. The slopes are not significantly different from each other ($F(1,38) = 2.608$, $p = 0.1146$).

Figure A3: Correlation of Right Hemisphere mPFC and PCC by PA or APOEε4 Group.

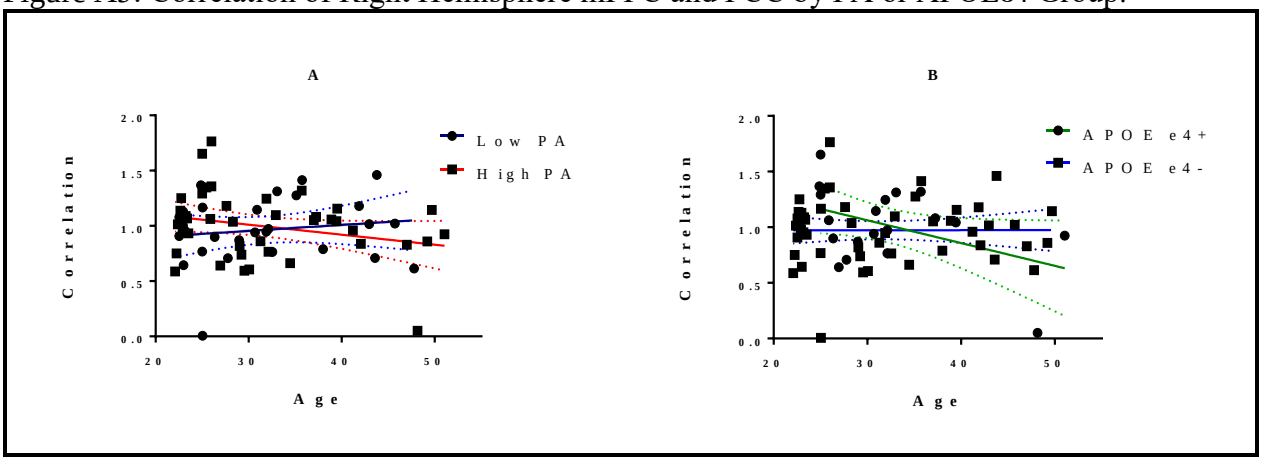

Legend: Panel A: Graphs show the linear regression line when plotting the correlation of the rs-fMRI timeseries of the mPFC and PCC in the right hemisphere versus age. Panel A: Comparing the regression lines of High and Low PA. Low PA: dark blue line and circle data points. High PA: red line and square data points. The slopes of the two equations are not significantly different ($F(1,65) = 2.565$, $p = 0.1141$). Panel B: Comparing the regression lines of APOE-ε4 carriers and non-carriers. APOE-ε4 carriers: green line and circle data points. APOE-ε4 non-carriers: blue line and square data points. The slopes of the two equations are not quite significantly different ($F(1,65) = 3.827$, $p = 0.0547$).

Equations of regression lines in Figure A3 generated by GraphPad Prism 7.0 software:

9) Low PA: $y = 0.005405x + 0.7924$

The slope is not significantly different from 0 ($F(1,25) = 0.5182$, $p = 0.4783$).

10) High PA: $y = -0.009046x + 1.282$

The slope is not significantly different from 0 ($F(1,40) = 3.009$, $p = 0.0905$).

11) APOE-ε4 positive: $y = -0.02046x + 1.676$

The slope is not significantly different from 0 ($F(1,17) = 4.098$, $p = 0.0589$).

12) APOE-ε4 negative: $y = 0.000072x + 0.9705$

The slope is not significantly different from 0 ($F(1,48) = 0.00024$, $p = 0.9877$).

Equations of regression lines in Figure A4 generated by GraphPad Prism 7.0 software.

13) Low PA APOE-ε4 positive: $y = -0.007033x + 0.8209$

The slope is not significantly different from 0 ($F(1,6) = 0.04698$, $p = 0.8356$).

14) Low PA APOE-ε4 negative: $y = 0.006829x + 0.7132$

The slope is not significantly different from 0 ($F(1,17) = 0.6331$, $p = 0.4372$).

15) High PA APOE-ε4 positive: $y = -0.02479x + 1.86$

The slope is not significantly different from 0 ($F(1,9) = 3.555$, $p = 0.0920$).

16) High PA APOE-ε4 negative: $y = -0.003892x + 1.112$

The slope is not significantly different from 0 ($F(1,29) = 0.5184$, $p = 0.4773$).

Figure A4: Effects of PA and APOE-ε4 Groups on Right Hemisphere mPFC-PCC correlation.

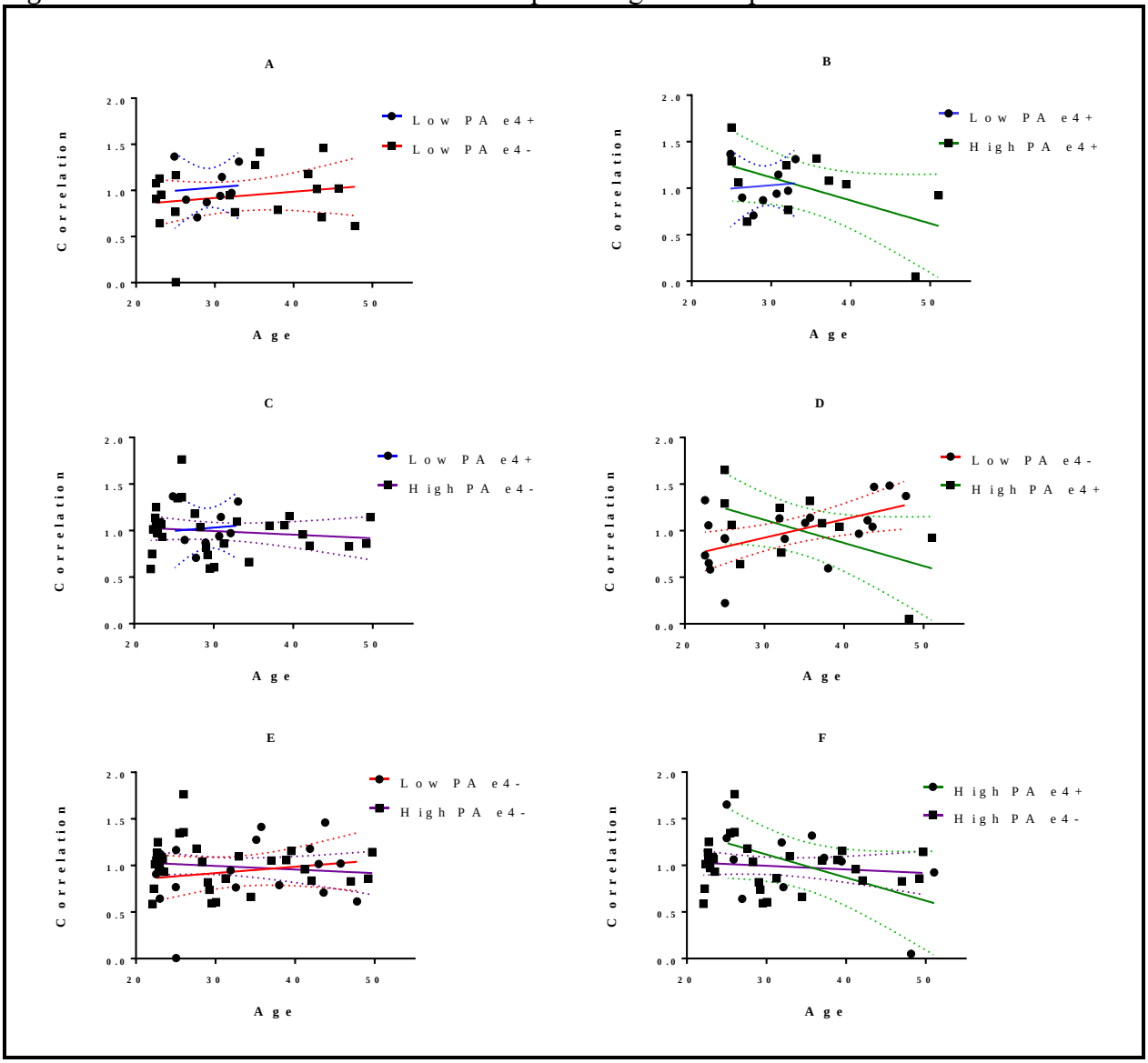

Legend: Graphs show the linear regression line when plotting the correlation of the rs-fMRI timeseries of the mPFC and PCC in the right hemisphere versus age. Blue line and circle data points: Low PA APOE-ε4 carriers; Red line and square data points: Low PA APOE-ε4 non-carriers; Green line square data points: High PA APOE-ε4 carriers; Purple line square data points: High PA APOEε4 non-carriers. Panel A: Comparing the regression lines of APOE-ε4 carriers and non-carriers in the Low PA category. The slopes of the regression lines are not significantly different from each other ($F(1,23) = 0.000023$, $p = 0.9962$); Panel B: Comparing the regression lines of APOE-ε4 carriers in the High and Low PA categories. The slopes are not significantly different from each other ($F(1,15) = 0.4986$, $p = 0.4909$); Panel C: Comparing the regression lines of Low PA APOE-ε4 carriers and High PA APOE-ε4 non-carriers. The slopes are not significantly different from each other ($F(1,35) = 1.1052$, $p = 0.7476$); Panel D: Comparing the regression lines of Low PA APOE-ε4 non-carriers and High PA APOE-ε4 carriers. The slopes are significantly different from each other ($F(1,26) = 10.64$, $p = 0.0031$); Panel E: Comparing the regression lines of APOE-ε4 non-carriers with High and Low PA levels. The slopes are not significantly different from each other ($F(1,46) = 1.263$, $p = 0.2670$); Panel F: Comparing the regression lines of APOE-ε4 carriers and non-carriers in the High PA category. The slopes are not significantly different from each other ($F(1,38) = 3.157$, $p = 0.0836$).

DMN Nodes

Figure A5: Node Strength of Right Precuneus by PA or APOE-ε4 Group.

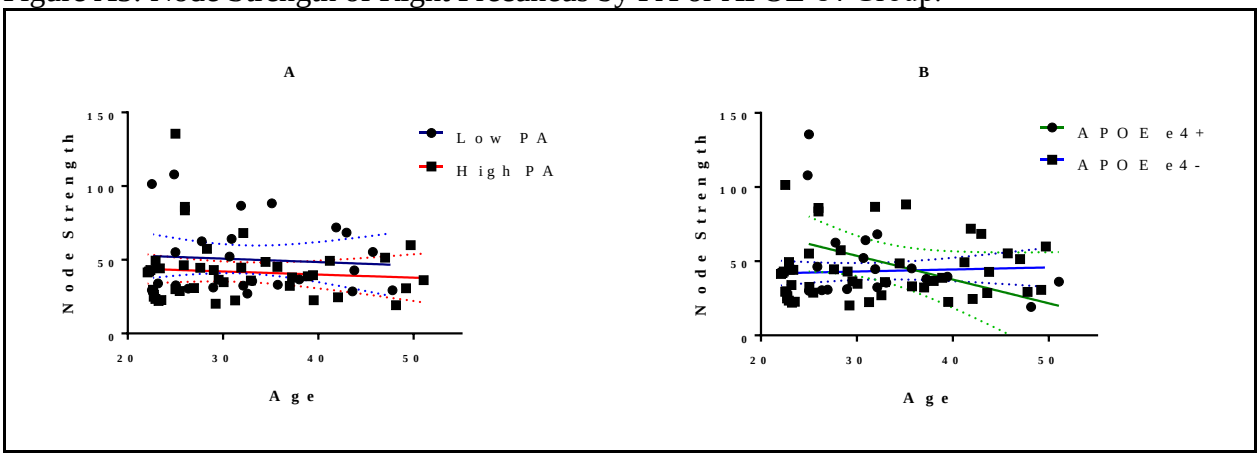

Legend: Panel A: Graphs show the linear regression line when plotting the node strength of the right precuneus versus age. Panel A: Comparing the regression lines of High and Low PA. Low PA: dark blue line and circle data points. High PA: red line and square data points. The slopes of the two equations are not significantly different ($F(1,65) = .001097$, $p = 0.9737$). Panel B: Comparing the regression lines of APOE-ε4 carriers and non-carriers. APOE-ε4 carriers: green line and circle data points. APOE-ε4 non-carriers: blue line and square data points. The slopes of the two equations are significantly different ($F(1,65) = 4.97$, $p = 0.0292$).

Equations of regression lines in Figure A5 generated by GraphPad Prism 7.0 software:

17) Low PA: $y = 0.23385x + 57.8$

The slope is not significantly different from 0 ($F(1,25) = 0.1572$, $p = 0.6951$).

18) High PA: $y = -0.2112x + 48.43$

The slope is not significantly different from 0 ($F(1,40) = 0.302$, $p = 0.5857$).

19) APOE-ε4 positive: $y = -1.601x + 101.7$

The slope is not significantly different from 0 ($F(1,17) = 3.523$, $p = 0.0778$).

20) APOE-ε4 negative: $y = 0.1388x + 38.9$

The slope is not significantly different from 0 ($F(1,48) = 0.186$, $p = 0.6682$).

Equations of regression lines in Figure A6 generated by GraphPad Prism 7.0 software.

21) Low PA APOE-ε4 positive: $y = -5.061x + 200.5$

The slope is not significantly different from 0 ($F(1,6) = 2.545$, $p = 0.1617$).

22) Low PA APOE-ε4 negative: $y = -0.03131x + 50.64$

The slope is not significantly different from 0 ($F(1,17) = 0.002656$, $p = 0.9595$).

23) High PA APOE-ε4 positive: $y = -1.49x + 99.79$

The slope is not significantly different from 0 ($F(1,9) = 2.034$, $p = 0.1876$).

24) High PA APOE-ε4 negative: $y = 0.121x + 35.69$

The slope is not significantly different from 0 ($F(1,29) = 0.1151$, $p = 0.7369$).

Figure A6: Node Strength of Right Precuneus versus Age by PA and APOE-ε4 Groups.

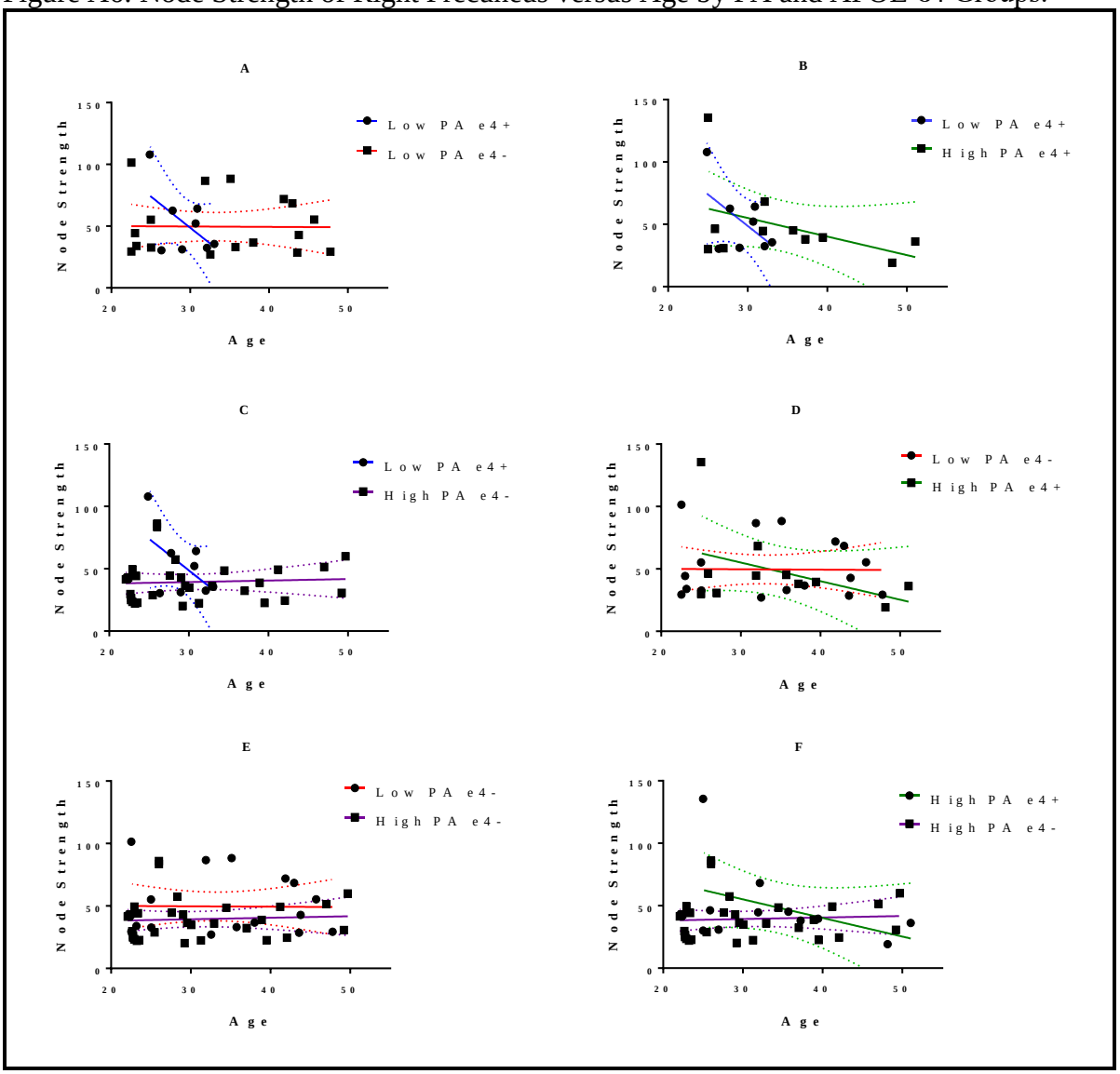

Legend: Graphs show the linear regression line when plotting the node strength of the right precuneus versus age. Blue line and circle data points: Low PA APOE-ε4 carriers; Red line and square data points: Low PA APOE-ε4 non-carriers; Green line square data points: High PA APOE-ε4 carriers; Purple line square data points: High PA APOE-ε4 non-carriers. Panel A: Comparing the regression lines of APOE-ε4 carriers and non-carriers in the Low PA category. The slopes of the regression lines are not significantly different from each other ($F(1,23) = 2.463$, $p = 0.1302$); Panel B: Comparing the regression lines of APOE-ε4 carriers in the High and Low PA categories. The slopes are not significantly different from each other ($F(1,15) = 0.8926$, $p = 0.3597$); Panel C: Comparing the regression lines of Low PA APOE-ε4 carriers and High PA APOE-ε4 non-carriers. The slopes are significantly different from each other ($F(1,35) = 0.0401$, $p = 4.546$); Panel D: Comparing the regression lines of Low PA APOE-ε4 non-carriers and High PA APOEε4 carriers. The slopes are not significantly different from each other ($F(1,26) = 1.672$, $p = 0.2074$); Panel E: Comparing the regression lines of APOE-ε4 non-carriers with High and Low PA levels. The slopes are not significantly different from each other ($F(1,46) = 0.05437$, $p = 0.8167$); Panel F: Comparing the regression lines of APOE-ε4 carriers and non-carriers in the High PA category. The slopes are not quite significantly different from each other ($F(1,38) = 3.641$, $p = 0.0639$).

Figure A7: Node Strength of Left Precuneus by PA or APOE-ε4 Group.

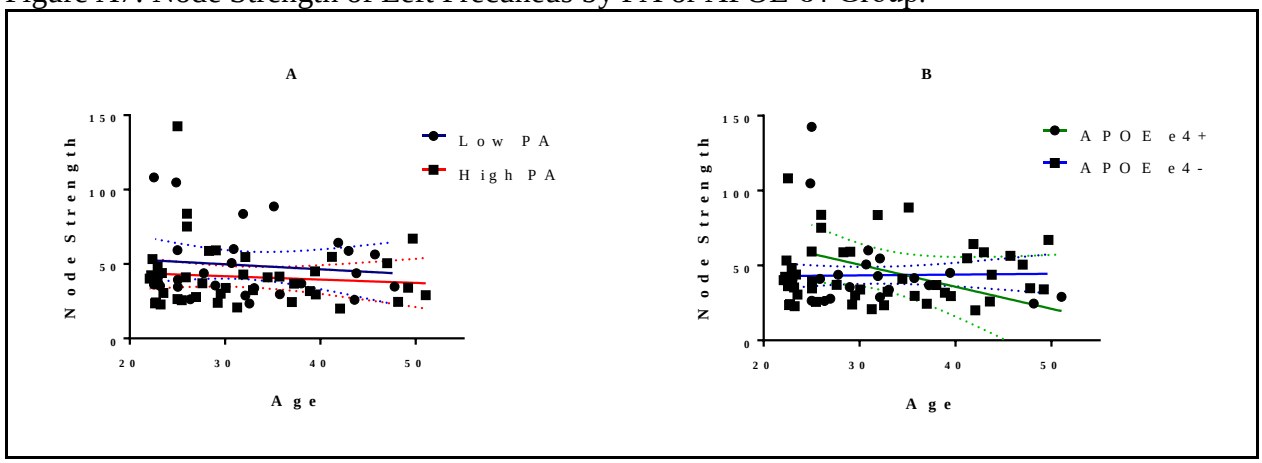

Legend: Panel A: Graphs show the linear regression line when plotting the node strength of the left precuneus versus age. Panel A: Comparing the regression lines of High and Low PA. Low PA: dark blue line and circle data points. High PA: red line and square data points. The slopes of the two equations are not significantly different ($F(1,65) = 0.02808$, $p = 0.8674$). Panel B: Comparing the regression lines of APOE-ε4 carriers and non-carriers. APOE-ε4 carriers: green line and circle data points. APOE-ε4 non-carriers: blue line and square data points. The slopes of the two equations are not quite significantly different ($F(1,65) = 3.695$, $p = 0.0590$).

Equations of regression lines in Figure A7 generated by GraphPad Prism 7.0 software:

25) Low PA: $y = -0.3408x + 60.07$

The slope is not significantly different from 0 ($F(1,25) = 0.3495$, $p = 0.5597$).

26) High PA: $y = -0.2259x + 48.58$

The slope is not significantly different from 0 ($F(1,40) = 0.3289$, $p = 0.5695$).

27) APOE-ε4 positive: $y = -1.473x + 94.64$

The slope is not significantly different from 0 ($F(1,17) = 2.727$, $p = 0.1170$).

28) APOE-ε4 negative: $y = 0.05336x + 41.78$

The slope is not significantly different from 0 ($F(1,48) = 0.02759$, $p = 0.8688$).

Equations of regression lines in Figure A8 generated by GraphPad Prism 7.0 software.

29) Low PA APOE-ε4 positive: $y = -4.547x + 181.4$

The slope is not significantly different from 0 ($F(1,6) = 2.093$, $p = 0.1981$).

30) Low PA APOE-ε4 negative: $y = -0.224x + 57.09$

The slope is not significantly different from 0 ($F(1,17) = 0.1395$, $p = 0.7134$).

31) High PA APOE-ε4 positive: $y = -1.431x + 95.8$

The slope is not significantly different from 0 ($F(1,9) = 1.616$, $p = 0.2355$).

32) High PA APOE-ε4 negative: $y = -0.1101x + 36.29$

The slope is not significantly different from 0 ($F(1,29) = 0.09401$, $p = 0.7613$).

Figure A8: Node Strength of Left Precuneus versus Age by PA and APOE-ε4 Groups.

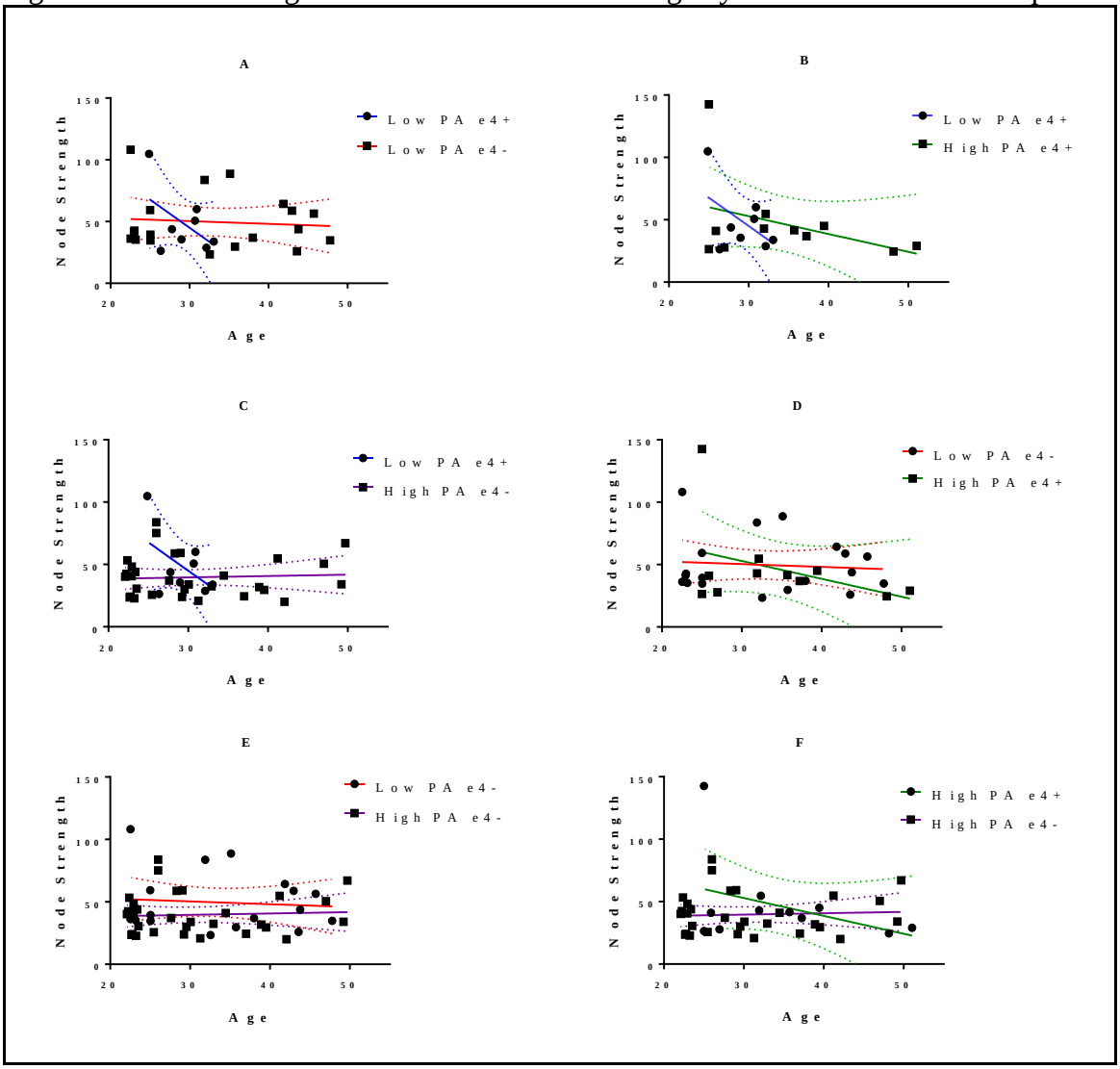

Legend: Graphs show the linear regression line when plotting the node strength of the left precuneus versus age. Blue line and circle data points: Low PA APOE-ε4 carriers; Red line and square data points: Low PA APOE-ε4 non-carriers; Green line square data points: High PA APOE-ε4 carriers; Purple line square data points: High PA APOE-ε4 non-carriers. Panel A: Comparing the regression lines of APOE-ε4 carriers and non-carriers in the Low PA category. The slopes of the regression lines are not significantly different from each other ($F(1,23) = 1.863$, $p = 0.1854$); Panel B: Comparing the regression lines of APOE-ε4 carriers in the High and Low PA categories. The slopes are not significantly different from each other ($F(1,15) = 0.6142$, $p = 0.4454$); Panel C: Comparing the regression lines of Low PA APOE-ε4 carriers and High PA APOE-ε4 non-carriers. The slopes are not quite significantly different from each other ($F(1,35) = 3.659$, $p = 0.0640$); Panel D: Comparing the regression lines of Low PA APOE-ε4 non-carriers and High PA APOEε4 carriers. The slopes are not significantly different from each other ($F(1,26) = 1.08$, $p = 0.3082$); Panel E: Comparing the regression lines of APOE-ε4 non-carriers with High and Low PA levels. The slopes are not significantly different from each other ($F(1,46) = 0.2636$, $p = 0.6101$); Panel F: Comparing the regression lines of APOE-ε4 carriers and non-carriers in the High PA category. The slopes are not quite significantly different from each other ($F(1,38) = 3.067$, $p = 0.0880$).

Figure A9: Node Strength of Right PCC by PA or APOE-ε4 Group.

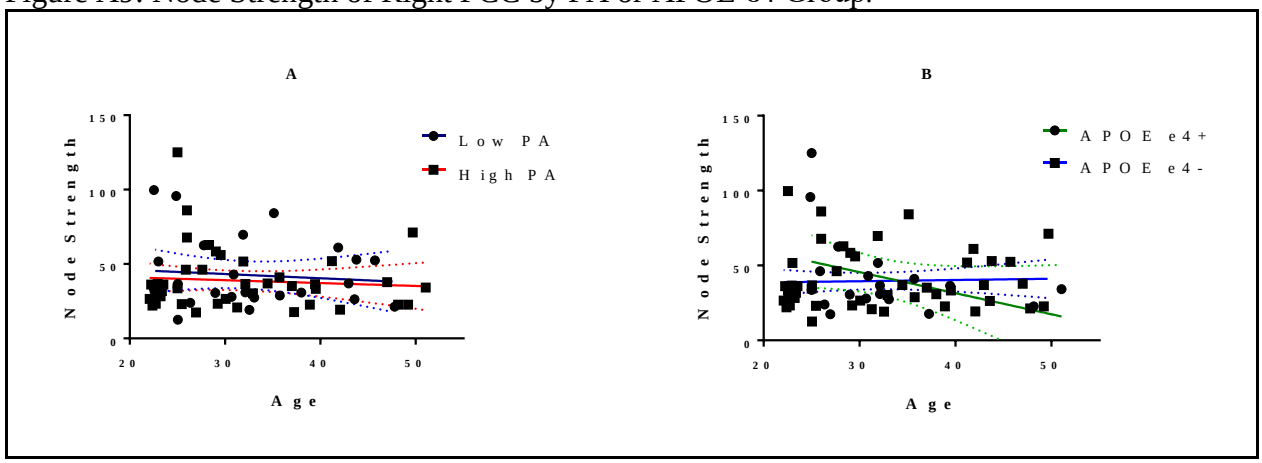

Legend: Panel A: Graphs show the linear regression line when plotting the node strength of the right PCC versus age. Panel A: Comparing the regression lines of High and Low PA. Low PA: dark blue line and circle data points. High PA: red line and square data points. The slopes of the two equations are not significantly different ($F(1,65) = 0.01917$, $p = 0.8903$). Panel B: Comparing the regression lines of APOE-ε4 carriers and non-carriers. APOE-ε4 carriers: green line and circle data points. APOE-ε4 non-carriers: blue line and square data points. The slopes of the two equations are not quite significantly different ($F(1,65) = 3.863$, $p = 0.0536$).

Equations of regression lines in Figure A9 generated by GraphPad Prism 7.0 software:

33) Low PA: $y = -0.285x + 51.83$

The slope is not significantly different from 0 ($F(1,25) = 0.2.497$, $p = 0.6217$).

34) High PA: $y = -0.1935x + 44.94$

The slope is not significantly different from 0 ($F(1,40) = 0.2699$, $p = 0.6063$).

35) APOE-ε4 positive: $y = -1.406x + 87.72$

The slope is not significantly different from 0 ($F(1,17) = 3.002$, $p = 0.1012$).

36) APOE-ε4 negative: $y = 0.0824x + 37.01$

The slope is not significantly different from 0 ($F(1,48) = 0.06795$, $p = 0.7955$).

Equations of regression lines in Figure A10 generated by GraphPad Prism 7.0 software.

37) Low PA APOE-ε4 positive: $y = -5.522x + 204.8$

The slope is not significantly different from 0 ($F(1,6) = 4.119$, $p = 0.0887$).

38) Low PA APOE-ε4 negative: $y = -0.1028x + 46.11$

The slope is not significantly different from 0 ($F(1,17) = 0.02933$, $p = 0.8660$).

39) High PA APOE-ε4 positive: $y = -1.302x + 86.83$

The slope is not significantly different from 0 ($F(1,9) = 1.685$, $p = 0.2266$).

40) High PA APOE-ε4 negative: $y = -0.003892x + 1.112$

The slope is not significantly different from 0 ($F(1,29) = 0.1576$, $p = 0.6943$).

Figure A10: Node Strength of Right PCC versus Age by PA and APOE-ε4 Groups.

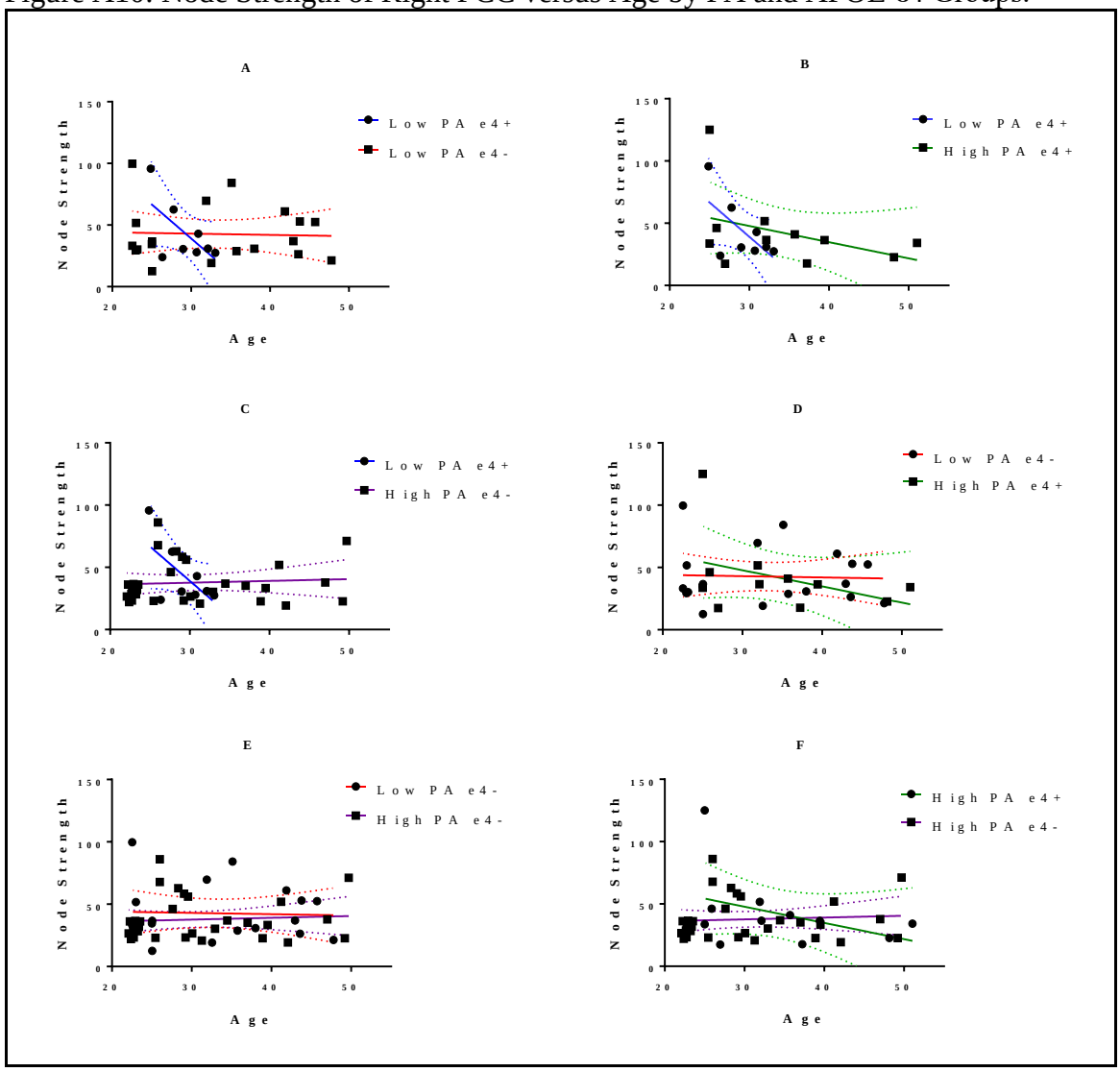

Legend: Graphs show the linear regression line when plotting the node strength of the right PCC versus age. Blue line and circle data points: Low PA APOE-ε4 carriers; Red line and square data points: Low PA APOE-ε4 non-carriers; Green line square data points: High PA APOE-ε4 carriers; Purple line square data points: High PA APOE-ε4 non-carriers. Panel A: Comparing the regression lines of APOE-ε4 carriers and non-carriers in the Low PA category. The slopes of the regression lines are not significantly different from each other ($F(1,23) = 3.133$, $p = 0.0900$); Panel B: Comparing the regression lines of APOE-ε4 carriers in the High and Low PA categories. The slopes are not significantly different from each other ($F(1,15) = 1.441$, $p = 0.2486$); Panel C: Comparing the regression lines of Low PA APOE-ε4 carriers and High PA APOE-ε4 non-carriers. The slopes are significantly different from each other ($F(1,35) = 5.678$, $p = 0.0227$); Panel D: Comparing the regression lines of Low PA APOE-ε4 non-carriers and High PA APOEε4 carriers. The slopes are not significantly different from each other ($F(1,26) = 1.187$, $p = 0.2860$); Panel E: Comparing the regression lines of APOE-ε4 non-carriers with High and Low PA levels. The slopes are not significantly different from each other ($F(1,46) = 0.1427$, $p = 0.7074$); Panel F: Comparing the regression lines of APOE-ε4 carriers and non-carriers in the High PA category. The slopes are not significantly different from each other ($F(1,38) = 2.975$, $p = 0.0927$).

Figure A11: Node Strength of Left PCC by PA or APOE-ε4 Group.

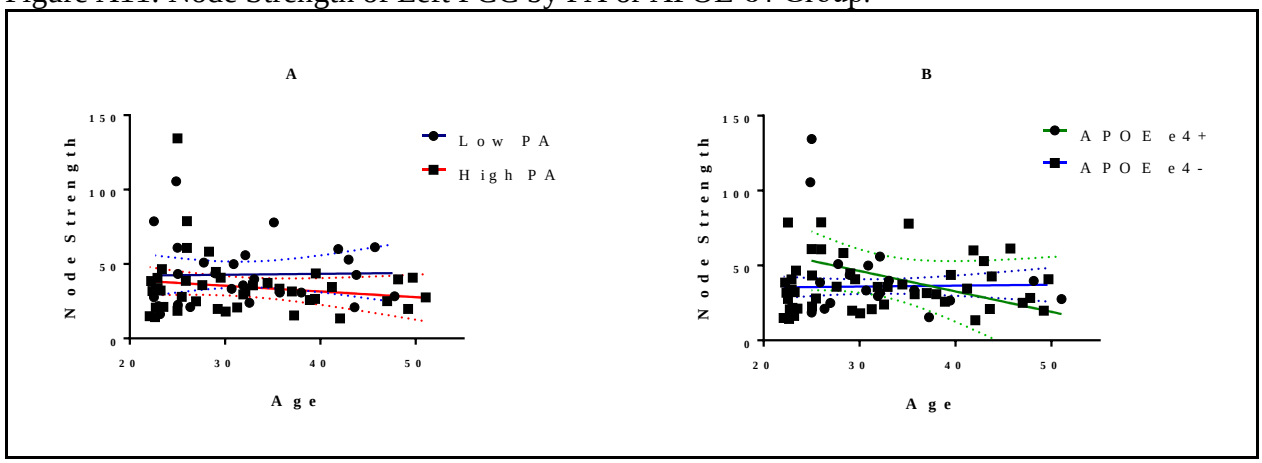

Legend: Panel A: Graphs show the linear regression line when plotting the node strength of the left PCC versus age. Panel A: Comparing the regression lines of High and Low PA. Low PA: dark blue line and circle data points. High PA: red line and square data points. The slopes of the two equations are not significantly different ($F(1,65) = 0.4879$, $p = 0.4879$). Panel B: Comparing the regression lines of APOE-ε4 carriers and non-carriers. APOE-ε4 carriers: green line and circle data points. APOE-ε4 non-carriers: blue line and square data points. The slopes of the two equations are not quite significantly different ($F(1,65) = 3.747$, $p = 0.0573$).

Equations of regression lines in Figure A11 generated by GraphPad Prism 7.0 software:

41) Low PA: $y = 0.06194x + 40.93$

The slope is not significantly different from 0 ($F(1,25) = 0.01332$, $p = 0.9090$).

42) High PA: $y = -0.3835x + 46.9$

The slope is not significantly different from 0 ($F(1,40) = 1.095$, $p = 0.3016$).

43) APOE-ε4 positive: $y = -1.364x + 87.24$

The slope is not significantly different from 0 ($F(1,17) = 2.261$, $p = 0.1510$).

44) APOE-ε4 negative: $y = 0.06218x + 34.03$

The slope is not significantly different from 0 ($F(1,48) = 0.05077$, $p = 0.8227$).

Equations of regression lines in Figure A12 generated by GraphPad Prism 7.0 software.

45) Low PA APOE-ε4 positive: $y = -3.57x + 154.8$

The slope is not significantly different from 0 ($F(1,6) = 1.203$, $p = 0.3148$).

46) Low PA APOE-ε4 negative: $y = 0.3402x + 28.66$

The slope is not significantly different from 0 ($F(1,17) = 0.4381$, $p = 0.5169$).

47) High PA APOE-ε4 positive: $y = -1.069x + 75.02$

The slope is not significantly different from 0 ($F(1,9) = 0.8583$, $p = 0.3784$).

48) High PA APOE-ε4 negative: $y = -0.2171x + 40.21$

The slope is not significantly different from 0 ($F(1,29) = 0.4764$, $p = 0.4955$).

Figure A12: Node Strength of Left PCC versus Age by PA and APOE-ε4 Groups.

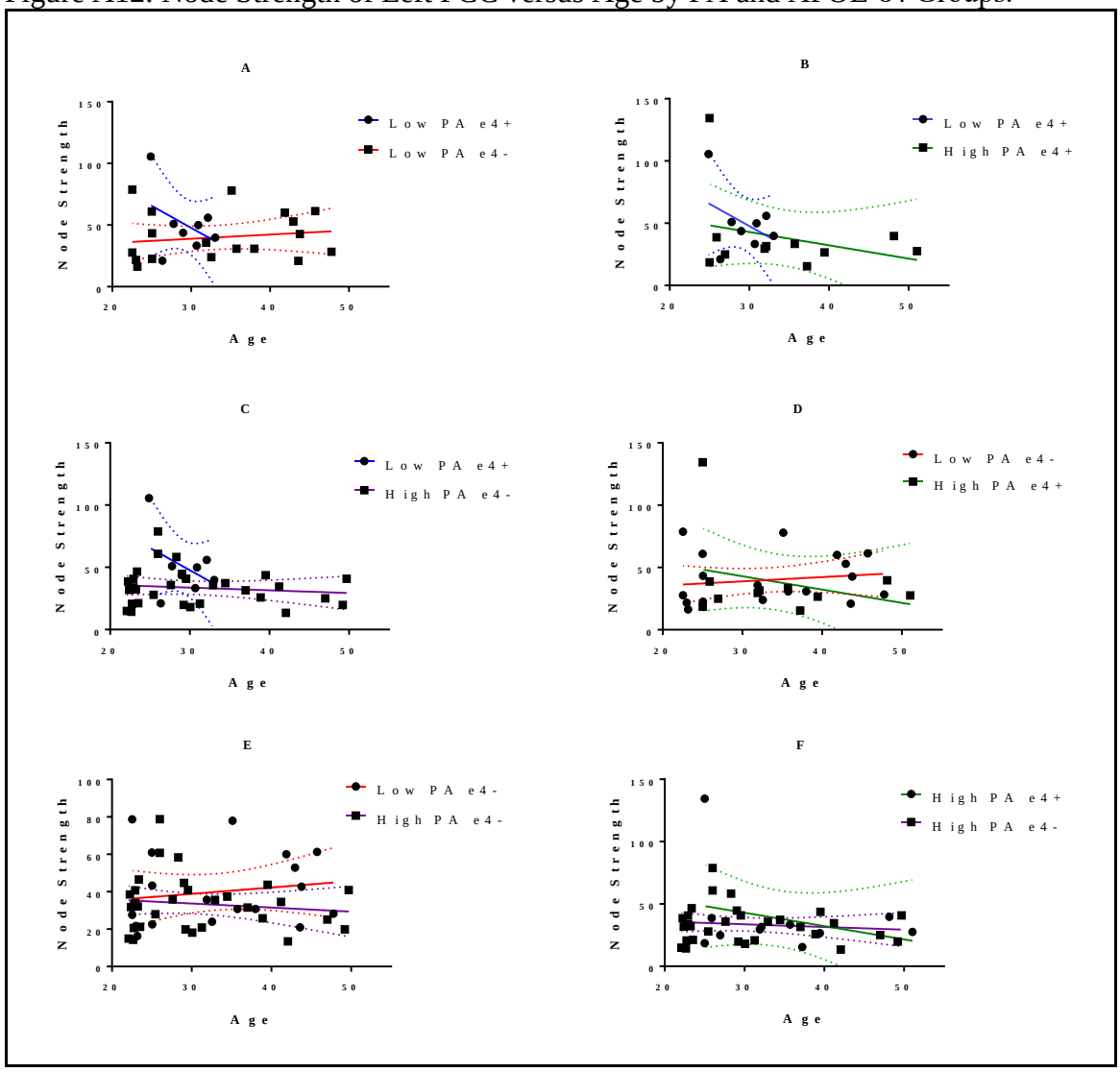

Legend: Graphs show the linear regression line when plotting the node strength of the left PCC versus age. Blue line and circle data points: Low PA APOE-ε4 carriers; Red line and square data points: Low PA APOE-ε4 non-carriers; Green line square data points: High PA APOE-ε4 carriers; Purple line square data points: High PA APOE-ε4 non-carriers. Panel A: Comparing the regression lines of APOE-ε4 carriers and non-carriers in the Low PA category. The slopes of the regression lines are not significantly different from each other ($F(1,23) = 1.849$, $p = 0.1871$); Panel B: Comparing the regression lines of APOE-ε4 carriers in the High and Low PA categories. The slopes are not significantly different from each other ($F(1,15) = 0.3742$, $p = 0.5499$); Panel C: Comparing the regression lines of Low PA APOE-ε4 carriers and High PA APOE-ε4 non-carriers. The slopes are not significantly different from each other ($F(1,35) = 2.214$, $p = 0.1457$); Panel D: Comparing the regression lines of Low PA APOE-ε4 non-carriers and High PA APOEε4 carriers. The slopes are not significantly different from each other ($F(1,26) = 1.651$, $p = 0.2102$); Panel E: Comparing the regression lines of APOE-ε4 non-carriers with High and Low PA levels. The slopes are not significantly different from each other ($F(1,46) = 0.9783$, $p = 0.3278$); Panel F: Comparing the regression lines of APOE-ε4 carriers and non-carriers in the High PA category. The slopes are not significantly different from each other ($F(1,38) = 1.021$, $p = 0.3187$).

Figure A13: Node Strength of Right Dorsal mPFC by PA or APOE-ε4 Group.

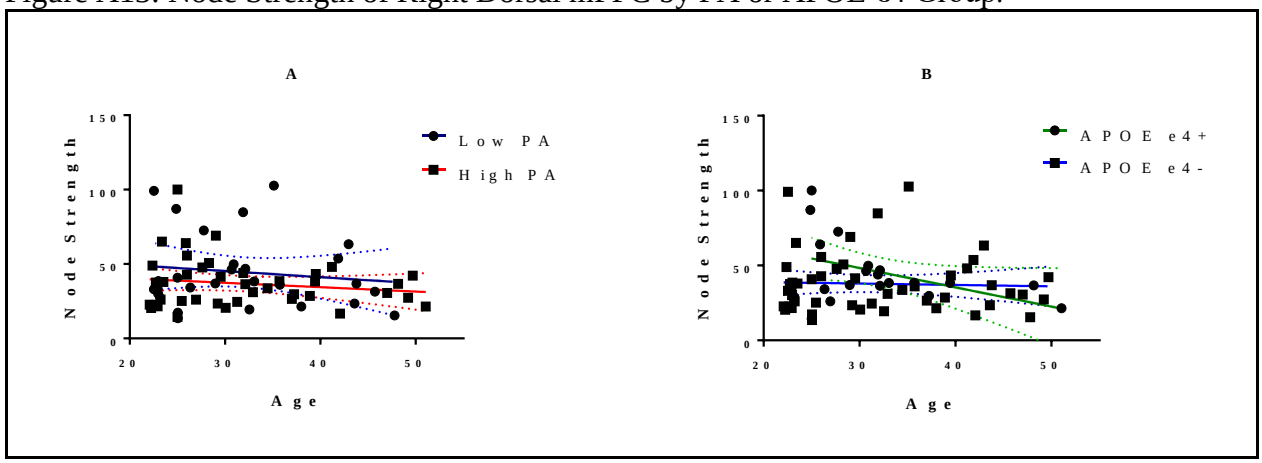

Legend: Panel A: Graphs show the linear regression line when plotting the node strength of the right dorsal mPFC versus age. Panel A: Comparing the regression lines of High and Low PA. Low PA: dark blue line and circle data points. High PA: red line and square data points. The slopes of the two equations are not significantly different ($F(1,65) = 0.196$, $p = 0.6595$). Panel B: Comparing the regression lines of APOE-ε4 carriers and non-carriers. APOE-ε4 carriers: green line and circle data points. APOE-ε4 non-carriers: blue line and square data points. The slopes of the two equations are not significantly different ($F(1,65) = 2.323$, $p = 0.1323$).

Equations of regression lines in Figure A13 generated by GraphPad Prism 7.0 software:

49) Low PA: $y = 0.2432x + 42.04$

The slope is not significantly different from 0 ($F(1,25) = 0.2026$, $p = 0.6565$).

50) High PA: $y = -0.03088x + 45$

The slope is not significantly different from 0 ($F(1,40) = 0.008$, $p = 0.9292$).

51) APOE-ε4 positive: $y = -0.0858x + 77.87$

The slope is not significantly different from 0 ($F(1,17) = 0.9106$, $p = 0.3533$).

52) APOE-ε4 negative: $y = 0.2805x + 35.34$

The slope is not significantly different from 0 ($F(1,48) = 1.029$, $p = 0.3155$).

Equations of regression lines in Figure A14 generated by GraphPad Prism 7.0 software.

53) Low PA APOE-ε4 positive: $y = -1.429x + 99.08$

The slope is not significantly different from 0 ($F(1,6) = 0.2208$, $p = 0.6550$).

54) Low PA APOE-ε4 negative: $y = 0.4613x + 31.47$

The slope is not significantly different from 0 ($F(1,17) = 0.6904$, $p = 0.4176$).

55) High PA APOE-ε4 positive: $y = -0.6173x + 69.26$

The slope is not significantly different from 0 ($F(1,9) = 0.3226$, $p = 0.5840$).

56) High PA APOE-ε4 negative: $y = -0.1074x + 39.33$

The slope is not significantly different from 0 ($F(1,29) = 0.1289$, $p = 0.7221$).

Figure A14: Node Strength of Right Dorsal mPFC versus Age by PA and APOE-ε4 Groups.

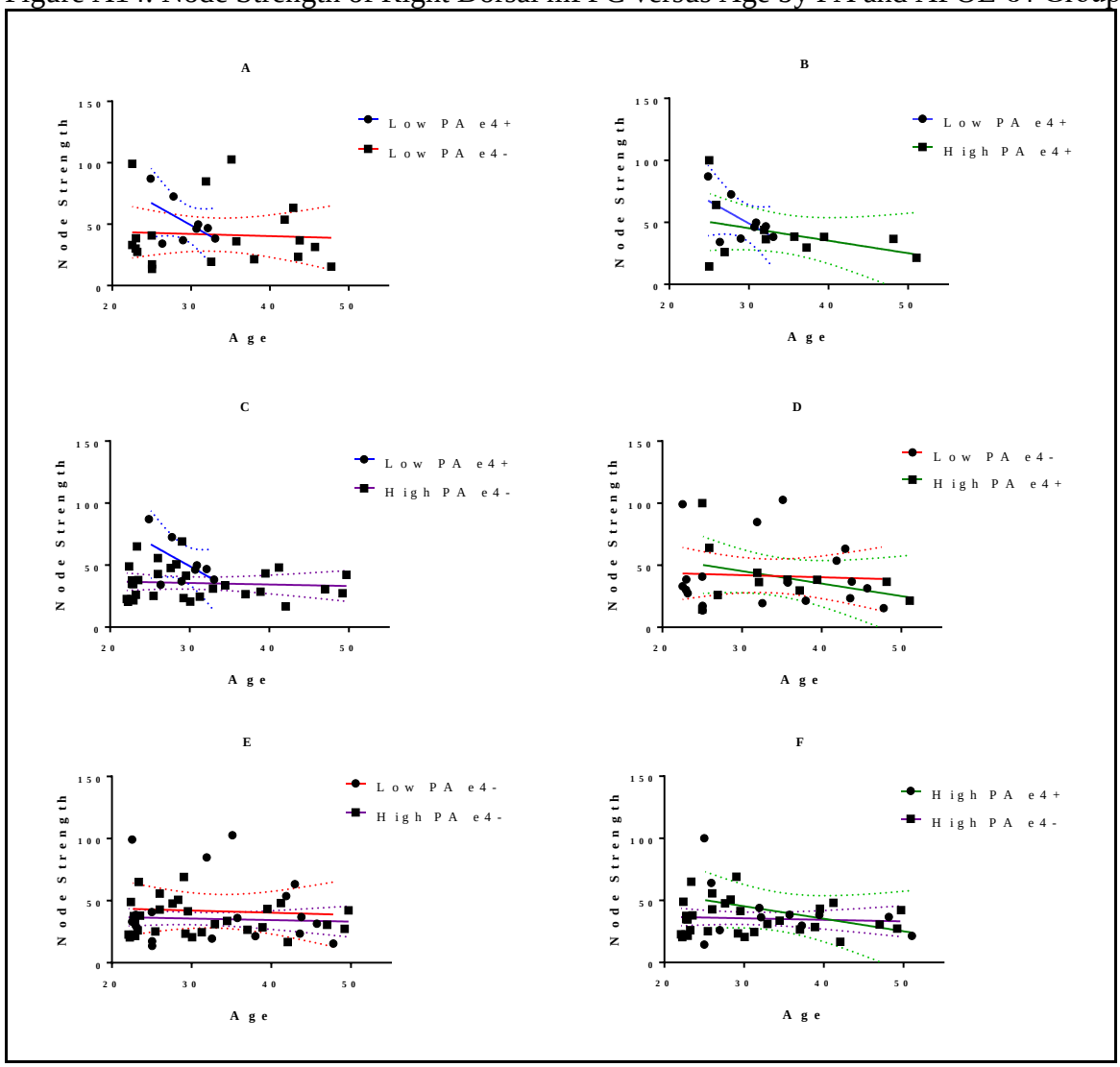

Legend: Graphs show the linear regression line when plotting the node strength of the right dorsal mPFC versus age. Blue line and circle data points: Low PA APOE-ε4 carriers; Red line and square data points: Low PA APOE-ε4 non-carriers; Green line square data points: High PA APOE-ε4 carriers; Purple line square data points: High PA APOE-ε4 non-carriers. Panel A: Comparing the regression lines of APOE-ε4 carriers and non-carriers in the Low PA category. The slopes of the regression lines are not significantly different from each other ($F(1,23) = 0.4057$, $p = 0.5304$); Panel B: Comparing the regression lines of APOE-ε4 carriers in the High and Low PA categories. The slopes are not significantly different from each other ($F(1,15) = 0.04466$, $p = 0.8355$); Panel C: Comparing the regression lines of Low PA APOE-ε4 carriers and High PA APOE-ε4 non-carriers. The slopes are not significantly different from each other ($F(1,36) = 0.5208$, $p = 0.4753$); Panel D: Comparing the regression lines of Low PA APOE-ε4 non-carriers and High PA APOEε4 carriers. The slopes are not significantly different from each other ($F(1,26) = 0.9644$, $p = 0.3351$); Panel E: Comparing the regression lines of APOE-ε4 non-carriers with High and Low PA levels. The slopes are not significantly different from each other ($F(1,46) = 0.3789$, $p = 0.5412$); Panel F: Comparing the regression lines of APOE-ε4 carriers and non-carriers in the High PA category. The slopes are not significantly different from each other ($F(1,38) = 1.769$, $p = 0.1915$).

Figure A15: Node Strength of Left Dorsal mPFC by PA or APOE-ε4 Group.

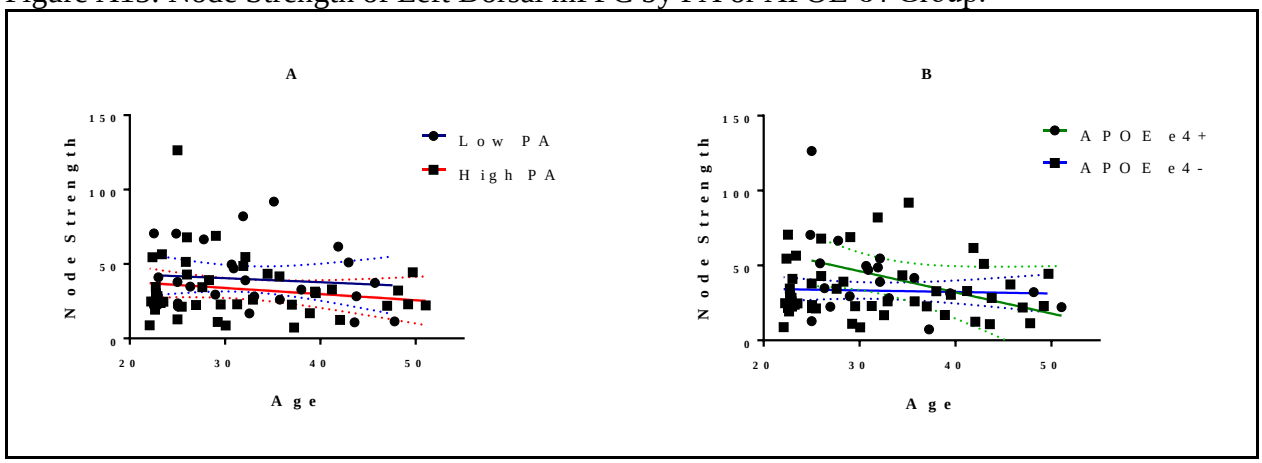

Legend: Panel A: Graphs show the linear regression line when plotting the node strength of the left dorsal mPFC versus age. Panel A: Comparing the regression lines of High and Low PA. Low PA: dark blue line and circle data points. High PA: red line and square data points. The slopes of the two equations are not significantly different ($F(1,65) = 0.0458$, $p = 0.8313$). Panel B: Comparing the regression lines of APOE-ε4 carriers and non-carriers. APOE-ε4 carriers: green line and circle data points. APOE-ε4 non-carriers: blue line and square data points. The slopes of the two equations are not quite significantly different ($F(1,65) = 3.125$, $p = 0.0818$).

Equations of regression lines in Figure A15 generated by GraphPad Prism 7.0 software:

57) Low PA: $y = -0.2711x + 48.61$

The slope is not significantly different from 0 ($F(1,25) = 0.2547$, $p = 0.6182$).

58) High PA: $y = -0.4107x + 46.22$

The slope is not significantly different from 0 ($F(1,40) = 1.169$, $p = 0.2861$).

59) APOE-ε4 positive: $y = -1.414x + 88.62$

The slope is not significantly different from 0 ($F(1,17) = 3.259$, $p = 0.0888$).

60) APOE-ε4 negative: $y = -0.1034x + 36.45$

The slope is not significantly different from 0 ($F(1,48) = 0.1096$, $p = 0.7421$).

Equations of regression lines in Figure A16 generated by GraphPad Prism 7.0 software.

61) Low PA APOE-ε4 positive: $y = -3.153x + 138.2$

The slope is not significantly different from 0 ($F(1,6) = 2.786$, $p = 0.1461$).

62) Low PA APOE-ε4 negative: $y = -0.066x + 39.73$

The slope is not significantly different from 0 ($F(1,17) = 0.01137$, $p = 0.9163$).

63) High PA APOE-ε4 positive: $y = -1.366x + 88.03$

The slope is not significantly different from 0 ($F(1,9) = 1.536$, $p = 0.2465$).

64) High PA APOE-ε4 negative: $y = -0.2303x + 37.55$

The slope is not significantly different from 0 ($F(1,29) = 0.4715$, $p = 0.4978$).

Figure A16: Node Strength of Left Dorsal mPFC versus Age by PA and APOE-ε4 Groups.

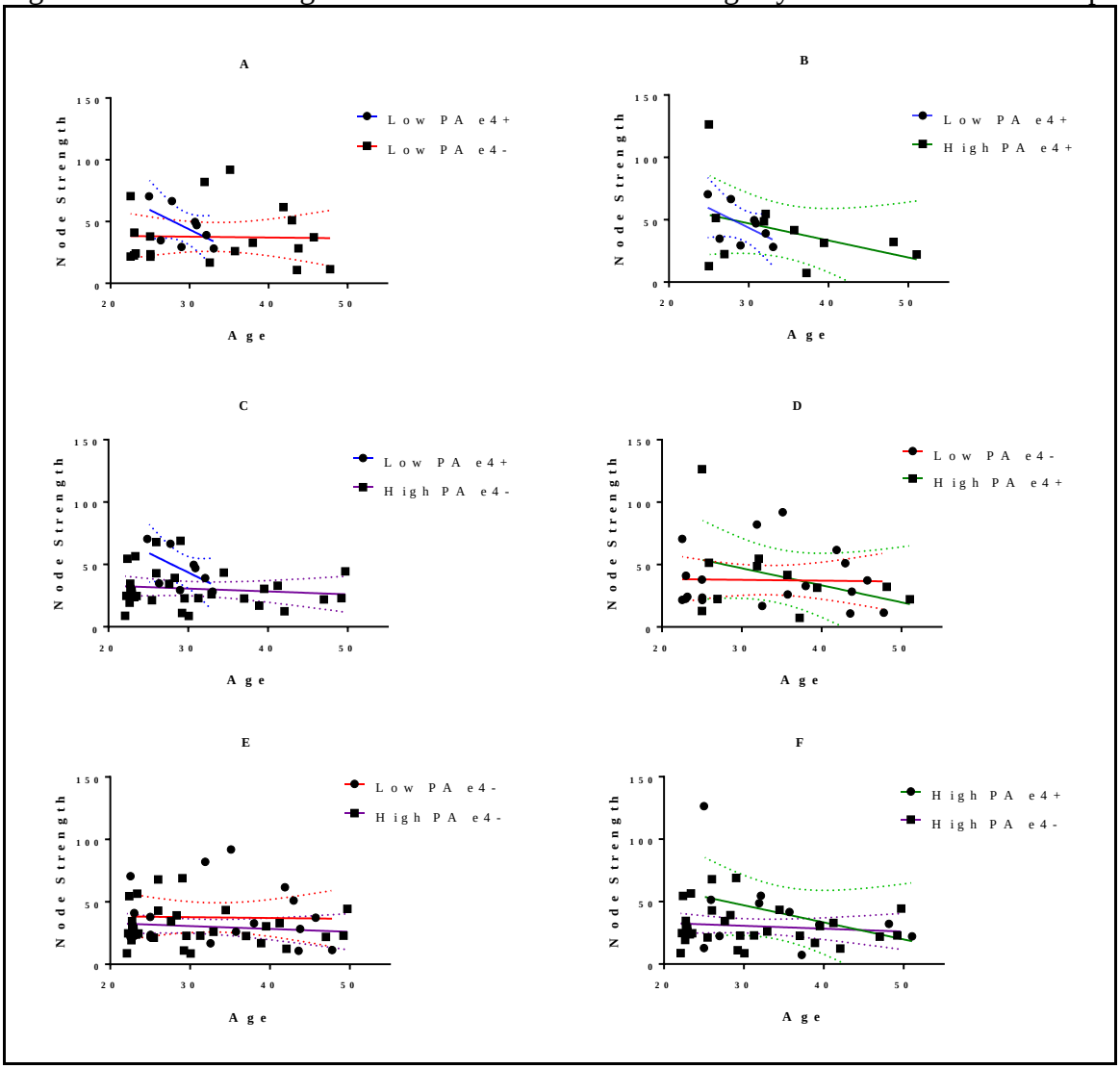

Legend: Graphs show the linear regression line when plotting the node strength of the left dorsal mPFC versus age. Blue line and circle data points: Low PA APOE-ε4 carriers; Red line and square data points: Low PA APOE-ε4 non-carriers; Green line square data points: High PA APOE-ε4 carriers; Purple line square data points: High PA APOE-ε4 non-carriers. Panel A: Comparing the regression lines of APOE-ε4 carriers and non-carriers in the Low PA category. The slopes of the regression lines are not significantly different from each other ($F(1,23) = 1.082$, $p = 0.3090$); Panel B: Comparing the regression lines of APOE-ε4 carriers in the High and Low PA categories. The slopes are not significantly different from each other ($F(1,15) = 0.2529$, $p = 0.6224$); Panel C: Comparing the regression lines of Low PA APOE-ε4 carriers and High PA APOE-ε4 non-carriers. The slopes are not significantly different from each other ($F(1,35) = 1.995$, $p = 0.1666$); Panel D: Comparing the regression lines of Low PA APOE-ε4 non-carriers and High PA APOEε4 carriers. The slopes are not significantly different from each other ($F(1,26) = 1.1238$, $p = 0.2760$); Panel E: Comparing the regression lines of APOE-ε4 non-carriers with High and Low PA levels. The slopes are not significantly different from each other ($F(1,46) = 0.06535$, $p = 0.7994$); Panel F: Comparing the regression lines of APOE-ε4 carriers and non-carriers in the High PA category. The slopes are not significantly different from each other ($F(1,38) = 1.814$, $p = 0.1860$).

Figure A17: Node Strength of Right Lateral mPFC by PA or APOE-ε4 Group.

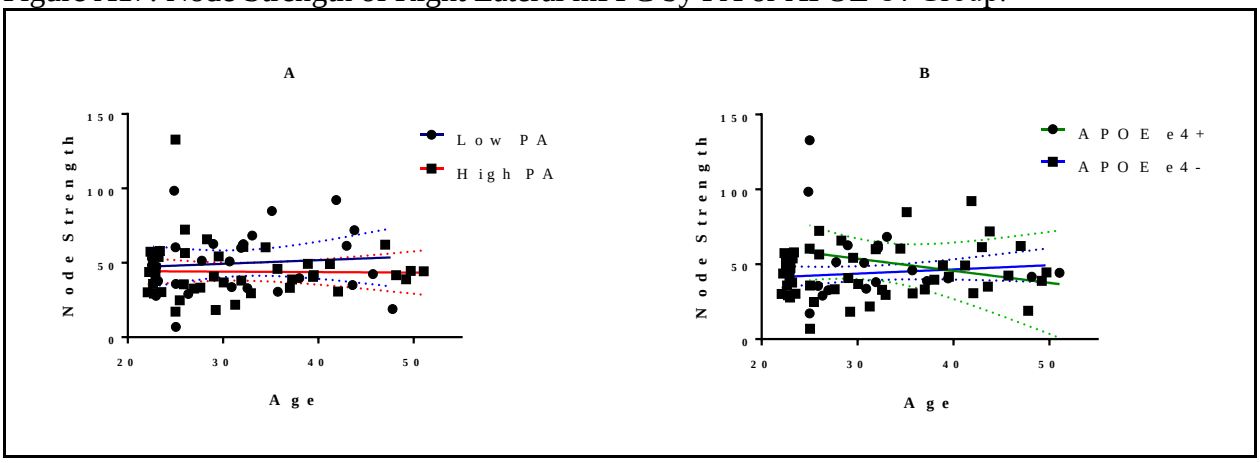

Legend: Panel A: Graphs show the linear regression line when plotting the node strength of the right lateral mPFC versus age. Panel A: Comparing the regression lines of High and Low PA. Low PA: dark blue line and circle data points. High PA: red line and square data points. The slopes of the two equations are not significantly different ($F(1,65) = 0.196$, $p = 0.6595$). Panel B: Comparing the regression lines of APOE-ε4 carriers and non-carriers. APOE-ε4 carriers: green line and circle data points. APOE-ε4 non-carriers: blue line and square data points. The slopes of the two equations are not significantly different ($F(1,65) = 2.323$, $p = 0.1323$).

Equations of regression lines in Figure A17 generated by GraphPad Prism 7.0 software:

65) Low PA: $y = 0.2432x + 42.04$

The slope is not significantly different from 0 ($F(1,25) = 0.2026$, $p = 0.6565$).

66) High PA: $y = -0.03088x + 45$

The slope is not significantly different from 0 ($F(1,40) = 0.008$, $p = 0.9292$).

67) APOE-ε4 positive: $y = -0.8058x + 77.87$

The slope is not significantly different from 0 ($F(1,17) = 0.9106$, $p = 0.3533$).

68) APOE-ε4 negative: $y = 0.2805 + 35.34$

The slope is not significantly different from 0 ($F(1,48) = 1.029$, $p = 0.3155$).

Equations of regression lines in Figure A18 generated by GraphPad Prism 7.0 software.

69) Low PA APOE-ε4 positive: $y = -1.429x + 99.08$

The slope is not significantly different from 0 ($F(1,6) = 0.2208$, $p = 0.6550$).

70) Low PA APOE-ε4 negative: $y = 0.4613x + 31.47$

The slope is not significantly different from 0 ($F(1,17) = 0.6904$, $p = 0.4176$).

71) High PA APOE-ε4 positive: $y = -0.6173x + 69.26$

The slope is not significantly different from 0 ($F(1,9) = 0.3226$, $p = 0.5840$).

72) High PA APOE-ε4 negative: $y = 0.1074x + 39.33$

The slope is not significantly different from 0 ($F(1,29) = 0.1289$, $p = 0.7221$).

Figure A18: Node Strength of Right Lateral mPFC versus Age by PA and APOE-ε4 Groups.

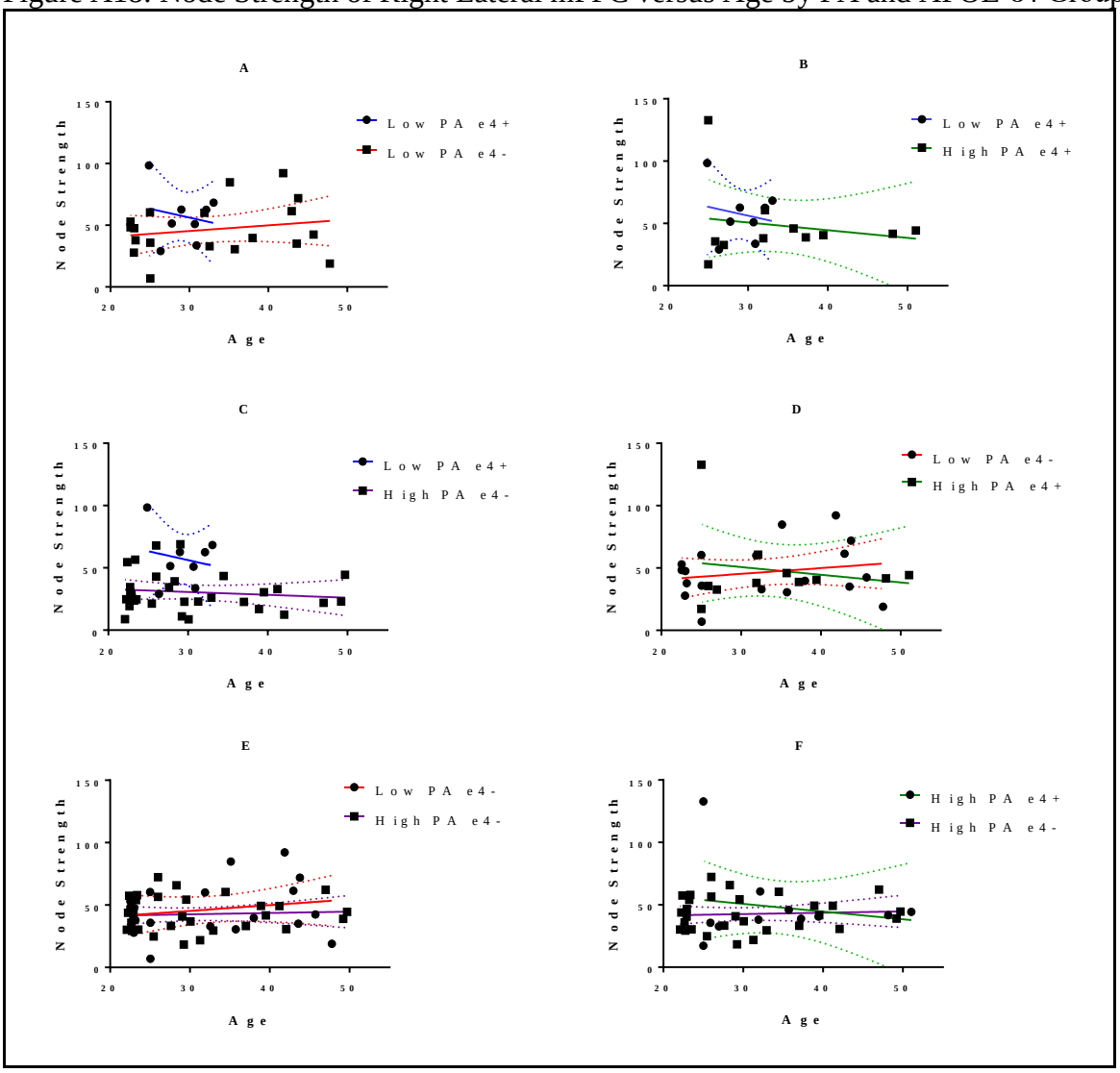

Legend: Graphs show the linear regression line when plotting the node strength of the right lateral mPFC versus age. Blue line and circle data points: Low PA APOE-ε4 carriers; Red line and square data points: Low PA APOE-ε4 non-carriers; Green line square data points: High PA APOE-ε4 carriers; Purple line square data points: High PA APOE-ε4 non-carriers. Panel A: Comparing the regression lines of APOE-ε4 carriers and non-carriers in the Low PA category. The slopes of the regression lines are not significantly different from each other ($F(1,23) = 0.4057$, $p = 0.5304$); Panel B: Comparing the regression lines of APOE-ε4 carriers in the High and Low PA categories. The slopes are not significantly different from each other ($F(1,15) = 0.04466$, $p = 0.8355$); Panel C: Comparing the regression lines of Low PA APOE-ε4 carriers and High PA APOE-ε4 non-carriers. The slopes are not significantly different from each other ($F(1,35) = 0.5208$, $p = 0.4753$); Panel D: Comparing the regression lines of Low PA APOE-ε4 non-carriers and High PA APOEε4 carriers. The slopes are not significantly different from each other ($F(1,26) = 0.9644$, $p = 0.3351$); Panel E: Comparing the regression lines of APOE-ε4 non-carriers with High and Low PA levels. The slopes are not significantly different from each other ($F(1,46) = 0.3789$, $p = 0.5412$); Panel F: Comparing the regression lines of APOE-ε4 carriers and non-carriers in the High PA category. The slopes are not significantly different from each other ($F(1,38) = 0.8264$, $p = 0.3691$).

Figure A19: Node Strength of Left Lateral mPFC by PA or APOE-ε4 Group.

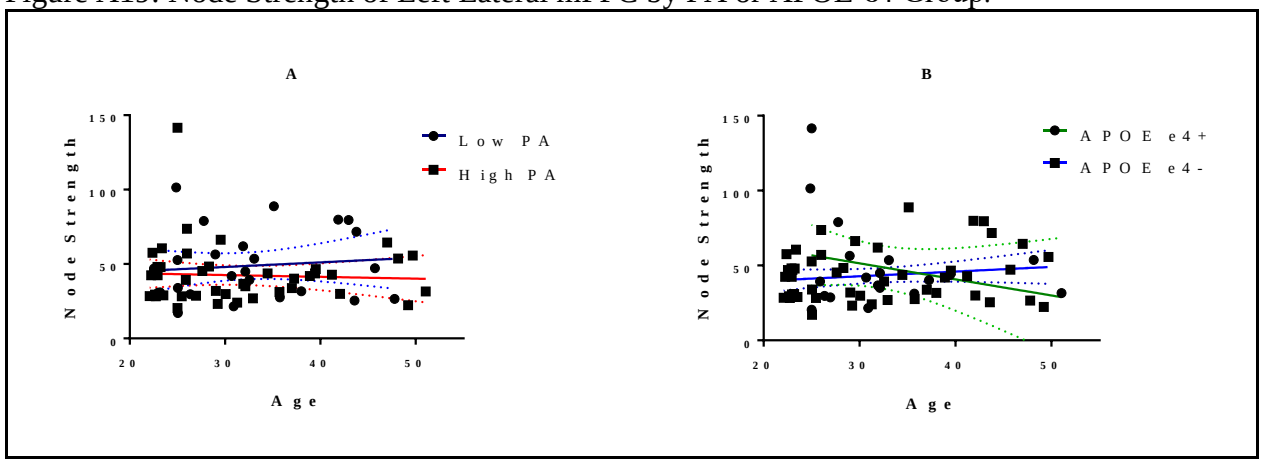

Legend: Panel A: Graphs show the linear regression line when plotting the node strength of the left lateral mPFC versus age. Panel A: Comparing the regression lines of High and Low PA. Low PA: dark blue line and circle data points. High PA: red line and square data points. The slopes of the two equations are not significantly different ($F(1,65) = 0.4414$, $p = 0.5088$). Panel B: Comparing the regression lines of APOE-ε4 carriers and non-carriers. APOE-ε4 carriers: green line and circle data points. APOE-ε4 non-carriers: blue line and square data points. The slopes of the two equations are not quite significantly different ($F(1,65) = 3.43$, $p = 0.0685$).

Equations of regression lines in Figure A19 generated by GraphPad Prism 7.0 software:

73) Low PA: $y = 0.3106x + 38.69$

The slope is not significantly different from 0 ($F(1,25) = 0.315$, $p = 0.5796$).

74) High PA: $y = -0.1205x + 46.2$

The slope is not significantly different from 0 ($F(1,40) = 0.107$, $p = 0.7453$).

75) APOE-ε4 positive: $y = -1.073x + 83.61$

The slope is not significantly different from 0 ($F(1,17) = 1.318$, $p = 0.2669$).

76) APOE-ε4 negative: $y = 0.3126x + 33.42$

The slope is not significantly different from 0 ($F(1,48) = 1.283$, $p = 0.2630$).

Equations of regression lines in Figure A20 generated by GraphPad Prism 7.0 software.

77) Low PA APOE-ε4 positive: $y = -4.758x + 193.2$

The slope is not significantly different from 0 ($F(1,6) = 2.262$, $p = 0.1833$).

78) Low PA APOE-ε4 negative: $y = 0.613x + 26.26$

The slope is not significantly different from 0 ($F(1,17) = 1.336$, $p = 0.2637$).

79) High PA APOE-ε4 positive: $y = -0.7428x + 71.2$

The slope is not significantly different from 0 ($F(1,9) = 0.3896$, $p = 0.5480$).

80) High PA APOE-ε4 negative: $y = -0.04094x + 40.01$

The slope is not significantly different from 0 ($F(1,29) = 0.01765$, $p = 0.8952$).

Figure A20: Node Strength of Left Lateral mPFC versus Age by PA and APOE-ε4 Groups.

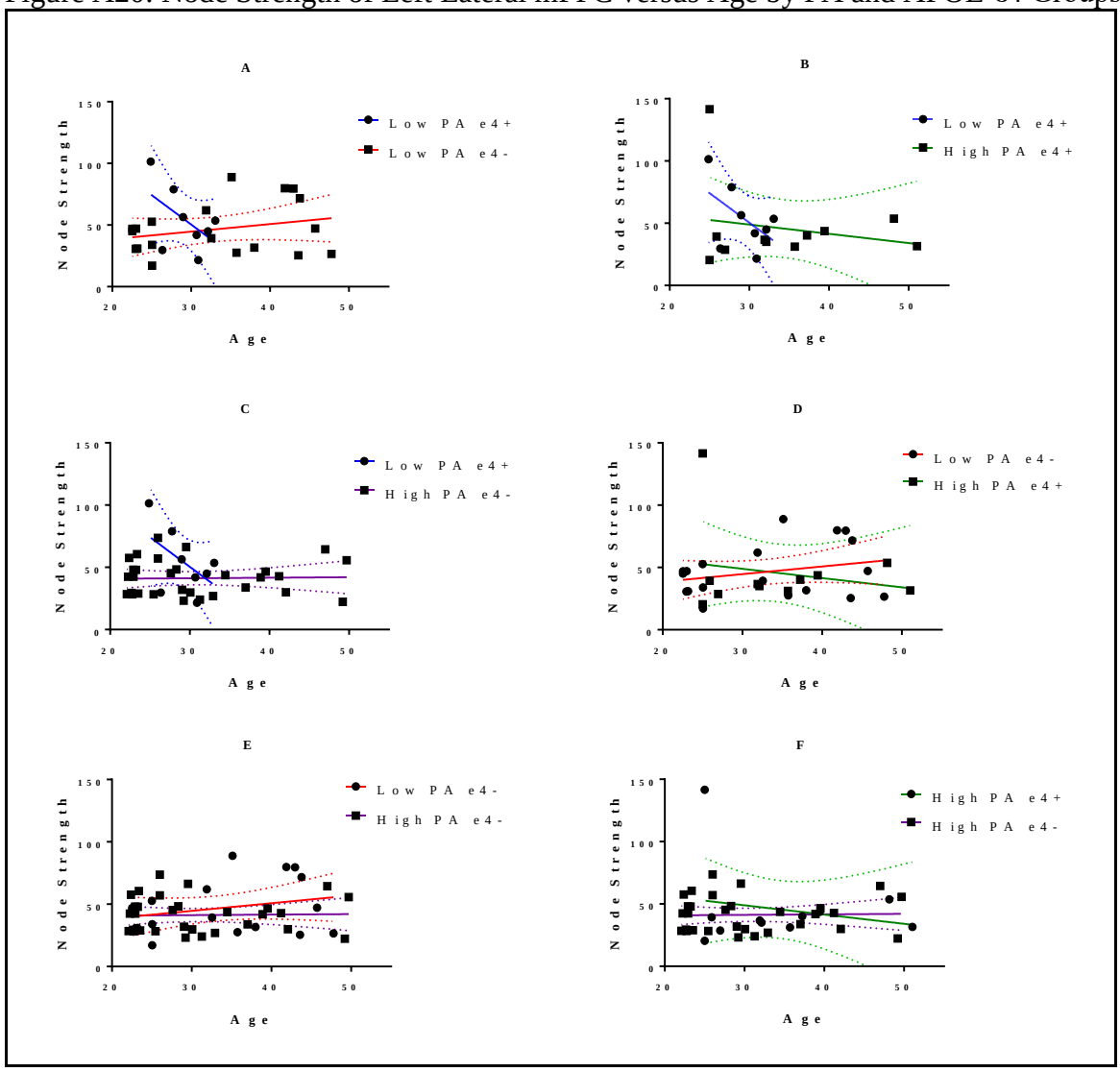

Legend: Graphs show the linear regression line when plotting the node strength of the left lateral mPFC versus age. Blue line and circle data points: Low PA APOE-ε4 carriers; Red line and square data points: Low PA APOE-ε4 non-carriers; Green line square data points: High PA APOE-ε4 carriers; Purple line square data points: High PA APOE-ε4 non-carriers. Panel A: Comparing the regression lines of APOE-ε4 carriers and non-carriers in the Low PA category. The slopes of the regression lines are not quite significantly different from each other ($F(1,23) = 3.409$, $p = 0.0777$); Panel B: Comparing the regression lines of APOE-ε4 carriers in the High and Low PA categories. The slopes are not significantly different from each other ($F(1,15) = 0.9357$, $p = 0.3487$); Panel C: Comparing the regression lines of Low PA APOE-ε4 carriers and High PA APOE-ε4 non-carriers. The slopes are significantly different from each other ($F(1,35) = 4.753$, $p = 0.0361$); Panel D: Comparing the regression lines of Low PA APOE-ε4 non-carriers and High PA APOEε4 carriers. The slopes are not significantly different from each other ($F(1,26) = 1.436$, $p = 0.2416$); Panel E: Comparing the regression lines of APOE-ε4 non-carriers with High and Low PA levels. The slopes are not significantly different from each other ($F(1,46) = 1.016$, $p = 0.3187$); Panel F: Comparing the regression lines of APOE-ε4 carriers and non-carriers in the High PA category. The slopes are not significantly different from each other ($F(1,38) = 0.8444$, $p = 0.3639$).

Figure A21: Node Strength of Right Hippocampal Head by PA or APOE-ε4 Group.

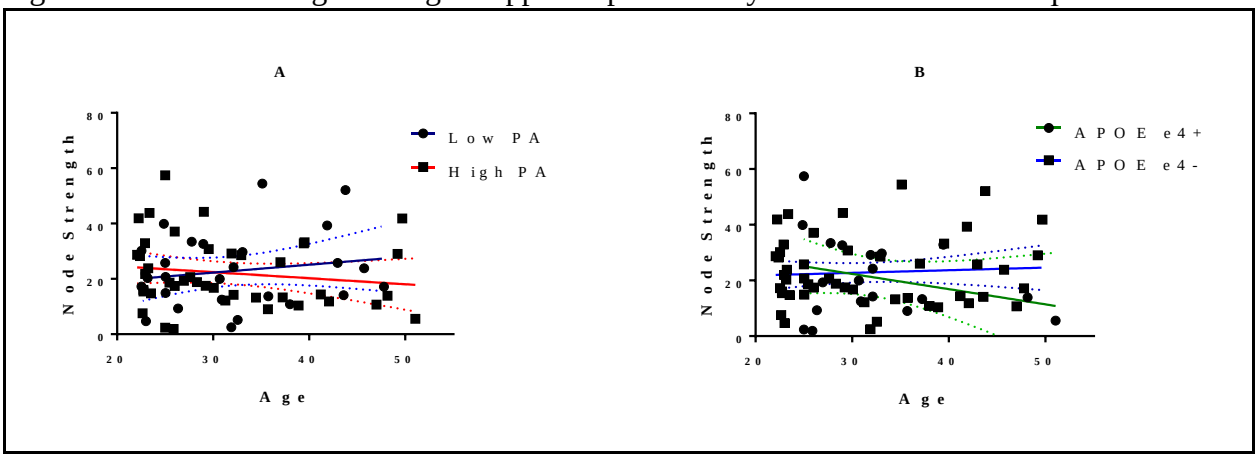

Legend: Panel A: Graphs show the linear regression line when plotting the node strength of the right hippocampal head versus age. Panel A: Comparing the regression lines of High and Low PA. Low PA: dark blue line and circle data points. High PA: red line and square data points. The slopes of the two equations are not significantly different ($F(1,65) = 1.687$, $p = 0.1986$). Panel B: Comparing the regression lines of APOE-ε4 carriers and non-carriers. APOE-ε4 carriers: green line and circle data points. APOE-ε4 non-carriers: blue line and square data points. The slopes of the two equations are not significantly different ($F(1,65) = 1.989$, $p = 0.1633$).

Equations of regression lines in Figure A21 generated by GraphPad Prism 7.0 software:

81) Low PA: $y = 0.2857x + 13.69$

The slope is not significantly different from 0 ($F(1,25) = 0.7716$, $p = 0.3881$).

82) High PA: $y = -0.2184x + 28.97$

The slope is not significantly different from 0 ($F(1,40) = 0.9575$, $p = 0.3337$).

83) APOE-ε4 positive: $y = -0.5465x + 38.73$

The slope is not significantly different from 0 ($F(1,17) = 1.47$, $p = 0.2420$).

84) APOE-ε4 negative: $y = 0.0945x + 19.89$

The slope is not significantly different from 0 ($F(1,48) = 0.2281$, $p = 0.6351$).

Equations of regression lines in Figure A22 generated by GraphPad Prism 7.0 software.

85) Low PA APOE-ε4 positive: $y = -0.8173x + 49.19$

The slope is not significantly different from 0 ($F(1,6) = 0.301$, $p = 0.6030$).

86) Low PA APOE-ε4 negative: $y = 0.3881x + 8.99$

The slope is not significantly different from 0 ($F(1,17) = 1.137$, $p = 0.3011$).

87) High PA APOE-ε4 positive: $y = -0.403x + 31.97$

The slope is not significantly different from 0 ($F(1,9) = 0.4667$, $p = 0.5117$).

88) High PA APOE-ε4 negative: $y = -0.084x + 26.06$

The slope is not significantly different from 0 ($F(1,29) = 0.1299$, $p = 0.7211$).

Figure A22: Node Strength of Right Hippocampal Head vs. Age by PA and APOE-ε4 Groups.

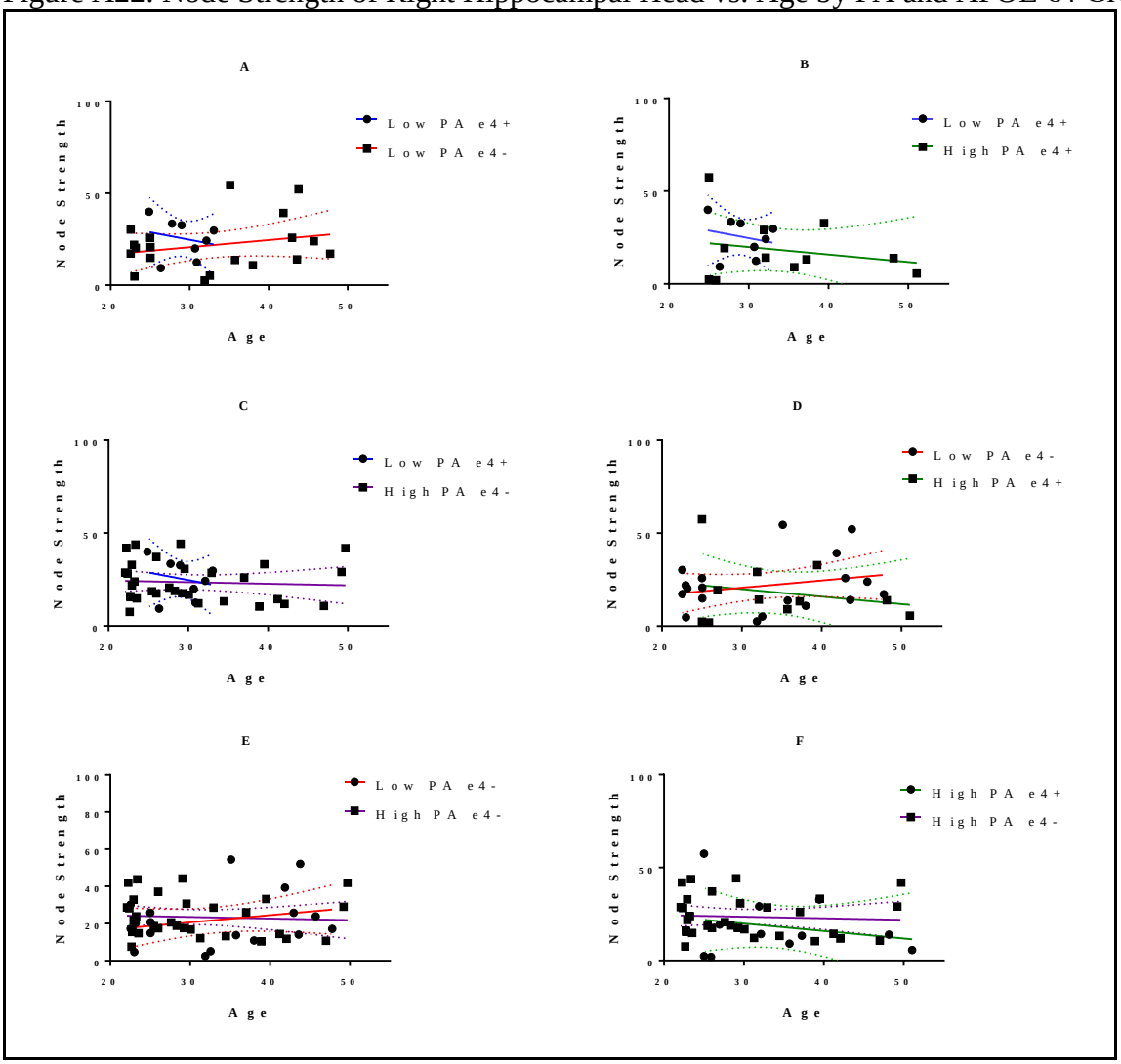

Legend: Graphs show the linear regression line when plotting the node strength of the right hippocampal head versus age. Blue line and circle data points: Low PA APOE-ε4 carriers; Red line and square data points: Low PA APOE-ε4 non-carriers; Green line square data points: High PA APOE-ε4 carriers; Purple line square data points: High PA APOE-ε4 non-carriers. Panel A: Comparing the regression lines of APOE-ε4 carriers and non-carriers in the Low PA category. The slopes of the regression lines are not significantly different from each other ($F(1,23) = 0.439$, $p = 0.5142$); Panel B: Comparing the regression lines of APOE-ε4 carriers in the High and Low PA categories. The slopes are not significantly different from each other ($F(1,15) = 0.04155$, $p = 0.8412$); Panel C: Comparing the regression lines of Low PA APOE-ε4 carriers and High PA APOE-ε4 non-carriers. The slopes are not significantly different from each other ($F(1,35) = 0.2496$, $p = 0.6205$); Panel D: Comparing the regression lines of Low PA APOE-ε4 non-carriers and High PA APOEε4 carriers. The slopes are not significantly different from each other ($F(1,26) = 1.443$, $p = 0.2404$); Panel E: Comparing the regression lines of APOE-ε4 non-carriers with High and Low PA levels. The slopes are not significantly different from each other ($F(1,46) = 1.339$, $p = 0.2531$); Panel F: Comparing the regression lines of APOE-ε4 carriers and non-carriers in the High PA category. The slopes are not significantly different from each other ($F(1,38) = 0.3828$, $p = 0.5398$).

Figure A23: Node Strength of Right Hippocampal Body by PA or APOE-ε4 Group.

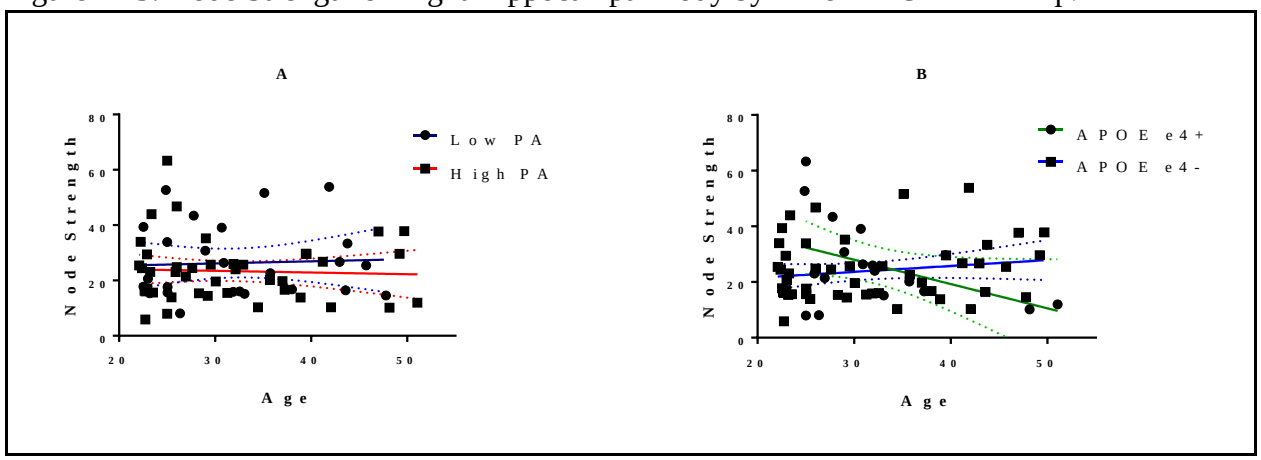

Legend: Panel A: Graphs show the linear regression line when plotting the node strength of the right hippocampal body versus age. Panel A: Comparing the regression lines of High and Low PA. Low PA: dark blue line and circle data points. High PA: red line and square data points. The slopes of the two equations are not significantly different ($F(1,65) = 0.1406$, $p = 0.7089$). Panel B: Comparing the regression lines of APOE-ε4 carriers and non-carriers. APOE-ε4 carriers: green line and circle data points. APOE-ε4 non-carriers: blue line and square data points. The slopes of the two equations are significantly different ($F(1,65) = 6.822$, $p = 0.0112$).

Equations of regression lines in Figure A23 generated by GraphPad Prism 7.0 software:

89) Low PA: $y = 0.07761x + 23.82$

The slope is not significantly different from 0 ($F(1,25) = 0.05739$, $p = 0.8126$).

90) High PA: $y = -0.06094x + 25.32$

The slope is not significantly different from 0 ($F(1,40) = 0.08814$, $p = 0.7681$).

91) APOE-ε4 positive: $y = -0.8732x + 54.2$

The slope is not significantly different from 0 ($F(1,17) = 3.986$, $p = 0.0621$).

92) APOE-ε4 negative: $y = 0.2115x + 17.31$

The slope is not significantly different from 0 ($F(1,48) = 1.458$, $p = 0.2331$).

Equations of regression lines in Figure A24 generated by GraphPad Prism 7.0 software.

93) Low PA APOE-ε4 positive: $y = -2.114x + 92.05$

The slope is not significantly different from 0 ($F(1,6) = 1.217$, $p = 0.3121$).

94) Low PA APOE-ε4 negative: $y = 0.2364x + 16.91$

The slope is not significantly different from 0 ($F(1,17) = 0.5552$, $p = 0.4664$).

95) High PA APOE-ε4 positive: $y = -0.7146x + 47.69$

The slope is not significantly different from 0 ($F(1,9) = 2.055$, $p = 0.1856$).

96) High PA APOE-ε4 negative: $y = -0.1847x + 17.86$

The slope is not significantly different from 0 ($F(1,29) = 0.7299$, $p = 0.3999$).

Figure A24: Node Strength of Right Hippocampal Body versus Age by PA and APOE-ε4 Groups.

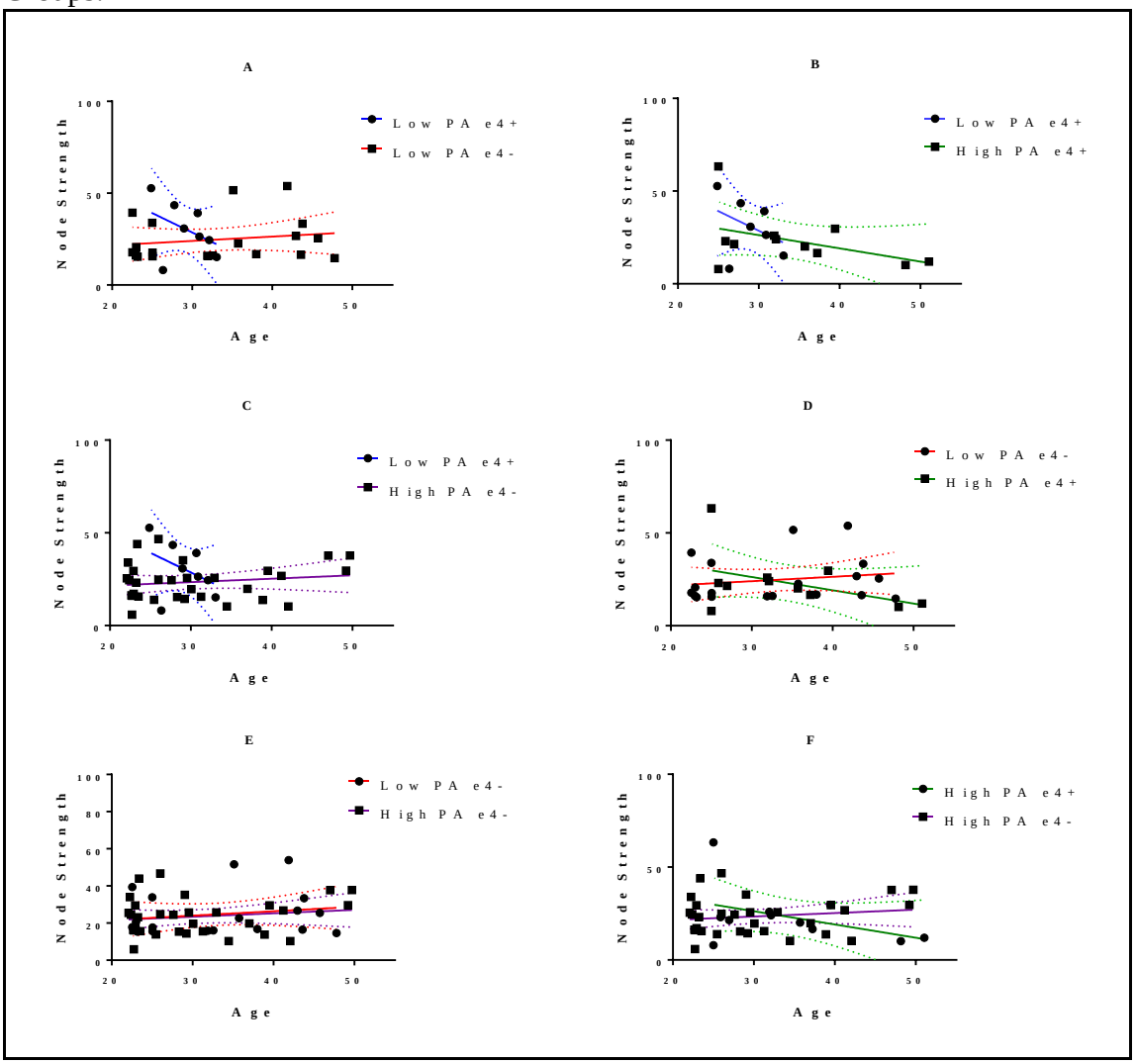

Legend: Graphs show the linear regression line when plotting the node strength of the right hippocampal body versus age. Blue line and circle data points: Low PA APOE-ε4 carriers; Red line and square data points: Low PA APOE-ε4 non-carriers; Green line square data points: High PA APOE-ε4 carriers; Purple line square data points: High PA APOE-ε4 non-carriers. Panel A: Comparing the regression lines of APOE-ε4 carriers and non-carriers in the Low PA category. The slopes of the regression lines are not significantly different from each other ($F(1,23) = 1.81$, $p = 0.1916$); Panel B: Comparing the regression lines of APOE-ε4 carriers in the High and Low PA categories. The slopes are not significantly different from each other ($F(1,15) = 0.5096$, $p = 0.4863$); Panel C: Comparing the regression lines of Low PA APOE-ε4 carriers and High PA APOE-ε4 non-carriers. The slopes are not significantly different from each other ($F(1,35) = 2.441$, $p = 0.1272$); Panel D: Comparing the regression lines of Low PA APOE-ε4 non-carriers and High PA APOEε4 carriers. The slopes are not significantly different from each other ($F(1,26) = 2.817$, $p = 0.1053$); Panel E: Comparing the regression lines of APOE-ε4 non-carriers with High and Low PA levels. The slopes are not significantly different from each other ($F(1,46) = 0.01976$, $p = 0.8888$); Panel F: Comparing the regression lines of APOE-ε4 carriers and non-carriers in the High PA category. The slopes are not quite significantly different from each other ($F(1,38) = 3.811$, $p = 0.0583$).

Figure A25: Node Strength of Right Hippocampal Tail by PA or APOE-ε4 Group.

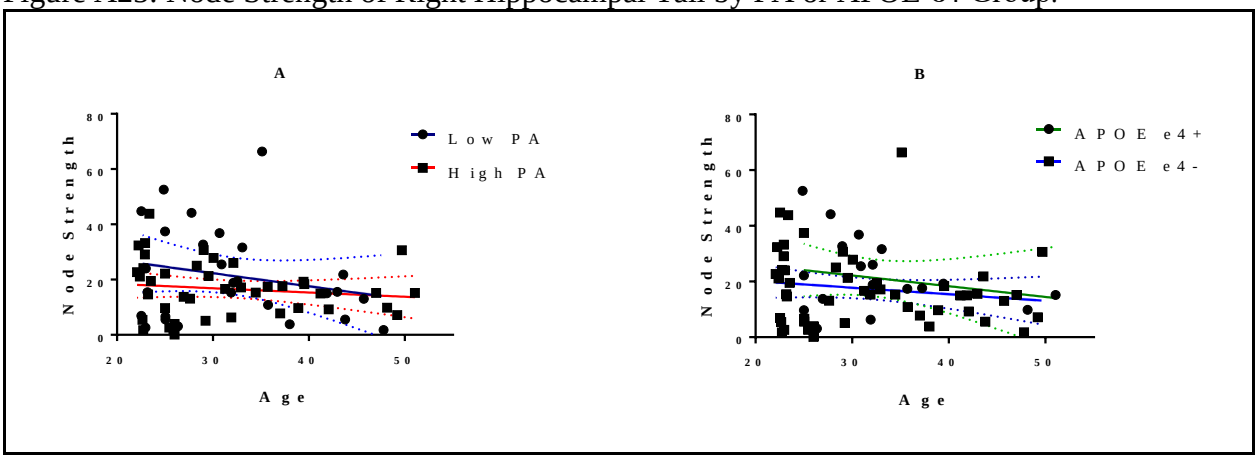

Legend: Panel A: Graphs show the linear regression line when plotting the node strength of the right hippocampal tail versus age. Panel A: Comparing the regression lines of High and Low PA. Low PA: dark blue line and circle data points. High PA: red line and square data points. The slopes of the two equations are not significantly different ($F(1,65) = 0.6444$, $p = 0.4251$). Panel B: Comparing the regression lines of APOE-ε4 carriers and non-carriers. APOE-ε4 carriers: green line and circle data points. APOE-ε4 non-carriers: blue line and square data points. The slopes of the two equations are not significantly different ($F(1,65) = 0.1023$, $p = 0.7501$).

Equations of regression lines in Figure A25 generated by GraphPad Prism 7.0 software:

97) Low PA: $y = -0.472x + 36.46$

The slope is not significantly different from 0 ($F(1,25) = 0.2635$, $p = 0.2635$).

98) High PA: $y = -0.1536x + 21.45$

The slope is not significantly different from 0 ($F(1,40) = 0.7329$, $p = 0.3970$).

99) APOE-ε4 positive: $y = -0.3856x + 33.74$

The slope is not significantly different from 0 ($F(1,17) = 0.7849$, $p = 0.3880$).

100) APOE-ε4 negative: $y = -0.2348x + 24.82$

The slope is not significantly different from 0 ($F(1,48) = 1.23$, $p = 0.2728$).

Equations of regression lines in Figure A26 generated by GraphPad Prism 7.0 software.

101) Low PA APOE-ε4 positive: $y = -1.154x + 64.53$

The slope is not significantly different from 0 ($F(1,6) = 0.2948$, $p = 0.6067$).

102) Low PA APOE-ε4 negative: $y = -0.2996x + 27.04$

The slope is not significantly different from 0 ($F(1,17) = 0.4623$, $p = 0.5057$).

103) High PA APOE-ε4 positive: $y = 0.07669x + 11.85$

The slope is not significantly different from 0 ($F(1,9) = 0.0272$, $p = 0.7745$).

104) High PA APOE-ε4 negative: $y = -0.2058x + 23.68$

The slope is not significantly different from 0 ($F(1,29) = 0.7815$, $p = 0.3839$).

Figure A26: Node Strength of Right Hippocampal Tail versus Age by PA and APOE-ε4 Groups.

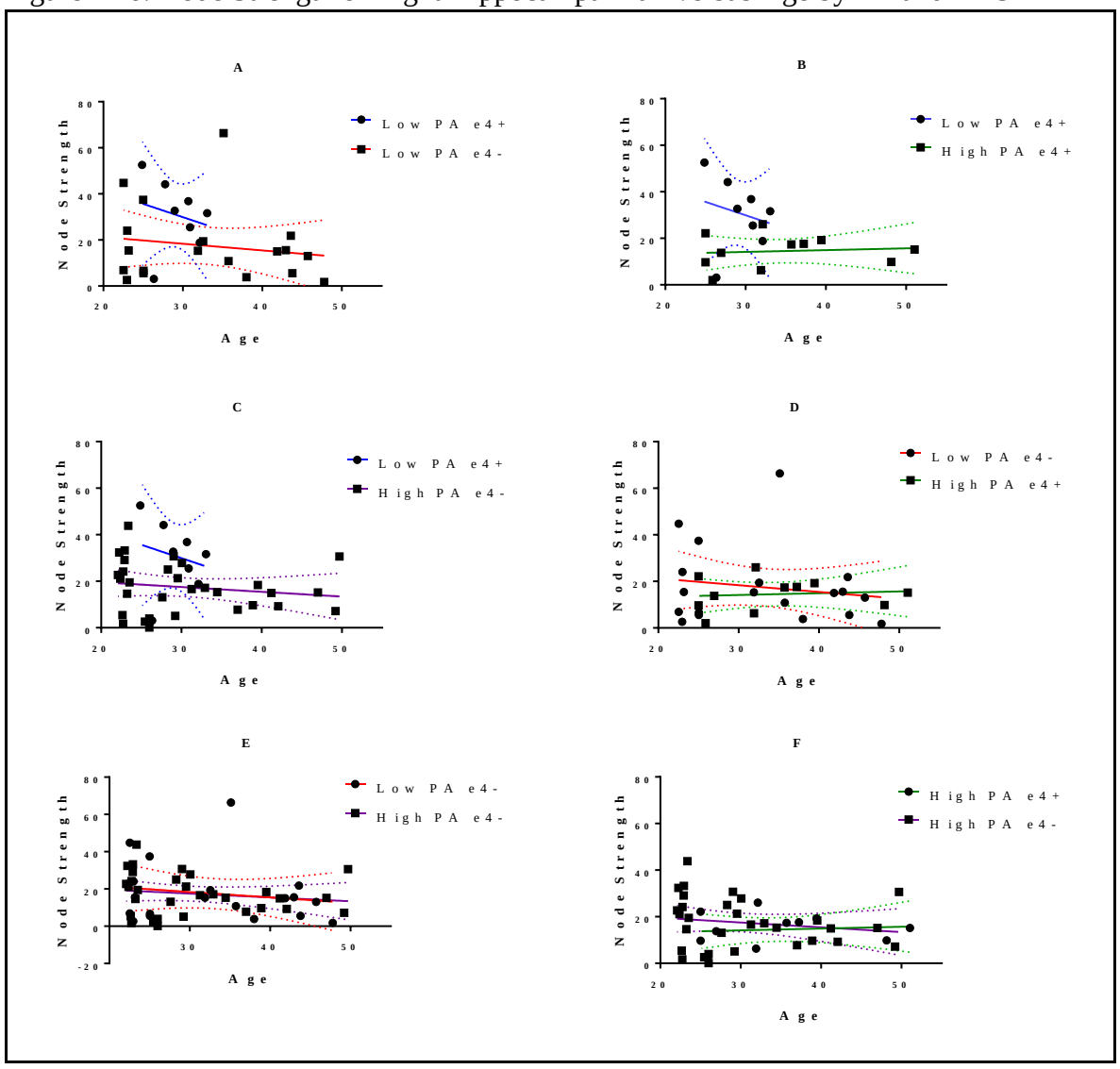

Legend: Graphs show the linear regression line when plotting the node strength of the right hippocampal tail versus age. Blue line and circle data points: Low PA APOE-ε4 carriers; Red line and square data points: Low PA APOE-ε4 non-carriers; Green line square data points: High PA APOE-ε4 carriers; Purple line square data points: High PA APOE-ε4 non-carriers. Panel A: Comparing the regression lines of APOE-ε4 carriers and non-carriers in the Low PA category. The slopes of the regression lines are not significantly different from each other ($F(1,23) = 0.1515$, $p = 0.7007$); Panel B: Comparing the regression lines of APOE-ε4 carriers in the High and Low PA categories. The slopes are not significantly different from each other ($F(1,15) = 0.5939$, $p = 0.4529$); Panel C: Comparing the regression lines of Low PA APOE-ε4 carriers and High PA APOE-ε4 non-carriers. The slopes are not significantly different from each other ($F(1,35) = 0.352$, $p = 0.5568$); Panel D: Comparing the regression lines of Low PA APOE-ε4 non-carriers and High PA APOEε4 carriers. The slopes are not significantly different from each other ($F(1,26) = 0.3562$, $p = 0.5558$); Panel E: Comparing the regression lines of APOE-ε4 non-carriers with High and Low PA levels. The slopes are not significantly different from each other ($F(1,46) = 0.0362$, $p = 0.8511$); Panel F: Comparing the regression lines of APOE-ε4 carriers and non-carriers in the High PA category. The slopes are not significantly different from each other ($F(1,38) = 0.4579$, $p = 0.5027$).

Figure A27: Node Strength of Left Hippocampal Head by PA or APOE-ε4 Group.

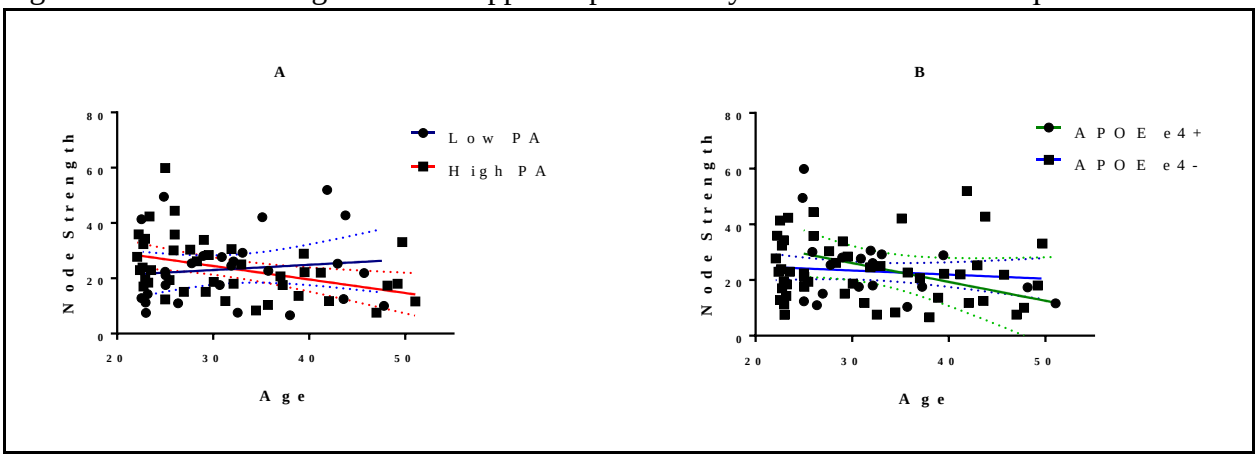

Legend: Panel A: Graphs show the linear regression line when plotting the node strength of the left hippocampal head versus age. Panel A: Comparing the regression lines of High and Low PA. Low PA: dark blue line and circle data points. High PA: red line and square data points. The slopes of the two equations are not quite significantly different ($F(1,65) = 3.958$, $p = 0.0509$). Panel B: Comparing the regression lines of APOE-ε4 carriers and non-carriers. APOE-ε4 carriers: green line and circle data points. APOE-ε4 non-carriers: blue line and square data points. The slopes of the two equations are not significantly different ($F(1,65) = 1.701$, $p = 0.1967$).

Equations of regression lines in Figure A27 generated by GraphPad Prism 7.0 software:

105) Low PA: $y = 0.1897x + 17.31$

The slope is not significantly different from 0 ($F(1,25) = 0.354$, $p = 0.5572$).

106) High PA: $y = -0.4888x + 39.12$

The slope is not significantly different from 0 ($F(1,40) = 7.503$, $p = 0.0092$).

107) APOE-ε4 positive: $y = -0.678x + 46.43$

The slope is not significantly different from 0 ($F(1,17) = 3.064$, $p = 0.0980$).

108) APOE-ε4 negative: $y = -0.1473x + 27.85$

The slope is not significantly different from 0 ($F(1,48) = .06666$, $p = 0.4183$).

Equations of regression lines in Figure A28 generated by GraphPad Prism 7.0 software.

109) Low PA APOE-ε4 positive: $y = -0.9895x + 55.86$

The slope is not significantly different from 0 ($F(1,6) = 0.4182$, $p = 0.5418$).

110) Low PA APOE-ε4 negative: $y = 0.311x + 11.63$

The slope is not significantly different from 0 ($F(1,17) = 0.80$, $p = 0.3836$).

111) High PA APOE-ε4 positive: $y = -0.642x + 44.99$

The slope is not significantly different from 0 ($F(1,9) = 1.764$, $p = 0.2169$).

112) High PA APOE-ε4 negative: $y = -0.4435x + 37.53$

The slope is not significantly different from 0 ($F(1,29) = 5.571$, $p = 0.0252$).

Figure A28: Node Strength of Left Hippocampal Head versus Age by PA and APOE-ε4 Groups.

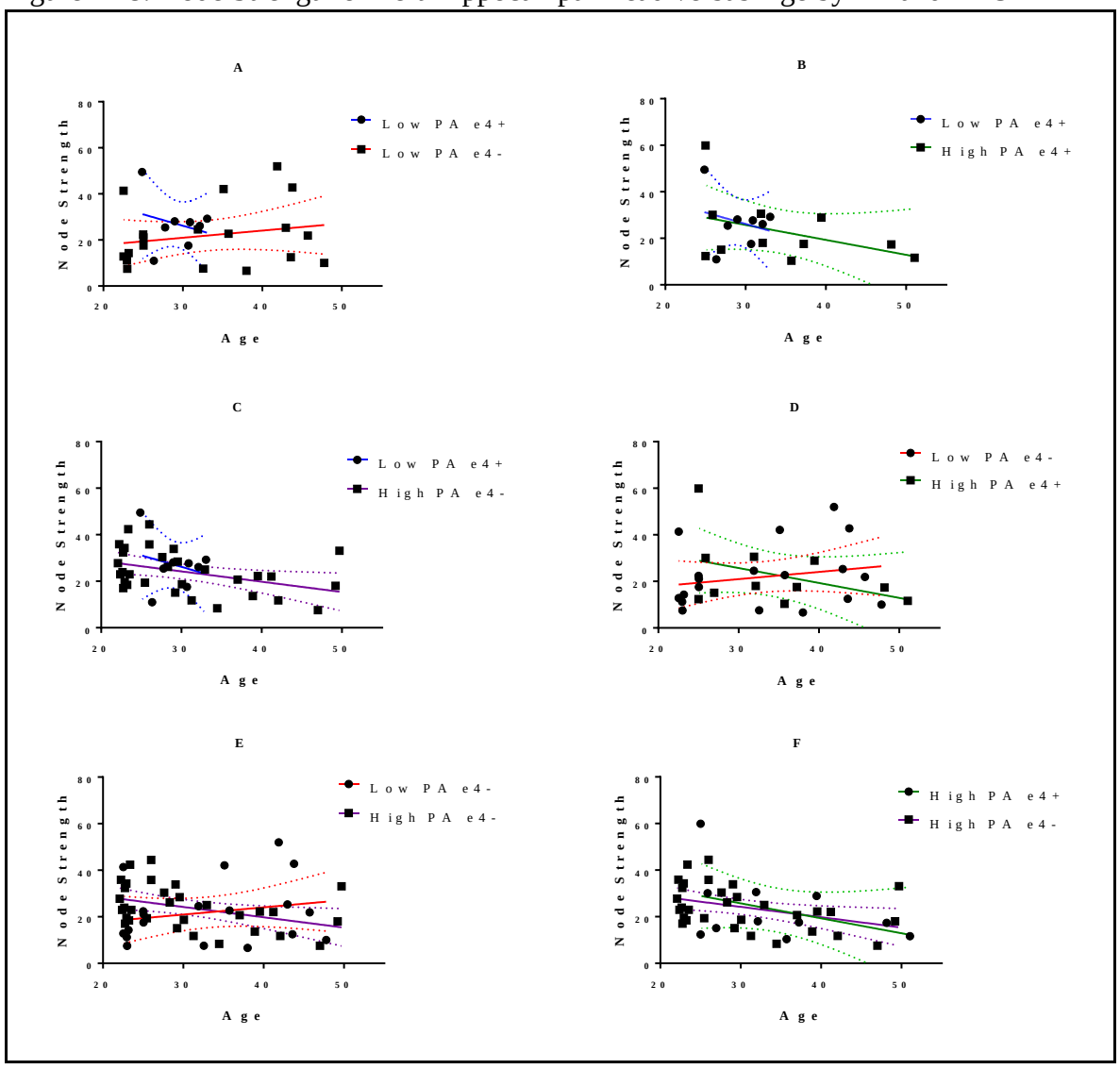

Legend: Graphs show the linear regression line when plotting the node strength of the left hippocampal head versus age. Blue line and circle data points: Low PA APOE-ε4 carriers; Red line and square data points: Low PA APOE-ε4 non-carriers; Green line square data points: High PA APOE-ε4 carriers; Purple line square data points: High PA APOE-ε4 non-carriers. Panel A: Comparing the regression lines of APOE-ε4 carriers and non-carriers in the Low PA category. The slopes of the regression lines are not significantly different from each other ($F(1,23) = 0.5444$, $p = 0.4681$); Panel B: Comparing the regression lines of APOE-ε4 carriers in the High and Low PA categories. The slopes are not significantly different from each other ($F(1,15) = 0.03849$, $p = 0.8471$); Panel C: Comparing the regression lines of Low PA APOE-ε4 carriers and High PA APOE-ε4 non-carriers. The slopes are not significantly different from each other ($F(1,35) = 0.1912$, $p = 0.6646$); Panel D: Comparing the regression lines of Low PA APOE-ε4 non-carriers and High PA APOEε4 carriers. The slopes are not significantly different from each other ($F(1,26) = 2.586$, $p = 0.1199$); Panel E: Comparing the regression lines of APOE-ε4 non-carriers with High and Low PA levels. The slopes are significantly different from each other ($F(1,46) = 4.378$, $p = 0.0419$); Panel F: Comparing the regression lines of APOE-ε4 carriers and non-carriers in the High PA category. The slopes are not significantly different from each other ($F(1,38) = 0.2248$, $p = 0.6382$).

Figure A29: Node Strength of Left Hippocampal Body by PA or APOE-ε4 Group.

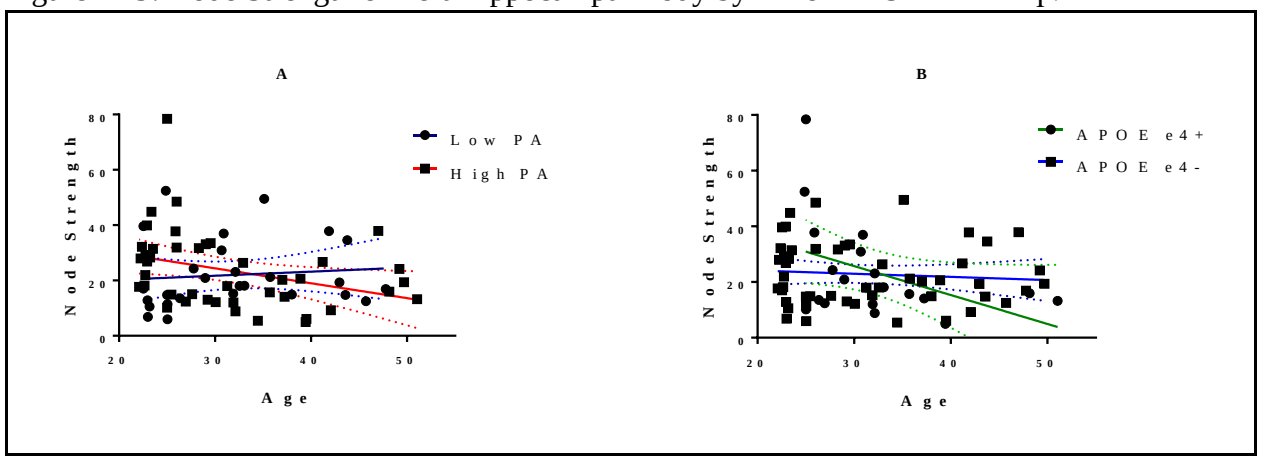

Legend: Panel A: Graphs show the linear regression line when plotting the node strength of the left hippocampal body versus age. Panel A: Comparing the regression lines of High and Low PA. Low PA: dark blue line and circle data points. High PA: red line and square data points. The slopes of the two equations are not quite significantly different ($F(1,65) = 3.025$, $p = 0.0867$). Panel B: Comparing the regression lines of APOE-ε4 carriers and non-carriers. APOE-ε4 carriers: green line and circle data points. APOE-ε4 non-carriers: blue line and square data points. The slopes of the two equations are significantly different ($F(1,65) = 4.031$, $p = 0.0488$).

Equations of regression lines in Figure A29 generated by GraphPad Prism 7.0 software:

113) Low PA: $y = 0.1476x + 17.29$

The slope is not significantly different from 0 ($F(1,25) = 0.2303$, $p = 0.6355$).

114) High PA: $y = -0.5394x + 40.57$

The slope is not significantly different from 0 ($F(1,40) = 5.143$, $p = 0.0288$).

115) APOE-ε4 positive: $y = -1.039x + 56.9$

The slope is not significantly different from 0 ($F(1,17) = 3.917$, $p = 0.0642$).

116) APOE-ε4 negative: $y = -0.113x + 26.36$

The slope is not significantly different from 0 ($F(1,48) = 0.3733$, $p = 0.5441$).

Equations of regression lines in Figure A30 generated by GraphPad Prism 7.0 software.

117) Low PA APOE-ε4 positive: $y = -1.572x + 73.67$

The slope is not significantly different from 0 ($F(1,6) = 0.91$, $p = 0.3769$).

118) Low PA APOE-ε4 negative: $y = 0.3274x + 8.852$

The slope is not significantly different from 0 ($F(1,17) = 1.167$, $p = 0.2952$).

119) High PA APOE-ε4 positive: $y = -0.946x + 52.87$

The slope is not significantly different from 0 ($F(1,9) = 1.788$, $p = 0.2140$).

120) High PA APOE-ε4 negative: $y = -0.3546x + 35.54$

The slope is not significantly different from 0 ($F(1,29) = 2.532$, $p = 0.1224$).

Figure A30: Node Strength of Left Hippocampal Body versus Age by PA and APOE-ε4 Groups.

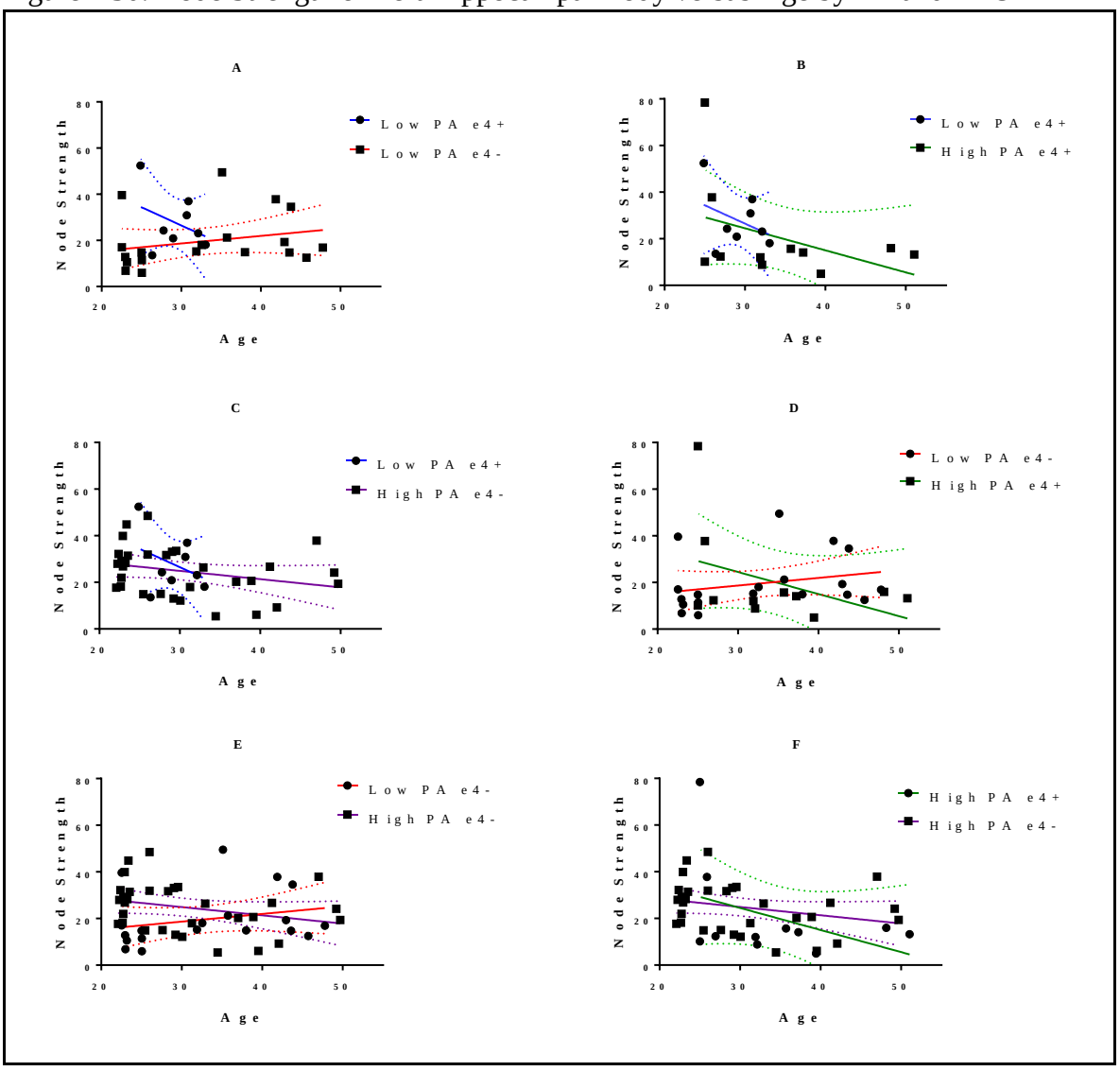

Legend: Graphs show the linear regression line when plotting the node strength of the left hippocampal body versus age. Blue line and circle data points: Low PA APOE-ε4 carriers; Red line and square data points: Low PA APOE-ε4 non-carriers; Green line square data points: High PA APOE-ε4 carriers; Purple line square data points: High PA APOE-ε4 non-carriers. Panel A: Comparing the regression lines of APOE-ε4 carriers and non-carriers in the Low PA category. The slopes of the regression lines are not significantly different from each other ($F(1,23) = 1.381$, $p = 0.2520$); Panel B: Comparing the regression lines of APOE-ε4 carriers in the High and Low PA categories. The slopes are not significantly different from each other ($F(1,15) = 0.06839$, $p = 0.7973$); Panel C: Comparing the regression lines of Low PA APOE-ε4 carriers and High PA APOE-ε4 non-carriers. The slopes are not significantly different from each other ($F(1,35) = 0.7092$, $p = 0.4054$); Panel D: Comparing the regression lines of Low PA APOE-ε4 non-carriers and High PA APOEε4 carriers. The slopes are not quite significantly different from each other ($F(1,26) = 3.699$, $p = 0.0654$); Panel E: Comparing the regression lines of APOE-ε4 non-carriers with High and Low PA levels. The slopes are not quite significantly different from each other ($F(1,46) = 3.476$, $p = 0.0686$); Panel F: Comparing the regression lines of APOE-ε4 carriers and non-carriers in the High PA category. The slopes are not significantly different from each other ($F(1,38) = 1.57$, $p = 0.2889$).

Figure A31: Node Strength of Left Hippocampal Tail by PA or APOE-ε4 Group.

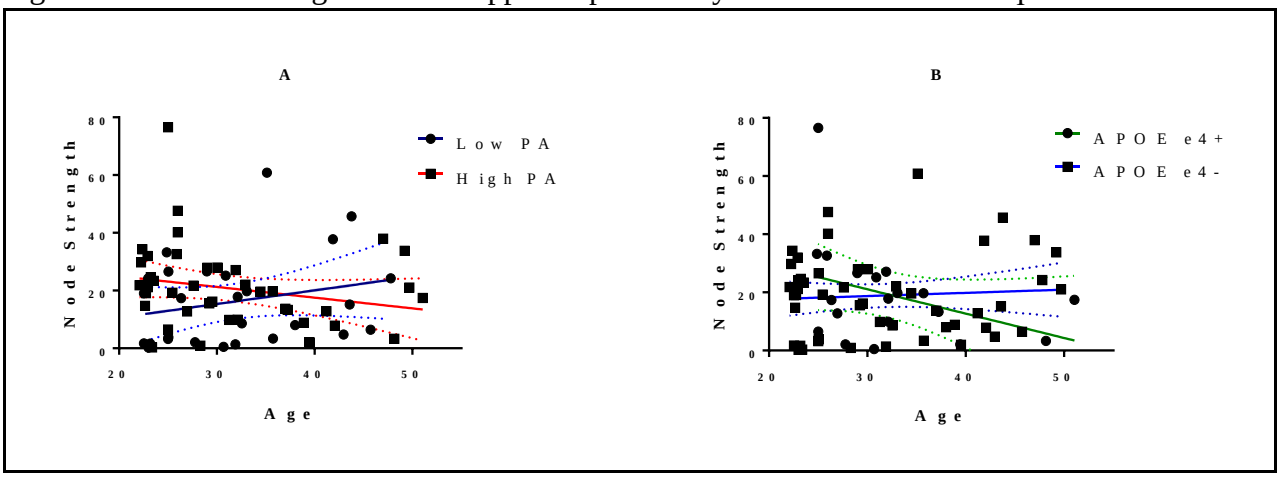

Legend: Panel A: Graphs show the linear regression line when plotting the node strength of the left hippocampal tail versus age. Panel A: Comparing the regression lines of High and Low PA. Low PA: dark blue line and circle data points. High PA: red line and square data points. The slopes of the two equations are not quite significantly different ($F(1,65) = 3.657$, $p = 0.0603$). Panel B: Comparing the regression lines of APOE-ε4 carriers and non-carriers. APOE-ε4 carriers: green line and circle data points. APOE-ε4 non-carriers: blue line and square data points. The slopes of the two equations are not quite significantly different ($F(1,65) = 3.265$, $p = 0.0754$).

Equations of regression lines in Figure A31 generated by GraphPad Prism 7.0 software:

121) Low PA: $y = 0.4717x + 1.196$

The slope is not significantly different from 0 ($F(1,25) = 1.577$, $p = 0.2208$).

122) High PA: $y = -0.371x + 3.238$

The slope is not significantly different from 0 ($F(1,40) = 2.196$, $p = 0.1462$).

123) APOE-ε4 positive: $y = -0.8382x + 46.21$

The slope is not significantly different from 0 ($F(1,17) = 2.552$, $p = 0.1286$).

124) APOE-ε4 negative: $y = 0.1106x + 15.4$

The slope is not significantly different from 0 ($F(1,48) = 0.2358$, $p = 0.6295$).

Equations of regression lines in Figure A32 generated by GraphPad Prism 7.0 software.

125) Low PA APOE-ε4 positive: $y = -0.8819x + 43.71$

The slope is not significantly different from 0 ($F(1,6) =$, $p = 0.3055$).

126) Low PA APOE-ε4 negative: $y = 0.577x + -3.466$

The slope is not significantly different from 0 ($F(1,17) = 1.809$, $p = 0.1963$).

127) High PA APOE-ε4 positive: $y = -1.022x + 55.3$

The slope is not significantly different from 0 ($F(1,9) = 2.168$, $p = 0.1750$).

128) High PA APOE-ε4 negative: $y = -0.1382x + 25.1$

The slope is not significantly different from 0 ($F(1,29) = 0.316$, $p = 0.5783$).

Figure A32: Node Strength of Left Hippocampal Tail versus Age by PA and APOE-ε4 Groups.

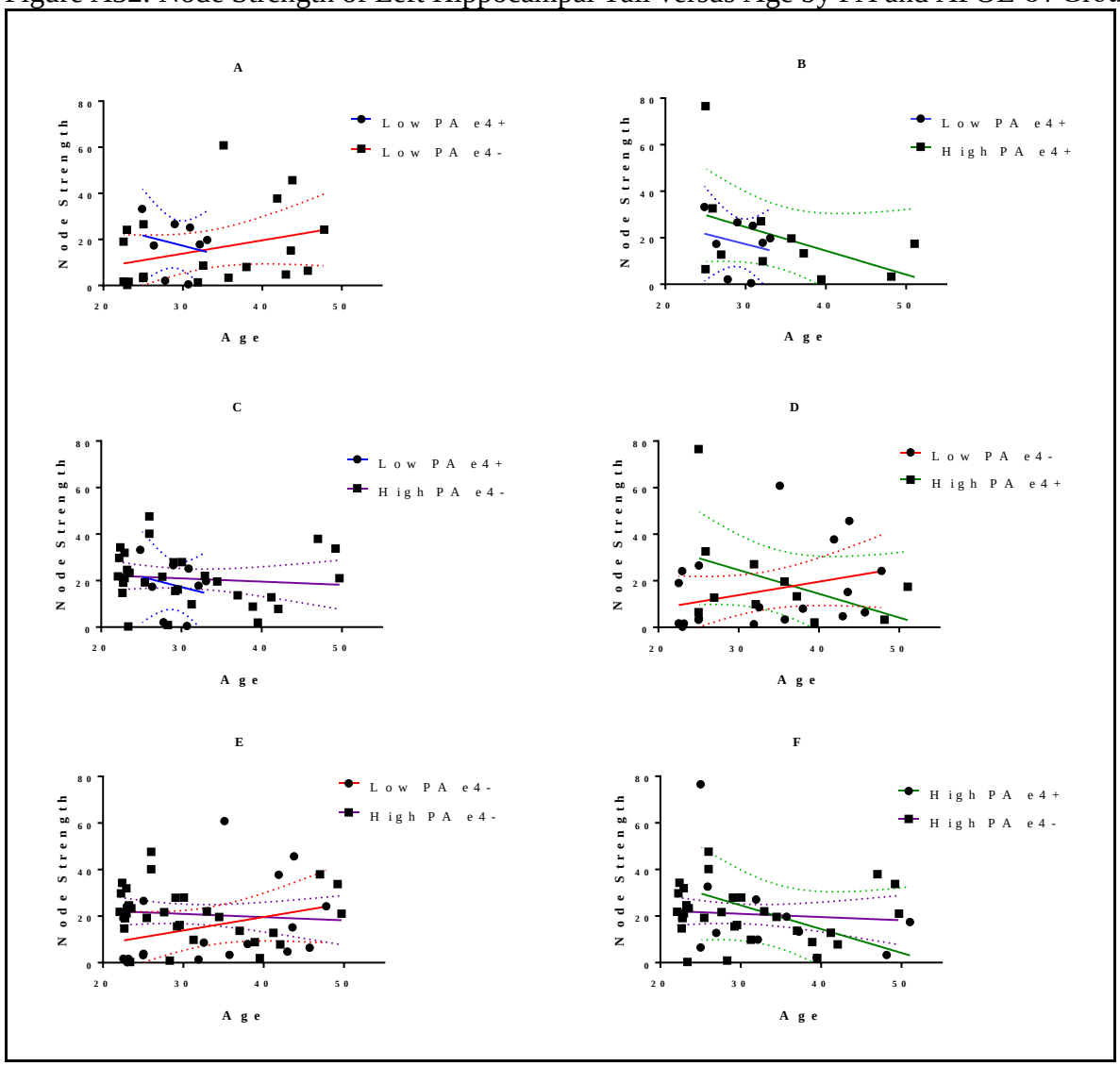

Legend: Graphs show the linear regression line when plotting the node strength of the left hippocampal tail versus age. Blue line and circle data points: Low PA APOE-ε4 carriers; Red line and square data points: Low PA APOE-ε4 non-carriers; Green line square data points: High PA APOE-ε4 carriers; Purple line square data points: High PA APOE-ε4 non-carriers. Panel A: Comparing the regression lines of APOE-ε4 carriers and non-carriers in the Low PA category. The slopes of the regression lines are not significantly different from each other ($F(1,23) = 0.4779$, $p = 0.4963$); Panel B: Comparing the regression lines of APOE-ε4 carriers in the High and Low PA categories. The slopes are not significantly different from each other ($F(1,15) = 0.003593$, $p = 0.9530$); Panel C: Comparing the regression lines of Low PA APOE-ε4 carriers and High PA APOE-ε4 non-carriers. The slopes are not significantly different from each other ($F(1,35) = 0.2295$, $p = 0.6349$); Panel D: Comparing the regression lines of Low PA APOE-ε4 non-carriers and High PA APOEε4 carriers. The slopes are significantly different from each other ($F(1,26) = 4.251$, $p = 0.0494$); Panel E: Comparing the regression lines of APOE-ε4 non-carriers with High and Low PA levels. The slopes are not significantly different from each other ($F(1,46) = 2.458$, $p = 0.1238$); Panel F: Comparing the regression lines of APOE-ε4 carriers and non-carriers in the High PA category. The slopes are not significantly different from each other ($F(1,38) = 2.395$, $p = 0.1300$).

Glossary

Amyloid	A general term for protein fragments that the body produces normally. Beta amyloid is a protein fragment snipped from an amyloid precursor protein (APP). In a healthy brain, these protein fragments are broken down and eliminated.
Brain plasticity	The ability of the brain to modify its own structure and function following changes within the body or in the external environment.
Clusters	Densely interconnected groups of brain regions.
Cognitive Reserve	The phenomenon that brain disruption does not completely predict cognitive performance. Also described as the ability to recruit brain networks.
CSF A_{42}	Cerebrospinal fluid beta-amyloid (1-42). A biomarker for AD.
Declarative Memory	The capacity for conscious recollection about facts and events and is the kind of memory that is impaired in amnesia and dependent on structures in the medial temporal lobe and midline diencephalon.
Dementia	General term for a decline in mental ability severe enough to interfere with daily life.
Diffusion tensor imaging	MRI-based neuroimaging technique which makes it possible to visualize the location, orientation, and anisotropy of the brain's white matter tracts.
Edge	Pairs of nodes are linked by edges, also called links or connections.
Electroencephalogram	Test that detects electrical activity in the brain using small electrodes on the scalp.
Episodic memory	Relates to the formation and retrieval of specific personal experiences and allow the recollection of past events.
Frontal-striatal circuit	Neural pathways that connect frontal lobe regions with the basal ganglia (striatum).

Functional connectivity	A measure of coherence of signals assumed to reflect the underlying white matter structural connectivity and synchronous neural activity.
Global efficiency	A measure of functional integration that is the average inverse shortest path length.
Hubs	Hubs may be identified on the basis of several network measures, including high degree, short average path length, or high betweenness centrality.
Local efficiency	A measure of functional segregation: efficiency within a module.
Modularity	Degree to which a given network can be decomposed into a set of non-overlapping, overlapping, or hierarchically arranged modules.
Network	Graph theory: Set of nodes (elements) and edges (relations). Neuroscience: spatially distributed, but functionally linked regions that continuously share information with each other.
Node	A network element which may represent a neuron, a neuronal population, a brain region, a brain voxel, or a recording electrode. Nodes are also referred to as vertices.
Node degree	The number of connections (incoming and outgoing) that are attached to a given node. Across the whole network, all node degrees are often summarized in a degree distribution.
Path length	In weighted graphs, the length of the path is the sum of the edge lengths, which can be derived by transforming the edge weights.
Pattern completion	Reconstruction of complete stored representations from partial inputs that are part of the stored representation.
Pattern separation	Process by which overlapping or similar inputs (representations) are transformed into less similar outputs.
Physical Activity	Any bodily movement produced by skeletal muscles that requires energy expenditure.
PiB PET imaging	One of the most common methods to detect amyloid plaques. Positron emission tomography (PET) scan using PiB as the radioactive substance that binds to beta amyloid.

Priming	The change in the ability to identify an object as a result of a specific encounter with the object.
Semantic memory	The acquisition and recall of general knowledge that is not tied to any specific personal experience and that can take a variety of forms: words, facts, numbers, and rules.
Small worldness	A property of networks that combines high clustering with a short characteristic path length compared to a population of random networks composed of the same number of nodes and connections.
VO_{2max}	Maximum volume of oxygen a body is capable of utilizing. Measure of cardiorespiratory fitness.

Bibliography

Achard, S., & Bullmore, E. (2007). Efficiency and cost of economical brain functional networks. *PLoS Comput Biol, 3*(2), e17.

Ainsworth, B. E., Leon, A. S., Richardson, M. T., Jacobs, D. R., & Paffenbarger, R. S. (1993). Accuracy of the College Alumnus Physical Activity Questionnaire. *J Clin Epidemiol, 46*(12), 1403-1411.

Albert, M. S. (2011). Changes in cognition. *Neurobiol Aging, 32 Suppl 1*, S58-63.

Albert, M. S., DeKosky, S. T., Dickson, D., Dubois, B., Feldman, H. H., Fox, N. C., et al. (2011). The diagnosis of mild cognitive impairment due to Alzheimer's disease: recommendations from the National Institute on Aging-Alzheimer's Association workgroups on diagnostic guidelines for Alzheimer's disease. *Alzheimers Dement, 7*(3), 270-279.

Allen, G., McColl, R., Barnard, H., Ringe, W. K., Fleckenstein, J., & Cullum, C. M. (2005). Magnetic resonance imaging of cerebellar-prefrontal and cerebellar-parietal functional connectivity. *Neuroimage, 28*(1), 39-48.

Alvarez, P., & Squire, L. R. (1994). Memory consolidation and the medial temporal lobe: a simple network model. *Proc Natl Acad Sci U S A, 91*(15), 7041-7045.

American College of Sports Medicine. (2010). *ACSM's guidelines for exercise testing and prescription* (8th ed. ed.). Philadelphia: Lippincott Williams & Wilkins.

Amieva, H., Jacqmin-Gadda, H., Orgogozo, J. M., Le Carret, N., Helmer, C., Letenneur, L., et al. (2005). The 9 year cognitive decline before dementia of the Alzheimer type: a prospective population-based study. *Brain, 128*(Pt 5), 1093-1101.

Andrews-Hanna, J. R., Snyder, A. Z., Vincent, J. L., Lustig, C., Head, D., Raichle, M. E., et al. (2007). Disruption of large-scale brain systems in advanced aging. *Neuron, 56*(5), 924-935.

Angevaren, M., Aufdemkampe, G., Verhaar, H. J., Aleman, A., & Vanhees, L. (2008). Physical activity and enhanced fitness to improve cognitive function in older people without known cognitive impairment. *Cochrane Database Syst Rev*(3), CD005381.

Arenaza-Urquijo, E. M., Landeau, B., La Joie, R., Mevel, K., Mézenge, F., Perrotin, A., et al. (2013). Relationships between years of education and gray matter volume, metabolism and functional connectivity in healthy elders. *Neuroimage, 83*, 450-457.

Baker, L. D., Frank, L. L., Foster-Schubert, K., Green, P. S., Wilkinson, C. W., McTiernan, A., et al. (2010). Aerobic exercise improves cognition for older adults with glucose intolerance, a risk factor for Alzheimer's disease. *J Alzheimers Dis, 22*(2), 569-579.

Baker, L. D., Frank, L. L., Foster-Schubert, K., Green, P. S., Wilkinson, C. W., McTiernan, A., et al. (2010). Effects of aerobic exercise on mild cognitive impairment: a controlled trial. *Arch Neurol, 67*(1), 71-79.

Bartzokis, G., Sultzer, D., Lu, P. H., Nuechterlein, K. H., Mintz, J., & Cummings, J. L. (2004). Heterogeneous age-related breakdown of white matter structural integrity: implications for cortical "disconnection" in aging and Alzheimer's disease. *Neurobiol Aging, 25*(7), 843-851.

Barulli, D., & Stern, Y. (2013). Efficiency, capacity, compensation, maintenance, plasticity: emerging concepts in cognitive reserve. *Trends Cogn Sci, 17*(10), 502-509.
Bassett, D. S., & Bullmore, E. (2006). Small-world brain networks. *Neuroscientist, 12*(6), 512-523.
Basu, R., Breda, E., Oberg, A. L., Powell, C. C., Dalla Man, C., Basu, A., et al. (2003). Mechanisms of the age-associated deterioration in glucose tolerance: contribution of alterations in insulin secretion, action, and clearance. *Diabetes, 52*(7), 1738-1748.
Ben, J., Soares, F. M., Cechetti, F., Vuaden, F. C., Bonan, C. D., Netto, C. A., et al. (2009). Exercise effects on activities of Na(+),K(+)-ATPase, acetylcholinesterase and adenine nucleotides hydrolysis in ovariectomized rats. *Brain Res, 1302*, 248-255.
Bender, A. R., Prindle, J. J., Brandmaier, A. M., & Raz, N. (2016). White matter and memory in healthy adults: Coupled changes over two years. *Neuroimage, 131*, 193-204.
Bennett, I. J., & Madden, D. J. (2014). Disconnected aging: cerebral white matter integrity and age-related differences in cognition. *Neuroscience, 276*, 187-205.
Benton, A., & Hamsher, K. (1978). *Multilingual Aphasia Examination: Manual of Instructions*. Iowa City: Associates A.
Binder, J. R., Desai, R. H., Graves, W. W., & Conant, L. L. (2009). Where is the semantic system? A critical review and meta-analysis of 120 functional neuroimaging studies. *Cereb Cortex, 19*(12), 2767-2796.
Boraxbekk, C. J., Salami, A., Wåhlin, A., & Nyberg, L. (2016). Physical activity over a decade modifies age-related decline in perfusion, gray matter volume, and functional connectivity of the posterior default-mode network-A multimodal approach. *Neuroimage, 131*, 133-141.
Borg, G. (1998). *Borg's Perceived Exertion and Pain Scales*. Champaign, IL: Human Kinetics.
Bu, G. (2009). Apolipoprotein E and its receptors in Alzheimer's disease: pathways, pathogenesis and therapy. *Nat Rev Neurosci, 10*(5), 333-344.
Buchman, A. S., Boyle, P. A., Yu, L., Shah, R. C., Wilson, R. S., & Bennett, D. A. (2012). Total daily physical activity and the risk of AD and cognitive decline in older adults. *Neurology, 78*(17), 1323-1329.
Buckner, R. L. (2004). Memory and executive function in aging and AD: multiple factors that cause decline and reserve factors that compensate. *Neuron, 44*(1), 195-208.
Buckner, R. L. (2013). The brain's default network: origins and implications for the study of psychosis. *Dialogues Clin Neurosci, 15*(3), 351-358.
Buckner, R. L., Andrews-Hanna, J. R., & Schacter, D. L. (2008). The brain's default network: anatomy, function, and relevance to disease. *Ann N Y Acad Sci, 1124*, 1-38.
Buckner, R. L., Krienen, F. M., Castellanos, A., Diaz, J. C., & Yeo, B. T. (2011). The organization of the human cerebellum estimated by intrinsic functional connectivity. *J Neurophysiol, 106*(5), 2322-2345.
Buckner, R. L., Sepulcre, J., Talukdar, T., Krienen, F. M., Liu, H., Hedden, T., et al. (2009). Cortical hubs revealed by intrinsic functional connectivity: mapping, assessment of stability, and relation to Alzheimer's disease. *J Neurosci, 29*(6), 1860-1873.
Buckner, R. L., Snyder, A. Z., Sanders, A. L., Raichle, M. E., & Morris, J. C. (2000). Functional brain imaging of young, nondemented, and demented older adults. *J Cogn Neurosci, 12 Suppl 2*, 24-34.

Buckner, R. L., Snyder, A. Z., Shannon, B. J., LaRossa, G., Sachs, R., Fotenos, A. F., et al. (2005). Molecular, structural, and functional characterization of Alzheimer's disease: evidence for a relationship between default activity, amyloid, and memory. *J Neurosci, 25*(34), 7709-7717.

Bullmore, E., & Sporns, O. (2009). Complex brain networks: graph theoretical analysis of structural and functional systems. *Nat Rev Neurosci, 10*(3), 186-198.

Burdette, J. H., Laurienti, P. J., Espeland, M. A., Morgan, A., Telesford, Q., Vechlekar, C. D., et al. (2010). Using network science to evaluate exercise-associated brain changes in older adults. *Front Aging Neurosci, 2*, 23.

Burkhalter, J., Fiumelli, H., Allaman, I., Chatton, J. Y., & Martin, J. L. (2003). Brain-derived neurotrophic factor stimulates energy metabolism in developing cortical neurons. *J Neurosci, 23*(23), 8212-8220.

Carreiras, M., Seghier, M. L., Baquero, S., Estévez, A., Lozano, A., Devlin, J. T., et al. (2009). An anatomical signature for literacy. *Nature, 461*(7266), 983-986.

Chen, G., Saad, Z. S., Britton, J. C., Pine, D. S., & Cox, R. W. (2013). Linear mixed-effects modeling approach to FMRI group analysis. *Neuroimage, 73*, 176-190.

Chen, K., Reiman, E. M., Alexander, G. E., Caselli, R. J., Gerkin, R., Bandy, D., et al. (2007). Correlations between apolipoprotein E epsilon4 gene dose and whole brain atrophy rates. *Am J Psychiatry, 164*(6), 916-921.

Chen, Y., Chen, K., Zhang, J., Li, X., Shu, N., Wang, J., et al. (2015). Disrupted functional and structural networks in cognitively normal elderly subjects with the APOE ε4 allele. *Neuropsychopharmacology, 40*(5), 1181-1191.

Chirles, T. J., Reiter, K., Weiss, L. R., Alfini, A. J., Nielson, K. A., & Smith, J. C. (2017). Exercise Training and Functional Connectivity Changes in Mild Cognitive Impairment and Healthy Elders. *J Alzheimers Dis*.

Chételat, G., & Fouquet, M. (2013). Neuroimaging biomarkers for Alzheimer's disease in asymptomatic APOE4 carriers. *Rev Neurol (Paris), 169*(10), 729-736.

Coffey, C. E., Saxton, J. A., Ratcliff, G., Bryan, R. N., & Lucke, J. F. (1999). Relation of education to brain size in normal aging: implications for the reserve hypothesis. *Neurology, 53*(1), 189-196.

Cohen, A. D., Price, J. C., Weissfeld, L. A., James, J., Rosario, B. L., Bi, W., et al. (2009). Basal cerebral metabolism may modulate the cognitive effects of Abeta in mild cognitive impairment: an example of brain reserve. *J Neurosci, 29*(47), 14770-14778.

Cook, D., O'Connor, P., Eubanks, S., Smith, J., & Lee, M. (1997). Naturally occurring muscle pain during exercise: Assessment and experimental evidence. *Medicine & Science in Sports & Exercise, 29*, 999-1012.

Corder, E. H., Saunders, A. M., Strittmatter, W. J., Schmechel, D. E., Gaskell, P. C., Small, G. W., et al. (1993). Gene dose of apolipoprotein E type 4 allele and the risk of Alzheimer's disease in late onset families. *Science, 261*(5123), 921-923.

Cosentino, S., Jefferson, A., Chute, D. L., Kaplan, E., & Libon, D. J. (2004). Clock drawing errors in dementia: neuropsychological and neuroanatomical considerations. *Cogn Behav Neurol, 17*(2), 74-84.

Cotman, C. W., & Berchtold, N. C. (2002). Exercise: a behavioral intervention to enhance brain health and plasticity. *Trends Neurosci, 25*(6), 295-301.

Cox, R. W. (1996). AFNI: software for analysis and visualization of functional magnetic resonance neuroimages. *Comput Biomed Res, 29*(3), 162-173.
Craik, F. I., Morris, L. W., Morris, R. G., & Loewen, E. R. (1990). Relations between source amnesia and frontal lobe functioning in older adults. *Psychol Aging, 5*(1), 148-151.
Damoiseaux, J. S., Prater, K. E., Miller, B. L., & Greicius, M. D. (2012). Functional connectivity tracks clinical deterioration in Alzheimer's disease. *Neurobiol Aging, 33*(4), 828.e819-830.
de Reus, M. A., & van den Heuvel, M. P. (2013). The parcellation-based connectome: limitations and extensions. *Neuroimage, 80*, 397-404.
Dean, D. C., Jerskey, B. A., Chen, K., Protas, H., Thiyyagura, P., Roontiva, A., et al. (2014). Brain differences in infants at differential genetic risk for late-onset Alzheimer disease: a cross-sectional imaging study. *JAMA Neurol, 71*(1), 11-22.
DeFronzo, R. A. (1981). Glucose intolerance and aging. *Diabetes Care, 4*(4), 493-501.
Dosenbach, N. U., Visscher, K. M., Palmer, E. D., Miezin, F. M., Wenger, K. K., Kang, H. C., et al. (2006). A core system for the implementation of task sets. *Neuron, 50*(5), 799-812.
Drzezga, A., Becker, J. A., Van Dijk, K. R. A., Sreenivasan, A., Talukdar, T., Sullivan, C., et al. (2011). Neuronal dysfunction and disconnection of cortical hubs in non-demented subjects with elevated amyloid burden. [Article]. *Brain, 134*, 1635-1646.
Dumanis, S. B., Tesoriero, J. A., Babus, L. W., Nguyen, M. T., Trotter, J. H., Ladu, M. J., et al. (2009). ApoE4 decreases spine density and dendritic complexity in cortical neurons in vivo. *J Neurosci, 29*(48), 15317-15322.
Eichenbaum, H. (2004). Hippocampus: cognitive processes and neural representations that underlie declarative memory. *Neuron, 44*(1), 109-120.
Engvig, A., Fjell, A. M., Westlye, L. T., Moberget, T., Sundseth, Ø., Larsen, V. A., et al. (2012). Memory training impacts short-term changes in aging white matter: a longitudinal diffusion tensor imaging study. *Hum Brain Mapp, 33*(10), 2390-2406.
Erickson, K. I., Voss, M. W., Prakash, R. S., Basak, C., Szabo, A., Chaddock, L., et al. (2011). Exercise training increases size of hippocampus and improves memory. *Proc Natl Acad Sci U S A, 108*(7), 3017-3022.
Erickson, K. I., Weinstein, A. M., & Lopez, O. L. (2012). Physical activity, brain plasticity, and Alzheimer's disease. *Arch Med Res, 43*(8), 615-621.
Etgen, T., Sander, D., Huntgeburth, U., Poppert, H., Förstl, H., & Bickel, H. (2010). Physical activity and incident cognitive impairment in elderly persons: the INVADE study. *Arch Intern Med, 170*(2), 186-193.
Ewers, M., Insel, P. S., Stern, Y., Weiner, M. W., & (ADNI), A. s. D. N. I. (2013). Cognitive reserve associated with FDG-PET in preclinical Alzheimer disease. *Neurology, 80*(13), 1194-1201.
Fair, D. A., Cohen, A. L., Dosenbach, N. U., Church, J. A., Miezin, F. M., Barch, D. M., et al. (2008). The maturing architecture of the brain's default network. *Proc Natl Acad Sci U S A, 105*(10), 4028-4032.
Fair, D. A., Cohen, A. L., Power, J. D., Dosenbach, N. U., Church, J. A., Miezin, F. M., et al. (2009). Functional brain networks develop from a "local to distributed" organization. *PLoS Comput Biol, 5*(5), e1000381.

Farrer, L. A., Cupples, L. A., Haines, J. L., Hyman, B., Kukull, W. A., Mayeux, R., et al. (1997). Effects of age, sex, and ethnicity on the association between apolipoprotein E genotype and Alzheimer disease. A meta-analysis. APOE and Alzheimer Disease Meta Analysis Consortium. *JAMA, 278*(16), 1349-1356.

Ferreira, J. M., Burnett, A. L., & Rameau, G. A. (2011). Activity-dependent regulation of surface glucose transporter-3. *J Neurosci, 31*(6), 1991-1999.

Fleisher, A. S., Sherzai, A., Taylor, C., Langbaum, J. B., Chen, K., & Buxton, R. B. (2009). Resting-state BOLD networks versus task-associated functional MRI for distinguishing Alzheimer's disease risk groups. *Neuroimage, 47*(4), 1678-1690.

Folstein, M. F., Folstein, S. E., & McHugh, P. R. (1975). "Mini-mental state". A practical method for grading the cognitive state of patients for the clinician. *J Psychiatr Res, 12*(3), 189-198.

Foster, D. J., & Wilson, M. A. (2006). Reverse replay of behavioural sequences in hippocampal place cells during the awake state. *Nature, 440*(7084), 680-683.

Foster, P. P. (2015). Role of physical and mental training in brain network configuration. *Front Aging Neurosci, 7*, 117.

Fouquet, M., Besson, F. L., Gonneaud, J., La Joie, R., & Chételat, G. (2014). Imaging brain effects of APOE4 in cognitively normal individuals across the lifespan. *Neuropsychol Rev, 24*(3), 290-299.

Fox, M. D., & Raichle, M. E. (2007). Spontaneous fluctuations in brain activity observed with functional magnetic resonance imaging. *Nat Rev Neurosci, 8*(9), 700-711.

Fox, M. D., Snyder, A. Z., Vincent, J. L., Corbetta, M., Van Essen, D. C., & Raichle, M. E. (2005). The human brain is intrinsically organized into dynamic, anticorrelated functional networks. *Proc Natl Acad Sci U S A, 102*(27), 9673-9678.

Fraser, M. A., Shaw, M. E., & Cherbuin, N. (2015). A systematic review and meta-analysis of longitudinal hippocampal atrophy in healthy human ageing. *Neuroimage, 112*, 364-374.

Fratiglioni, L., Paillard-Borg, S., & Winblad, B. (2004). An active and socially integrated lifestyle in late life might protect against dementia. *Lancet Neurol, 3*(6), 343-353.

Gaser, C., & Schlaug, G. (2003). Brain structures differ between musicians and non-musicians. *J Neurosci, 23*(27), 9240-9245.

Gates, N., Fiatarone Singh, M. A., Sachdev, P. S., & Valenzuela, M. (2013). The effect of exercise training on cognitive function in older adults with mild cognitive impairment: a meta-analysis of randomized controlled trials. *Am J Geriatr Psychiatry, 21*(11), 1086-1097.

Gauthier, S., Reisberg, B., Zaudig, M., Petersen, R. C., Ritchie, K., Broich, K., et al. (2006). Mild cognitive impairment. *Lancet, 367*(9518), 1262-1270.

Golanov, E. V., Yamamoto, S., & Reis, D. J. (1994). Spontaneous waves of cerebral blood flow associated with a pattern of electrocortical activity. *Am J Physiol, 266*(1 Pt 2), R204-214.

Goveas, J. S., Xie, C., Chen, G., Li, W., Ward, B. D., Franczak, M. B., et al. (2013). Functional network endophenotypes unravel the effects of apolipoprotein E epsilon 4 in middle-aged adults. *PLoS One, 8*(2), e55902.

Goveas, J. S., Xie, C., Ward, B. D., Wu, Z., Li, W., Franczak, M., et al. (2011). Recovery of hippocampal network connectivity correlates with cognitive improvement in mild

Alzheimer's disease patients treated with donepezil assessed by resting-state fMRI. *J Magn Reson Imaging, 34*(4), 764-773.
Grande, G., Vanacore, N., Maggiore, L., Cucumo, V., Ghiretti, R., Galimberti, D., et al. (2014). Physical activity reduces the risk of dementia in mild cognitive impairment subjects: a cohort study. *J Alzheimers Dis, 39*(4), 833-839.
Greicius, M. (2008). Resting-state functional connectivity in neuropsychiatric disorders. *Curr Opin Neurol, 21*(4), 424-430.
Greicius, M. D., & Menon, V. (2004). Default-mode activity during a passive sensory task: uncoupled from deactivation but impacting activation. *J Cogn Neurosci, 16*(9), 1484-1492.
Greicius, M. D., Srivastava, G., Reiss, A. L., & Menon, V. (2004). Default-mode network activity distinguishes Alzheimer's disease from healthy aging: evidence from functional MRI. *Proc Natl Acad Sci U S A, 101*(13), 4637-4642.
Greicius, M. D., Supekar, K., Menon, V., & Dougherty, R. F. (2009). Resting-state functional connectivity reflects structural connectivity in the default mode network. *Cereb Cortex, 19*(1), 72-78.
Guerra-Carrillo, B., Mackey, A. P., & Bunge, S. A. (2014). Resting-state fMRI: a window into human brain plasticity. *Neuroscientist, 20*(5), 522-533.
Gómez-Isla, T., Price, J. L., McKeel, D. W., Morris, J. C., Growdon, J. H., & Hyman, B. T. (1996). Profound loss of layer II entorhinal cortex neurons occurs in very mild Alzheimer's disease. *J Neurosci, 16*(14), 4491-4500.
Habeck, C., Hilton, H. J., Zarahn, E., Flynn, J., Moeller, J., & Stern, Y. (2003). Relation of cognitive reserve and task performance to expression of regional covariance networks in an event-related fMRI study of nonverbal memory. *Neuroimage, 20*(3), 1723-1733.
Habeck, C., & Moeller, J. R. (2011). Intrinsic functional-connectivity networks for diagnosis: just beautiful pictures? *Brain Connect, 1*(2), 99-103.
Hall, C. B., Derby, C., LeValley, A., Katz, M. J., Verghese, J., & Lipton, R. B. (2007). Education delays accelerated decline on a memory test in persons who develop dementia. *Neurology, 69*(17), 1657-1664.
Harrison, T. M., Burggren, A. C., Small, G. W., & Bookheimer, S. Y. (2016). Altered memory-related functional connectivity of the anterior and posterior hippocampus in older adults at increased genetic risk for Alzheimer's disease. *Hum Brain Mapp, 37*(1), 366-380.
Head, D., Buckner, R. L., Shimony, J. S., Williams, L. E., Akbudak, E., Conturo, T. E., et al. (2004). Differential vulnerability of anterior white matter in nondemented aging with minimal acceleration in dementia of the Alzheimer type: evidence from diffusion tensor imaging. *Cereb Cortex, 14*(4), 410-423.
Head, D., Bugg, J. M., Goate, A. M., Fagan, A. M., Mintun, M. A., Benzinger, T., et al. (2012). Exercise Engagement as a Moderator of the Effects of APOE Genotype on Amyloid Deposition. *Arch Neurol, 69*(5), 636-643.
Head, D., Snyder, A. Z., Girton, L. E., Morris, J. C., & Buckner, R. L. (2005). Frontal-hippocampal double dissociation between normal aging and Alzheimer's disease. *Cereb Cortex, 15*(6), 732-739.

Heath, G. W., Gavin, J. R., Hinderliter, J. M., Hagberg, J. M., Bloomfield, S. A., & Holloszy, J. O. (1983). Effects of exercise and lack of exercise on glucose tolerance and insulin sensitivity. *J Appl Physiol Respir Environ Exerc Physiol, 55*(2), 512-517.

Hedden, T., & Gabrieli, J. D. (2004). Insights into the ageing mind: a view from cognitive neuroscience. *Nat Rev Neurosci, 5*(2), 87-96.

Hedden, T., Van Dijk, K. R., Becker, J. A., Mehta, A., Sperling, R. A., Johnson, K. A., et al. (2009). Disruption of functional connectivity in clinically normal older adults harboring amyloid burden. *J Neurosci, 29*(40), 12686-12694.

Heise, V., Filippini, N., Trachtenberg, A. J., Suri, S., Ebmeier, K. P., & Mackay, C. E. (2014). Apolipoprotein E genotype, gender and age modulate connectivity of the hippocampus in healthy adults. *Neuroimage, 98*, 23-30.

Heisz, J. J., Gould, M., & McIntosh, A. R. (2015). Age-related shift in neural complexity related to task performance and physical activity. *J Cogn Neurosci, 27*(3), 605-613.

Heyn, P., Abreu, B. C., & Ottenbacher, K. J. (2004). The effects of exercise training on elderly persons with cognitive impairment and dementia: a meta-analysis. *Arch Phys Med Rehabil, 85*(10), 1694-1704.

Hillary, F. G., Rajtmajer, S. M., Roman, C. A., Medaglia, J. D., Slocomb-Dluzen, J. E., Calhoun, V. D., et al. (2014). The rich get richer: brain injury elicits hyperconnectivity in core subnetworks. *PLoS One, 9*(8), e104021.

Hillary, F. G., Roman, C. A., Venkatesan, U., Rajtmajer, S. M., Bajo, R., & Castellanos, N. D. (2015). Hyperconnectivity is a fundamental response to neurological disruption. *Neuropsychology, 29*(1), 59-75.

Hofstetter, S., Tavor, I., Tzur Moryosef, S., & Assaf, Y. (2013). Short-term learning induces white matter plasticity in the fornix. *J Neurosci, 33*(31), 12844-12850.

Holtzman, D. M., Herz, J., & Bu, G. (2012). Apolipoprotein E and apolipoprotein E receptors: normal biology and roles in Alzheimer disease. *Cold Spring Harb Perspect Med, 2*(3), a006312.

Honea, R. A., Vidoni, E., Harsha, A., & Burns, J. M. (2009). Impact of APOE on the healthy aging brain: a voxel-based MRI and DTI study. *J Alzheimers Dis, 18*(3), 553-564.

Honey, C. J., Kötter, R., Breakspear, M., & Sporns, O. (2007). Network structure of cerebral cortex shapes functional connectivity on multiple time scales. *Proc Natl Acad Sci U S A, 104*(24), 10240-10245.

Huang, C., Wahlund, L. O., Svensson, L., Winblad, B., & Julin, P. (2002). Cingulate cortex hypoperfusion predicts Alzheimer's disease in mild cognitive impairment. *BMC Neurol, 2*, 9.

Huang, P., Fang, R., Li, B. Y., & Chen, S. D. (2016). Exercise-Related Changes of Networks in Aging and Mild Cognitive Impairment Brain. *Front Aging Neurosci, 8*, 47.

Intlekofer, K. A., & Cotman, C. W. (2013). Exercise counteracts declining hippocampal function in aging and Alzheimer's disease. *Neurobiol Dis, 57*, 47-55.

Jack, C. R., Knopman, D. S., Jagust, W. J., Shaw, L. M., Aisen, P. S., Weiner, M. W., et al. (2010). Hypothetical model of dynamic biomarkers of the Alzheimer's pathological cascade. *Lancet Neurol, 9*(1), 119-128.

Jack, C. R., Petersen, R. C., Xu, Y. C., Waring, S. C., O'Brien, P. C., Tangalos, E. G., et al. (1997). Medial temporal atrophy on MRI in normal aging and very mild Alzheimer's disease. *Neurology, 49*(3), 786-794.

Jagust, W. J., Landau, S. M., & Initiative, A. s. D. N. (2012). Apolipoprotein E, not fibrillar β-amyloid, reduces cerebral glucose metabolism in normal aging. *J Neurosci, 32*(50), 18227-18233.

Jeurissen, B., Leemans, A., Tournier, J. D., Jones, D. K., & Sijbers, J. (2013). Investigating the prevalence of complex fiber configurations in white matter tissue with diffusion magnetic resonance imaging. *Hum Brain Mapp, 34*(11), 2747-2766.

Johansen-Berg, H. (2012). The future of functionally-related structural change assessment. *Neuroimage, 62*(2), 1293-1298.

Jurica, P., Leitten, C., & Mattis, S. (2001). *Dementia Rating Scale-2 Professional Manual*. Lutz, Florida: Psychological Assessment Resources.

Kamijo, K., O'Leary, K. C., Pontifex, M. B., Themanson, J. R., & Hillman, C. H. (2010). The relation of aerobic fitness to neuroelectric indices of cognitive and motor task preparation. *Psychophysiology, 47*(5), 814-821.

Kenet, T., Bibitchkov, D., Tsodyks, M., Grinvald, A., & Arieli, A. (2003). Spontaneously emerging cortical representations of visual attributes. *Nature, 425*(6961), 954-956.

Kesner, R. P., Lee, I., & Gilbert, P. (2004). A behavioral assessment of hippocampal function based on a subregional analysis. *Rev Neurosci, 15*(5), 333-351.

Klados, M. A., Styliadis, C., Frantzidis, C. A., Paraskevopoulos, E., & Bamidis, P. D. (2016). Beta-Band Functional Connectivity is Reorganized in Mild Cognitive Impairment after Combined Computerized Physical and Cognitive Training. *Front Neurosci, 10*, 55.

Kleemeyer, M. M., Kühn, S., Prindle, J., Bodammer, N. C., Brechtel, L., Garthe, A., et al. (2016). Changes in fitness are associated with changes in hippocampal microstructure and hippocampal volume among older adults. *Neuroimage, 131*, 155-161.

Knickmeyer, R. C., Wang, J., Zhu, H., Geng, X., Woolson, S., Hamer, R. M., et al. (2014). Common variants in psychiatric risk genes predict brain structure at birth. *Cereb Cortex, 24*(5), 1230-1246.

Knopman, D. S., Jack, C. R., Wiste, H. J., Lundt, E. S., Weigand, S. D., Vemuri, P., et al. (2014). 18F-fluorodeoxyglucose positron emission tomography, aging, and apolipoprotein E genotype in cognitively normal persons. *Neurobiol Aging, 35*(9), 2096-2106.

Koch, W., Teipel, S., Mueller, S., Benninghoff, J., Wagner, M., Bokde, A. L. W., et al. (2012). Diagnostic power of default mode network resting state fMRI in the detection of Alzheimer's disease. *Neurobiology of Aging, 33*(3), 466-478.

Kramer, A. F., Erickson, K. I., & Colcombe, S. J. (2006). Exercise, cognition, and the aging brain. *J Appl Physiol (1985), 101*(4), 1237-1242.

Körding, K. P., & Wolpert, D. M. (2006). Bayesian decision theory in sensorimotor control. *Trends Cogn Sci, 10*(7), 319-326.

Laurin, D., Verreault, R., Lindsay, J., MacPherson, K., & Rockwood, K. (2001). Physical activity and risk of cognitive impairment and dementia in elderly persons. *Arch Neurol, 58*(3), 498-504.

Lautenschlager, N. T., Cox, K. L., Flicker, L., Foster, J. K., van Bockxmeer, F. M., Xiao, J., et al. (2008). Effect of physical activity on cognitive function in older adults at risk for Alzheimer disease: a randomized trial. *JAMA, 300*(9), 1027-1037.

Li, W., Antuono, P. G., Xie, C., Chen, G., Jones, J. L., Ward, B. D., et al. (2012). Changes in regional cerebral blood flow and functional connectivity in the cholinergic pathway associated with cognitive performance in subjects with mild Alzheimer's disease after 12-week donepezil treatment. *Neuroimage, 60*(2), 1083-1091.

Lomax, R. G., & Hahs-Vaughn, D. L. (2012). *Statistical Concepts: A Second Course* (Fourth Edition ed.).

Matura, S., Prvulovic, D., Jurcoane, A., Hartmann, D., Miller, J., Scheibe, M., et al. (2014). Differential effects of the ApoE4 genotype on brain structure and function. *Neuroimage, 89*, 81-91.

Mazzeo, R. S., & Tanaka, H. (2001). Exercise prescription for the elderly: current recommendations. *Sports Med, 31*(11), 809-818.

McKenna, F., Koo, B. B., Killiany, R., & Initiative, A. s. D. N. (2015). Comparison of ApoE-related brain connectivity differences in early MCI and normal aging populations: an fMRI study. *Brain Imaging Behav*.

Middleton, L. E., Barnes, D. E., Lui, L. Y., & Yaffe, K. (2010). Physical activity over the life course and its association with cognitive performance and impairment in old age. *J Am Geriatr Soc, 58*(7), 1322-1326.

Middleton, L. E., Manini, T. M., Simonsick, E. M., Harris, T. B., Barnes, D. E., Tylavsky, F., et al. (2011). Activity energy expenditure and incident cognitive impairment in older adults. *Arch Intern Med, 171*(14), 1251-1257.

Miller, L. A., Spitznagel, M. B., Busko, S., Potter, V., Juvancic-Heltzel, J., Istenes, N., et al. (2011). Structured exercise does not stabilize cognitive function in individuals with mild cognitive impairment residing in a structured living facility. *Int J Neurosci, 121*(4), 218-223.

Morris, J. C., Roe, C. M., Xiong, C., Fagan, A. M., Goate, A. M., Holtzman, D. M., et al. (2010). APOE predicts amyloid-beta but not tau Alzheimer pathology in cognitively normal aging. *Ann Neurol, 67*(1), 122-131.

Nyberg, L., Bäckman, L., Erngrund, K., Olofsson, U., & Nilsson, L. G. (1996). Age differences in episodic memory, semantic memory, and priming: relationships to demographic, intellectual, and biological factors. *J Gerontol B Psychol Sci Soc Sci, 51*(4), P234-240.

O'Dwyer, L., Lamberton, F., Matura, S., Tanner, C., Scheibe, M., Miller, J., et al. (2012). Reduced hippocampal volume in healthy young ApoE4 carriers: an MRI study. *PLoS One, 7*(11), e48895.

Oberlin, L. E., Verstynen, T. D., Burzynska, A. Z., Voss, M. W., Prakash, R. S., Chaddock-Heyman, L., et al. (2016). White matter microstructure mediates the relationship between cardiorespiratory fitness and spatial working memory in older adults. *Neuroimage, 131*, 91-101.

Okuizumi, K., Onodera, O., Tanaka, H., Kobayashi, H., Tsuji, S., Takahashi, H., et al. (1994). ApoE-epsilon 4 and early-onset Alzheimer's. *Nat Genet, 7*(1), 10-11.

Oldfield, R. C. (1971). The assessment and analysis of handedness: the Edinburgh inventory. *Neuropsychologia, 9*(1), 97-113.

Ott, A., Stolk, R. P., Hofman, A., van Harskamp, F., Grobbee, D. E., & Breteler, M. M. (1996). Association of diabetes mellitus and dementia: the Rotterdam Study. *Diabetologia, 39*(11), 1392-1397.

Paffenbarger, R. S., Blair, S. N., Lee, I. M., & Hyde, R. T. (1993). Measurement of physical activity to assess health effects in free-living populations. *Med Sci Sports Exerc, 25*(1), 60-70.

Paffenbarger, R. S., Wing, A. L., & Hyde, R. T. (1978). Physical activity as an index of heart attack risk in college alumni. *Am J Epidemiol, 108*(3), 161-175.

Park, D. C., Smith, A. D., Lautenschlager, G., Earles, J. L., Frieske, D., Zwahr, M., et al. (1996). Mediators of long-term memory performance across the life span. *Psychol Aging, 11*(4), 621-637.

Paus, T., Pesaresi, M., & French, L. (2014). White matter as a transport system. *Neuroscience, 276*, 117-125.

Pereira, A. C., Huddleston, D. E., Brickman, A. M., Sosunov, A. A., Hen, R., McKhann, G. M., et al. (2007). An in vivo correlate of exercise-induced neurogenesis in the adult dentate gyrus. *Proc Natl Acad Sci U S A, 104*(13), 5638-5643.

Perkins, M., Wolf, A. B., Chavira, B., Shonebarger, D., Meckel, J. P., Leung, L., et al. (2016). Altered Energy Metabolism Pathways in the Posterior Cingulate in Young Adult Apolipoprotein E ε4 Carriers. *J Alzheimers Dis, 53*(1), 95-106.

Persson, J., Pudas, S., Nilsson, L. G., & Nyberg, L. (2014). Longitudinal assessment of default-mode brain function in aging. *Neurobiol Aging, 35*(9), 2107-2117.

Peters, A. (2002). The effects of normal aging on myelin and nerve fibers: a review. *J Neurocytol, 31*(8-9), 581-593.

Petersen, R. C. (2004). Mild cognitive impairment as a diagnostic entity. *J Intern Med, 256*(3), 183-194.

Petersen, R. C., Smith, G. E., Waring, S. C., Ivnik, R. J., Tangalos, E. G., & Kokmen, E. (1999). Mild cognitive impairment: clinical characterization and outcome. *Arch Neurol, 56*(3), 303-308.

Pievani, M., de Haan, W., Wu, T., Seeley, W. W., & Frisoni, G. B. (2011). Functional network disruption in the degenerative dementias. [Review]. *Lancet Neurology, 10*(9), 829-843.

Pievani, M., Filippini, N., van den Heuvel, M. P., Cappa, S. F., & Frisoni, G. B. (2014). Brain connectivity in neurodegenerative diseases--from phenotype to proteinopathy. *Nat Rev Neurol, 10*(11), 620-633.

Pihlajamaki, M., & Sperling, R. A. (2009). Functional MRI assessment of task-induced deactivation of the default mode network in Alzheimer's disease and at-risk older individuals. *Behavioural Neurology, 21*(1-2), 77-91.

Plassman, B. L., Welsh-Bohmer, K. A., Bigler, E. D., Johnson, S. C., Anderson, C. V., Helms, M. J., et al. (1997). Apolipoprotein E epsilon 4 allele and hippocampal volume in twins with normal cognition. *Neurology, 48*(4), 985-989.

Pouget, A., Dayan, P., & Zemel, R. S. (2003). Inference and computation with population codes. *Annu Rev Neurosci, 26*, 381-410.

Power, J. D., Barnes, K. A., Snyder, A. Z., Schlaggar, B. L., & Petersen, S. E. (2012). Spurious but systematic correlations in functional connectivity MRI networks arise from subject motion. *Neuroimage, 59*(3), 2142-2154.

Power, J. D., Fair, D. A., Schlaggar, B. L., & Petersen, S. E. (2010). The development of human functional brain networks. *Neuron, 67*(5), 735-748.
Raichle, M. E. (2011). The restless brain. *Brain Connect, 1*(1), 3-12.
Raichle, M. E., & Mintun, M. A. (2006). Brain work and brain imaging. *Annu Rev Neurosci, 29*, 449-476.
Raichlen, D. A., Bharadwaj, P. K., Fitzhugh, M. C., Haws, K. A., Torre, G. A., Trouard, T. P., et al. (2016). Differences in Resting State Functional Connectivity between Young Adult Endurance Athletes and Healthy Controls. *Front Hum Neurosci, 10*, 610.
Raz, N., Lindenberger, U., Rodrigue, K. M., Kennedy, K. M., Head, D., Williamson, A., et al. (2005). Regional brain changes in aging healthy adults: general trends, individual differences and modifiers. *Cereb Cortex, 15*(11), 1676-1689.
Reiman, E. M., Caselli, R. J., Yun, L. S., Chen, K., Bandy, D., Minoshima, S., et al. (1996). Preclinical evidence of Alzheimer's disease in persons homozygous for the epsilon 4 allele for apolipoprotein E. *N Engl J Med, 334*(12), 752-758.
Reiman, E. M., Chen, K., Alexander, G. E., Caselli, R. J., Bandy, D., Osborne, D., et al. (2004). Functional brain abnormalities in young adults at genetic risk for late-onset Alzheimer's dementia. *Proc Natl Acad Sci U S A, 101*(1), 284-289.
Reiman, E. M., Chen, K., Liu, X., Bandy, D., Yu, M., Lee, W., et al. (2009). Fibrillar amyloid-beta burden in cognitively normal people at 3 levels of genetic risk for Alzheimer's disease. *Proc Natl Acad Sci U S A, 106*(16), 6820-6825.
Reiter, K., Nielson, K. A., Smith, T. J., Weiss, L. R., Alfini, A. J., & Smith, J. C. (2015). Improved Cardiorespiratory Fitness Is Associated with Increased Cortical Thickness in Mild Cognitive Impairment. *J Int Neuropsychol Soc, 21*(10), 757-767.
Reuter-Lorenz, P. A., & Park, D. C. (2010). Human neuroscience and the aging mind: a new look at old problems. *J Gerontol B Psychol Sci Soc Sci, 65*(4), 405-415.
Reuter-Lorenz, P. A., & Park, D. C. (2014). How does it STAC up? Revisiting the scaffolding theory of aging and cognition. *Neuropsychol Rev, 24*(3), 355-370.
Rey, A. (1964). *L'examen clinique en psychologic*. Paris: Presses Universitaires de France Paris.
Rogers, M. A., Yamamoto, C., King, D. S., Hagberg, J. M., Ehsani, A. A., & Holloszy, J. O. (1988). Improvement in glucose tolerance after 1 wk of exercise in patients with mild NIDDM. *Diabetes Care, 11*(8), 613-618.
Rolandsson, O., Backeström, A., Eriksson, S., Hallmans, G., & Nilsson, L. G. (2008). Increased glucose levels are associated with episodic memory in nondiabetic women. *Diabetes, 57*(2), 440-443.
Rubinov, M., & Sporns, O. (2010). Complex network measures of brain connectivity: uses and interpretations. *Neuroimage, 52*(3), 1059-1069.
Rushworth, M. F., Walton, M. E., Kennerley, S. W., & Bannerman, D. M. (2004). Action sets and decisions in the medial frontal cortex. *Trends Cogn Sci, 8*(9), 410-417.
Salinas, E., & Sejnowski, T. J. (2001). Correlated neuronal activity and the flow of neural information. *Nat Rev Neurosci, 2*(8), 539-550.
Sanz-Arigita, E. J., Schoonheim, M. M., Damoiseaux, J. S., Rombouts, S., Maris, E., Barkhof, F., et al. (2010). Loss of 'Small-World' Networks in Alzheimer's Disease: Graph Analysis of fMRI Resting-State Functional Connectivity. [Article]. *Plos One, 5*(11), 14.

Saunders, A. M., Schmader, K., Breitner, J. C., Benson, M. D., Brown, W. T., Goldfarb, L., et al. (1993). Apolipoprotein E epsilon 4 allele distributions in late-onset Alzheimer's disease and in other amyloid-forming diseases. *Lancet, 342*(8873), 710-711.

Scarmeas, N., Luchsinger, J. A., Schupf, N., Brickman, A. M., Cosentino, S., Tang, M. X., et al. (2009). Physical activity, diet, and risk of Alzheimer disease. *JAMA, 302*(6), 627-637.

Scarmeas, N., Zarahn, E., Anderson, K. E., Hilton, J., Flynn, J., Van Heertum, R. L., et al. (2003). Cognitive reserve modulates functional brain responses during memory tasks: a PET study in healthy young and elderly subjects. *Neuroimage, 19*(3), 1215-1227.

Schacter, D. L. (1997). The cognitive neuroscience of memory: perspectives from neuroimaging research. *Philos Trans R Soc Lond B Biol Sci, 352*(1362), 1689-1695.

Schacter, D. L. (2000). Memory systems of 1999. In E. Tulving & F. I. Craik (Eds.), *The Oxford handbook of memory* (Vol. 1, pp. 627-643). Oxford: Oxford University Press.

Schaie, K. W., & Willis, S. L. (2010). The Seattle Longitudinal Study of Adult Cognitive Development. *ISSBD Bull, 57*(1), 24-29.

Schuit, A. J., Feskens, E. J. M., Launer, L. J., & Kromhout, D. (2001). Physical activity and cognitive decline, the role of the apolipoprotein e4 allele. *Medicine and Science in Sports and Exercise, 33*(5), 772-777.

Seals, D. R., Hagberg, J. M., Allen, W. K., Hurley, B. F., Dalsky, G. P., Ehsani, A. A., et al. (1984). Glucose tolerance in young and older athletes and sedentary men. *J Appl Physiol Respir Environ Exerc Physiol, 56*(6), 1521-1525.

Seals, D. R., Hagberg, J. M., Hurley, B. F., Ehsani, A. A., & Holloszy, J. O. (1984). Effects of endurance training on glucose tolerance and plasma lipid levels in older men and women. *JAMA, 252*(5), 645-649.

Sexton, C. E., Betts, J. F., Demnitz, N., Dawes, H., Ebmeier, K. P., & Johansen-Berg, H. (2016). A systematic review of MRI studies examining the relationship between physical fitness and activity and the white matter of the ageing brain. *Neuroimage, 131*, 81-90.

Shatz, C. J. (1996). Emergence of order in visual system development. *J Physiol Paris, 90*(3-4), 141-150.

Shaw, P., Lerch, J. P., Pruessner, J. C., Taylor, K. N., Rose, A. B., Greenstein, D., et al. (2007). Cortical morphology in children and adolescents with different apolipoprotein E gene polymorphisms: an observational study. *Lancet Neurol, 6*(6), 494-500.

Sheline, Y. I., Morris, J. C., Snyder, A. Z., Price, J. L., Yan, Z., D'Angelo, G., et al. (2010). APOE4 allele disrupts resting state fMRI connectivity in the absence of amyloid plaques or decreased CSF Aβ42. *J Neurosci, 30*(50), 17035-17040.

Shu, H., Shi, Y., Chen, G., Wang, Z., Liu, D., Yue, C., et al. (2016). Opposite Neural Trajectories of Apolipoprotein E ϵ4 and ϵ2 Alleles with Aging Associated with Different Risks of Alzheimer's Disease. *Cereb Cortex, 26*(4), 1421-1429.

Small, G. W., Mazziotta, J. C., Collins, M. T., Baxter, L. R., Phelps, M. E., Mandelkern, M. A., et al. (1995). Apolipoprotein E type 4 allele and cerebral glucose metabolism in relatives at risk for familial Alzheimer disease. *JAMA, 273*(12), 942-947.

Small, S. A., Schobel, S. A., Buxton, R. B., Witter, M. P., & Barnes, C. A. (2011). A pathophysiological framework of hippocampal dysfunction in ageing and disease. *Nat Rev Neurosci, 12*(10), 585-601.

Smith, A. (1991). *Symbol Digit Modalities Test*. Los Angeles: Western Psychological Services.

Smith, J. C., Lancaster, M. A., Nielson, K. A., Woodard, J. L., Seidenberg, M., Durgerian, S., et al. (2016). Interactive effects of physical activity and APOE-ε4 on white matter tract diffusivity in healthy elders. *Neuroimage, 131*, 102-112.

Smith, J. C., Nielson, K. A., Antuono, P., Lyons, J. A., Hanson, R. J., Butts, A. M., et al. (2013). Semantic memory functional MRI and cognitive function after exercise intervention in mild cognitive impairment. *J Alzheimers Dis, 37*(1), 197-215.

Smith, J. C., Nielson, K. A., Woodard, J. L., Seidenberg, M., Durgerian, S., Antuono, P., et al. (2011). Interactive effects of physical activity and APOE-ε4 on BOLD semantic memory activation in healthy elders. *Neuroimage, 54*(1), 635-644.

Smith, J. C., Nielson, K. A., Woodard, J. L., Seidenberg, M., Durgerian, S., Hazlett, K. E., et al. (2014). Physical activity reduces hippocampal atrophy in elders at genetic risk for Alzheimer's disease. *Front Aging Neurosci, 6*, 61.

Smith, J. C., Nielson, K. A., Woodard, J. L., Seidenberg, M., & Rao, S. M. (2013). Physical activity and brain function in older adults at increased risk for Alzheimer's disease. *Brain Sci, 3*(1), 54-83.

Smith, J. C., Nielson, K. A., Woodard, J. L., Seidenberg, M., & Rao, S. M. (2013). Physical activity and brain function in older adults at increased risk for Alzheimer's disease. *Brain Sciences, 3*, 54-83.

Sperling, R. A., Aisen, P. S., Beckett, L. A., Bennett, D. A., Craft, S., Fagan, A. M., et al. (2011). Toward defining the preclinical stages of Alzheimer's disease: recommendations from the National Institute on Aging-Alzheimer's Association workgroups on diagnostic guidelines for Alzheimer's disease. *Alzheimers Dement, 7*(3), 280-292.

Sporns, O. (2011). *Networks of the Brain*. Cambridge: The MIT Press.

Sporns, O., Honey, C. J., & Kötter, R. (2007). Identification and classification of hubs in brain networks. *PLoS One, 2*(10), e1049.

Squire, L. R. (2004). Memory systems of the brain: a brief history and current perspective. *Neurobiol Learn Mem, 82*(3), 171-177.

Stern, Y. (2003). The concept of cognitive reserve: a catalyst for research. *J Clin Exp Neuropsychol, 25*(5), 589-593.

Stern, Y. (2006). Cognitive reserve and Alzheimer disease. *Alzheimer Dis Assoc Disord, 20*(3 Suppl 2), S69-74.

Stern, Y. (2009). Cognitive reserve. *Neuropsychologia, 47*(10), 2015-2028.

Stern, Y., Alexander, G. E., Prohovnik, I., & Mayeux, R. (1992). Inverse relationship between education and parietotemporal perfusion deficit in Alzheimer's disease. *Ann Neurol, 32*(3), 371-375.

Stern, Y., Habeck, C., Moeller, J., Scarmeas, N., Anderson, K. E., Hilton, H. J., et al. (2005). Brain networks associated with cognitive reserve in healthy young and old adults. *Cereb Cortex, 15*(4), 394-402.

Stranahan, A. M., & Mattson, M. P. (2011). Bidirectional metabolic regulation of neurocognitive function. *Neurobiol Learn Mem, 96*(4), 507-516.

Stranahan, A. M., & Mattson, M. P. (2012). Metabolic reserve as a determinant of cognitive aging. *J Alzheimers Dis, 30 Suppl 2*, S5-13.

Tarumi, T., Gonzales, M. M., Fallow, B., Nualnim, N., Lee, J., Tanaka, H., et al. (2013). Aerobic fitness and cognitive function in midlife: an association mediated by plasma insulin. *Metab Brain Dis, 28*(4), 727-730.

Thomas, A. G., Dennis, A., Rawlings, N. B., Stagg, C. J., Matthews, L., Morris, M., et al. (2016). Multi-modal characterization of rapid anterior hippocampal volume increase associated with aerobic exercise. *Neuroimage, 131*, 162-170.

Thompson, W. K., Hallmayer, J., O'Hara, R., & Initiative, A. s. D. N. (2011). Design considerations for characterizing psychiatric trajectories across the lifespan: application to effects of APOE-ε4 on cerebral cortical thickness in Alzheimer's disease. *Am J Psychiatry, 168*(9), 894-903.

Thompson, W. R., Gordon, N. F., & Pescatello, L. S. (Eds.). (2010). *ACSM's Guidelines for Exercise Testing and Prescription*. Baltimore: Lippincott Williams & Wilkins.

Tomasi, D., Wang, G. J., & Volkow, N. D. (2013). Energetic cost of brain functional connectivity. *Proc Natl Acad Sci U S A, 110*(33), 13642-13647.

Trachtenberg, A. J., Filippini, N., Cheeseman, J., Duff, E. P., Neville, M. J., Ebmeier, K. P., et al. (2012). The effects of APOE on brain activity do not simply reflect the risk of Alzheimer's disease. *Neurobiol Aging, 33*(3), 618.e611-618.e613.

Trachtenberg, A. J., Filippini, N., Ebmeier, K. P., Smith, S. M., Karpe, F., & Mackay, C. E. (2012). The effects of APOE on the functional architecture of the resting brain. *Neuroimage, 59*(1), 565-572.

Trejo, J. L., Carro, E., & Torres-Aleman, I. (2001). Circulating insulin-like growth factor I mediates exercise-induced increases in the number of new neurons in the adult hippocampus. *J Neurosci, 21*(5), 1628-1634.

Vaishnavi, S. N., Vlassenko, A. G., Rundle, M. M., Snyder, A. Z., Mintun, M. A., & Raichle, M. E. (2010). Regional aerobic glycolysis in the human brain. *Proc Natl Acad Sci U S A, 107*(41), 17757-17762.

Valla, J., Yaari, R., Wolf, A. B., Kusne, Y., Beach, T. G., Roher, A. E., et al. (2010). Reduced posterior cingulate mitochondrial activity in expired young adult carriers of the APOE ε4 allele, the major late-onset Alzheimer's susceptibility gene. *J Alzheimers Dis, 22*(1), 307-313.

van den Heuvel, M. P., & Sporns, O. (2013). An anatomical substrate for integration among functional networks in human cortex. *J Neurosci, 33*(36), 14489-14500.

van Praag, H., Shubert, T., Zhao, C., & Gage, F. H. (2005). Exercise enhances learning and hippocampal neurogenesis in aged mice. *J Neurosci, 25*(38), 8680-8685.

Varoquaux, G., & Craddock, R. C. (2013). Learning and comparing functional connectomes across subjects. *Neuroimage, 80*, 405-415.

Velayudhan, L., Poppe, M., Archer, N., Proitsi, P., Brown, R. G., & Lovestone, S. (2010). Risk of developing dementia in people with diabetes and mild cognitive impairment. *Br J Psychiatry, 196*(1), 36-40.

Vincent, J. L., Kahn, I., Snyder, A. Z., Raichle, M. E., & Buckner, R. L. (2008). Evidence for a frontoparietal control system revealed by intrinsic functional connectivity. *J Neurophysiol, 100*(6), 3328-3342.

Vincent, J. L., Patel, G. H., Fox, M. D., Snyder, A. Z., Baker, J. T., Van Essen, D. C., et al. (2007). Intrinsic functional architecture in the anaesthetized monkey brain. *Nature, 447*(7140), 83-86.

Vincent, J. L., Snyder, A. Z., Fox, M. D., Shannon, B. J., Andrews, J. R., Raichle, M. E., et al. (2006). Coherent spontaneous activity identifies a hippocampal-parietal memory network. *J Neurophysiol, 96*(6), 3517-3531.

Vos, S. B., Jones, D. K., Jeurissen, B., Viergever, M. A., & Leemans, A. (2012). The influence of complex white matter architecture on the mean diffusivity in diffusion tensor MRI of the human brain. *Neuroimage, 59*(3), 2208-2216.

Voss, M. W., Prakash, R. S., Erickson, K. I., Basak, C., Chaddock, L., Kim, J. S., et al. (2010). Plasticity of brain networks in a randomized intervention trial of exercise training in older adults. *Front Aging Neurosci, 2*.

Voss, M. W., Weng, T. B., Burzynska, A. Z., Wong, C. N., Cooke, G. E., Clark, R., et al. (2016). Fitness, but not physical activity, is related to functional integrity of brain networks associated with aging. *Neuroimage, 131*, 113-125.

Voytek, B., & Knight, R. T. (2015). Dynamic network communication as a unifying neural basis for cognition, development, aging, and disease. *Biol Psychiatry, 77*(12), 1089-1097.

Walhovd, K. B., Johansen-Berg, H., & Káradóttir, R. T. (2014). Unraveling the secrets of white matter--bridging the gap between cellular, animal and human imaging studies. *Neuroscience, 276*, 2-13.

Wang, L., Laviolette, P., O'Keefe, K., Putcha, D., Bakkour, A., Van Dijk, K. R., et al. (2010). Intrinsic connectivity between the hippocampus and posteromedial cortex predicts memory performance in cognitively intact older individuals. *Neuroimage, 51*(2), 910-917.

Wang, L., Negreira, A., LaViolette, P., Bakkour, A., Sperling, R. A., & Dickerson, B. C. (2010). Intrinsic interhemispheric hippocampal functional connectivity predicts individual differences in memory performance ability. *Hippocampus, 20*(3), 345-351.

Wang, X., Casadio, M., Weber, K. A., Mussa-Ivaldi, F. A., & Parrish, T. B. (2014). White matter microstructure changes induced by motor skill learning utilizing a body machine interface. *Neuroimage, 88*, 32-40.

Ward, A. M., Schultz, A. P., Huijbers, W., Van Dijk, K. R., Hedden, T., & Sperling, R. A. (2014). The parahippocampal gyrus links the default-mode cortical network with the medial temporal lobe memory system. *Hum Brain Mapp, 35*(3), 1061-1073.

Wechsler, D. (1997). *WAIS-III/WMS-III technical manual*. San Antonio: Psychological Corporation.

Weiss, A. P., Dewitt, I., Goff, D., Ditman, T., & Heckers, S. (2005). Anterior and posterior hippocampal volumes in schizophrenia. *Schizophr Res, 73*(1), 103-112.

Weng, T. B., Pierce, G. L., Darling, W. G., Falk, D., Magnotta, V. A., & Voss, M. W. (2017). The Acute Effects of Aerobic Exercise on the Functional Connectivity of Human Brain Networks. *Brain Plasticity, 2*(2), 171-190.

West, R. L. (1996). An application of prefrontal cortex function theory to cognitive aging. *Psychol Bull, 120*(2), 272-292.

Westlye, E. T., Lundervold, A., Rootwelt, H., Lundervold, A. J., & Westlye, L. T. (2011). Increased Hippocampal Default Mode Synchronization during Rest in Middle-Aged and

Elderly APOE epsilon 4 Carriers: Relationships with Memory Performance. *Journal of Neuroscience, 31*(21), 7775-7783.
Wheeler-Kingshott, C. A., & Cercignani, M. (2009). About "axial" and "radial" diffusivities. *Magn Reson Med, 61*(5), 1255-1260.
Wisdom, N. M., Callahan, J. L., & Hawkins, K. A. (2011). The effects of apolipoprotein E on non-impaired cognitive functioning: a meta-analysis. *Neurobiol Aging, 32*(1), 63-74.
Wishart, H. A., Saykin, A. J., McAllister, T. W., Rabin, L. A., McDonald, B. C., Flashman, L. A., et al. (2006). Regional brain atrophy in cognitively intact adults with a single APOE epsilon4 allele. *Neurology, 67*(7), 1221-1224.
Woo, C. W., Krishnan, A., & Wager, T. D. (2014). Cluster-extent based thresholding in fMRI analyses: pitfalls and recommendations. *Neuroimage, 91*, 412-419.
Woodard, J. L., Sugarman, M. A., Nielson, K. A., Smith, J. C., Seidenberg, M., Durgerian, S., et al. (2012). Lifestyle and genetic contributions to cognitive decline and hippocampal structure and function in healthy aging. *Curr Alzheimer Res, 9*(4), 436-446.
Xie, C., Bai, F., Yu, H., Shi, Y., Yuan, Y., Chen, G., et al. (2012). Abnormal insula functional network is associated with episodic memory decline in amnestic mild cognitive impairment. *Neuroimage, 63*(1), 320-327.
Yamasaki, T., Muranaka, H., Kaseda, Y., Mimori, Y., & Tobimatsu, S. (2012). Understanding the Pathophysiology of Alzheimer's Disease and Mild Cognitive Impairment: A Mini Review on fMRI and ERP Studies. *Neurol Res Int, 2012*, 719056.
Yassa, M. A., & Stark, C. E. (2011). Pattern separation in the hippocampus. *Trends Neurosci, 34*(10), 515-525.
Yen, C. H., Yeh, C. J., Wang, C. C., Liao, W. C., Chen, S. C., Chen, C. C., et al. (2010). Determinants of cognitive impairment over time among the elderly in Taiwan: results of the national longitudinal study. *Arch Gerontol Geriatr, 50 Suppl 1*, S53-57.
Yesavage, J. A. (1988). Geriatric Depression Scale. *Psychopharmacol Bull, 24*(4), 709-711.
Ylikoski, A., Erkinjuntti, T., Raininko, R., Sarna, S., Sulkava, R., & Tilvis, R. (1995). White matter hyperintensities on MRI in the neurologically nondiseased elderly. Analysis of cohorts of consecutive subjects aged 55 to 85 years living at home. *Stroke, 26*(7), 1171-1177.
Zalesky, A., Fornito, A., & Bullmore, E. (2012). On the use of correlation as a measure of network connectivity. *Neuroimage, 60*(4), 2096-2106.
Zarahn, E., Aguirre, G. K., & D'Esposito, M. (1997). Empirical analyses of BOLD fMRI statistics. I. Spatially unsmoothed data collected under null-hypothesis conditions. *Neuroimage, 5*(3), 179-197.
Zhang, H. Y., Wang, S. J., Xing, J., Liu, B., Ma, Z. L., Yang, M., et al. (2009). Detection of PCC functional connectivity characteristics in resting-state fMRI in mild Alzheimer's disease. [Article]. *Behavioural Brain Research, 197*(1), 103-108.
Zhao, X., Liu, Y., Wang, X., Liu, B., Xi, Q., Guo, Q., et al. (2012). Disrupted small-world brain networks in moderate Alzheimer's disease: a resting-state FMRI study. *PLoS One, 7*(3), e33540.
Zhou, Y., Dougherty, J. H., Hubner, K. F., Bai, B., Cannon, R. L., & Hutson, R. K. (2008). Abnormal connectivity in the posterior cingulate and hippocampus in early Alzheimer's disease and mild cognitive impairment. *Alzheimers Dement, 4*(4), 265-270.